LIGO-Virgo-KAGRA network for hunting gravitational waves

- Underground and Cryogenic interferometric 3 km gravitational-wave detector at Kamioka, Japan

Contents

(c) KAGRA Collaboration / Rey.Hori

LSC LIGO Scientific Collaboration

VIRGO

KAGRA

Hisaaki Shinkai (Osaka Inst. Tech.)
真貝寿明（大阪工業大学）

http://www.oit.ac.jp/is/shinkai/

JGW-G2113518

LIGO-Virgo-KAGRA network for hunting gravitational waves

Contents

(c) KAGRA Collaboration / Rey.Hori

Hisaaki Shinkai (Osaka Inst. Tech.)
真貝寿明（大阪工業大学）

First Detection (2015 Sep 14)

Feb 2016, LIGO announced the first detection of GW (GW150914). The source was Binary BHs.

Oct 2017, LIGO/Virgo announced the first GW detection from Binary NSs (GW170817).

2017 Nobel Prize

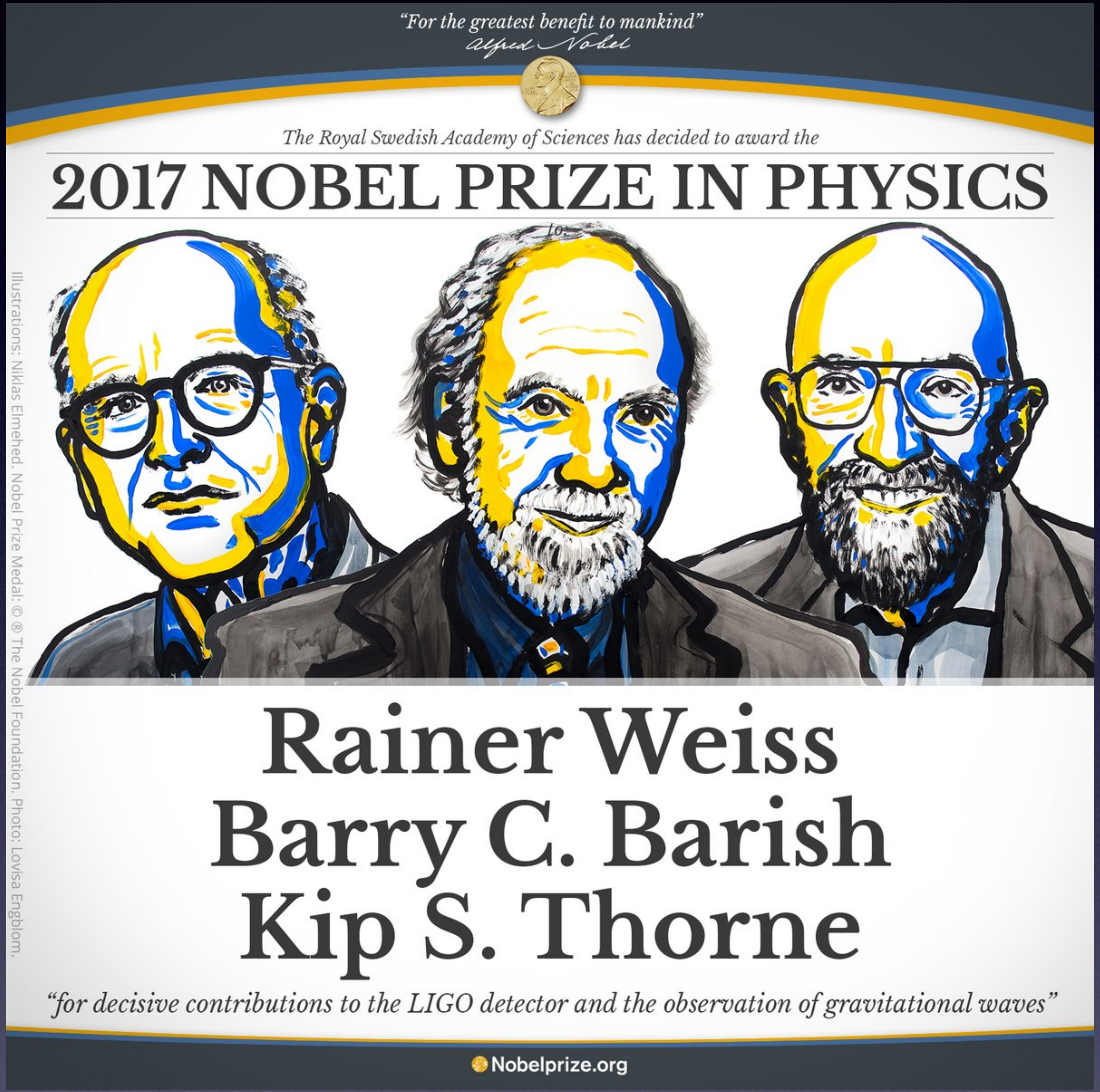

Oct 2017, Royal Swedish academy of science announced the physics prize goes to GW project.

Gravitational Wave

from binary BH-BH, NS-NS, BH-NS

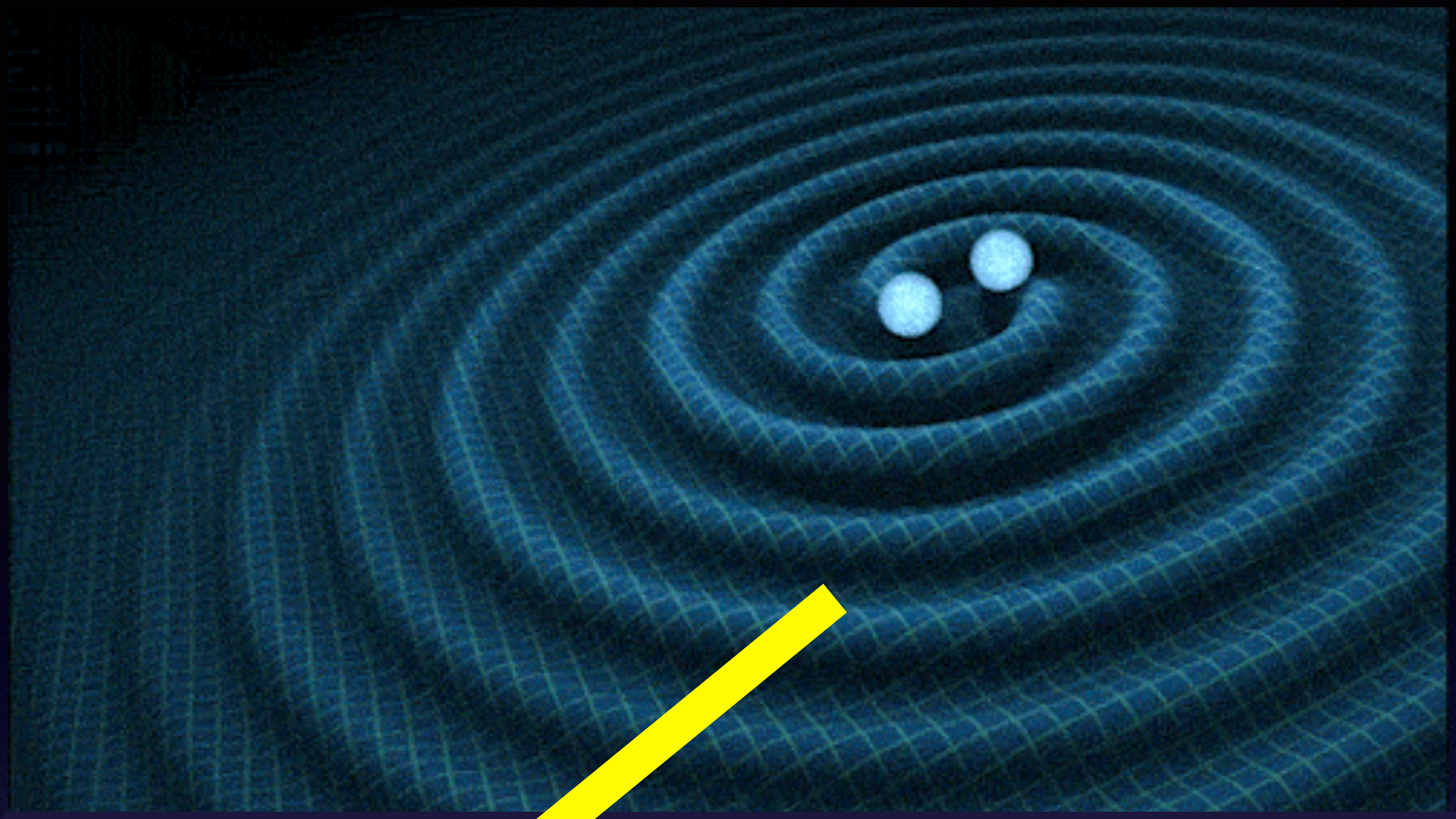

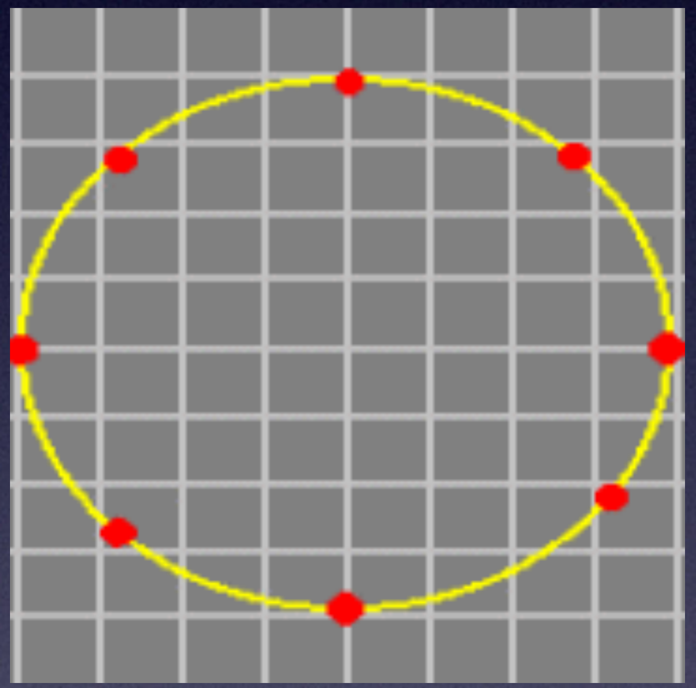

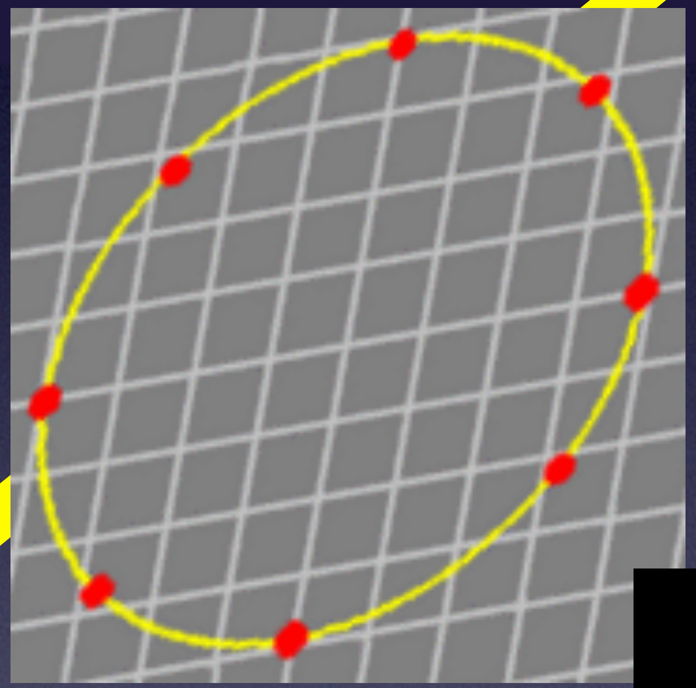

typical amplitude 10^{-22}

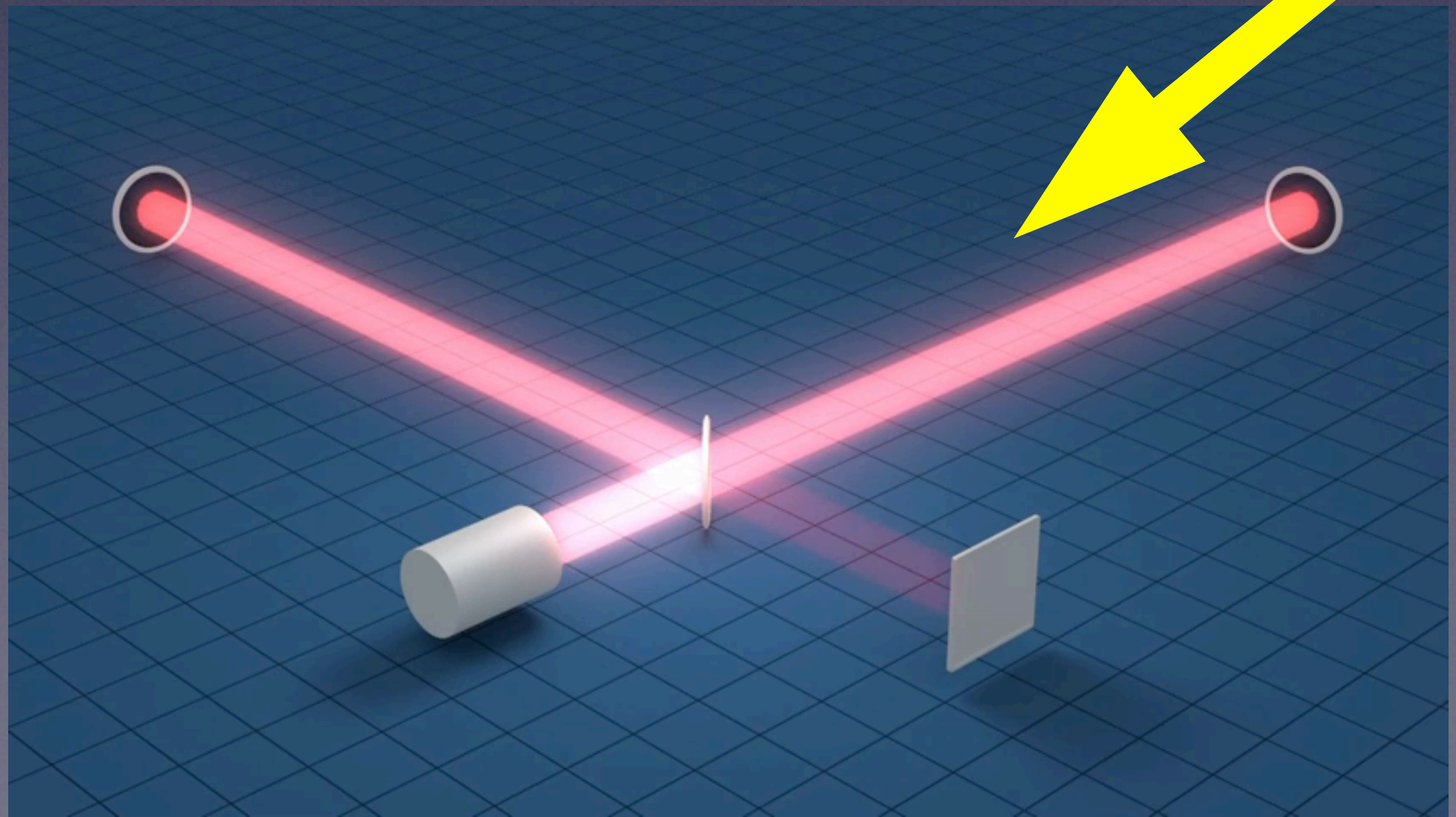

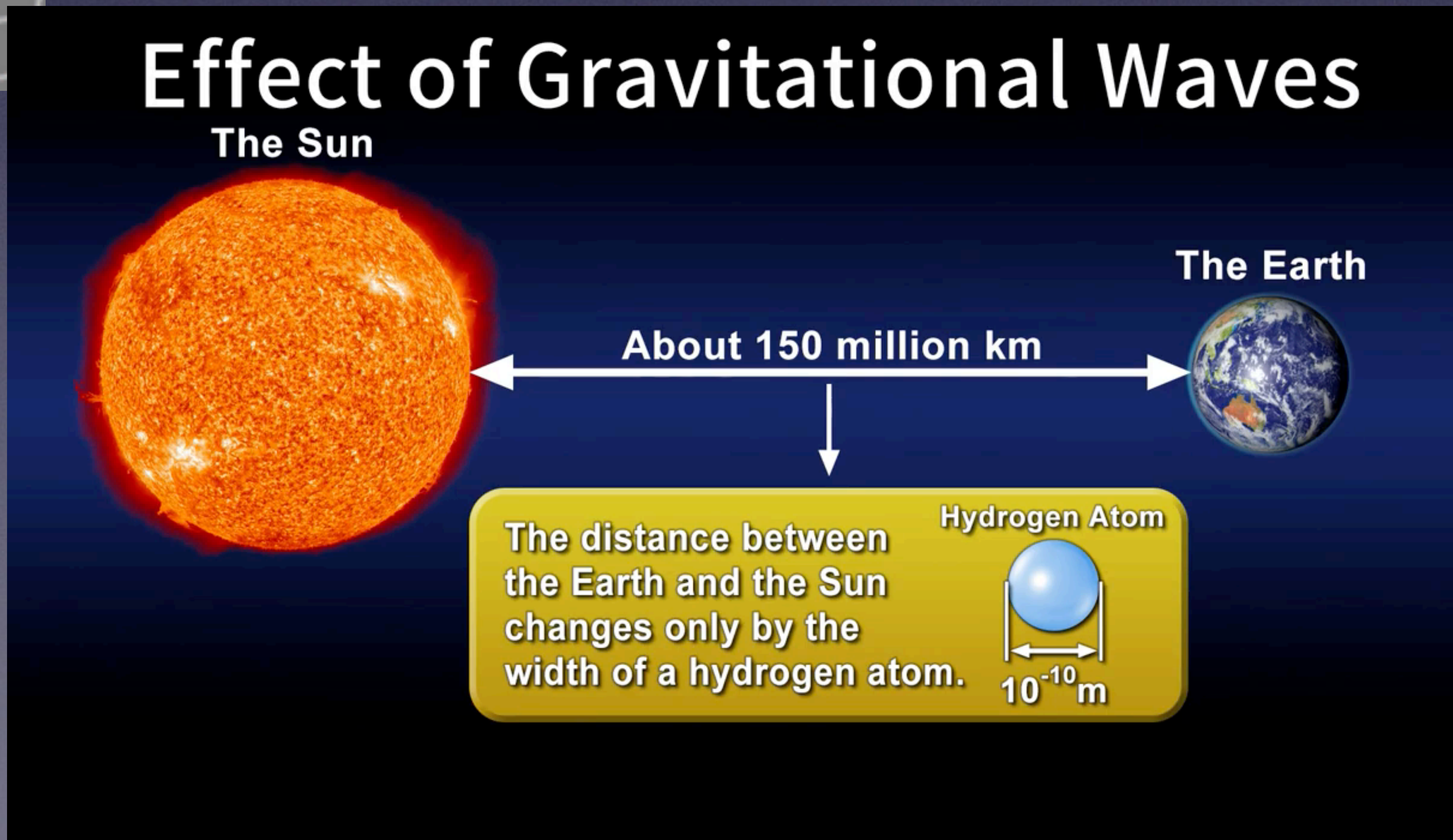

What we can learn from GW (from a binary merger) ?

merger phase

amplitude

inspiral phase

ringdown phase

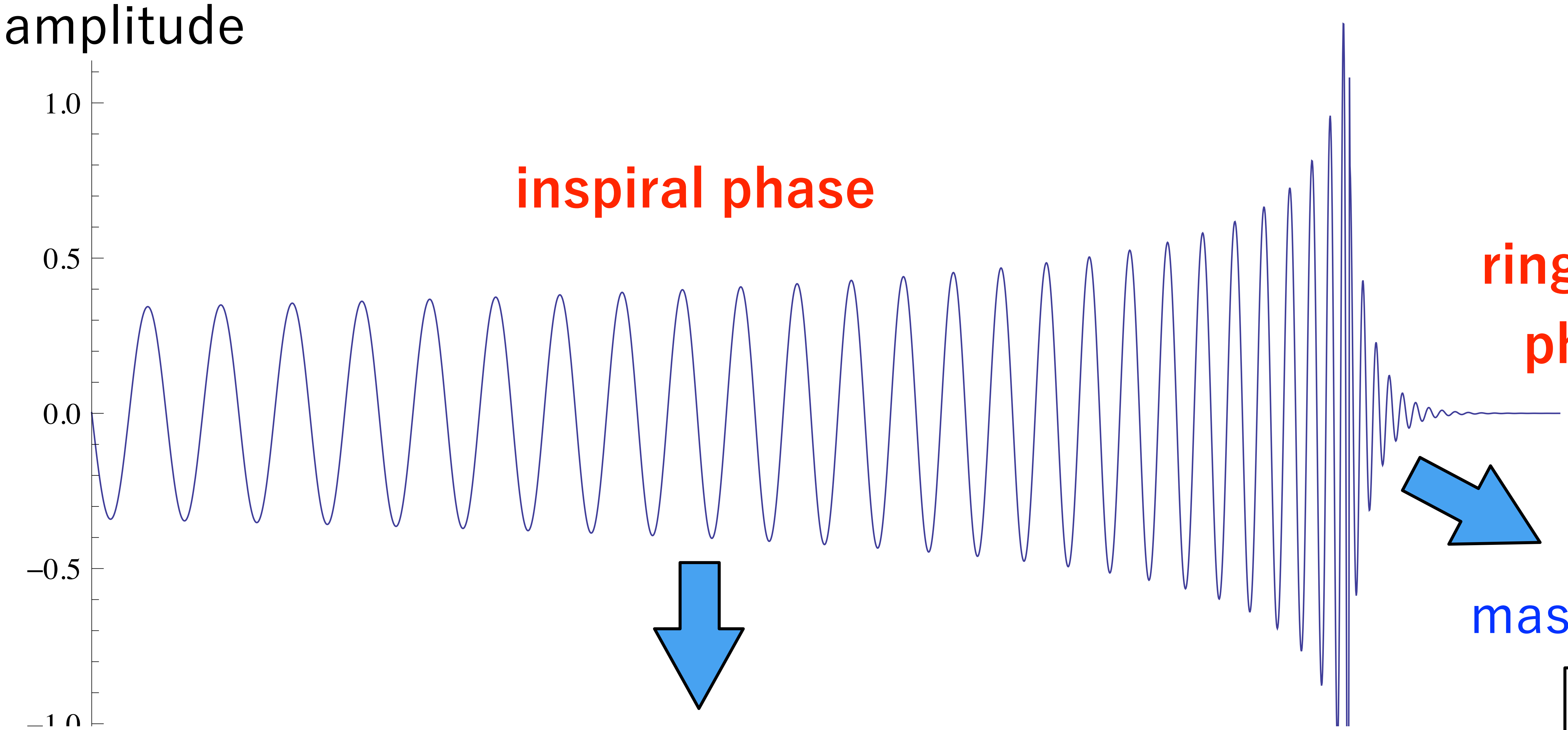

mass, spin

mass, spin, orbital parameters, tidal, distance, polarization

$$(m_1, m_2, \mathbf{s}_1, \mathbf{s}_2, \iota, \mathbf{n}, t_c, \varphi_c, \psi, r)$$

statistics

- nuclear matter EOS
- binary formation scenario
- galaxy formation scenario
- cosmological parameters

test of GR

unified theory

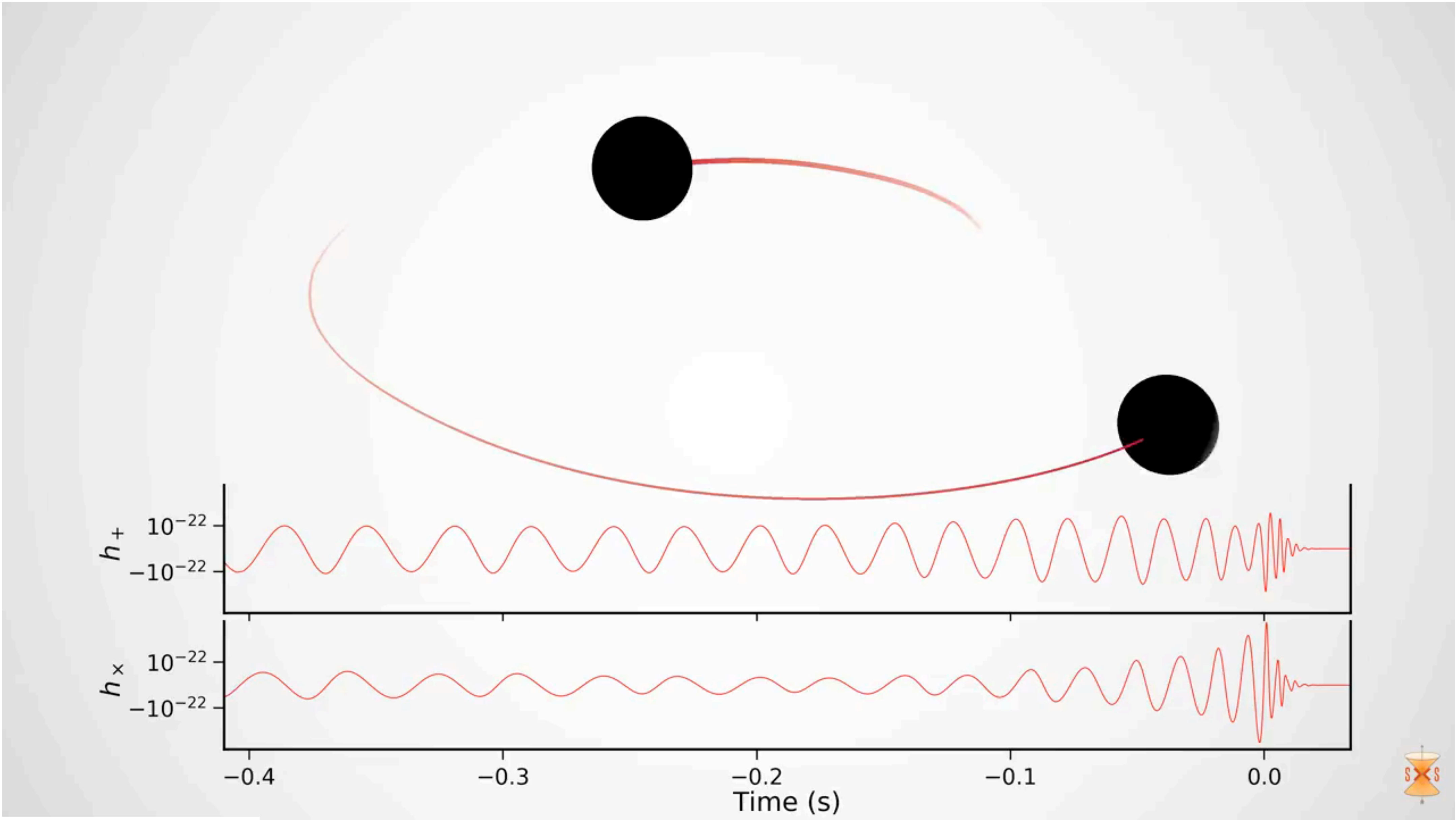

http://ligo.org/detections/GW170104.php

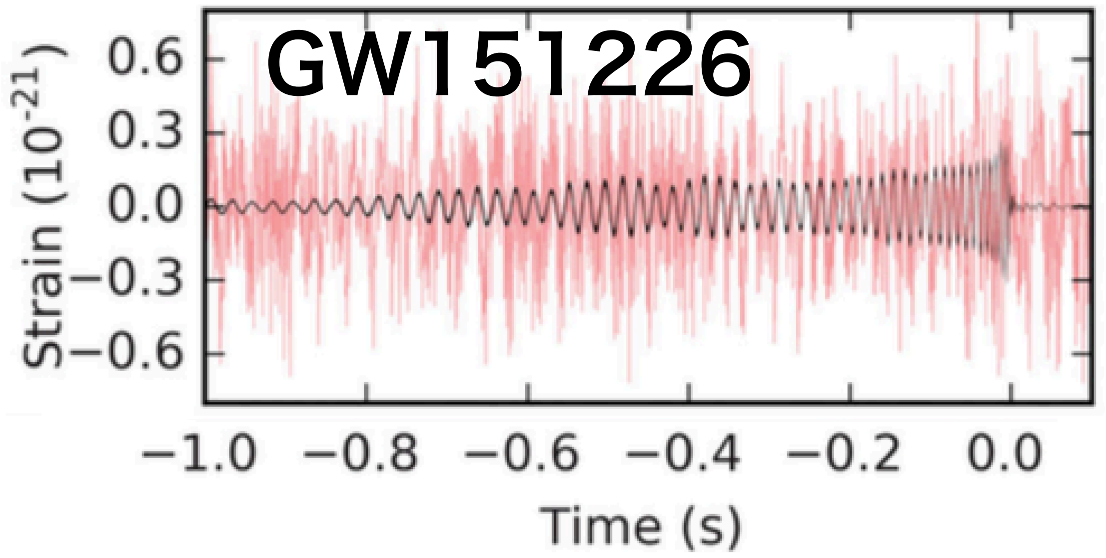

standard way is to use matched filtering technique
necessary for GW templates in hand

Sensitivity requirements for the detectors

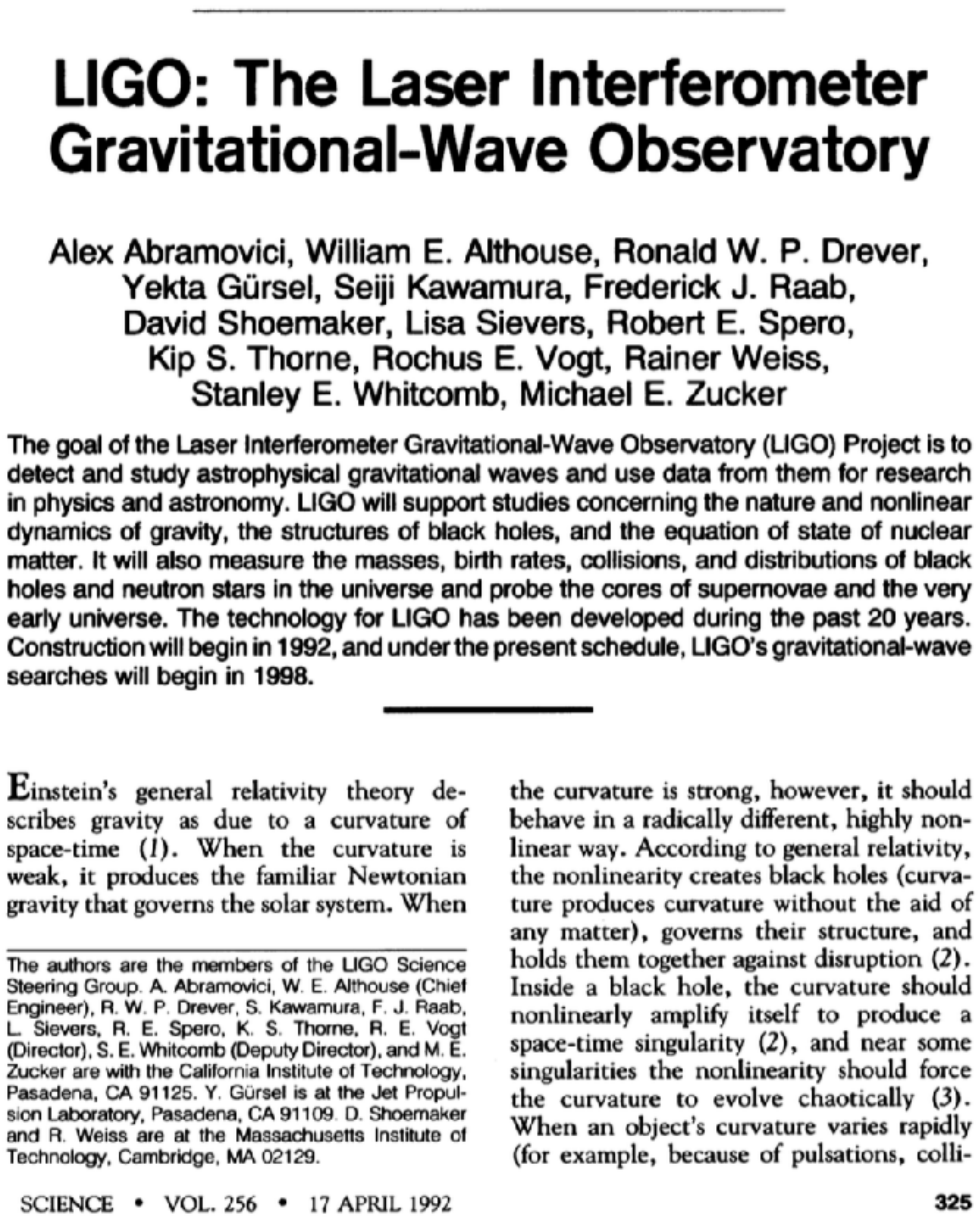

LIGO: The Laser Interferometer Gravitational-Wave Observatory

Alex Abramovici, William E. Althouse, Ronald W. P. Drever, Yekta Gürsel, Seiji Kawamura, Frederick J. Raab, David Shoemaker, Lisa Sievers, Robert E. Spero, Kip S. Thorne, Rochus E. Vogt, Rainer Weiss, Stanley E. Whitcomb, Michael E. Zucker

The goal of the Laser Interferometer Gravitational-Wave Observatory (LIGO) Project is to detect and study astrophysical gravitational waves and use data from them for research in physics and astronomy. LIGO will support studies concerning the nature and nonlinear dynamics of gravity, the structures of black holes, and the equation of state of nuclear matter. It will also measure the masses, birth rates, collisions, and distributions of black holes and neutron stars in the universe and probe the cores of supernovae and the very early universe. The technology for LIGO has been developed during the past 20 years. Construction will begin in 1992, and under the present schedule, LIGO's gravitational-wave searches will begin in 1998.

Einstein's general relativity theory describes gravity as due to a curvature of space-time (1). When the curvature is weak, it produces the familiar Newtonian gravity that governs the solar system. When the curvature is strong, however, it should behave in a radically different, highly nonlinear way. According to general relativity, the nonlinearity creates black holes (curvature produces curvature without the aid of any matter), governs their structure, and holds them together against disruption (2). Inside a black hole, the curvature should nonlinearly amplify itself to produce a space-time singularity (2), and near some singularities the nonlinearity should force the curvature to evolve chaotically (3). When an object's curvature varies rapidly (for example, because of pulsations, colli-

The authors are the members of the LIGO Science Steering Group. A. Abramovici, W. E. Althouse (Chief Engineer), R. W. P. Drever, S. Kawamura, F. J. Raab, L. Sievers, R. E. Spero, K. S. Thorne, R. E. Vogt (Director), S. E. Whitcomb (Deputy Director), and M. E. Zucker are with the California Institute of Technology, Pasadena, CA 91125. Y. Gürsel is at the Jet Propulsion Laboratory, Pasadena, CA 91109. D. Shoemaker and R. Weiss are at the Massachusetts Institute of Technology, Cambridge, MA 02129.

SCIENCE • VOL. 256 • 17 APRIL 1992 325

Science 256 (1992) 325

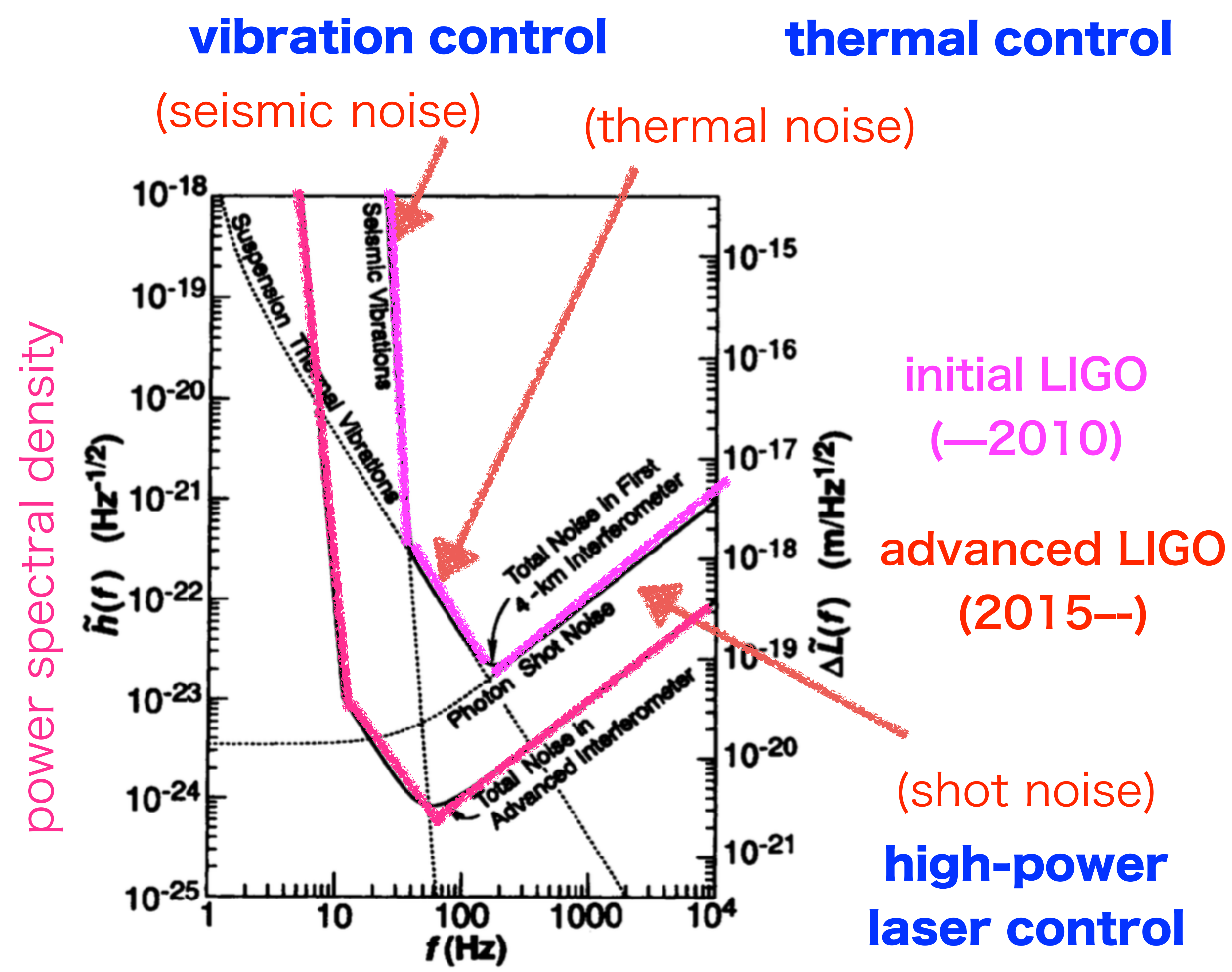

Fig. 7. The expected total noise in each of LIGO's first 4-km interferometers (upper solid curve) and in a more advanced interferometer (lower solid curve). The dashed curves show various contributions to the first interferometer's noise.

GW International Network

4 km

4 km

600 m

3 km

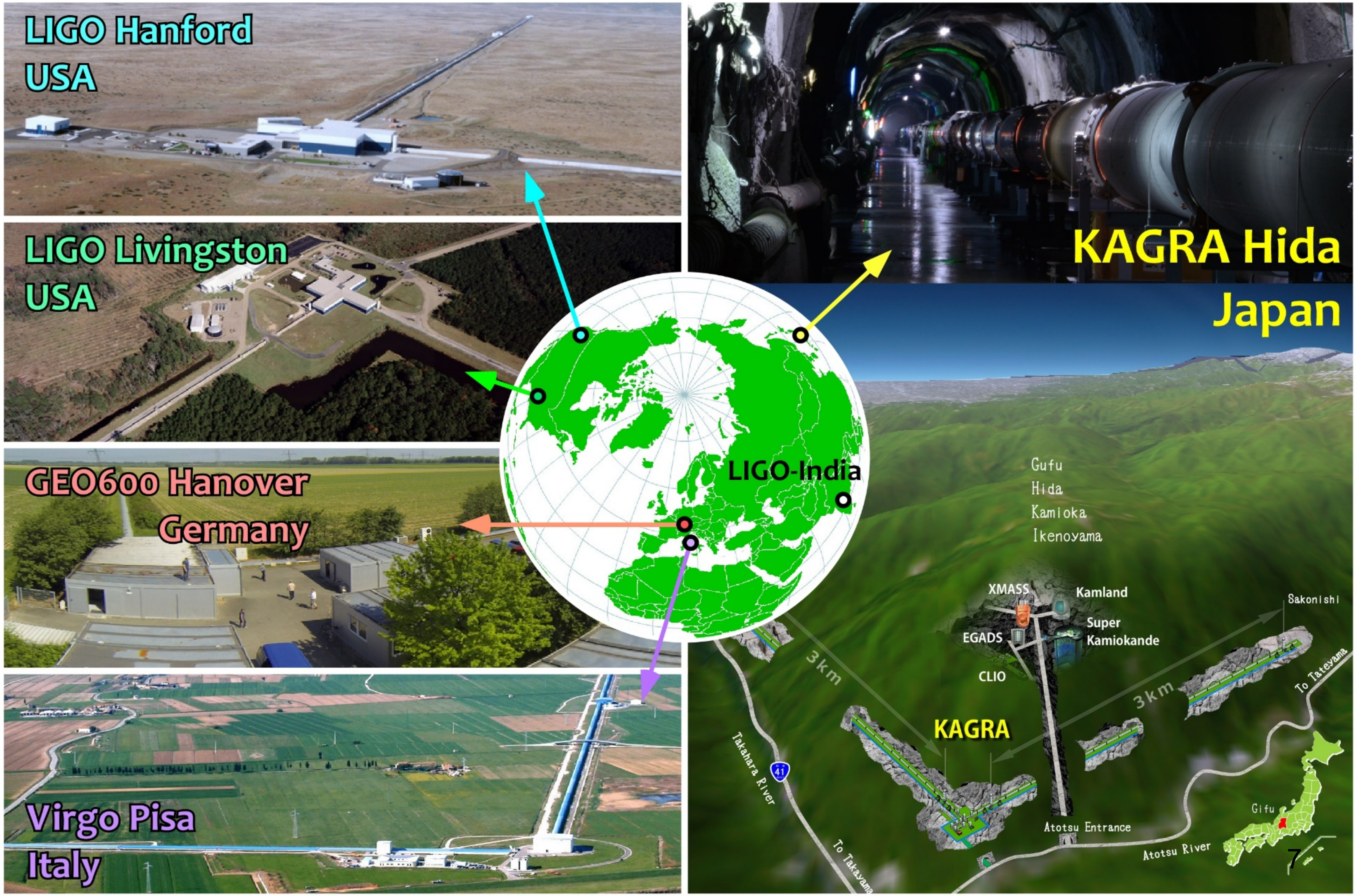

3 km

LIGO, Virgo and KAGRA

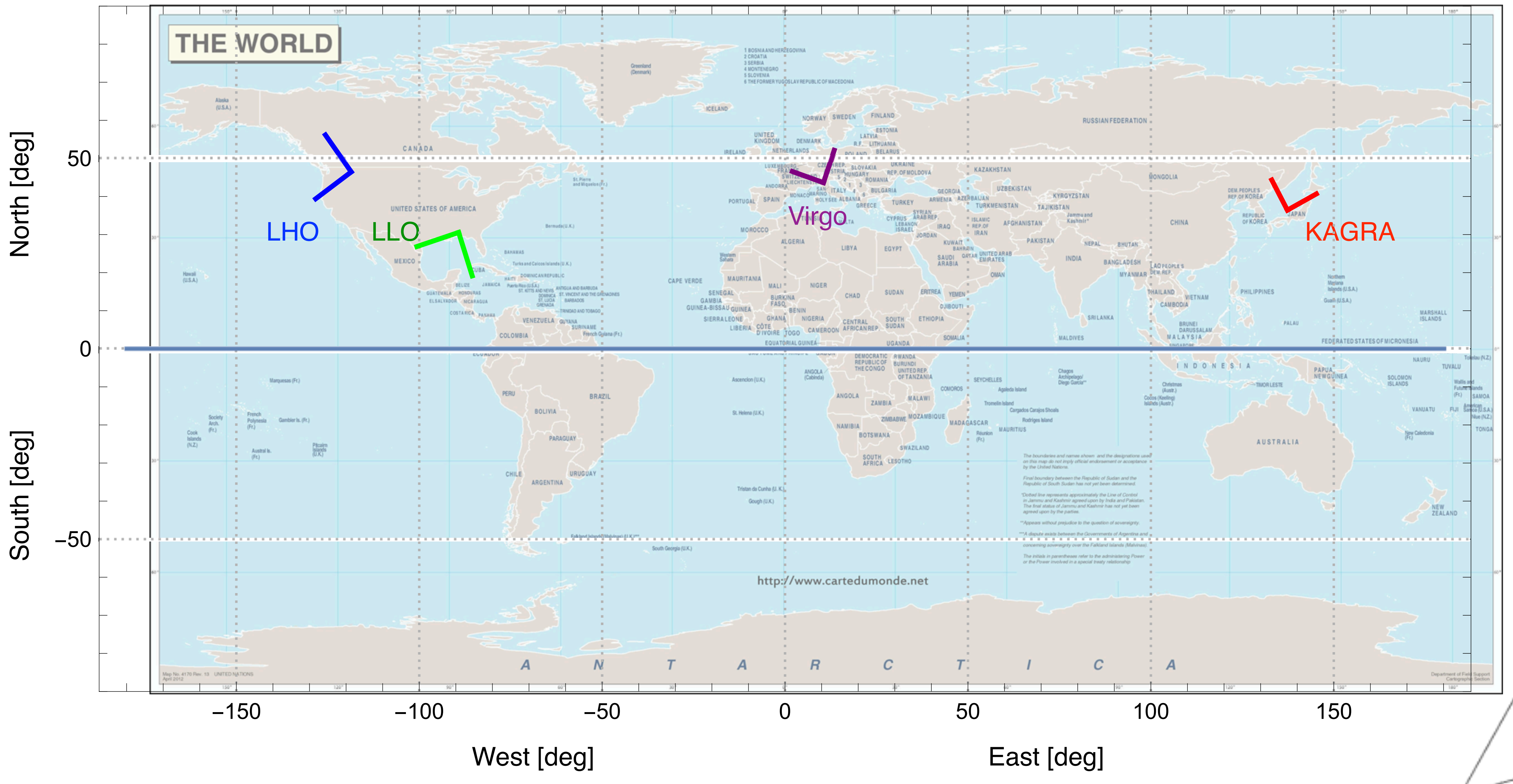

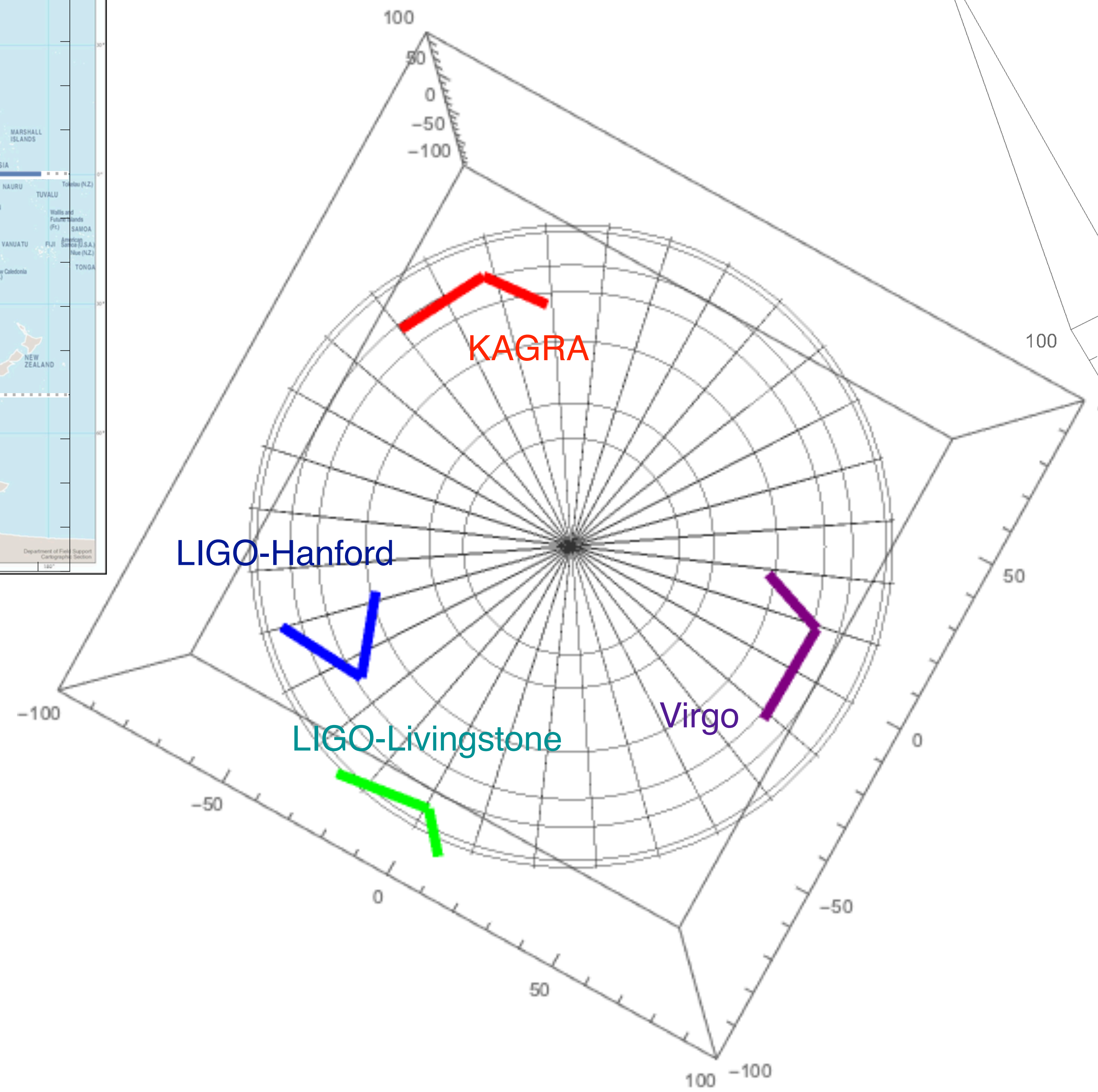

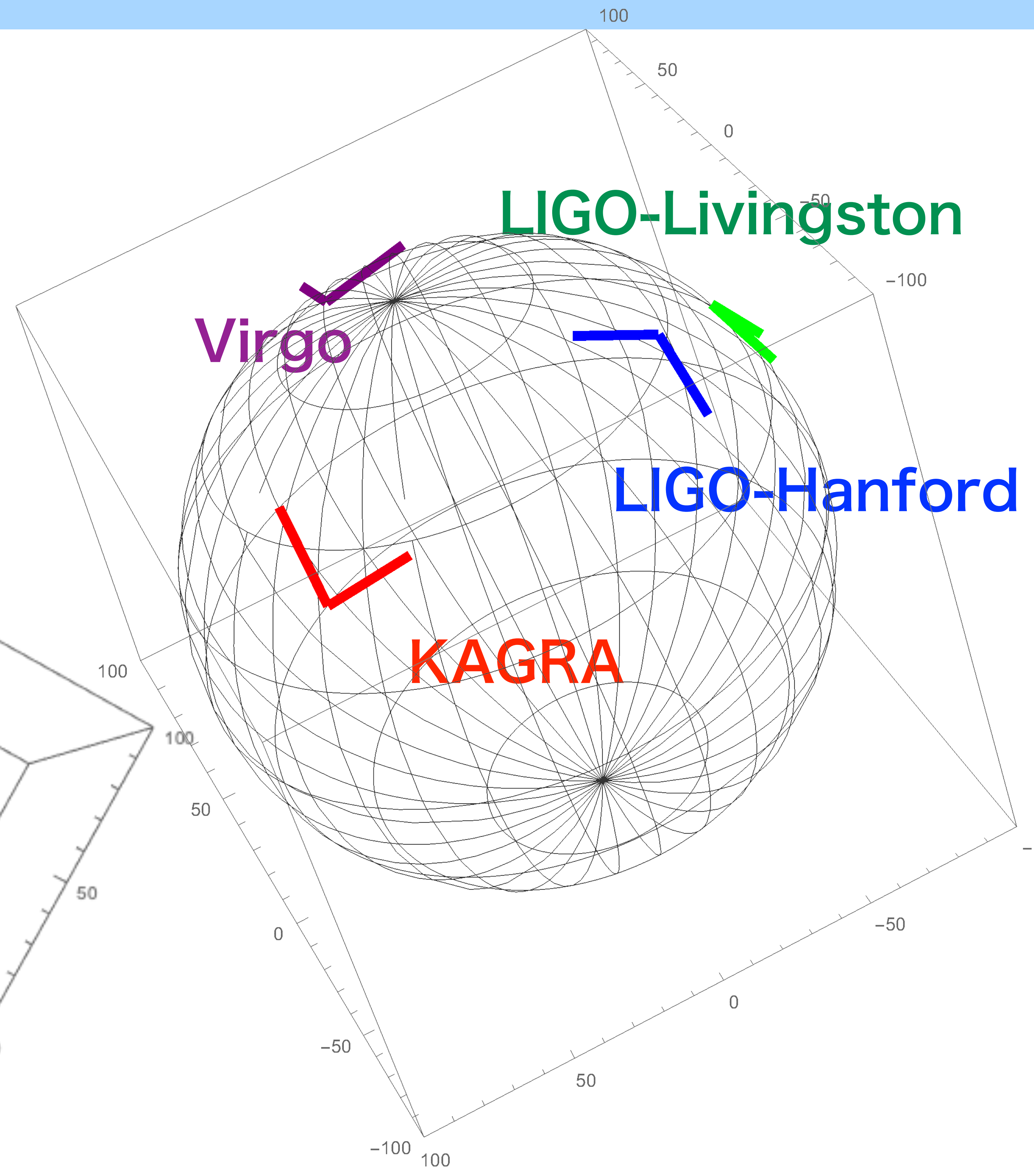

more precise GW source localization
more certain GW source parameters
more chances to hunt GW events
more information of GW polarization
more ideas for GW researches
more man power

Table 1 Geometry of LIGO, Virgo & KAGRA detectors.

Detector	arm length	Latitude	Longitude	X-arm	Y-arm
LIGO Hanford (LHO)	4 km	46°27′19″ N	119°24′28″ W	N 36° W	W 36° S
LIGO Livingston (LLO)	4 km	30°33′46″ N	90°46′27″ W	N 18° S	S 18° E
Virgo	3 km	43°37′53″ N	10°30′16″ E	N 19° E	W 19° N
KAGRA	3 km	36°24′36″ N	137°18′36″ E	E 28.3° N	N 28.3° W

GW International Network

KAGRA joined international network October 2019.

LIGO

1330 members

860 authors

101 groups

20 countries

VIRGO


Virgo Collaboration

Virgo is a European collaboration with about 360 authors from 89 institutes

Advanced Virgo (AdV) and AdV+: upgrades of the Virgo interferometric detector

Participation by scientists from France, Italy, Belgium, The Netherlands, Poland, Hungary, Spain, Germany

- Institutes in Virgo Steering Committee
  - APC Paris
  - ARTEMIS Nice
  - IFAE Barcelona
  - ILM and Navier
  - INFN Firenze-Urbino
  - INFN Genova
  - INFN Napoli
  - INFN Perugia
  - INFN Pisa
  - INFN Roma La Sapienza
  - INFN Roma Tor Vergata
  - INFN Trento-Padova
  - LAL Orsay ESPCI Paris
  - LAPP Annecy
  - LKB Paris
  - LMA Lyon
  - Maastricht University
  - Nikhef Amsterdam
  - POLGRAW(Poland)
  - University Nijmegen
  - RMKI Budapest
  - UCLouvain, ULiege
  - Univ. of Barcelona
  - University of Sannio
  - Univ. of Valencia
  - University of Jena

Advanced Virgo project has been formally completed on July 31, 2017

Part of the international network of 2nd generation detectors

Started O3 run on April 1, 2019

8 European countries

2

465 members

360 authors

96 groups

8 countries

KAGRA

460 members

200 authors

114 groups

14 regions

LSC spokesperson

Patrick Brady

Virgo spokesperson

Giovanni Losurdo

KSC board chair

2021 Aug.

HS **Jun'ichi Yokoyama**

Sensitivity Curve

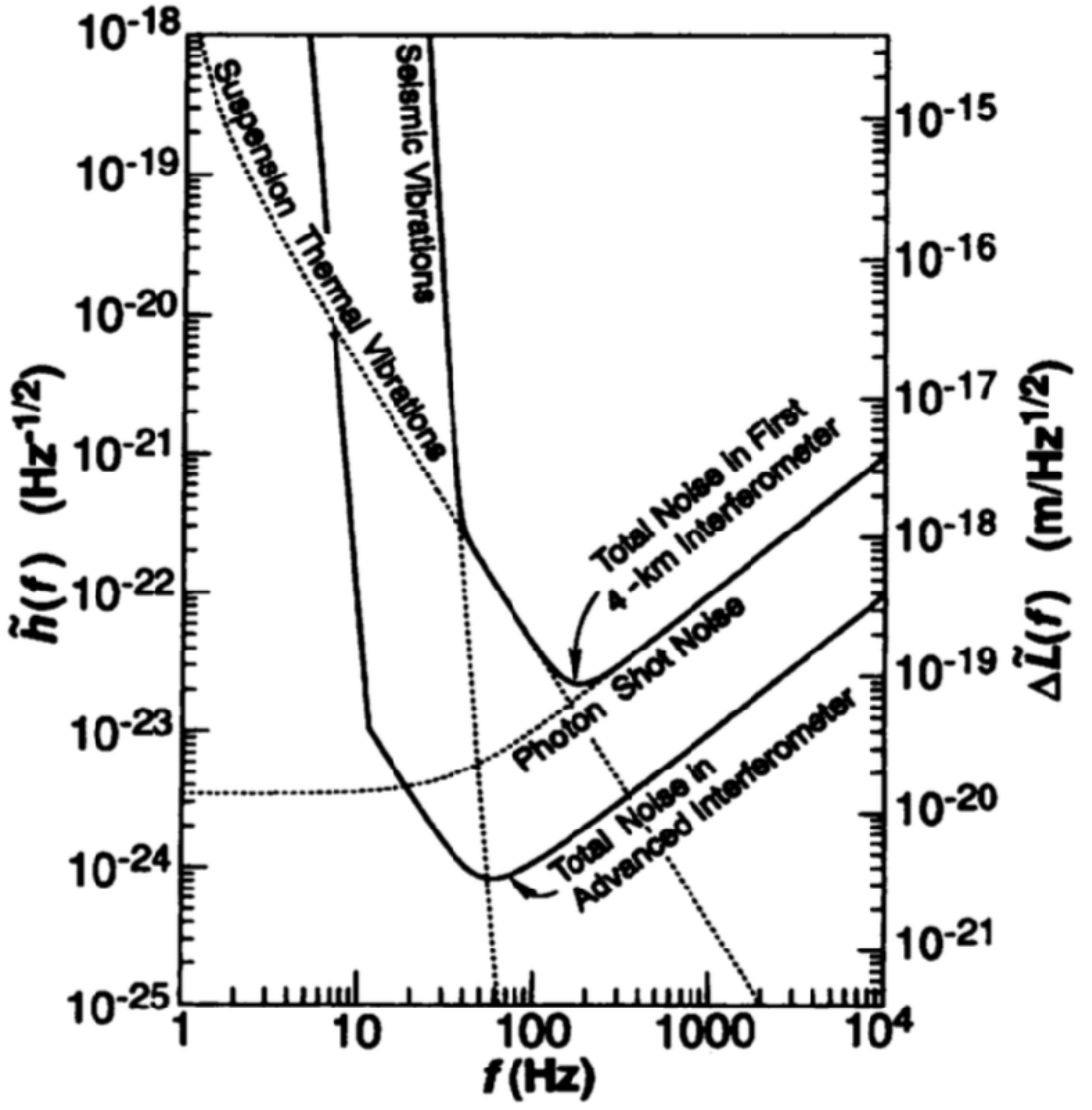

Fig. 7. The expected total noise in each of LIGO's first 4-km interferometers (upper solid curve) and in a more advanced interferometer (lower solid curve). The dashed curves show various contributions to the first interferometer's noise.

Science 256 (1992) 325

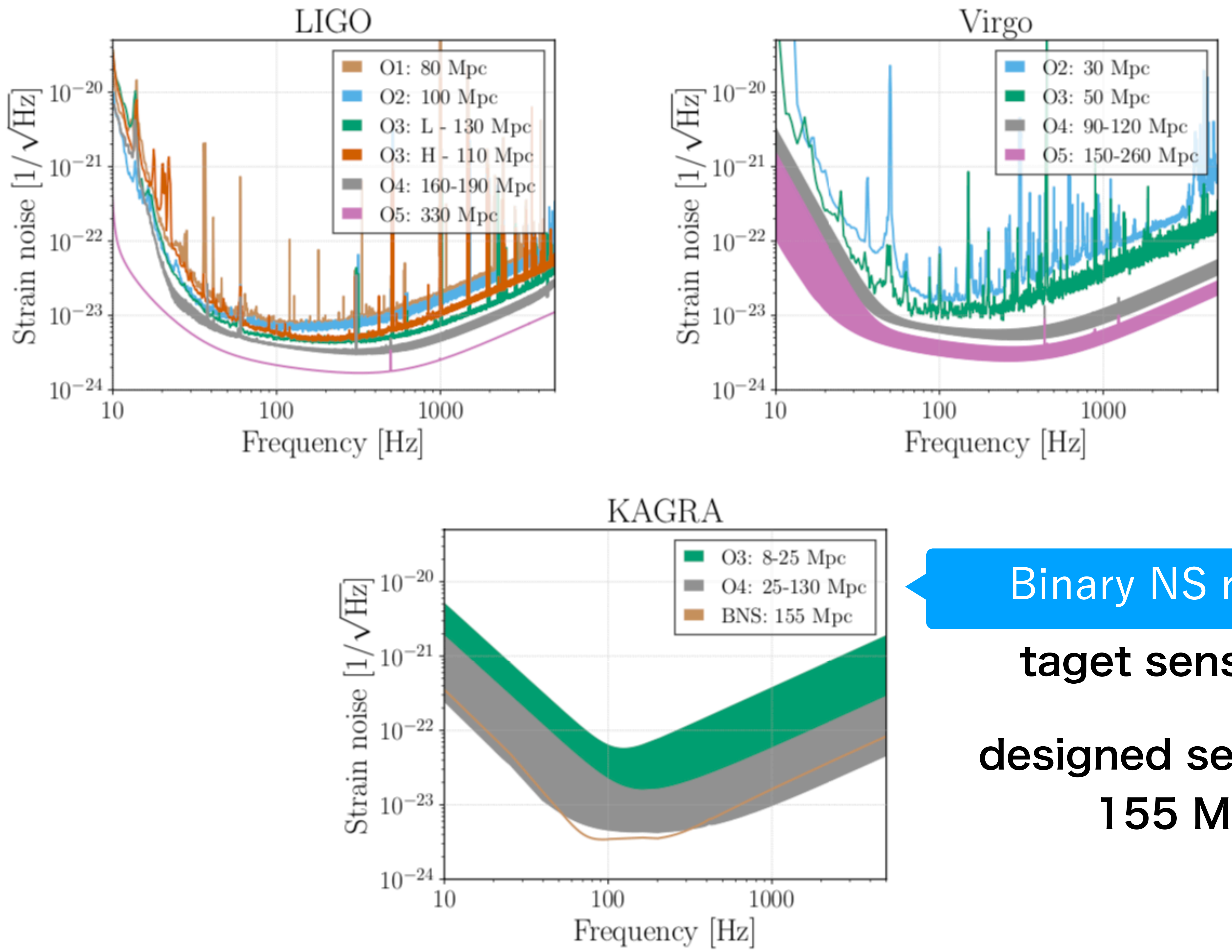

Binary NS range

taget sensitivity

designed sensitivity
155 Mpc

LVK collaboration, Living Rev Relativ (2020) 23:3
https://link.springer.com/article/10.1007/s41114-020-00026-9
[1304.0670ver2020Jan]

Sensitivity Curve

Sensitivity History

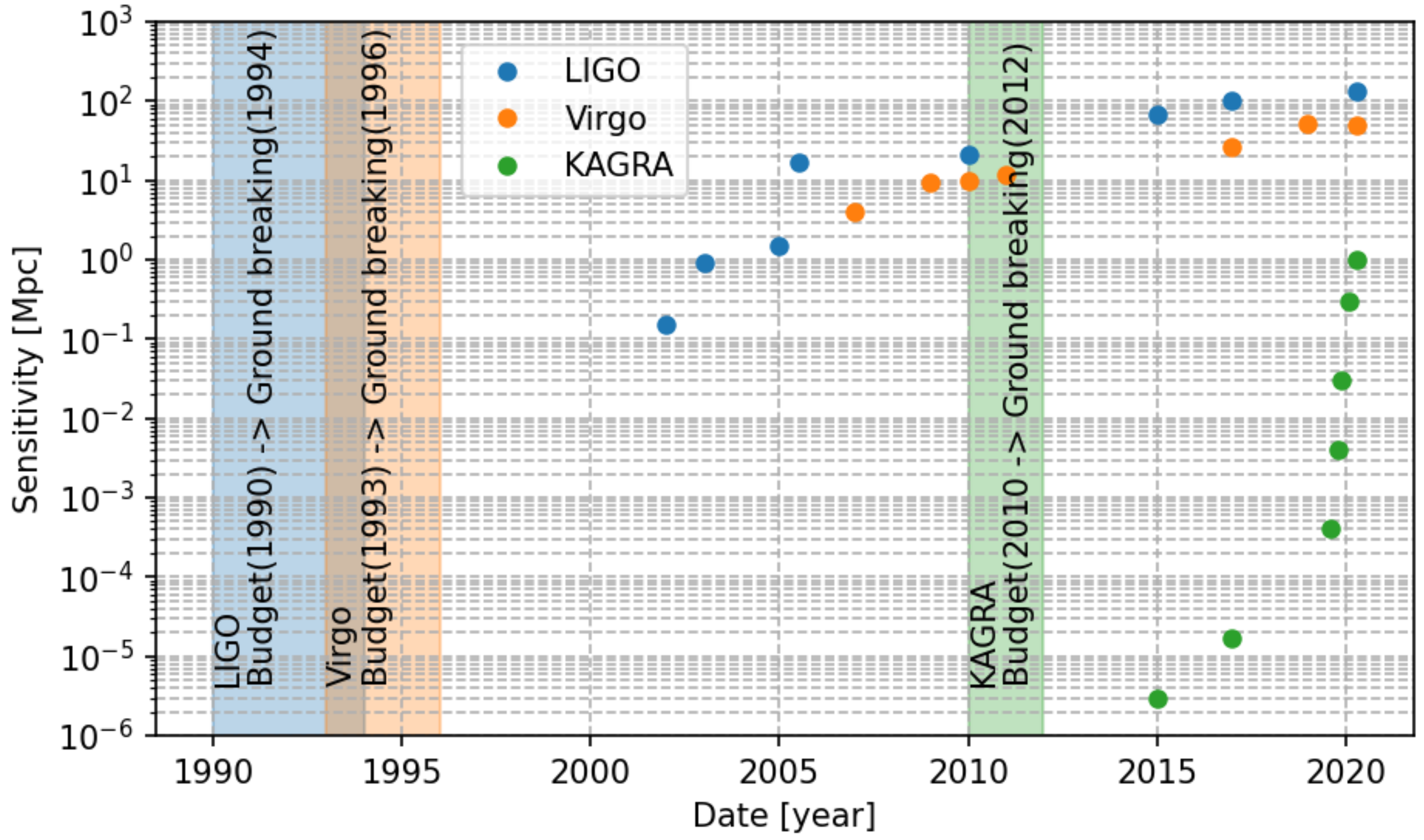

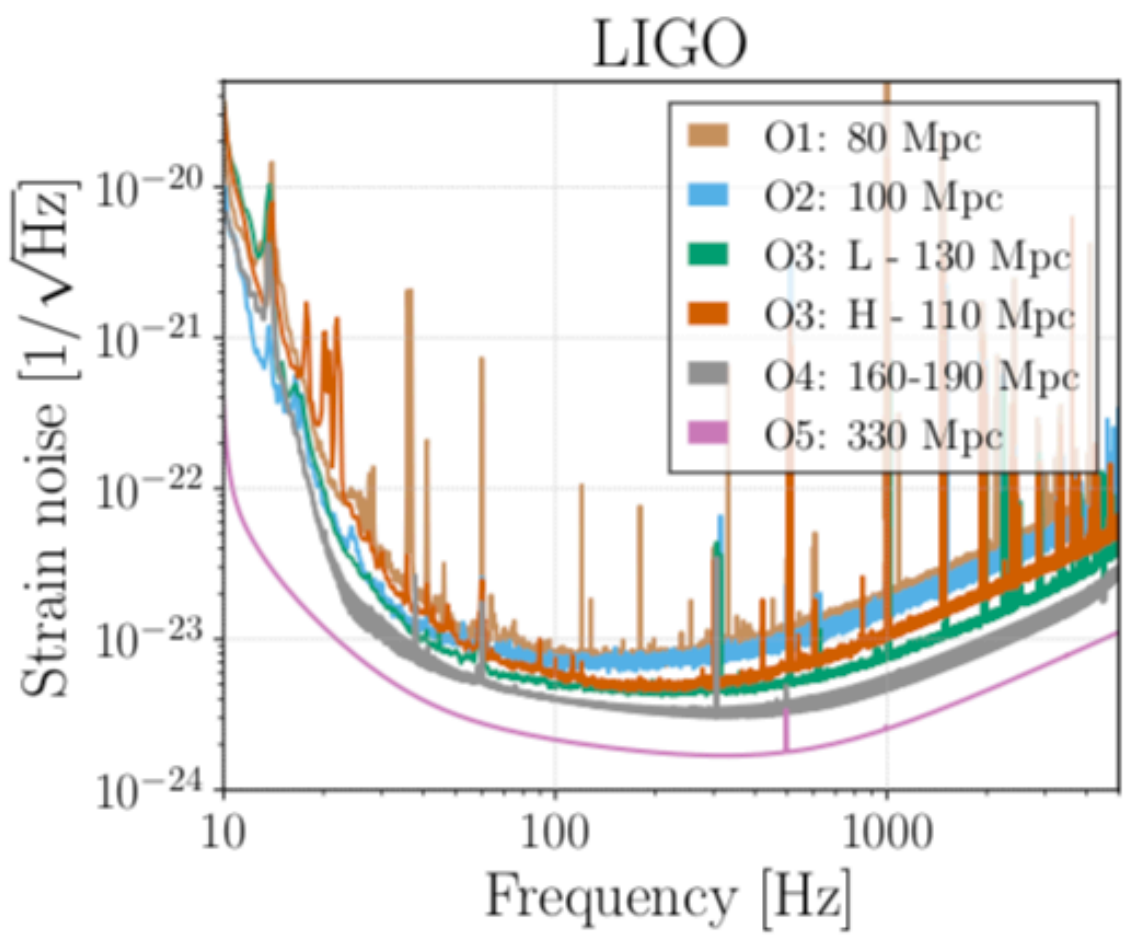

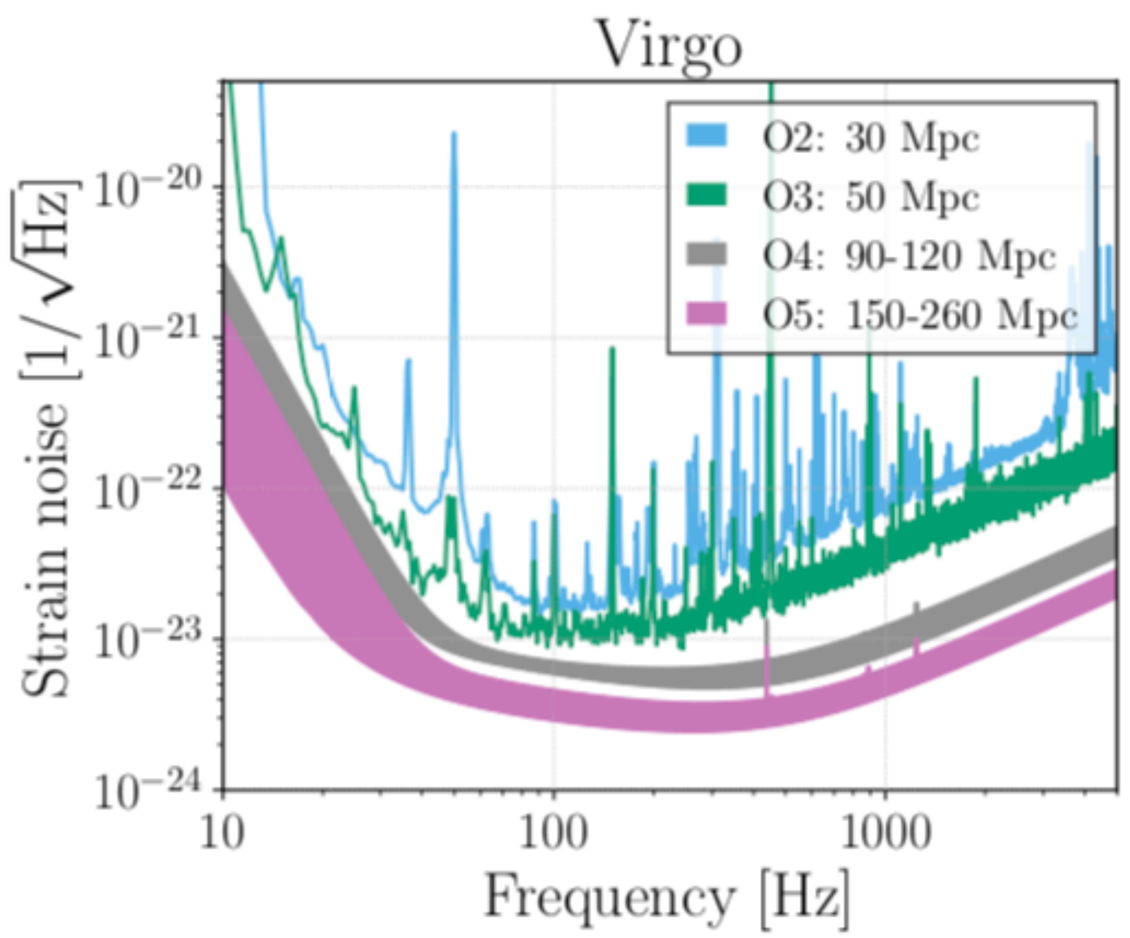

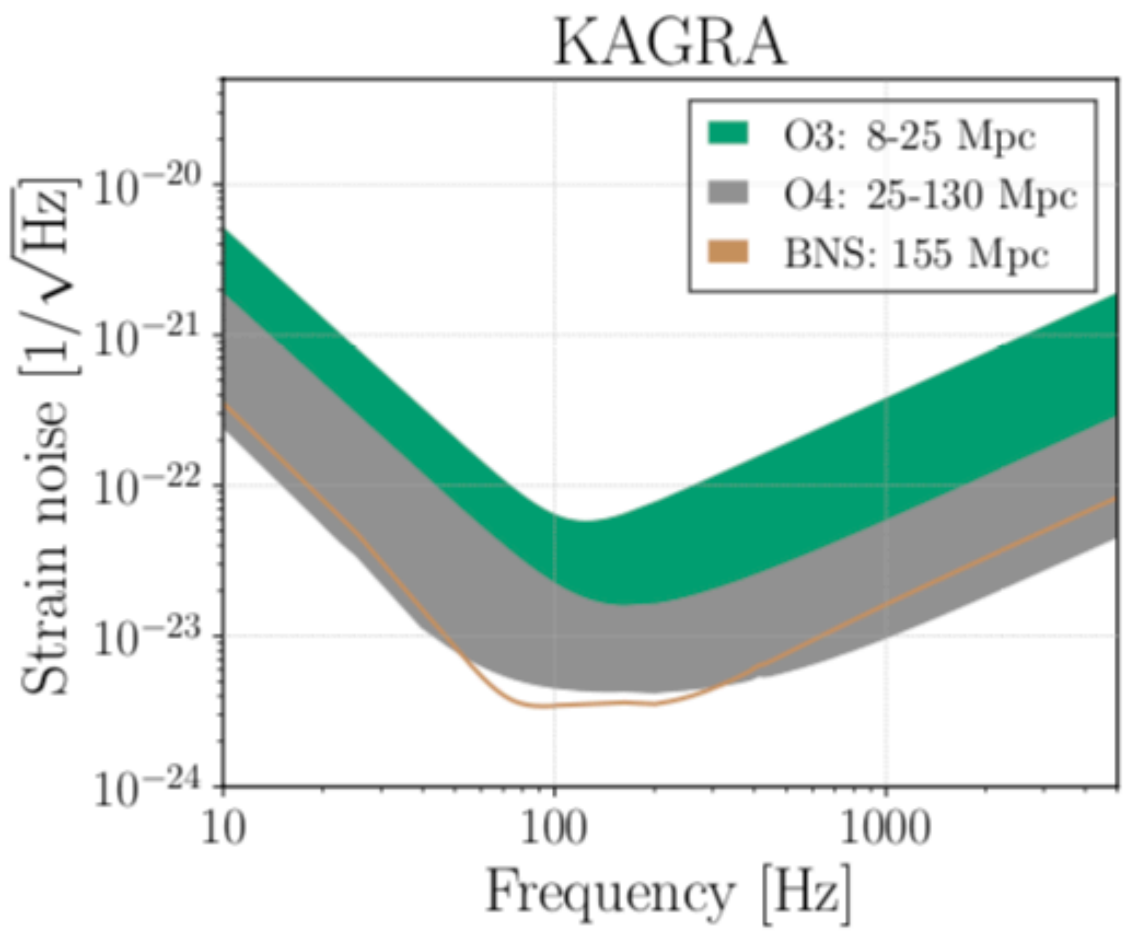

Binary NS range

taget sensitivity

designed sensitivity
155 Mpc

LVK collaboration, Living Rev Relativ (2020) 23:3
https://link.springer.com/article/10.1007/s41114-020-00026-9
[1304.0670ver2020Jan]

LIGO-Virgo-KAGRA network for hunting gravitational waves

Contents

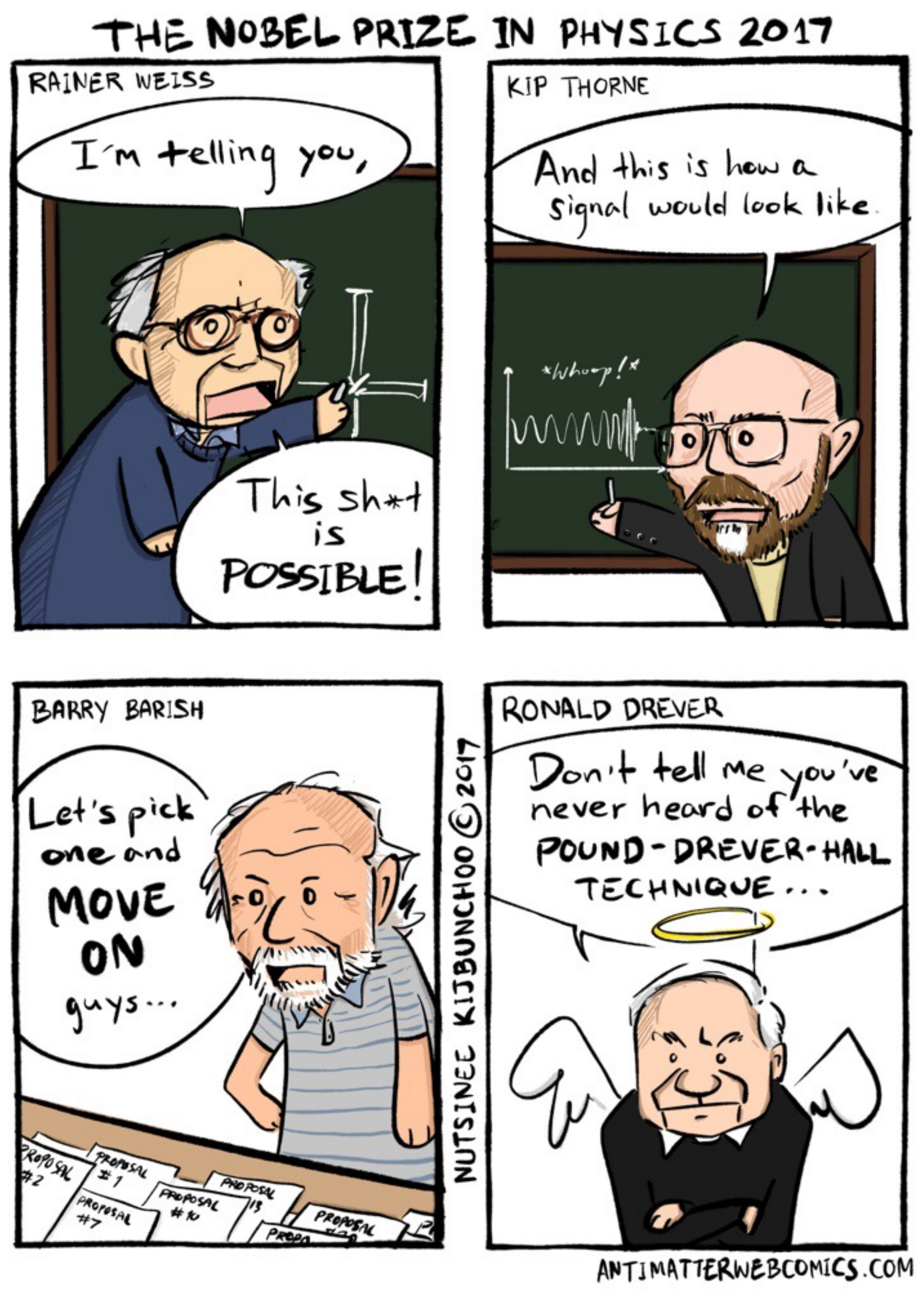

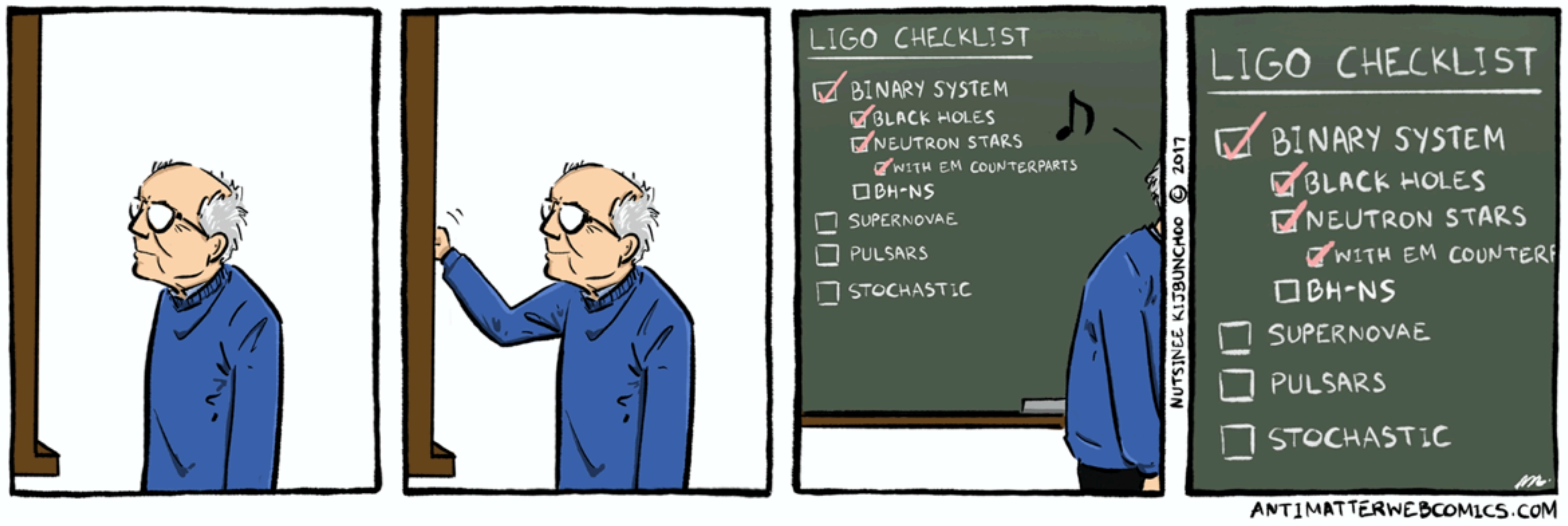

https://antimatterwebcomics.com/comic/physics-nobel-prize-2017/
https://antimatterwebcomics.com/comic/gw170817/

Observation Period

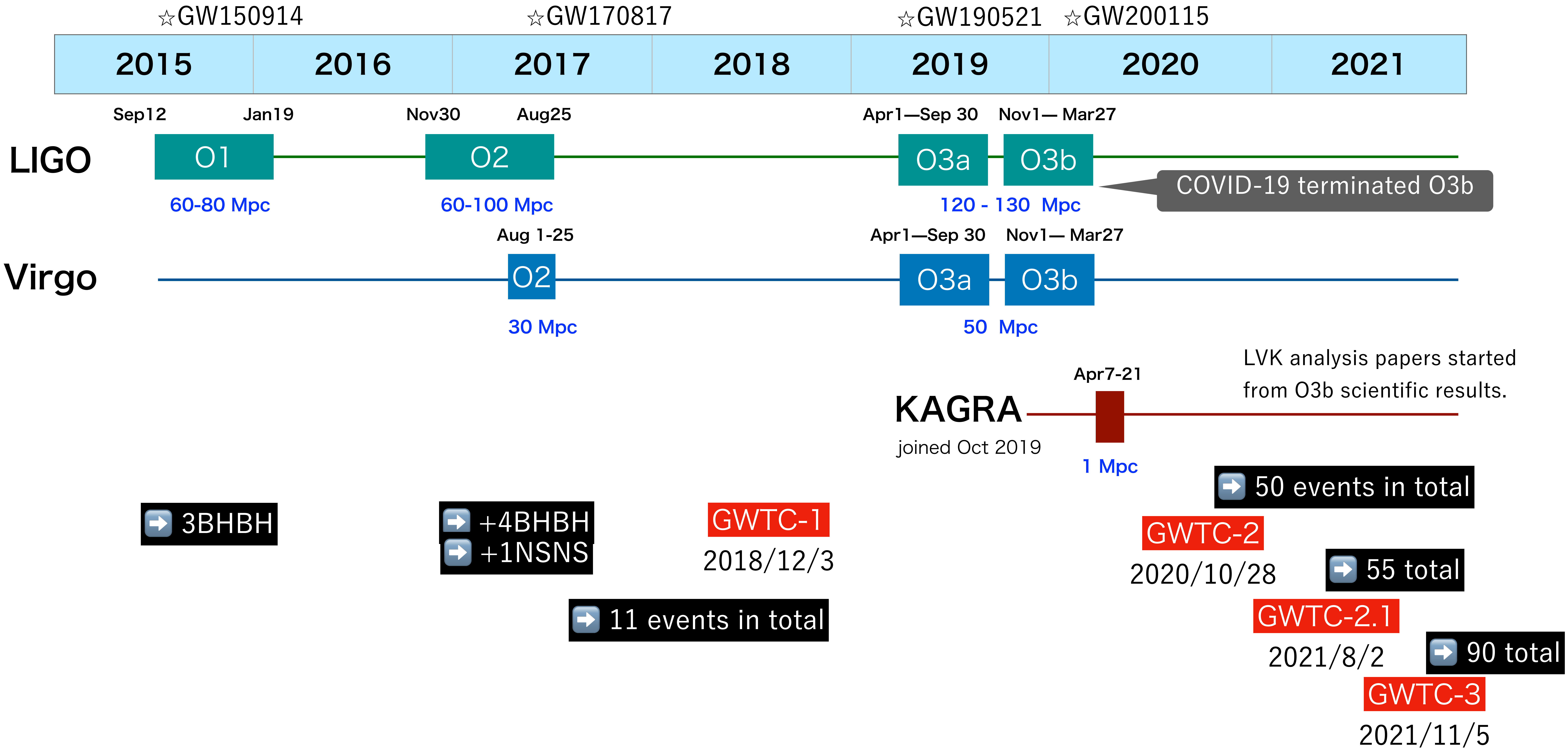

Observation Period

2015	2016	2017	2018	2019	2020	2021

LIGO

- O1: Sep12 – Jan19, 60-80 Mpc
- O2: Nov30 – Aug25, 60-100 Mpc
- O3a: Apr1—Sep 30; O3b: Nov1— Mar27, 120 - 130 Mpc

COVID-19 terminated O3b

Virgo

- O2: Aug 1-25, 30 Mpc
- O3a: Apr1—Sep 30; O3b: Nov1— Mar27, 50 Mpc

KAGRA

joined Oct 2019

Apr7-21, 1 Mpc

LVK analysis papers started from O3b scientific results.

GWTC-2 2020/10/28 ➡️ 50 events in total

GWTC-2.1 2021/8/2 ➡️ 55 total

GWTC-3 2021/11/5 ➡️ 90 total

Public Alert started from O3a

https://gracedb.ligo.org

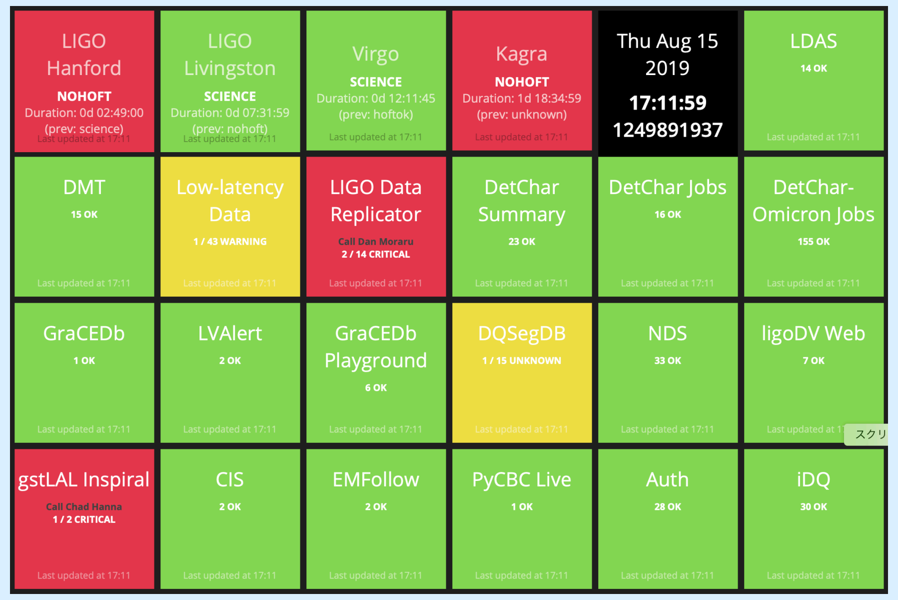

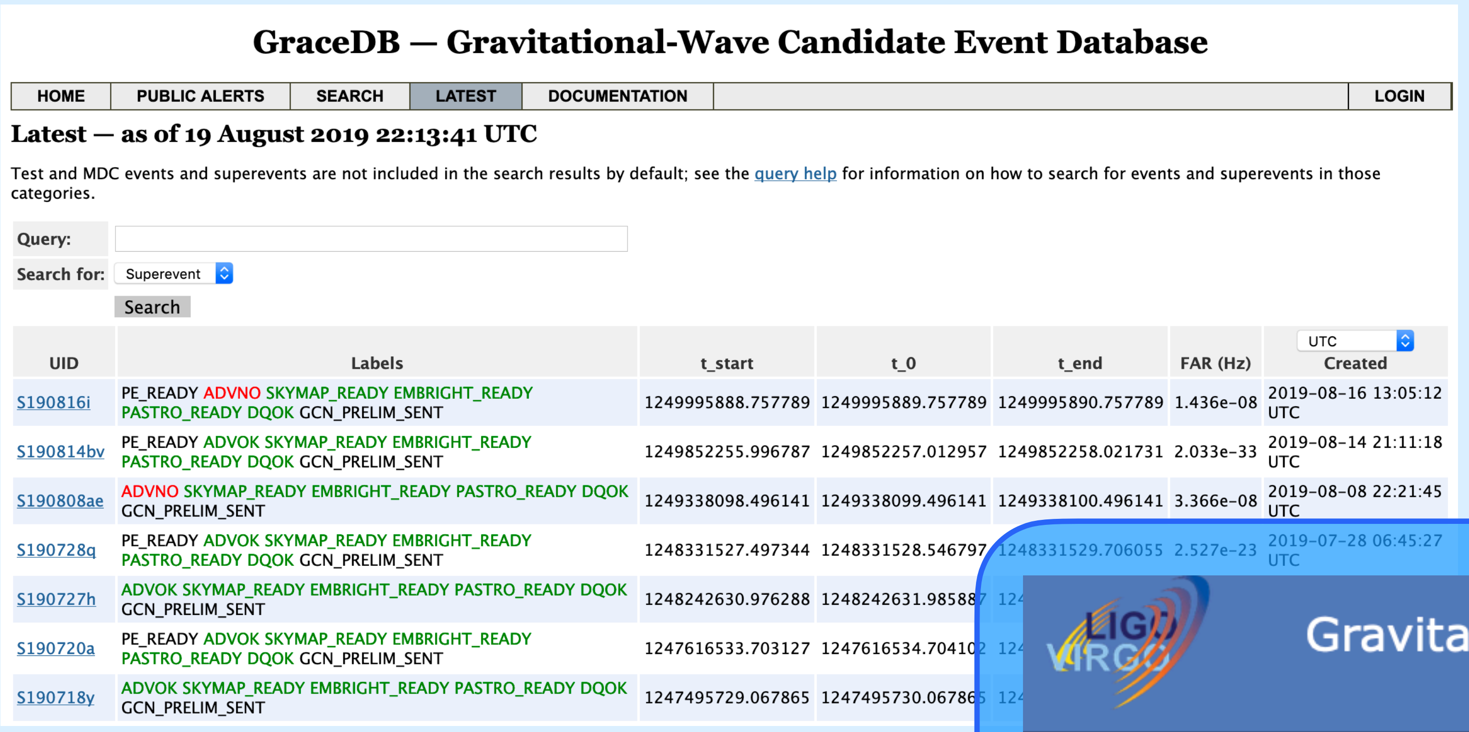

https://monitor.ligo.org/gwstatus

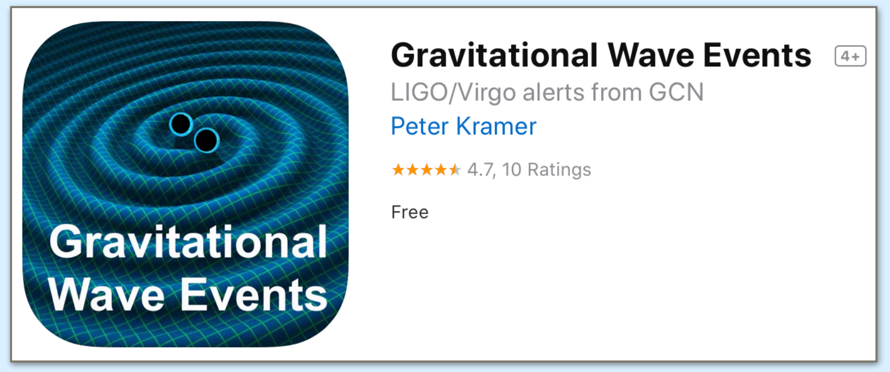

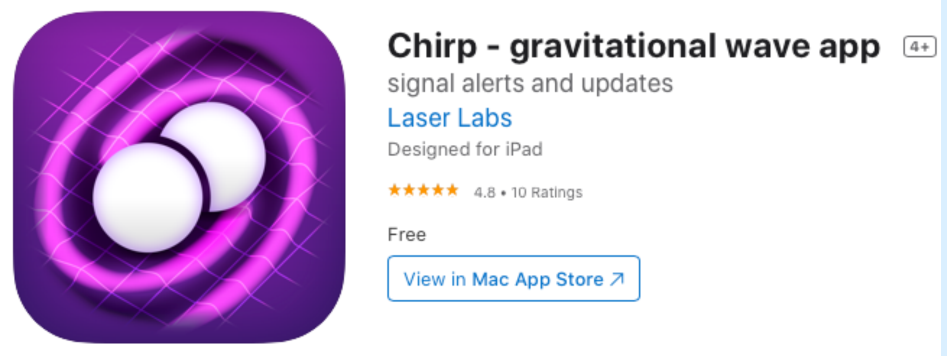

https://www.gw-openscience.org

O1 (2015/9/12 - 2016/1/19)

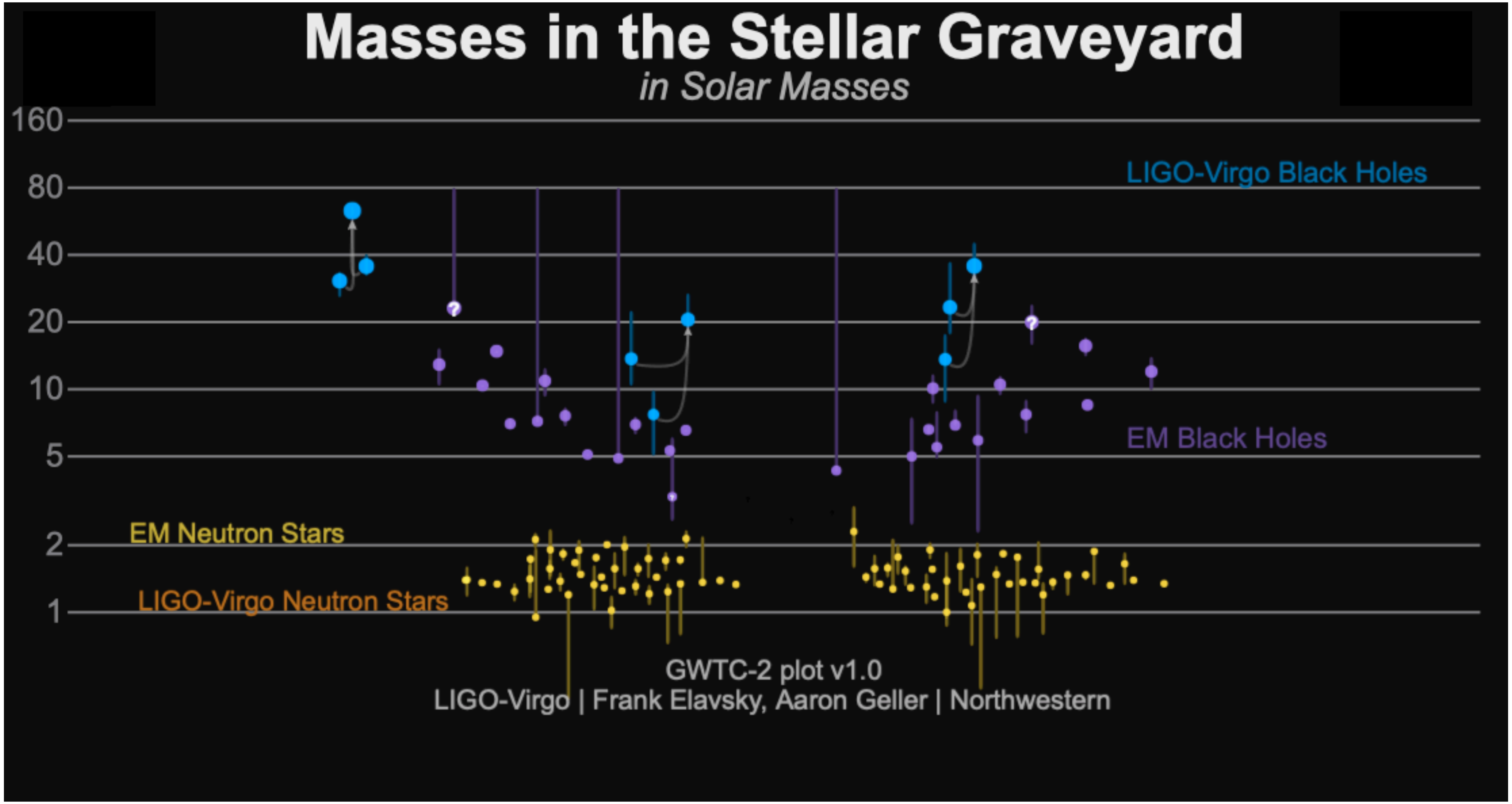

3 BHBH

GW150914: the first ever detection of gravitational waves from the merger of two black holes more than a billion light years away

https://media.ligo.northwestern.edu/gallery/mass-plot

GW transient catalog

O2 (2016/11/30 - 2017/8/25)   After O2 : GWTC1 (2018/12/3 released)

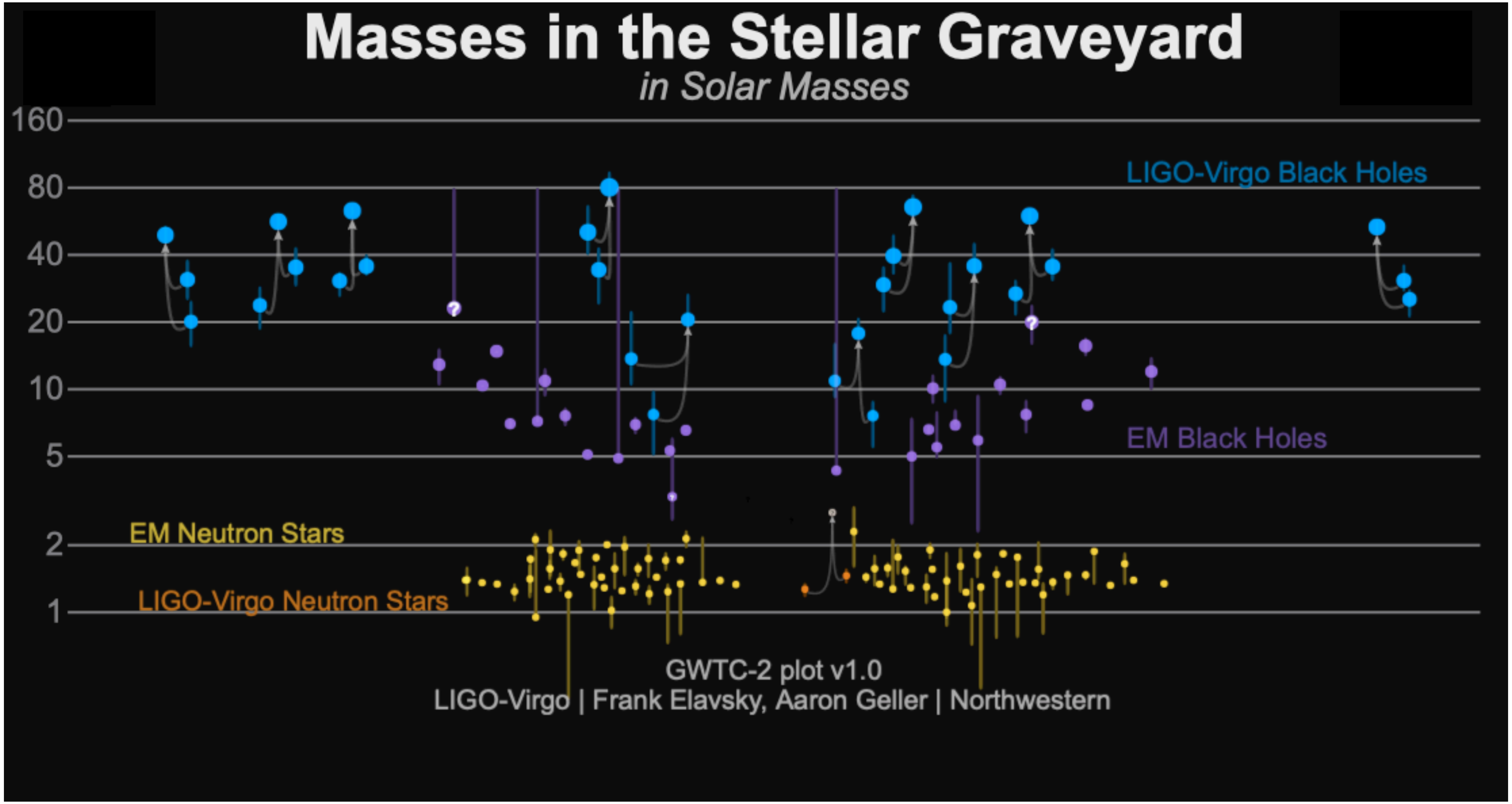

10 BHBH
1 NSNS

- GW170814: the first GW signal measured by the three-detector network, also from a binary black hole (BBH) merger;
- GW170817: the first GW signal measured from a binary neutron star (BNS) merger — and also the first event observed in light, by dozens of telescopes across the entire electromagnetic spectrum.

https://media.ligo.northwestern.edu/gallery/mass-plot

GW transient catalog

O3a (2019/4/1 - 2019/9/30) After O3a : **GWTC2** (2020/10/28 released)

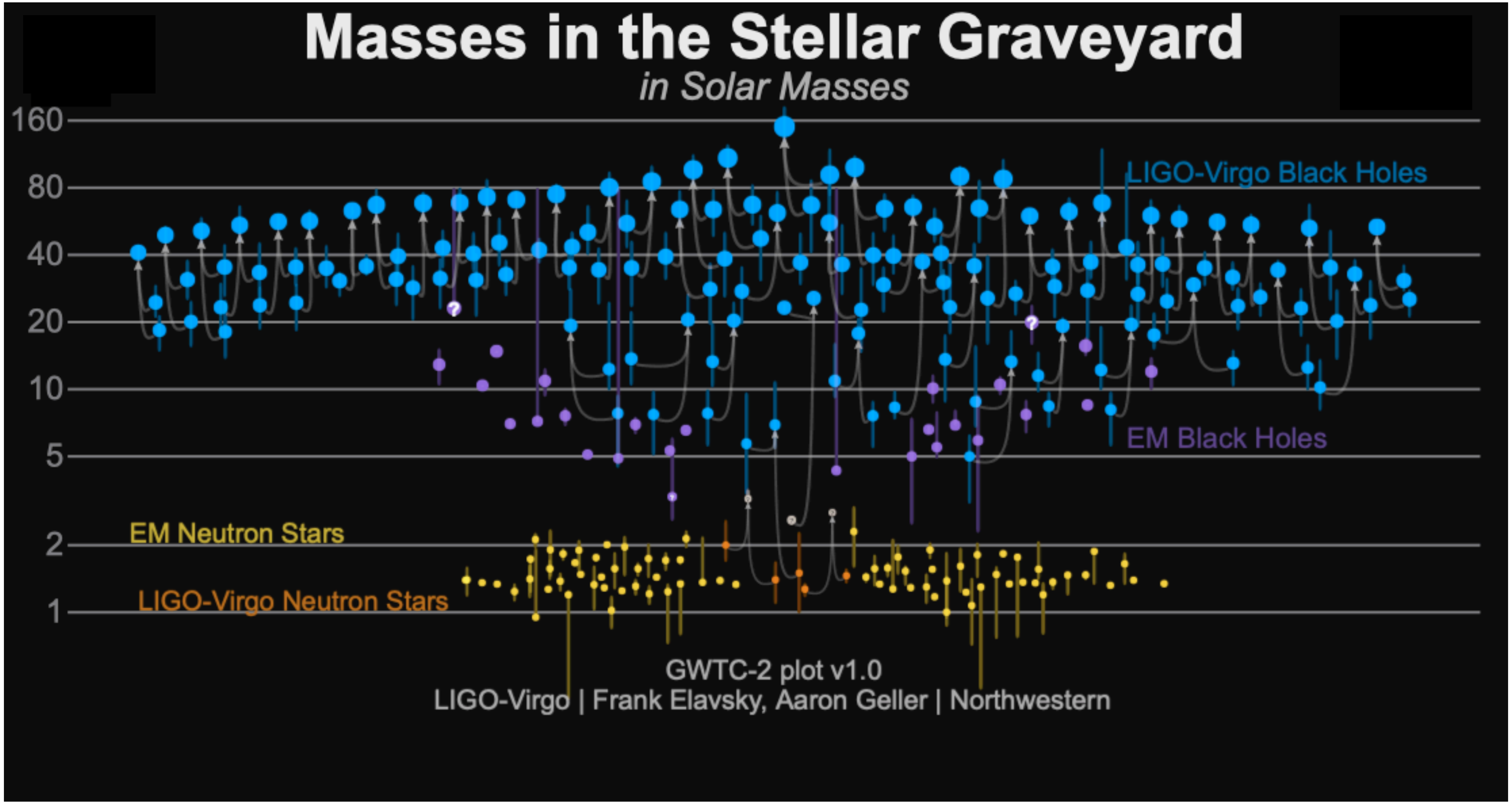

46 BHBH
2 NSNS
2 BH+?

- GW190412: the first BBH with definitively asymmetric component masses, which also shows evidence for higher harmonics
- GW190425: the second gravitational-wave event consistent with a BNS, following GW170817
- GW190426_152155: a low-mass event consistent with either an NSBH or BBH
- GW190514_065416: a BBH with the smallest effective aligned spin of all O3a events
- GW190517_055101: a BBH with the largest effective aligned spin of all O3a events
- GW190521: a BBH with total mass over 150 times the mass of the Sun
- GW190814: a highly asymmetric system of ambiguous nature, corresponding to the merger of a 23 solar mass black hole with a 2.6 solar mass compact object, making the latter either the lightest black hole or heaviest neutron star observed in a compact binary
- GW190924_021846: likely the lowest-mass BBH, with both black holes exceeding 3 solar masses

GW transient catalog

O3b (2019/11/1 - 2020/3/27) After O3b : **GWTC-3** (2021/11/7 released)

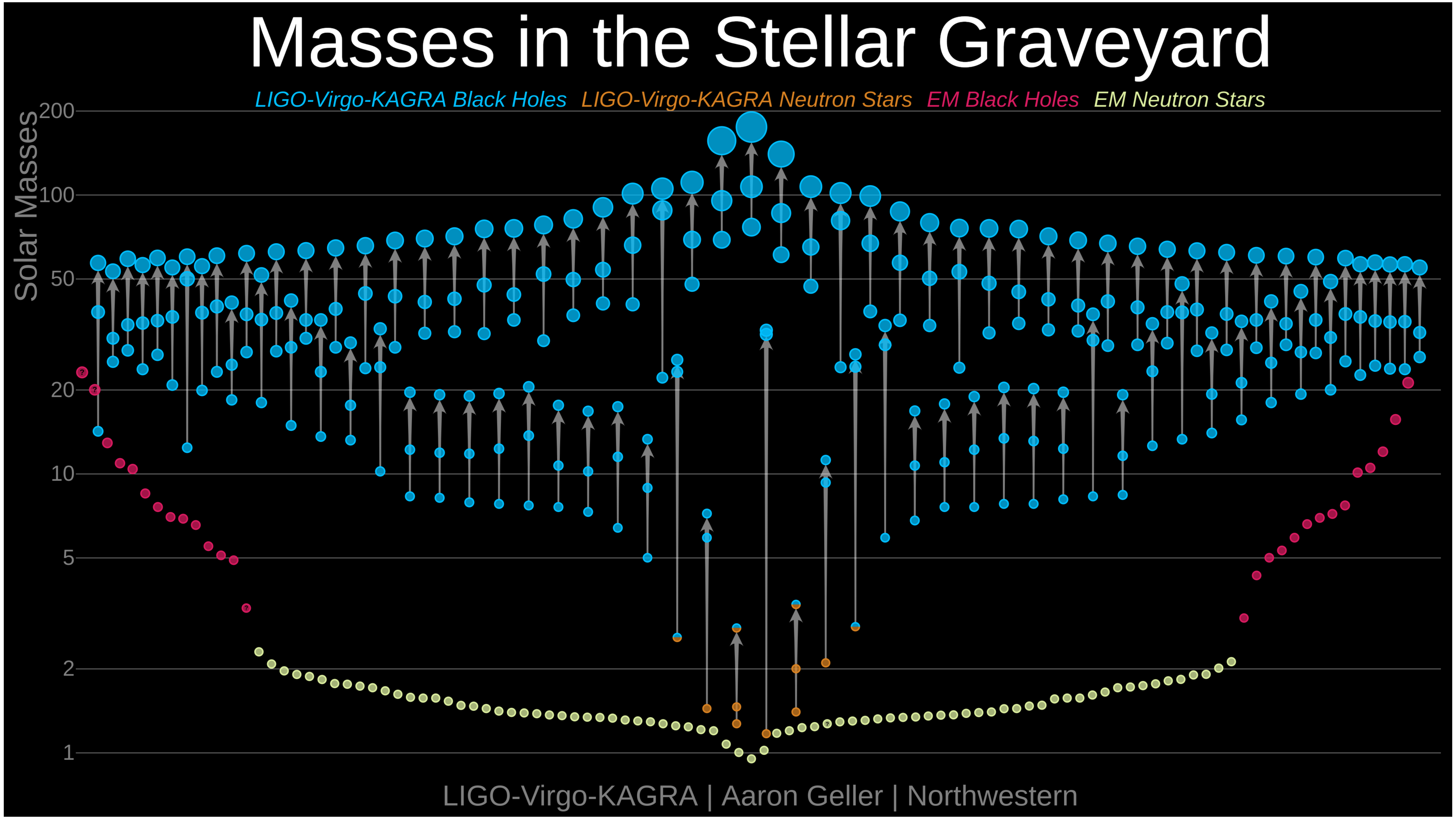

https://media.ligo.northwestern.edu/gallery/mass-plot

GW transient catalog

O3b (2020/11/1 - 2021/3/27) **After O3b : GWTC-3 (2021/11/7 released)**

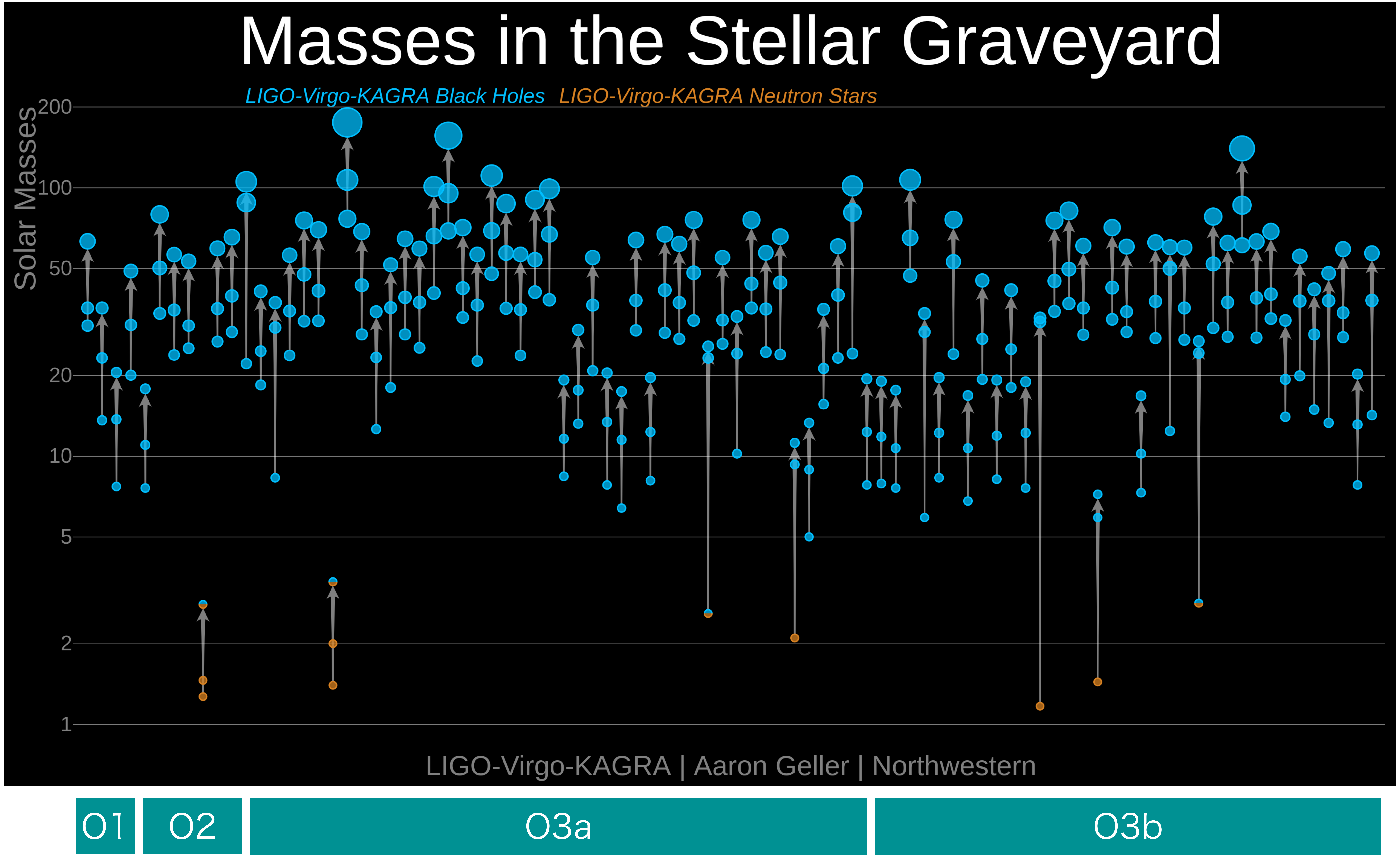

BHs

unknowns
(2.5-5M)

NSs

https://media.ligo.northwestern.edu/gallery/mass-plot

of Detections

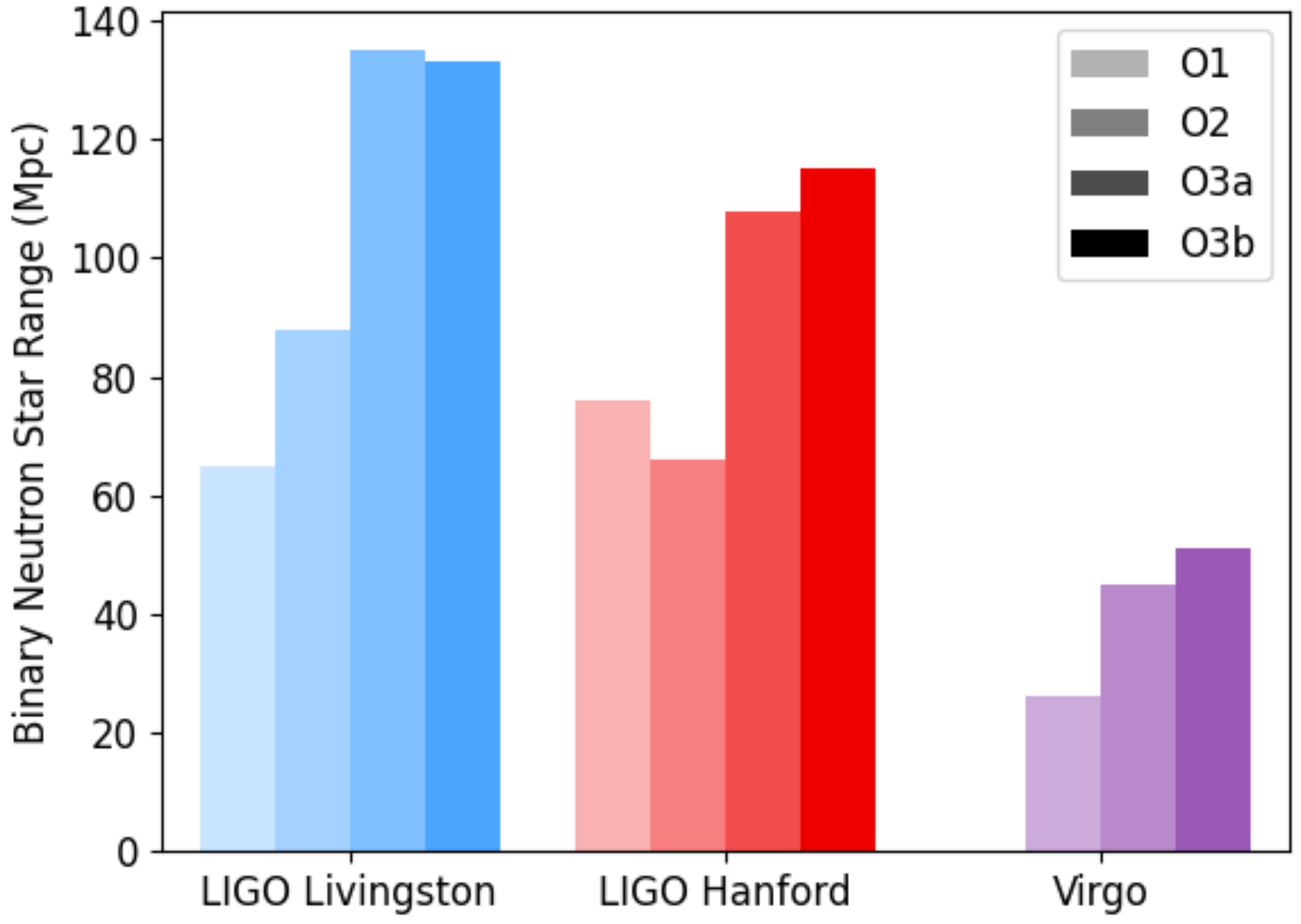

Event Rate is consistent with O3a/O3b

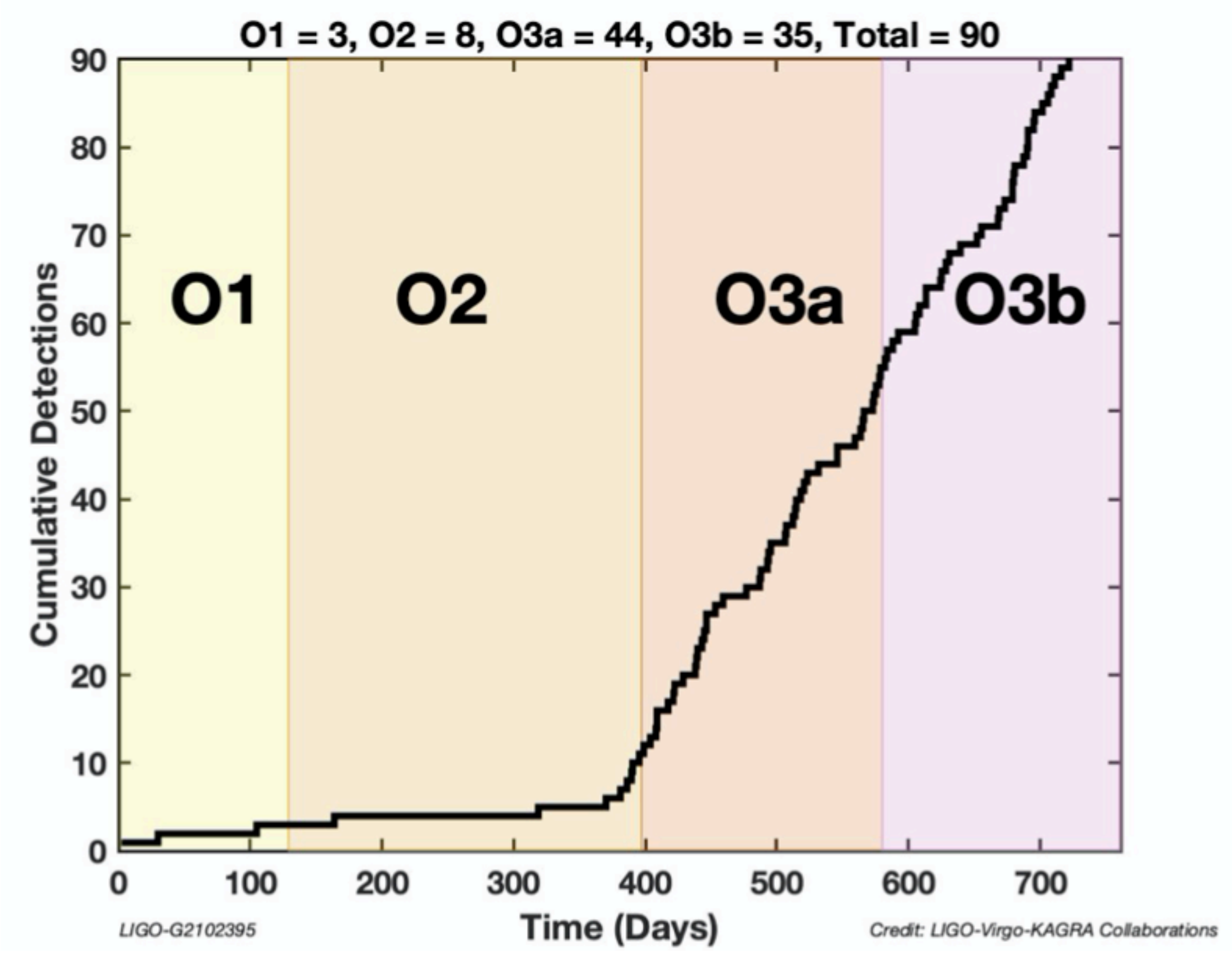

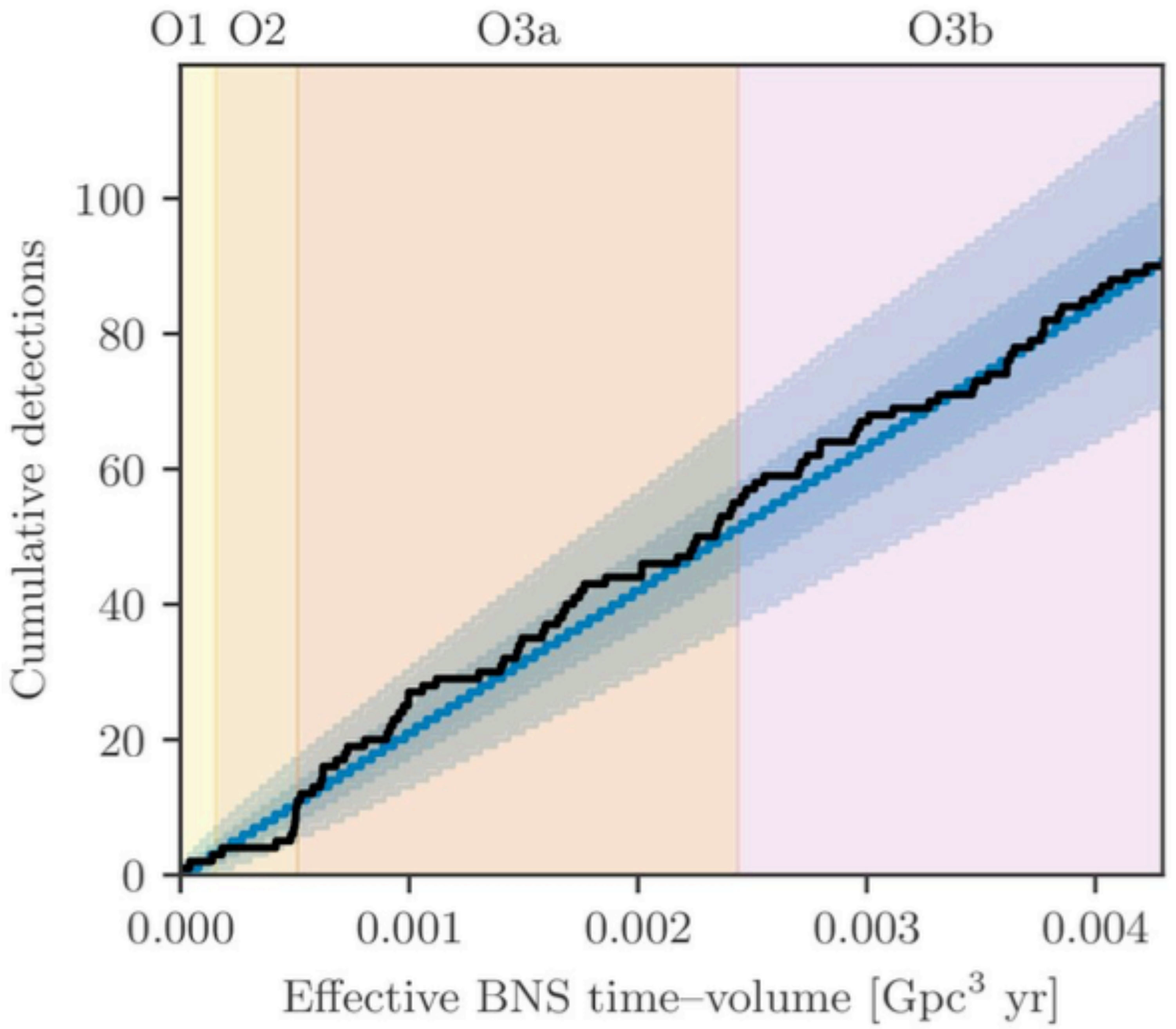

It’s hard to publish a review of GW Astronomy

"Rika Nenpyo 2022" (Annual Scientific Databook, Ed. by NAOJ, Maruzen Publishing Co.) newly includes data pages of gravitational waves, prepared by Takahiro Tanaka and HS.
The deadline of the draft was July this year, so the contents are of GWTC2.

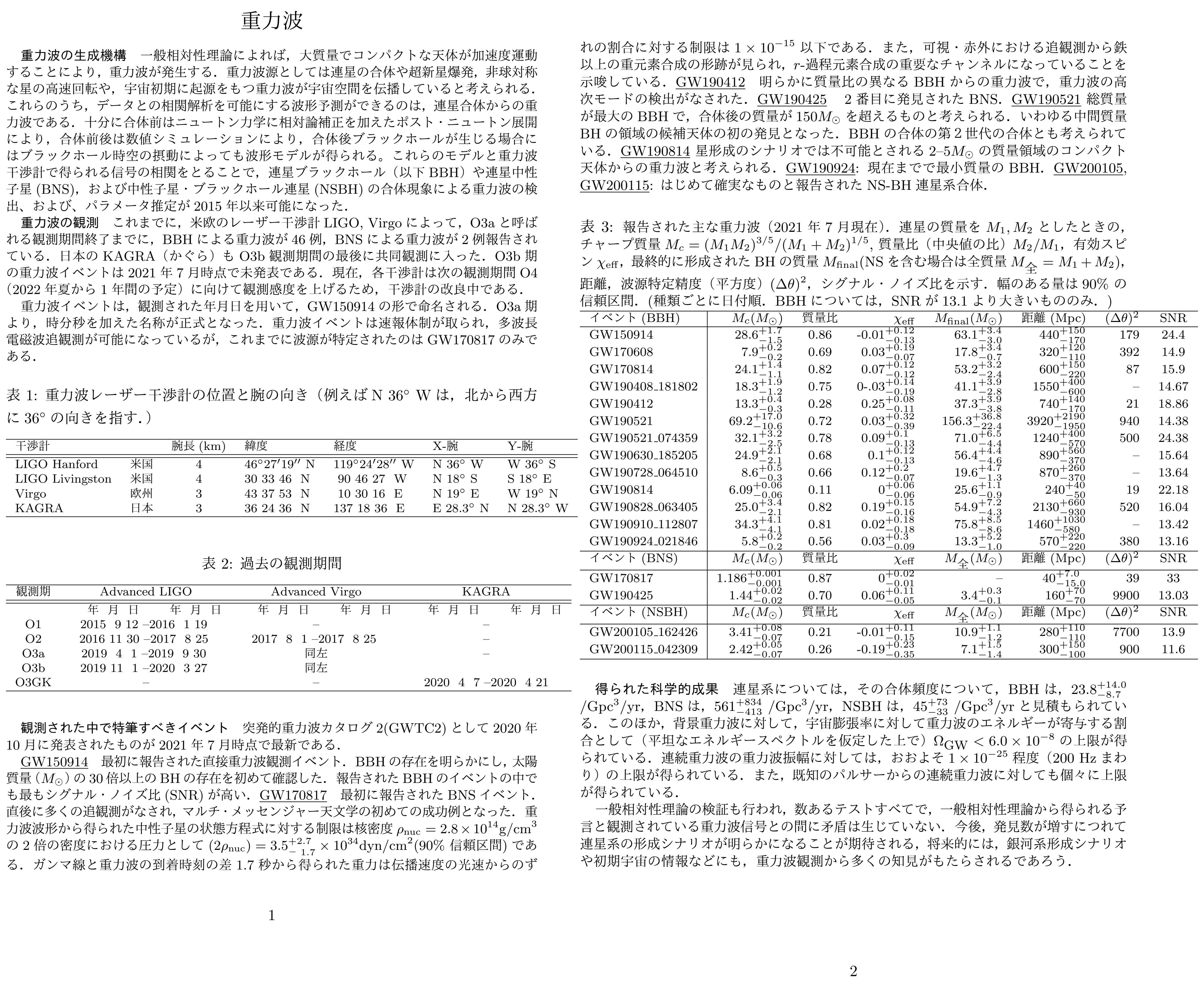

重力波

重力波の生成機構　一般相対性理論によれば，大質量でコンパクトな天体が加速度運動することにより，重力波が発生する．重力波源としては連星の合体や超新星爆発，非球対称な星の高速回転や，宇宙初期に起源をもつ重力波が宇宙空間を伝播していると考えられる．これらのうち，データとの相関解析を可能にする波形予測ができるのは，連星合体からの重力波である．十分に合体前はニュートン力学に相対論補正を加えたポスト・ニュートン展開により，合体前後は数値シミュレーションにより，合体後ブラックホールが生じる場合にはブラックホール時空の摂動によっても波形モデルが得られる。これらのモデルと重力波干渉計で得られる信号の相関をとることで，連星ブラックホール（以下 BBH）や連星中性子星 (BNS)，および中性子星・ブラックホール連星 (NSBH) の合体現象による重力波の検出、および、パラメータ推定が 2015 年以来可能になった．

重力波の観測　これまでに，米欧のレーザー干渉計 LIGO, Virgo によって，O3a と呼ばれる観測期間終了までに，BBH による重力波が 46 例，BNS による重力波が 2 例報告されている．日本の KAGRA（かぐら）も O3b 観測期間の最後に共同観測に入った．O3b 期の重力波イベントは 2021 年 7 月時点で未発表である．現在，各干渉計は次の観測期間 O4（2022 年夏から 1 年間の予定）に向けて観測感度を上げるため，干渉計の改良中である．

重力波イベントは，観測された年月日を用いて，GW150914 の形で命名される．O3a 期より，時分秒を加えた名称が正式となった．重力波イベントは速報体制が取られ，多波長電磁波追観測が可能になっているが，これまでに波源が特定されたのは GW170817 のみである．

表 1: 重力波レーザー干渉計の位置と腕の向き（例えば N 36° W は，北から西方に 36° の向きを指す．）

干渉計		腕長 (km)	緯度	経度	X-腕	Y-腕
LIGO Hanford	米国	4	46°27′19″ N	119°24′28″ W	N 36° W	W 36° S
LIGO Livingston	米国	4	30 33 46 N	90 46 27 W	N 18° S	S 18° E
Virgo	欧州	3	43 37 53 N	10 30 16 E	N 19° E	W 19° N
KAGRA	日本	3	36 24 36 N	137 18 36 E	E 28.3° N	N 28.3° W

表 2: 過去の観測期間

観測期	Advanced LIGO	Advanced Virgo	KAGRA
	年 月 日 年 月 日	年 月 日 年 月 日	年 月 日 年 月 日
O1	2015 9 12 –2016 1 19	–	–
O2	2016 11 30 –2017 8 25	2017 8 1 –2017 8 25	–
O3a	2019 4 1 –2019 9 30	同左	–
O3b	2019 11 1 –2020 3 27	同左	
O3GK	–	–	2020 4 7 –2020 4 21

観測された中で特筆すべきイベント　突発的重力波カタログ 2(GWTC2) として 2020 年 10 月に発表されたものが 2021 年 7 月時点で最新である．

GW150914　最初に報告された直接重力波観測イベント．BBH の存在を明らかにし，太陽質量（$M_\odot$）の 30 倍以上の BH の存在を初めて確認した．報告された BBH のイベントの中でも最もシグナル・ノイズ比 (SNR) が高い．GW170817　最初に報告された BNS イベント．直後に多くの追観測がなされ，マルチ・メッセンジャー天文学の初めての成功例となった．重力波波形から得られた中性子星の状態方程式に対する制限は核密度 $\rho_{\rm nuc} = 2.8 \times 10^{14}{\rm g/cm^3}$ の 2 倍の密度における圧力として $(2\rho_{\rm nuc}) = 3.5^{+2.7}_{-1.7} \times 10^{34}{\rm dyn/cm^2}$(90% 信頼区間) である．ガンマ線と重力波の到着時刻の差 1.7 秒から得られた重力は伝播速度の光速からのずれの割合に対する制限は 1×10^{-15} 以下である．また，可視・赤外における追観測から鉄以上の重元素合成の形跡が見られ，r-過程元素合成の重要なチャンネルになっていることを示唆している．GW190412　明らかに質量比の異なる BBH からの重力波で，重力波の高次モードの検出がなされた．GW190425　2 番目に発見された BNS．GW190521 総質量が最大の BBH で，合体後の質量が $150M_\odot$ を超えるものと考えられる．いわゆる中間質量 BH の領域の候補天体の初の発見となった．BBH の合体の第 2 世代の合体とも考えられている．GW190814 星形成のシナリオでは不可能とされる 2–5$M_\odot$ の質量領域のコンパクト天体からの重力波と考えられる．GW190924: 現在までで最小質量の BBH．GW200105, GW200115: はじめて確実なものと報告された NS-BH 連星系合体．

1

表 3: 報告された主な重力波（2021 年 7 月現在）．連星の質量を M_1, M_2 としたときの，チャープ質量 $M_c = (M_1M_2)^{3/5}/(M_1+M_2)^{1/5}$, 質量比（中央値の比）$M_2/M_1$，有効スピン $\chi_{\rm eff}$，最終的に形成された BH の質量 $M_{\rm final}$(NS を含む場合は全質量 $M_{全} = M_1 + M_2$)，距離，波源特定精度（平方度）$(\Delta\theta)^2$，シグナル・ノイズ比を示す．幅のある量は 90% の信頼区間．(種類ごとに日付順．BBH については，SNR が 13.1 より大きいもののみ．)

イベント (BBH)	$M_c(M_\odot)$	質量比	$\chi_{\rm eff}$	$M_{\rm final}(M_\odot)$	距離 (Mpc)	$(\Delta\theta)^2$	SNR
GW150914	$28.6^{+1.7}_{-1.5}$	0.86	$-0.01^{+0.12}_{-0.13}$	$63.1^{+3.4}_{-3.0}$	440^{+150}_{-170}	179	24.4
GW170608	$7.9^{+0.2}_{-0.2}$	0.69	$0.03^{+0.19}_{-0.07}$	$17.8^{+3.4}_{-0.7}$	320^{+120}_{-110}	392	14.9
GW170814	$24.1^{+1.4}_{-1.1}$	0.82	$0.07^{+0.12}_{-0.12}$	$53.2^{+3.2}_{-2.4}$	600^{+150}_{-220}	87	15.9
GW190408_181802	$18.3^{+1.9}_{-1.2}$	0.75	$0\text{-}.03^{+0.14}_{-0.19}$	$41.1^{+3.9}_{-2.8}$	1550^{+400}_{-600}	–	14.67
GW190412	$13.3^{+0.4}_{-0.3}$	0.28	$0.25^{+0.08}_{-0.11}$	$37.3^{+3.9}_{-3.8}$	740^{+140}_{-170}	21	18.86
GW190521	$69.2^{+17.0}_{-10.6}$	0.72	$0.03^{+0.32}_{-0.39}$	$156.3^{+36.8}_{-22.4}$	3920^{+2190}_{-1950}	940	14.38
GW190521_074359	$32.1^{+3.2}_{-2.5}$	0.78	$0.09^{+0.1}_{-0.13}$	$71.0^{+6.5}_{-4.4}$	1240^{+400}_{-570}	500	24.38
GW190630_185205	$24.9^{+2.1}_{-2.1}$	0.68	$0.1^{+0.12}_{-0.13}$	$56.4^{+4.4}_{-4.6}$	890^{+560}_{-370}	–	15.64
GW190728_064510	$8.6^{+0.5}_{-0.3}$	0.66	$0.12^{+0.2}_{-0.07}$	$19.6^{+4.7}_{-1.3}$	870^{+260}_{-370}	–	13.64
GW190814	$6.09^{+0.06}_{-0.06}$	0.11	$0^{+0.06}_{-0.06}$	$25.6^{+1.1}_{-0.9}$	240^{+40}_{-50}	19	22.18
GW190828_063405	$25.0^{+3.4}_{-2.1}$	0.82	$0.19^{+0.15}_{-0.16}$	$54.9^{+7.2}_{-4.3}$	2130^{+660}_{-930}	520	16.04
GW190910_112807	$34.3^{+4.1}_{-4.1}$	0.81	$0.02^{+0.18}_{-0.18}$	$75.8^{+8.5}_{-8.6}$	1460^{+1030}_{-580}	–	13.42
GW190924_021846	$5.8^{+0.2}_{-0.2}$	0.56	$0.03^{+0.3}_{-0.09}$	$13.3^{+5.2}_{-1.0}$	570^{+220}_{-220}	380	13.16
イベント (BNS)	$M_c(M_\odot)$	質量比	$\chi_{\rm eff}$	$M_{全}(M_\odot)$	距離 (Mpc)	$(\Delta\theta)^2$	SNR
GW170817	$1.186^{+0.001}_{-0.001}$	0.87	$0^{+0.02}_{-0.01}$	–	$40^{+7.0}_{-15.0}$	39	33
GW190425	$1.44^{+0.02}_{-0.02}$	0.70	$0.06^{+0.11}_{-0.05}$	$3.4^{+0.3}_{-0.1}$	160^{+70}_{-70}	9900	13.03
イベント (NSBH)	$M_c(M_\odot)$	質量比	$\chi_{\rm eff}$	$M_{全}(M_\odot)$	距離 (Mpc)	$(\Delta\theta)^2$	SNR
GW200105_162426	$3.41^{+0.08}_{-0.07}$	0.21	$-0.01^{+0.11}_{-0.15}$	$10.9^{+1.1}_{-1.2}$	280^{+110}_{-110}	7700	13.9
GW200115_042309	$2.42^{+0.05}_{-0.07}$	0.26	$-0.19^{+0.23}_{-0.35}$	$7.1^{+1.5}_{-1.4}$	300^{+150}_{-100}	900	11.6

得られた科学的成果　連星系については，その合体頻度について，BBH は，$23.8^{+14.0}_{-8.7}$ /Gpc^3/yr，BNS は，561^{+834}_{-413} /Gpc^3/yr，NSBH は，45^{+73}_{-33} /Gpc^3/yr と見積もられている．このほか，背景重力波に対して，宇宙膨張率に対して重力波のエネルギーが寄与する割合として（平坦なエネルギースペクトルを仮定した上で）$\Omega_{\rm GW} < 6.0 \times 10^{-8}$ の上限が得られている．連続重力波の重力波振幅に対しては，おおよそ 1×10^{-25} 程度（200 Hz まわり）の上限が得られている．また，既知のパルサーからの連続重力波に対しても個々に上限が得られている．

一般相対性理論の検証も行われ，数あるテストすべてで，一般相対性理論から得られる予言と観測されている重力波信号との間に矛盾は生じていない．今後，発見数が増すにつれて連星系の形成シナリオが明らかになることが期待される，将来的には，銀河系形成シナリオや初期宇宙の情報などにも，重力波観測から多くの知見がもたらされるであろう．

2

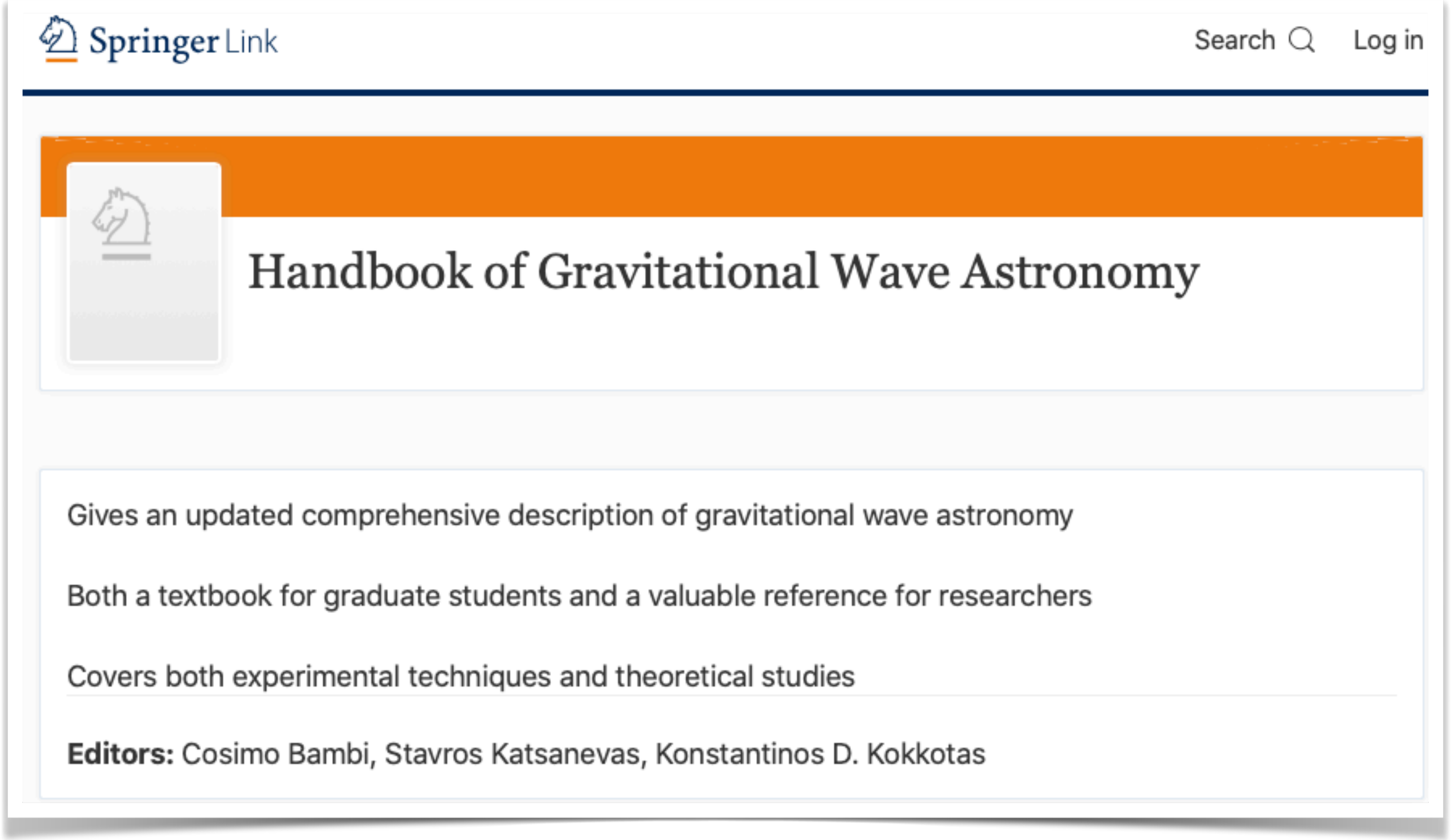

Springer Handbook of GW Astronomy will be ready in 2022.
The deadline of the draft was May this year, so the contents are of GWTC2.

➡️ 50 events in total

GWTC-2

2020/10/28

➡️ 55 total

GWTC-2.1

2021/8/2

➡️ 90 total

GWTC-3

2021/11/5

GW150914　The First Detection of GW　36M+29M=62M

PRL 116, 061102 (2016)　Selected for a Viewpoint in Physics　PHYSICAL REVIEW LETTERS　week ending 12 FEBRUARY 2016

Observation of Gravitational Waves from a Binary Black Hole Merger

B. P. Abbott et al.*
(LIGO Scientific Collaboration and Virgo Collaboration)
(Received 21 January 2016; published 11 February 2016)

On September 14, 2015 at 09:50:45 UTC the two detectors of the Laser Interferometer Gravitational-Wave Observatory simultaneously observed a transient gravitational-wave signal. The signal sweeps upwards in frequency from 35 to 250 Hz with a peak gravitational-wave strain of 1.0×10^{-21}. It matches the waveform predicted by general relativity for the inspiral and merger of a pair of black holes and the ringdown of the resulting single black hole. The signal was observed with a matched-filter signal-to-noise ratio of 24 and a false alarm rate estimated to be less than 1 event per 203 000 years, equivalent to a significance greater than 5.1σ. The source lies at a luminosity distance of 410^{+160}_{-180} Mpc corresponding to a redshift $z = 0.09^{+0.03}_{-0.04}$. In the source frame, the initial black hole masses are $36^{+5}_{-4} M_\odot$ and $29^{+4}_{-4} M_\odot$, and the final black hole mass is $62^{+4}_{-4} M_\odot$, with $3.0^{+0.5}_{-0.5} M_\odot c^2$ radiated in gravitational waves. All uncertainties define 90% credible intervals. These observations demonstrate the existence of binary stellar-mass black hole systems. This is the first direct detection of gravitational waves and the first observation of a binary black hole merger.

DOI: 10.1103/PhysRevLett.116.061102

＊The First Detection of GW

＊Existence of Binary BH

＊Existence of BH at 30M

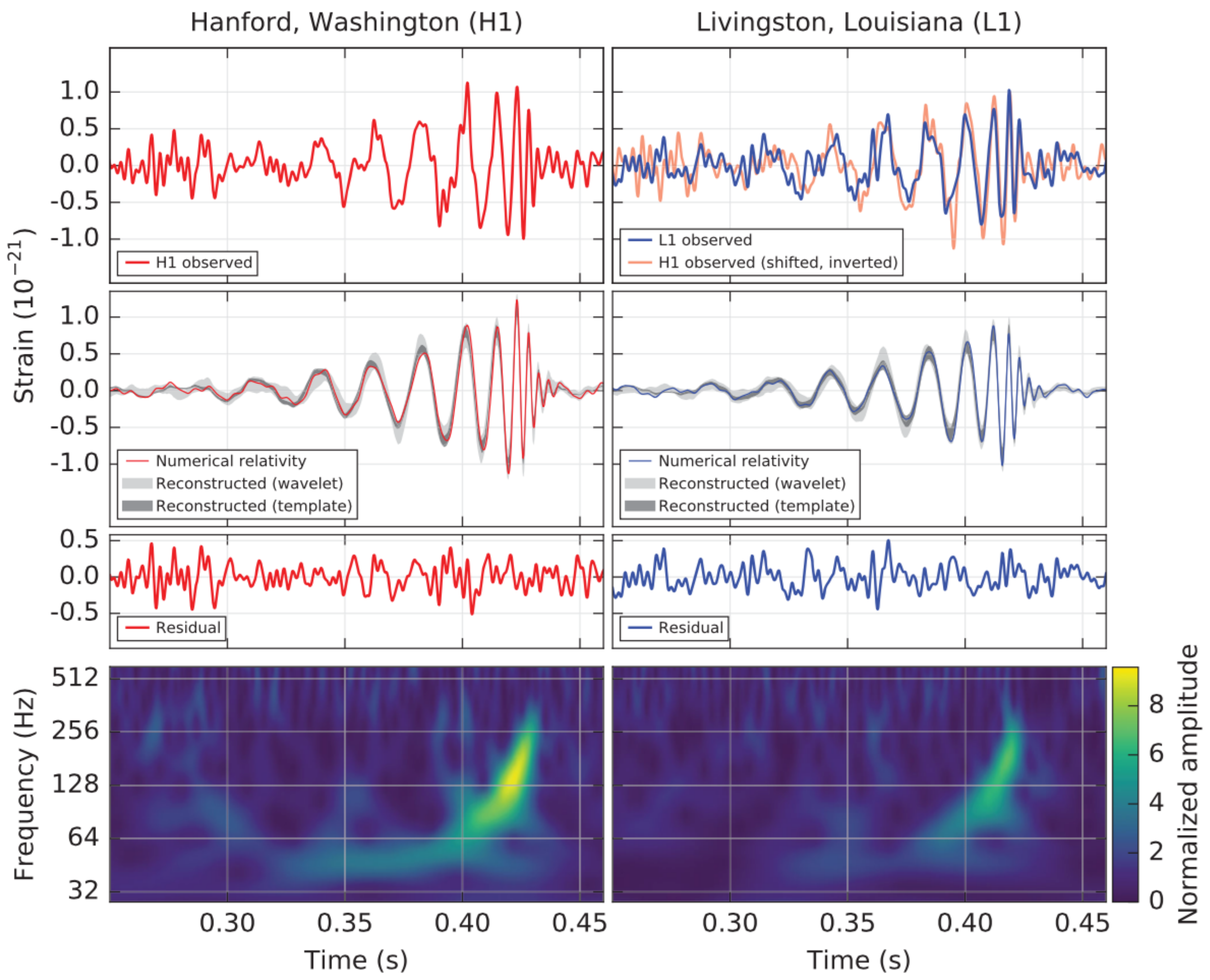

FIG. 1. The gravitational-wave event GW150914 observed by the LIGO Hanford (H1, left column panels) and Livingston (L1, right column panels) detectors. Times are shown relative to September 14, 2015 at 09:50:45 UTC. For visualization, all time series are filtered with a 35–350 Hz bandpass filter to suppress large fluctuations outside the detectors' most sensitive frequency band, and band-reject filters to remove the strong instrumental spectral lines seen in the Fig. 3 spectra. *Top row, left:* H1 strain. *Top row, right:* L1 strain. GW150914 arrived first at L1 and $6.9^{+0.5}_{-0.4}$ ms later at H1; for a visual comparison, the H1 data are also shown, shifted in time by this amount and inverted (to account for the detectors' relative orientations). *Second row:* Gravitational-wave strain projected onto each detector in the 35–350 Hz band. Solid lines show a numerical relativity waveform for a system with parameters consistent with those recovered from GW150914 [37,38] confirmed to 99.9% by an independent calculation based on [15]. Shaded areas show 90% credible regions for two independent waveform reconstructions. One (dark gray) models the signal using binary black hole template waveforms [39]. The other (light gray) does not use an astrophysical model, but instead calculates the strain signal as a linear combination of sine-Gaussian wavelets [40,41]. These reconstructions have a 94% overlap, as shown in [39]. *Third row:* Residuals after subtracting the filtered numerical relativity waveform from the filtered detector time series. *Bottom row:* A time-frequency representation [42] of the strain data, showing the signal frequency increasing over time.

GW150914: FACTSHEET

BACKGROUND IMAGES: TIME-FREQUENCY TRACE (TOP) AND TIME-SERIES (BOTTOM) IN THE TWO LIGO DETECTORS; SIMULATION OF BLACK HOLE HORIZONS (MIDDLE-TOP), BEST FIT WAVEFORM (MIDDLE-BOTTOM)

first direct detection of gravitational waves (GW) and first direct observation of a black hole binary

observed by	LIGO L1, H1
source type	black hole (BH) binary
date	14 Sept 2015
time	09:50:45 UTC
likely distance	0.75 to 1.9 Gly 230 to 570 Mpc
redshift	0.054 to 0.136
signal-to-noise ratio	24
false alarm prob.	< 1 in 5 million
false alarm rate	< 1 in 200,000 yr
Source Masses	M⊙
total mass	60 to 70
primary BH	32 to 41
secondary BH	25 to 33
remnant BH	58 to 67
mass ratio	0.6 to 1
primary BH spin	< 0.7
secondary BH spin	< 0.9
remnant BH spin	0.57 to 0.72
signal arrival time delay	arrived in L1 7 ms before H1
likely sky position	Southern Hemisphere
likely orientation	face-on/off
resolved to	~600 sq. deg.

duration from 30 Hz	~ 200 ms
# cycles from 30 Hz	~10
peak GW strain	1×10^{-21}
peak displacement of interferometers arms	±0.002 fm
frequency/wavelength at peak GW strain	150 Hz, 2000 km
peak speed of BHs	~ 0.6 c
peak GW luminosity	3.6×10^{56} erg s^{-1}
radiated GW energy	2.5-3.5 M⊙
remnant ringdown freq.	~ 250 Hz
remnant damping time	~ 4 ms
remnant size, area	180 km, 3.5×10^5 km^2
consistent with general relativity?	passes all tests performed
graviton mass bound	< 1.2×10^{-22} eV
coalescence rate of binary black holes	2 to 400 Gpc^{-3} yr^{-1}
online trigger latency	~ 3 min
# offline analysis pipelines	5
CPU hours consumed	~ 50 million (=20,000 PCs run for 100 days)
papers on Feb 11, 2016	13
# researchers	~1000, 80 institutions in 15 countries

Detector noise introduces errors in measurement. Parameter ranges correspond to 90% credible bounds.
Acronyms: L1=LIGO Livingston, H1=LIGO Hanford; Gly=giga lightyear=9.46×10^{12} km; Mpc=mega parsec=3.2 million lightyear, Gpc=10^3 Mpc, fm=femtometer=10^{-15} m, M⊙=1 solar mass=2×10^{30} kg

GW150914　The First Detection of GW　36M+29M=62M

★ Distance was determined（400±170 Mpc,　z=0.054—0.136）
but not a particular direction

★Comparing with various simulations,
binary parameters were determined.

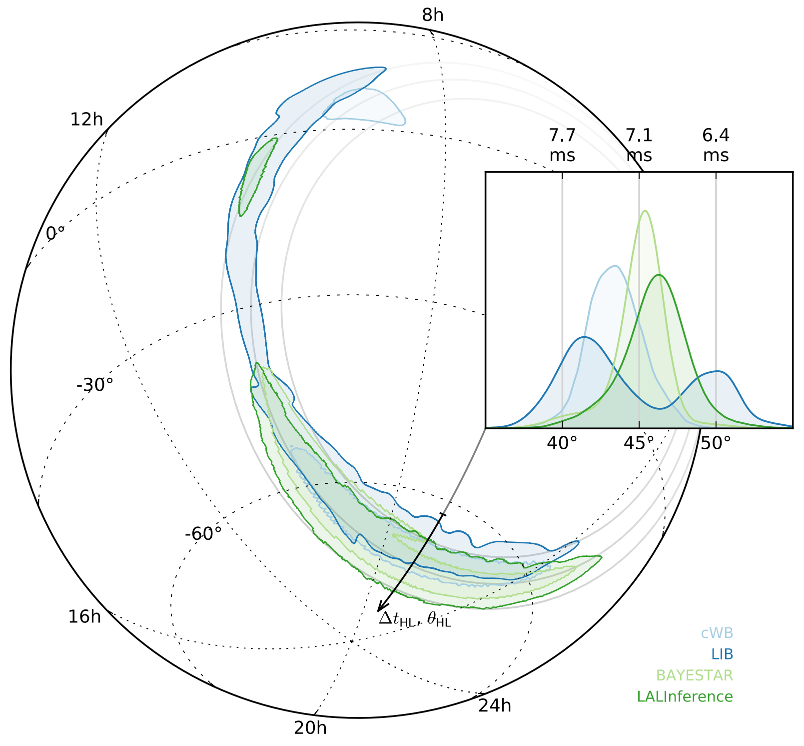

Localization and broadband follow-up of the gravitational-wave transient GW150914

This article is under preparation by the LIGO Scientific Collaboration, the Virgo collaboration, and partner observing facilities. The full version will be posted on or after February 15, 2016. It will describe the rapid detection and position reconstruction of the gravitational-wave signal an the broadband follow-up campaign by 21 teams of observers, spanning radio, optical, near-infrared, X-ray, and gamma-ray wavelengths with ground- and space-based facilities.

LIGO DCC

LIGO Document P1500227-v6

Home　Recent Changes　Topics

Localization and broadband follow-up of the gravitational-wave transient GW150914

Document #: LIGO-P1500227-v6
Document type: P - Publications
Login to modify

Abstract: This article is under preparation by the LIGO Scientific Collaboration, the Virgo collaboration, and partner observing facilities. The full version will be posted on or after February 15, 2016. It will describe the rapid detection and position reconstruction of the gravitational-wave signal and the broadband follow-up campaign by 21 teams of observers, spanning radio, optical, near-infrared, X-ray, and gamma-ray wavelengths with ground- and space-based facilities.

Other Versions:

Files in Document:

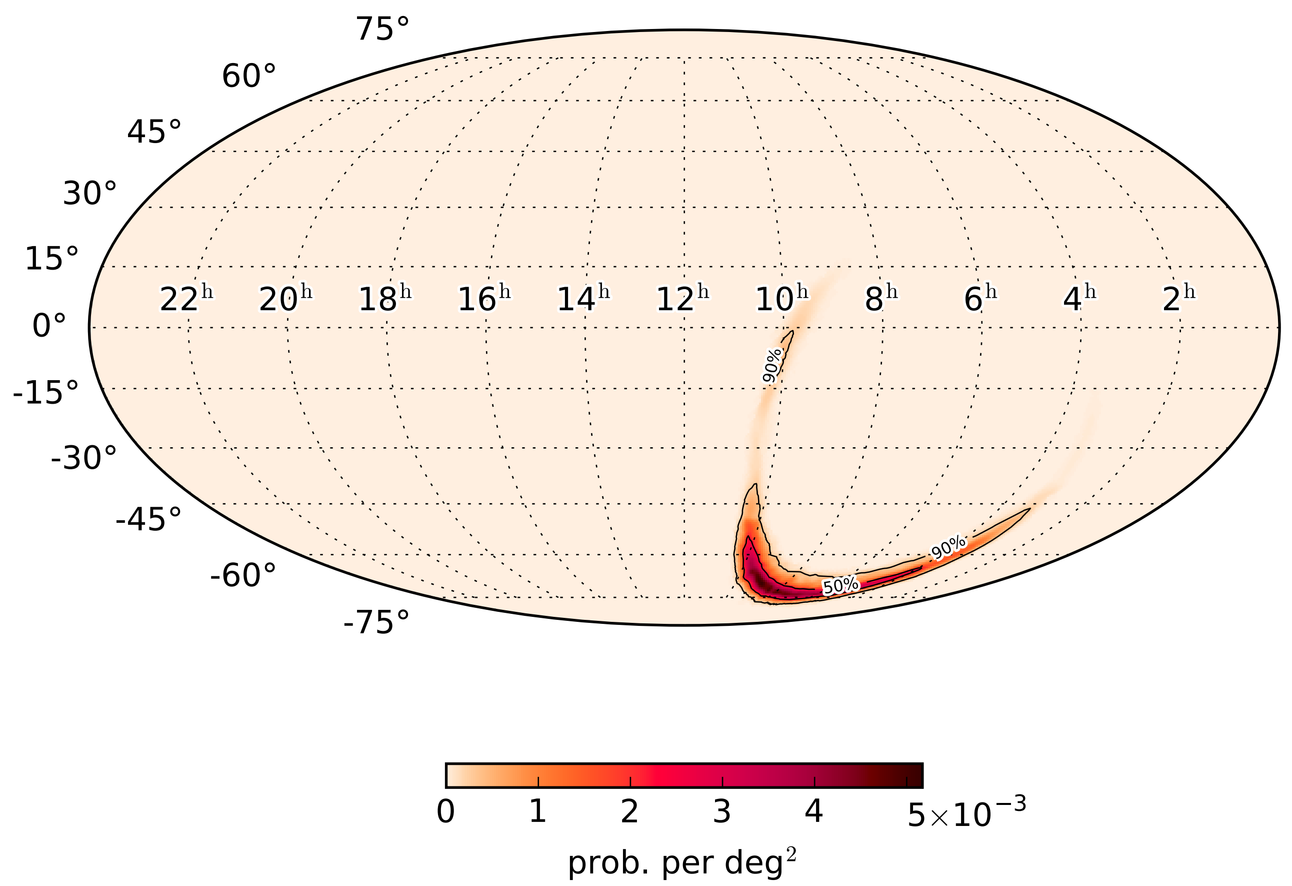

LALInference sky map (GCN 18858) Mollweide projection plot

600 squared degree

arXiv:1606.01262

B. P. ABBOTT *et al.*　　PHYSICAL REVIEW D **94,** 064035 (2016)

APPENDIX B: SIMULATION RANKINGS

In this appendix, we enumerate the simulations used in this work, ordered by one measure of their similarity with the data ($\ln L$, in Table III). For nonprecessing binaries, Fig. 6 provides a visual illustration of some trends in $\ln L$ versus mass ratio and the two component spins.

TABLE III. *Peak Marginalized* $\ln L$ *I: Consistency between simulations*: Peak value of the marginalized log likelihood $\ln L$ [Eq. (7)] evaluated using a lower frequency $f_{\rm low} = 30$ Hz and all modes with $l \leq 2$; the simulation key, described in Table II [an asterisk (*) denotes a new simulation motivated by GW150914, and a (+) denotes one of the simulations reported in LVC-detect [1]]; the *initial* spins of the simulation (using – to denote zero, to enhance readability); the initial $\chi_{\rm eff}$; the total (redshifted) mass of the best fit; and the starting frequency (in Hz) of the best fit. Though omitting information accessible to the longest simulations, this choice of low-frequency cutoff eliminates systematic biases associated with simulation duration, which differs across our archive, as seen by the last column.

$\ln L$	Key	q	$\chi_{1,x}$	$\chi_{1,y}$	$\chi_{1,z}$	$\chi_{2,x}$	$\chi_{2,y}$	$\chi_{2,z}$	$\chi_{\rm eff}$	$M_z/M_\odot$	$f_{\rm start}$(Hz)
272.2	SXS:BBH:0310(*)	1.221	⋯	⋯	⋯	⋯	⋯	⋯	0.00	73.0	15.1
272.1	D12_q1.00_a-0.25_0.25_n100(*)	1.0	⋯	⋯	0.250	⋯	⋯	−0.250	−0.00	73.2	20.5
272.1	SXS:BBH:0002[S]	1.0	⋯	⋯	⋯	⋯	⋯	⋯	0.00	73.2	10.0
271.8	D11_q0.75_a0.0_0.0_n100(*)	1.333	⋯	⋯	⋯	⋯	⋯	⋯	−0.00	72.1	23.1
271.8	SXS:BBH:0305(*+)	1.221	⋯	⋯	0.330	⋯	⋯	−0.440	−0.02	74.2	14.8
271.6	SXS:BBH:0218	1.0	⋯	⋯	−0.500	⋯	⋯	0.500	0.00	73.3	10.6
271.6	SXS:BBH:0198	1.202	⋯	⋯	⋯	⋯	⋯	⋯	0.00	73.4	12.7
271.6	SXS:BBH:0307(*)	1.228	⋯	⋯	0.320	⋯	⋯	−0.580	−0.08	70.0	17.0
271.6	GT:BBH:476	1.0	⋯	⋯	−0.200	⋯	⋯	−0.200	−0.20	67.9	24.3
271.6	S0_D10.04_q1.3333_a0.45_-0.80_n100	1.334	⋯	⋯	0.450	⋯	⋯	−0.801	−0.09	71.9	27.9
271.5	D12.00_q0.85_a0.0_0.0_n100(*)	1.176	⋯	⋯	⋯	⋯	⋯	⋯	−0.00	73.0	20.6
271.5	D12.25_q0.82_a-0.44_0.33_n100(*+)	1.22	⋯	⋯	0.330	⋯	⋯	−0.440	−0.02	72.9	20.2
271.5	SXS:BBH:0312(*)	1.203	⋯	⋯	0.390	⋯	⋯	−0.480	−0.00	73.9	14.8
271.4	SXS:BBH:0127	1.34	0.010	−0.077	−0.017	−0.061	−0.065	−0.179	−0.09	71.5	14.3
271.4	SXS:BBH:0115	1.07	0.019	0.013	−0.204	0.243	−0.067	0.291	0.04	74.1	13.8
271.3	SXS:BBH:0213	1.0	⋯	⋯	−0.800	⋯	⋯	0.800	0.00	73.2	11.7
271.3	UD_D10.01_q1.00_a0.4_n100	1.0	⋯	⋯	0.400	⋯	⋯	−0.400	−0.00	73.4	26.7
271.2	D12_q1.00_a-0.25_0.00_n100(*)	1.0	⋯	⋯	⋯	⋯	⋯	−0.250	−0.12	69.4	21.8
271.2	SXS:BBH:0222	1.0	⋯	⋯	−0.300	⋯	⋯	⋯	−0.15	69.1	12.3
271.2	SXS:BBH:0217	1.0	⋯	⋯	−0.600	⋯	⋯	0.600	0.00	73.2	11.9

GW170817 First Binary Neutron Stars & Follow-up Observations

＊First detection from binary NSs

LIGO Hanford＋Livingston + Virgo
Inspiral period 60 sec, 150 cycles.
localization 30 sq. deg

27 min: Alert for astronomers
5h14m: location information sent out

1.74 sec: GRB was detected.

Multi-Messenger Astronomy was established
Opt, IR, X-ray, gamma-ray, ….

Announced October 2017.
62 papers and preprints appeared on the day of press release.

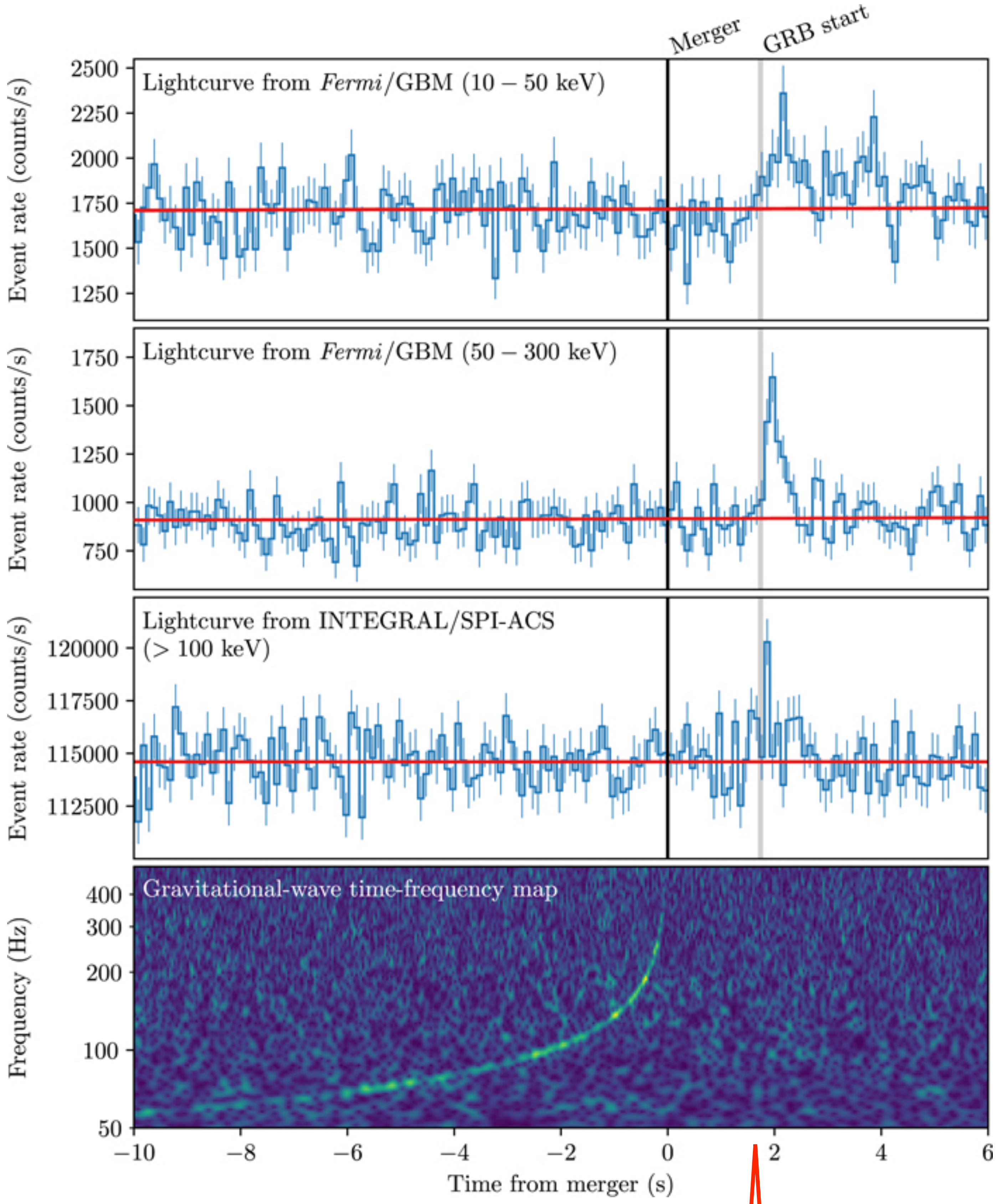

Fermi & INTEGRAL detected GRB 1.7 sec later the merger.

PRL 119 (2017) 161101

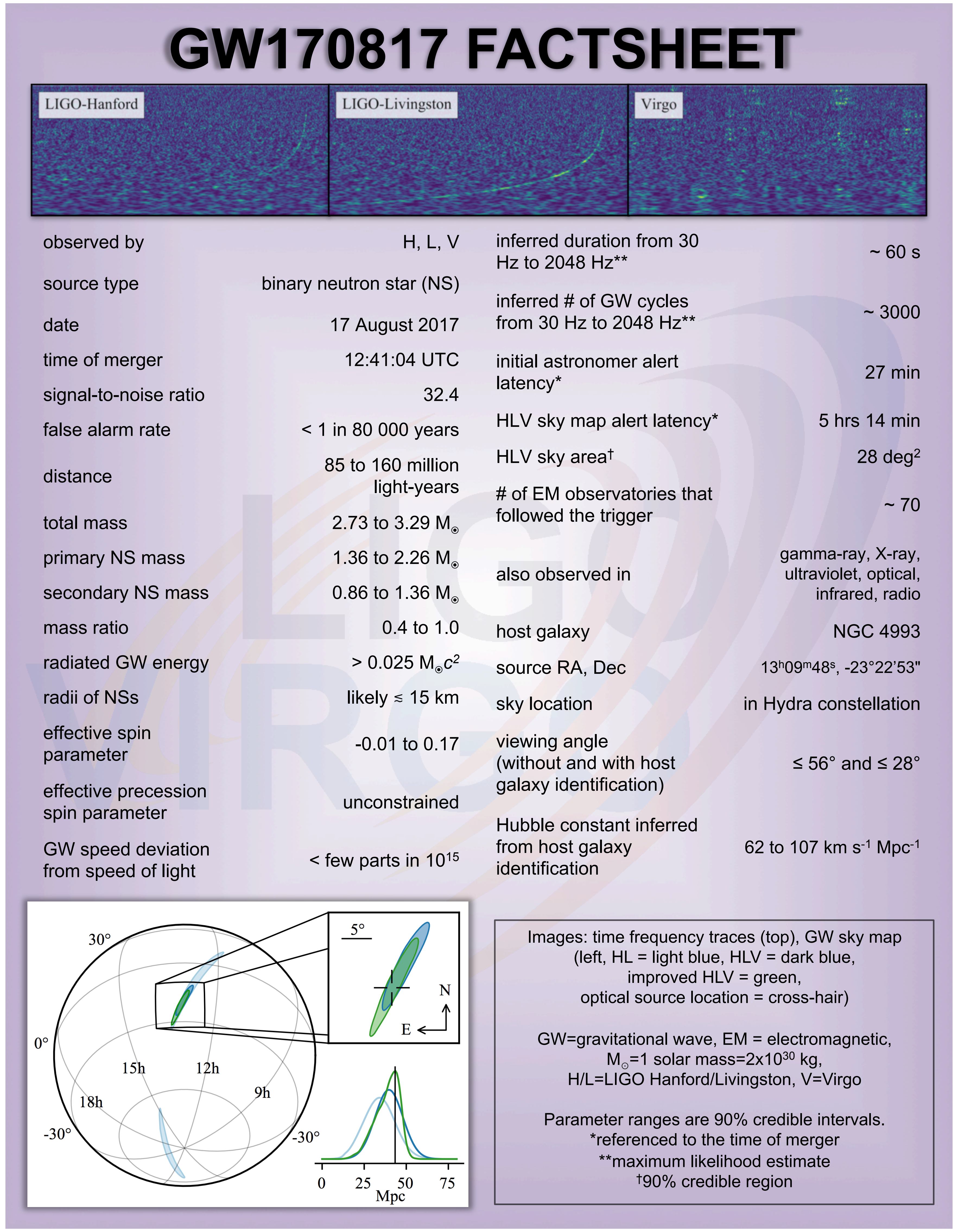

GW170817 constraints to EOS

LIGO/Virgo, PRL 119 (2017) 161101

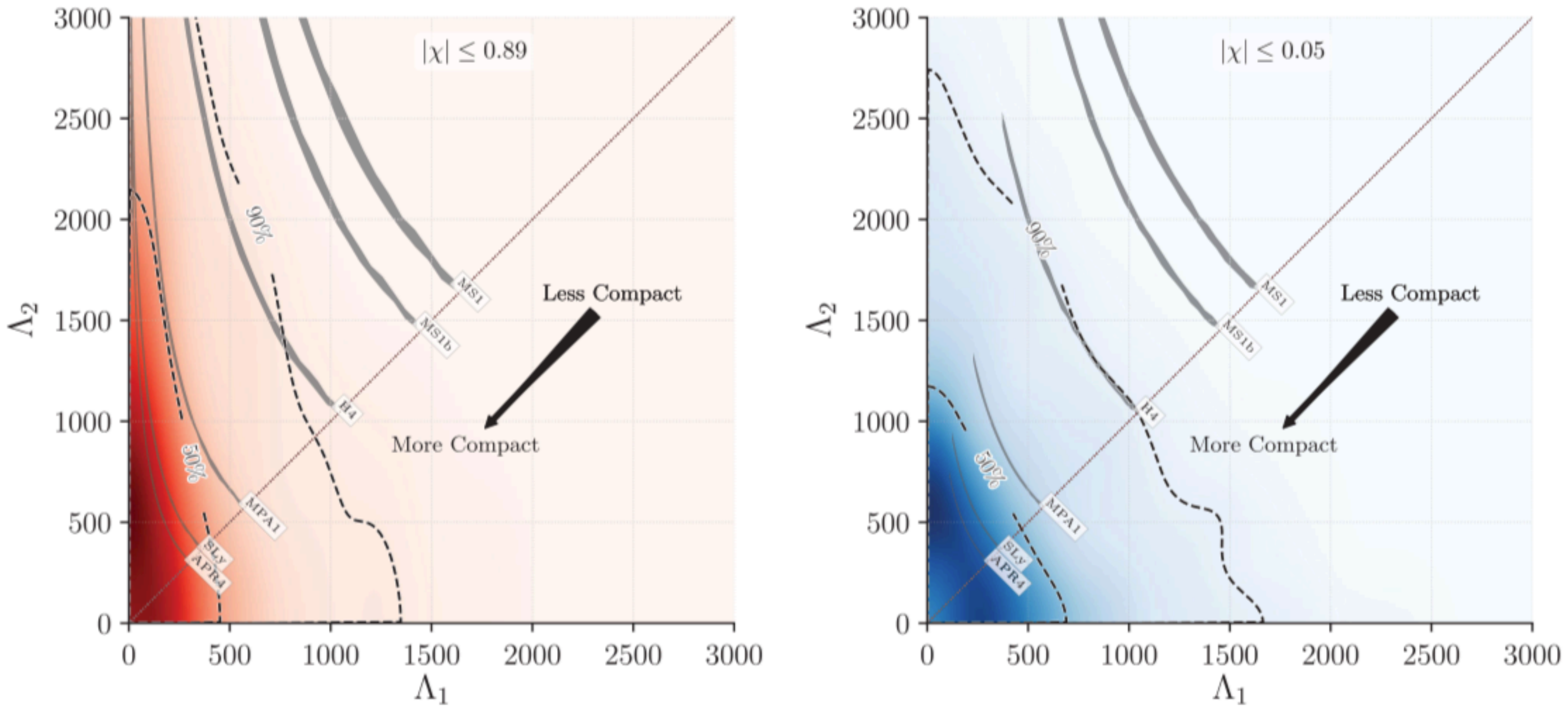

Tidal deformability Λ, quadrupole moment Q_{ij}, tidal field E_{ij}

$$Q_{ij} = -\left(\frac{GM}{c^2R}\right)^5 \frac{R^5}{G}\Lambda E_{ij}$$

$$\tilde{\Lambda} = \frac{16}{13}\frac{(m_1+12m_2)m_1^4\Lambda_1 + (m_2+12m_1)m_2^4\Lambda_2}{(m_1+m_2)^5}$$

$$\tilde{\Lambda}(1.4M_\odot) \lesssim 800 \Rightarrow R(1.4M_\odot) \lesssim 13\text{–}14\ \text{km}$$

Initial result preferred soft EOS, but now changed

LIGO/Virgo, PRL 121 (2018) 161101

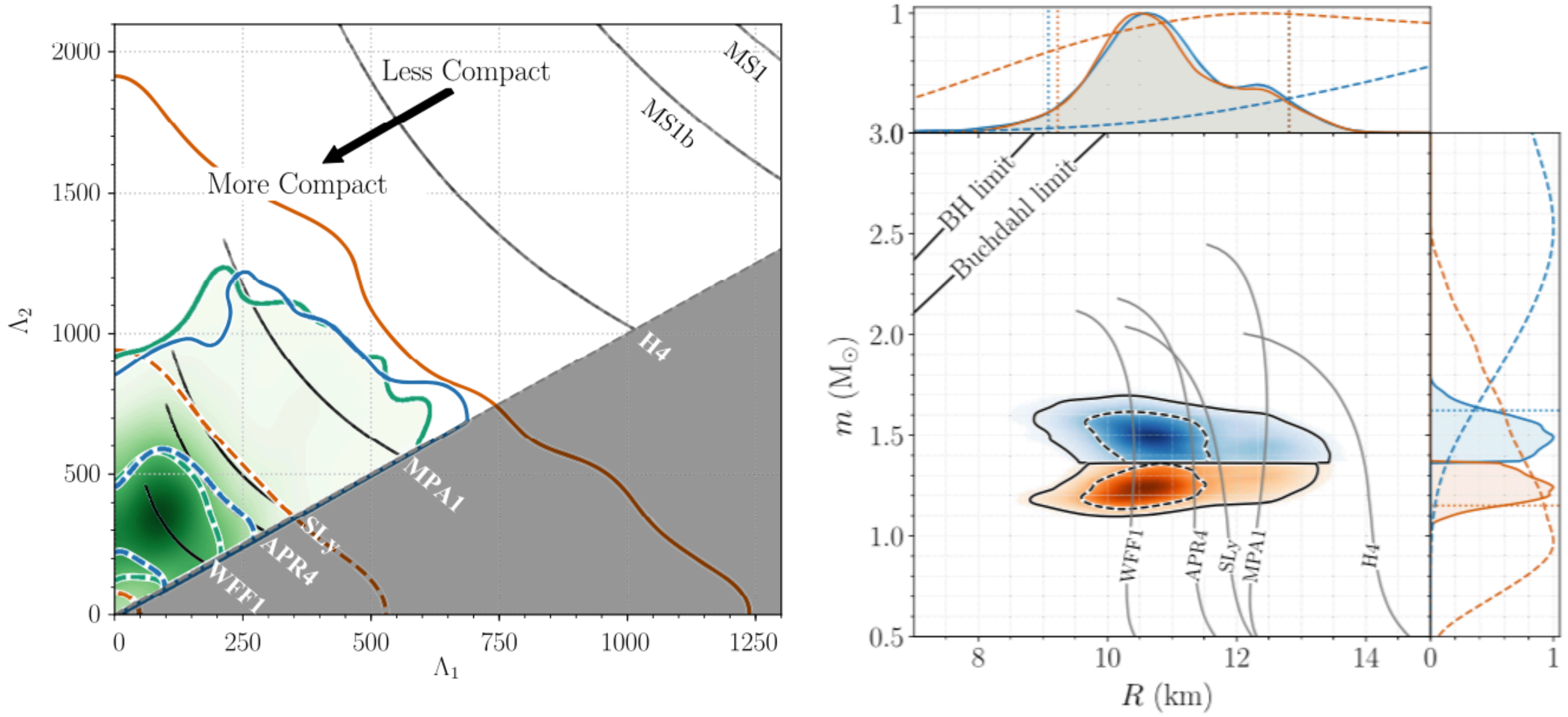

Capono+, Nat. Astro. 4 (2020) 625 (arXiv: 1908.10352)

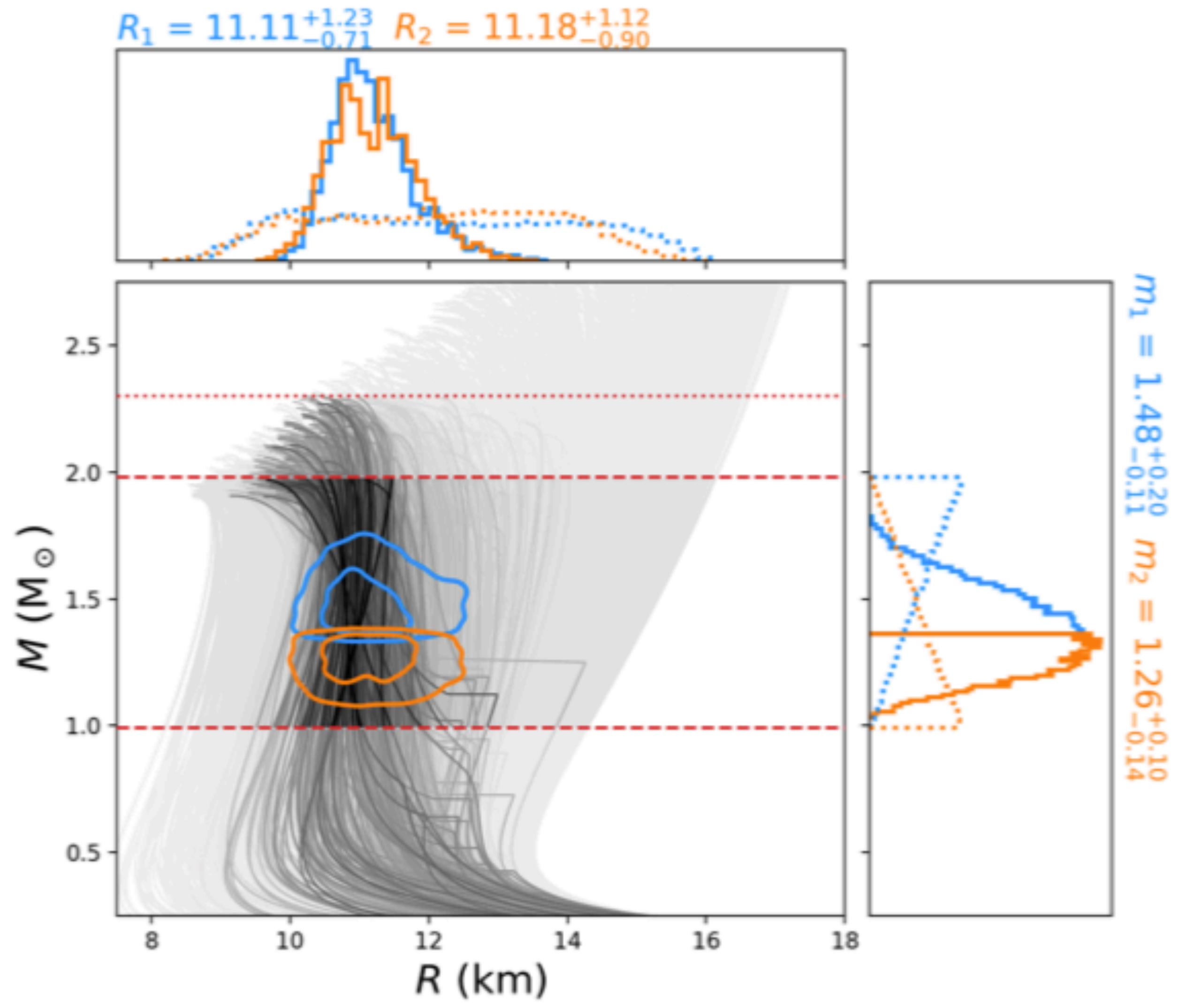

GWTC-2

Gravitational Wave Transient Catalog 2

PHYSICAL REVIEW X **11,** 021053 (2021)

arXiv:2010.14527

GWTC-2: Compact Binary Coalescences Observed by LIGO and Virgo during the First Half of the Third Observing Run

R. Abbott *et al.*[*]
(LIGO Scientific Collaboration and Virgo Collaboration)

(Received 30 October 2020; revised 23 February 2021; accepted 20 April 2021; published 9 June 2021)

*39 events in O3a

50 events in total

* False-Alarm Rate < 2 / 1 yr

* GWyymmdd_hhmmss for new events

- GW190412: the first BBH with definitively asymmetric component masses, which also shows evidence for higher harmonics
- GW190425: the second gravitational-wave event consistent with a BNS, following GW170817
- GW190426_152155: a low-mass event consistent with either an NSBH or BBH
- GW190514_065416: a BBH with the smallest effective aligned spin of all O3a events
- GW190517_055101: a BBH with the largest effective aligned spin of all O3a events
- GW190521: a BBH with total mass over 150 times the mass of the Sun
- GW190814: a highly asymmetric system of ambiguous nature, corresponding to the merger of a 23 solar mass black hole with a 2.6 solar mass compact object, making the latter either the lightest black hole or heaviest neutron star observed in a compact binary
- GW190924_021846: likely the lowest-mass BBH, with both black holes exceeding 3 solar masses

arXiv:2010.14529 Test of GR

arXiv:2010.14533 Population properties

Event	M ($M_\odot$)	$\mathcal{M}$ ($M_\odot$)	m_1 ($M_\odot$)	m_2 ($M_\odot$)	$\chi_{\rm eff}$	$D_{\rm L}$ (Gpc)	z	$M_{\rm f}$ ($M_\odot$)	$\chi_{\rm f}$	$\Delta\Omega$ (deg^2)	SNR
GW190408_181802	$42.9^{+4.1}_{-2.9}$	$18.3^{+1.8}_{-1.2}$	$24.5^{+5.1}_{-3.4}$	$18.3^{+3.2}_{-3.5}$	$-0.03^{+0.13}_{-0.19}$	$1.58^{+0.40}_{-0.59}$	$0.30^{+0.06}_{-0.10}$	$41.0^{+3.8}_{-2.7}$	$0.67^{+0.06}_{-0.07}$	140	$15.3^{+0.2}_{-0.3}$
GW190412	$38.4^{+3.8}_{-3.7}$	$13.3^{+0.4}_{-0.3}$	$30.0^{+4.7}_{-5.1}$	$8.3^{+1.6}_{-0.9}$	$0.25^{+0.08}_{-0.11}$	$0.74^{+0.14}_{-0.17}$	$0.15^{+0.03}_{-0.03}$	$37.3^{+3.9}_{-3.9}$	$0.67^{+0.05}_{-0.06}$	21	$18.9^{+0.2}_{-0.3}$
GW190413_052954	$56.9^{+13.1}_{-8.9}$	$24.0^{+5.4}_{-3.7}$	$33.4^{+12.4}_{-7.4}$	$23.4^{+6.7}_{-6.3}$	$0.01^{+0.29}_{-0.33}$	$4.10^{+2.41}_{-1.89}$	$0.66^{+0.30}_{-0.27}$	$54.3^{+12.4}_{-8.4}$	$0.69^{+0.12}_{-0.13}$	1400	$8.9^{+0.4}_{-0.8}$
GW190413_134308	$76.1^{+15.9}_{-10.6}$	$31.9^{+7.3}_{-4.6}$	$45.4^{+13.6}_{-9.6}$	$30.9^{+10.2}_{-9.6}$	$-0.01^{+0.24}_{-0.28}$	$5.15^{+2.44}_{-2.34}$	$0.80^{+0.30}_{-0.31}$	$72.8^{+15.2}_{-10.3}$	$0.69^{+0.10}_{-0.12}$	520	$10.0^{+0.4}_{-0.5}$
GW190421_213856	$71.8^{+12.5}_{-8.6}$	$30.7^{+5.5}_{-3.9}$	$40.6^{+10.4}_{-6.6}$	$31.4^{+7.5}_{-8.2}$	$-0.05^{+0.23}_{-0.26}$	$3.15^{+1.37}_{-1.42}$	$0.53^{+0.18}_{-0.21}$	$68.6^{+11.7}_{-8.1}$	$0.68^{+0.10}_{-0.11}$	1000	$10.7^{+0.2}_{-0.4}$
GW190424_180648	$70.7^{+13.4}_{-9.8}$	$30.3^{+5.7}_{-4.2}$	$39.5^{+10.9}_{-6.9}$	$31.0^{+7.4}_{-7.3}$	$0.15^{+0.22}_{-0.22}$	$2.55^{+1.56}_{-1.33}$	$0.45^{+0.22}_{-0.21}$	$67.1^{+12.5}_{-9.2}$	$0.75^{+0.08}_{-0.09}$	26000	$10.4^{+0.2}_{-0.4}$
GW190425	$3.4^{+0.3}_{-0.1}$	$1.44^{+0.02}_{-0.02}$	$2.0^{+0.6}_{-0.3}$	$1.4^{+0.3}_{-0.3}$	$0.06^{+0.11}_{-0.05}$	$0.16^{+0.07}_{-0.07}$	$0.03^{+0.01}_{-0.02}$	–	–	9900	$12.4^{+0.3}_{-0.4}$
GW190426_152155	$7.2^{+3.5}_{-1.5}$	$2.41^{+0.08}_{-0.08}$	$5.7^{+4.0}_{-2.3}$	$1.5^{+0.8}_{-0.5}$	$-0.03^{+0.33}_{-0.30}$	$0.38^{+0.19}_{-0.16}$	$0.08^{+0.04}_{-0.03}$	–	–	1400	$8.7^{+0.5}_{-0.6}$
GW190503_185404	$71.3^{+9.3}_{-8.0}$	$30.1^{+4.2}_{-4.0}$	$42.9^{+9.2}_{-7.8}$	$28.5^{+7.5}_{-7.9}$	$-0.02^{+0.20}_{-0.26}$	$1.52^{+0.71}_{-0.66}$	$0.29^{+0.11}_{-0.11}$	$68.2^{+8.7}_{-7.5}$	$0.67^{+0.09}_{-0.12}$	94	$12.4^{+0.2}_{-0.3}$
GW190512_180714	$35.6^{+3.9}_{-3.4}$	$14.5^{+1.3}_{-1.0}$	$23.0^{+5.4}_{-5.7}$	$12.5^{+3.5}_{-2.5}$	$0.03^{+0.13}_{-0.13}$	$1.49^{+0.53}_{-0.59}$	$0.28^{+0.09}_{-0.10}$	$34.2^{+3.9}_{-3.4}$	$0.65^{+0.07}_{-0.07}$	230	$12.2^{+0.2}_{-0.4}$
GW190513_205428	$53.6^{+8.6}_{-5.9}$	$21.5^{+3.6}_{-1.9}$	$35.3^{+9.6}_{-9.0}$	$18.1^{+7.3}_{-4.2}$	$0.12^{+0.29}_{-0.18}$	$2.16^{+0.94}_{-0.80}$	$0.39^{+0.14}_{-0.13}$	$51.3^{+8.1}_{-5.8}$	$0.69^{+0.14}_{-0.12}$	490	$12.9^{+0.3}_{-0.4}$
GW190514_065416	$64.2^{+16.6}_{-9.6}$	$27.4^{+6.9}_{-4.3}$	$36.9^{+13.4}_{-7.3}$	$27.5^{+8.2}_{-7.7}$	$-0.16^{+0.28}_{-0.32}$	$4.93^{+2.76}_{-2.41}$	$0.77^{+0.34}_{-0.33}$	$61.6^{+16.0}_{-9.2}$	$0.64^{+0.11}_{-0.14}$	2400	$8.2^{+0.3}_{-0.6}$
GW190517_055101	$61.9^{+10.0}_{-9.6}$	$26.0^{+4.2}_{-4.0}$	$36.4^{+11.8}_{-7.8}$	$24.8^{+6.9}_{-7.1}$	$0.53^{+0.20}_{-0.19}$	$2.11^{+1.79}_{-1.00}$	$0.38^{+0.26}_{-0.16}$	$57.8^{+9.4}_{-9.1}$	$0.87^{+0.05}_{-0.07}$	460	$10.7^{+0.4}_{-0.6}$
GW190519_153544	$104.2^{+14.5}_{-14.9}$	$43.5^{+6.8}_{-6.8}$	$64.5^{+11.3}_{-13.2}$	$39.9^{+11.0}_{-10.6}$	$0.33^{+0.19}_{-0.22}$	$2.85^{+2.02}_{-1.14}$	$0.49^{+0.27}_{-0.17}$	$98.7^{+13.5}_{-14.2}$	$0.80^{+0.07}_{-0.12}$	770	$15.6^{+0.2}_{-0.3}$
GW190521	$157.9^{+37.4}_{-20.9}$	$66.9^{+15.5}_{-9.2}$	$91.4^{+29.3}_{-17.5}$	$66.8^{+20.7}_{-20.7}$	$0.06^{+0.31}_{-0.37}$	$4.53^{+2.30}_{-2.13}$	$0.72^{+0.29}_{-0.29}$	$150.3^{+35.8}_{-20.0}$	$0.73^{+0.11}_{-0.14}$	940	$14.2^{+0.3}_{-0.3}$
GW190521_074359	$74.4^{+6.8}_{-4.6}$	$31.9^{+3.1}_{-2.4}$	$42.1^{+5.9}_{-4.9}$	$32.7^{+5.4}_{-6.2}$	$0.09^{+0.10}_{-0.13}$	$1.28^{+0.38}_{-0.57}$	$0.25^{+0.06}_{-0.10}$	$70.7^{+6.4}_{-4.2}$	$0.72^{+0.05}_{-0.07}$	500	$25.8^{+0.1}_{-0.2}$
GW190527_092055	$58.5^{+27.9}_{-10.6}$	$24.2^{+11.9}_{-4.4}$	$36.2^{+19.1}_{-9.5}$	$22.8^{+12.7}_{-8.1}$	$0.13^{+0.29}_{-0.28}$	$3.10^{+4.85}_{-1.64}$	$0.53^{+0.61}_{-0.25}$	$55.9^{+26.4}_{-10.1}$	$0.73^{+0.12}_{-0.16}$	3800	$8.1^{+0.4}_{-1.0}$
GW190602_175927	$114.1^{+18.5}_{-15.7}$	$48.3^{+8.6}_{-8.0}$	$67.2^{+16.0}_{-12.6}$	$47.4^{+13.4}_{-16.6}$	$0.10^{+0.25}_{-0.25}$	$2.99^{+2.02}_{-1.26}$	$0.51^{+0.27}_{-0.19}$	$108.8^{+17.2}_{-14.8}$	$0.71^{+0.10}_{-0.13}$	720	$12.8^{+0.2}_{-0.3}$
GW190620_030421	$90.1^{+17.3}_{-12.1}$	$37.5^{+7.8}_{-5.7}$	$55.4^{+15.8}_{-12.0}$	$35.0^{+11.6}_{-11.4}$	$0.34^{+0.21}_{-0.25}$	$3.16^{+1.67}_{-1.43}$	$0.54^{+0.22}_{-0.21}$	$85.4^{+15.9}_{-11.4}$	$0.80^{+0.08}_{-0.14}$	6700	$12.1^{+0.3}_{-0.4}$
GW190630_185205	$58.8^{+4.7}_{-4.8}$	$24.8^{+2.1}_{-2.0}$	$35.0^{+6.9}_{-5.7}$	$23.6^{+5.2}_{-5.1}$	$0.10^{+0.12}_{-0.13}$	$0.93^{+0.56}_{-0.40}$	$0.19^{+0.10}_{-0.07}$	$56.1^{+4.5}_{-4.6}$	$0.70^{+0.06}_{-0.07}$	1300	$15.6^{+0.2}_{-0.3}$
GW190701_203306	$94.1^{+11.6}_{-9.3}$	$40.2^{+5.2}_{-4.7}$	$53.6^{+11.7}_{-7.8}$	$40.8^{+8.3}_{-11.5}$	$-0.06^{+0.23}_{-0.28}$	$2.14^{+0.79}_{-0.73}$	$0.38^{+0.12}_{-0.12}$	$90.0^{+10.8}_{-8.6}$	$0.67^{+0.09}_{-0.12}$	45	$11.3^{+0.2}_{-0.4}$
GW190706_222641	$101.6^{+17.9}_{-13.5}$	$42.0^{+8.4}_{-6.2}$	$64.0^{+15.2}_{-15.2}$	$38.5^{+12.5}_{-12.4}$	$0.32^{+0.25}_{-0.30}$	$5.07^{+2.57}_{-2.11}$	$0.79^{+0.31}_{-0.28}$	$96.3^{+16.7}_{-13.2}$	$0.80^{+0.08}_{-0.17}$	610	$12.6^{+0.2}_{-0.4}$
GW190707_093326	$20.0^{+1.9}_{-1.3}$	$8.5^{+0.6}_{-0.4}$	$11.5^{+3.3}_{-1.7}$	$8.4^{+1.4}_{-1.6}$	$-0.05^{+0.10}_{-0.08}$	$0.80^{+0.37}_{-0.38}$	$0.16^{+0.07}_{-0.07}$	$19.2^{+1.9}_{-1.3}$	$0.66^{+0.03}_{-0.04}$	1300	$13.3^{+0.2}_{-0.4}$
GW190708_232457	$30.8^{+2.5}_{-1.8}$	$13.1^{+0.9}_{-0.6}$	$17.5^{+4.7}_{-2.3}$	$13.1^{+2.0}_{-2.7}$	$0.02^{+0.10}_{-0.08}$	$0.90^{+0.33}_{-0.40}$	$0.18^{+0.06}_{-0.07}$	$29.4^{+2.5}_{-1.7}$	$0.69^{+0.04}_{-0.04}$	14000	$13.1^{+0.2}_{-0.3}$
GW190719_215514	$55.8^{+16.3}_{-10.0}$	$22.7^{+5.9}_{-3.7}$	$35.2^{+16.9}_{-9.9}$	$20.2^{+8.1}_{-6.5}$	$0.35^{+0.28}_{-0.32}$	$4.61^{+2.84}_{-2.17}$	$0.73^{+0.35}_{-0.30}$	$52.9^{+15.6}_{-9.5}$	$0.80^{+0.10}_{-0.16}$	2300	$8.3^{+0.3}_{-1.0}$
GW190720_000836	$21.3^{+4.3}_{-2.3}$	$8.9^{+0.5}_{-0.8}$	$13.3^{+6.6}_{-3.0}$	$7.8^{+2.2}_{-2.2}$	$0.18^{+0.14}_{-0.12}$	$0.81^{+0.71}_{-0.33}$	$0.16^{+0.12}_{-0.06}$	$20.3^{+4.5}_{-2.3}$	$0.72^{+0.06}_{-0.05}$	510	$11.0^{+0.3}_{-0.8}$
GW190727_060333	$65.8^{+10.9}_{-7.4}$	$28.1^{+4.9}_{-3.4}$	$37.2^{+9.4}_{-5.9}$	$28.8^{+6.6}_{-7.9}$	$0.12^{+0.26}_{-0.25}$	$3.60^{+1.56}_{-1.51}$	$0.60^{+0.20}_{-0.22}$	$62.6^{+10.2}_{-7.0}$	$0.73^{+0.10}_{-0.10}$	860	$11.9^{+0.3}_{-0.5}$
GW190728_064510	$20.5^{+4.5}_{-1.3}$	$8.6^{+0.5}_{-0.3}$	$12.2^{+7.1}_{-2.2}$	$8.1^{+1.7}_{-2.6}$	$0.12^{+0.19}_{-0.07}$	$0.89^{+0.25}_{-0.37}$	$0.18^{+0.05}_{-0.07}$	$19.5^{+4.6}_{-1.3}$	$0.71^{+0.04}_{-0.04}$	410	$13.0^{+0.2}_{-0.4}$
GW190731_140936	$67.1^{+15.3}_{-10.2}$	$28.4^{+6.8}_{-4.5}$	$39.3^{+11.8}_{-8.2}$	$28.0^{+8.9}_{-8.4}$	$0.08^{+0.24}_{-0.24}$	$3.97^{+2.56}_{-2.07}$	$0.65^{+0.32}_{-0.30}$	$63.9^{+14.4}_{-9.8}$	$0.71^{+0.10}_{-0.12}$	3000	$8.6^{+0.2}_{-0.5}$
GW190803_022701	$62.7^{+11.8}_{-8.4}$	$26.7^{+5.2}_{-3.8}$	$36.1^{+10.2}_{-6.7}$	$26.7^{+7.1}_{-7.6}$	$-0.01^{+0.25}_{-0.26}$	$3.69^{+2.04}_{-1.69}$	$0.61^{+0.26}_{-0.24}$	$59.9^{+11.2}_{-7.9}$	$0.69^{+0.10}_{-0.11}$	1500	$8.6^{+0.3}_{-0.5}$
GW190814	$25.8^{+1.0}_{-0.9}$	$6.09^{+0.06}_{-0.06}$	$23.2^{+1.1}_{-1.0}$	$2.59^{+0.08}_{-0.09}$	$0.00^{+0.06}_{-0.06}$	$0.24^{+0.04}_{-0.05}$	$0.05^{+0.009}_{-0.010}$	$25.6^{+1.0}_{-0.9}$	$0.28^{+0.02}_{-0.02}$	19	$24.9^{+0.1}_{-0.2}$
GW190828_063405	$57.5^{+7.5}_{-4.4}$	$24.8^{+3.3}_{-2.0}$	$31.8^{+5.8}_{-3.9}$	$25.9^{+4.4}_{-4.6}$	$0.19^{+0.15}_{-0.16}$	$2.22^{+0.63}_{-0.95}$	$0.40^{+0.09}_{-0.15}$	$54.5^{+6.9}_{-4.0}$	$0.76^{+0.06}_{-0.07}$	520	$16.2^{+0.2}_{-0.3}$
GW190828_065509	$34.1^{+5.5}_{-4.5}$	$13.3^{+1.2}_{-0.9}$	$23.8^{+7.2}_{-7.0}$	$10.2^{+3.5}_{-2.1}$	$0.08^{+0.16}_{-0.16}$	$1.66^{+0.63}_{-0.61}$	$0.31^{+0.10}_{-0.10}$	$32.9^{+5.7}_{-4.5}$	$0.65^{+0.09}_{-0.08}$	640	$10.0^{+0.3}_{-0.5}$
GW190909_114149	$71.2^{+54.3}_{-15.0}$	$29.5^{+17.5}_{-6.3}$	$43.2^{+50.7}_{-12.2}$	$27.6^{+13.0}_{-10.9}$	$-0.03^{+0.44}_{-0.36}$	$4.77^{+3.70}_{-2.66}$	$0.75^{+0.45}_{-0.37}$	$68.3^{+52.5}_{-14.5}$	$0.68^{+0.16}_{-0.18}$	4200	$8.1^{+0.4}_{-0.7}$
GW190910_112807	$78.7^{+9.5}_{-9.0}$	$33.9^{+4.3}_{-3.9}$	$43.5^{+7.6}_{-6.2}$	$35.1^{+6.3}_{-7.0}$	$0.02^{+0.19}_{-0.18}$	$1.57^{+1.07}_{-0.64}$	$0.29^{+0.17}_{-0.11}$	$75.0^{+8.7}_{-8.5}$	$0.70^{+0.08}_{-0.07}$	10000	$14.1^{+0.2}_{-0.3}$
GW190915_235702	$59.5^{+7.5}_{-6.2}$	$25.1^{+3.1}_{-2.6}$	$34.9^{+9.5}_{-6.2}$	$24.4^{+5.5}_{-6.0}$	$0.03^{+0.19}_{-0.24}$	$1.70^{+0.71}_{-0.64}$	$0.32^{+0.11}_{-0.11}$	$56.8^{+7.1}_{-5.8}$	$0.71^{+0.09}_{-0.11}$	380	$13.6^{+0.2}_{-0.3}$
GW190924_021846	$13.9^{+5.1}_{-0.9}$	$5.8^{+0.2}_{-0.2}$	$8.8^{+7.0}_{-2.0}$	$5.0^{+1.3}_{-1.9}$	$0.03^{+0.30}_{-0.09}$	$0.57^{+0.22}_{-0.22}$	$0.12^{+0.04}_{-0.04}$	$13.3^{+5.2}_{-1.0}$	$0.67^{+0.05}_{-0.05}$	380	$11.5^{+0.3}_{-0.4}$
GW190929_012149	$90.6^{+21.2}_{-14.1}$	$34.3^{+8.6}_{-6.5}$	$64.7^{+22.4}_{-18.9}$	$25.7^{+14.4}_{-9.7}$	$0.03^{+0.27}_{-0.27}$	$3.68^{+2.98}_{-1.68}$	$0.61^{+0.38}_{-0.24}$	$87.5^{+20.7}_{-14.1}$	$0.64^{+0.17}_{-0.23}$	1800	$9.8^{+0.8}_{-0.6}$
GW190930_133541	$20.3^{+9.0}_{-1.5}$	$8.5^{+0.5}_{-0.5}$	$12.3^{+12.5}_{-2.3}$	$7.8^{+1.7}_{-3.3}$	$0.14^{+0.31}_{-0.15}$	$0.78^{+0.37}_{-0.33}$	$0.16^{+0.07}_{-0.06}$	$19.3^{+9.3}_{-1.5}$	$0.72^{+0.07}_{-0.06}$	1800	$9.5^{+0.3}_{-0.5}$

GWTC-2

Gravitational Wave Transient Catalog 2

PHYSICAL REVIEW X **11,** 021053 (2021)

arXiv:2010.14527

GWTC-2: Compact Binary Coalescences Observed by LIGO and Virgo during the First Half of the Third Observing Run

R. Abbott *et al.*[*]
(LIGO Scientific Collaboration and Virgo Collaboration)

(Received 30 October 2020; revised 23 February 2021; accepted 20 April 2021; published 9 June 2021)

*39 events in O3a
50 events in total

* False-Alarm Rate < 2 / 1 yr

* GWyymmdd_hhmmss for new events

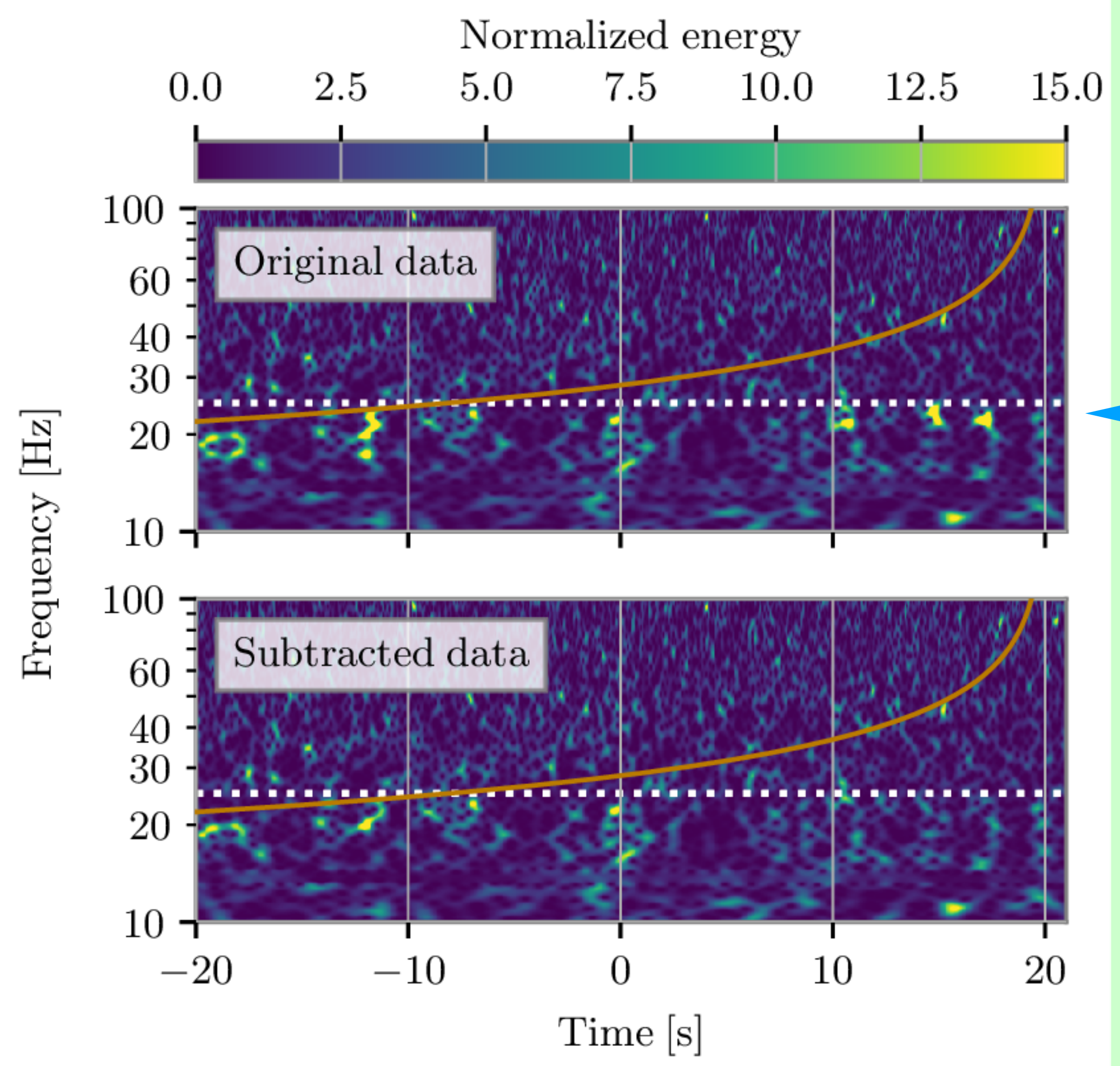

"glitch"

one source of "glitch" is the scatter of the laser

GWTC-2.1

Gravitational Wave Transient Catalog 2.1

arXiv:2108.01045

* re-calibrated data in O3a
* includes 1201 events of FAR < 2 / 1 day
* 44 events P_{astro} > 0.5 （8 new in O3a)
* 3 events retracted since P_{astro} < 0.5

55 events in total

$P_{astro}+P_{terre}=1$

noise

- GW190917 _114630 (P_{astro} = 0.77) potentially NSBH
- GW190426 _190642 (P_{astro} = 0.75) total mass 185 M -> 175M final (maximum ever)
- GW190403 _051519 (P_{astro} = 0.61) & GW190805 _211137(P_{astro} = 0.95) have χ > 0.8 BH

	GWTC-2	GWTC-2.1
BHBH	add 36 (total 46)	+8 -3 (51)
NSNS	+1 (2)	+0 (2)
NSBH		
BH+unknown	+ 2 (2)	+0 (2)
Total	+ 39 (50)	+5 (55)

GW190521 Discovery of IMBH (1)

PRL 125 (2020) 101102

PHYSICAL REVIEW LETTERS **125,** 101102 (2020)

Editors' Suggestion Featured in Physics

GW190521: A Binary Black Hole Merger with a Total Mass of 150 $M_\odot$

R. Abbott *et al.**
(LIGO Scientific Collaboration and Virgo Collaboration)

(Received 30 May 2020; revised 19 June 2020; accepted 9 July 2020; published 2 September 2020; corrected 23 October 2020)

On May 21, 2019 at 03:02:29 UTC Advanced LIGO and Advanced Virgo observed a short duration gravitational-wave signal, GW190521, with a three-detector network signal-to-noise ratio of 14.7, and an estimated false-alarm rate of 1 in 4900 yr using a search sensitive to generic transients. If GW190521 is from a quasicircular binary inspiral, then the detected signal is consistent with the merger of two black holes with masses of 85^{+21}_{-14} $M_\odot$ and 66^{+17}_{-18} $M_\odot$ (90% credible intervals). We infer that the primary black hole mass lies within the gap produced by (pulsational) pair-instability supernova processes, with only a 0.32% probability of being below 65 $M_\odot$. We calculate the mass of the remnant to be 142^{+28}_{-16} $M_\odot$, which can be considered an intermediate mass black hole (IMBH). The luminosity distance of the source is $5.3^{+2.4}_{-2.6}$ Gpc, corresponding to a redshift of $0.82^{+0.28}_{-0.34}$. The inferred rate of mergers similar to GW190521 is $0.13^{+0.30}_{-0.11}$ $\mathrm{Gpc}^{-3}\,\mathrm{yr}^{-1}$.

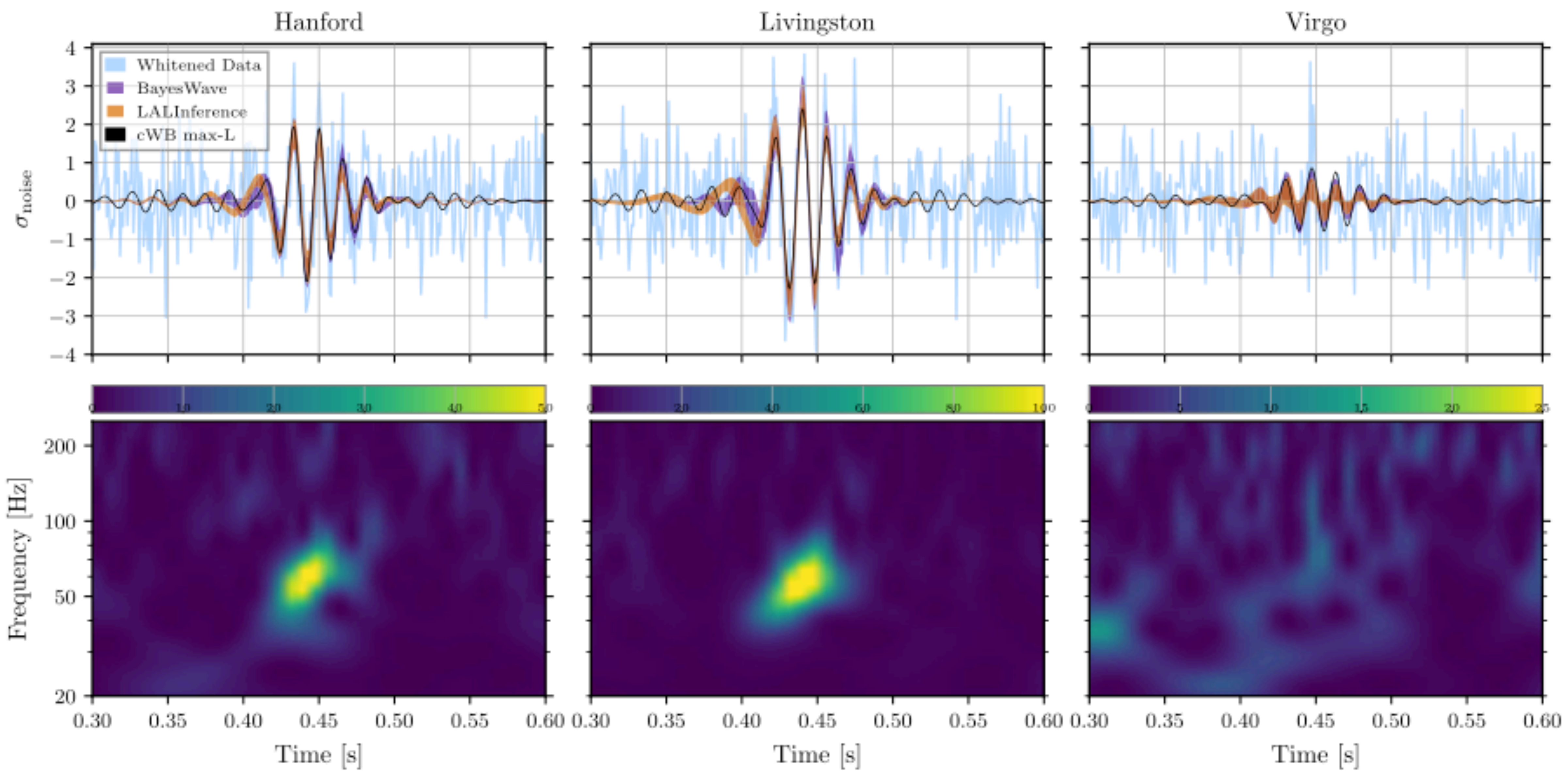

Mass 85^{+21}_{-14} Msun + 66^{+17}_{-18} Msun -> 142^{+28}_{-16} Msun

Distance $5.3^{+2.4}_{-2.6}$ Gpc, z= $0.82^{+0.28}_{-0.34}$

100 10^5 Msun

Stellar-mass BH **Intermediate-massBH** **Super-massive BH**

Existence of BH over 100 Msun !

No formation scenario for BH over 65 Msun in the standard model.

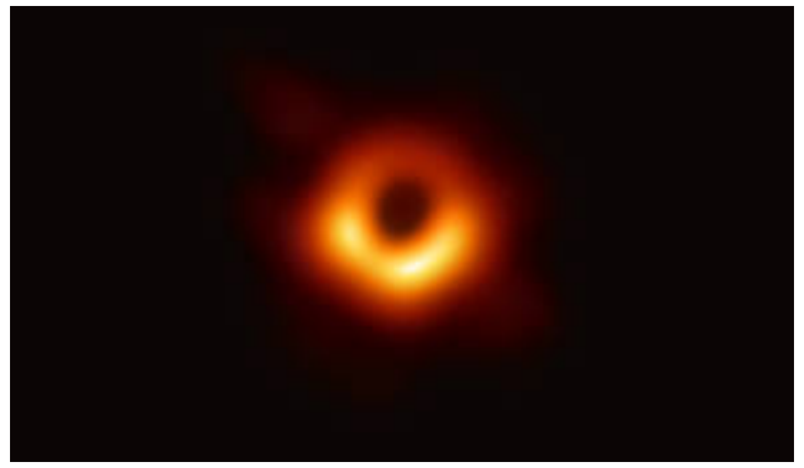

M87 by EHT

mass $6.5\ 10^9$Msun

distance

55 Mly

16.9 Mpc

LIGO/Virgo

GW190521 Discovery of IMBH (2)

PRL 125 (2020) 101102

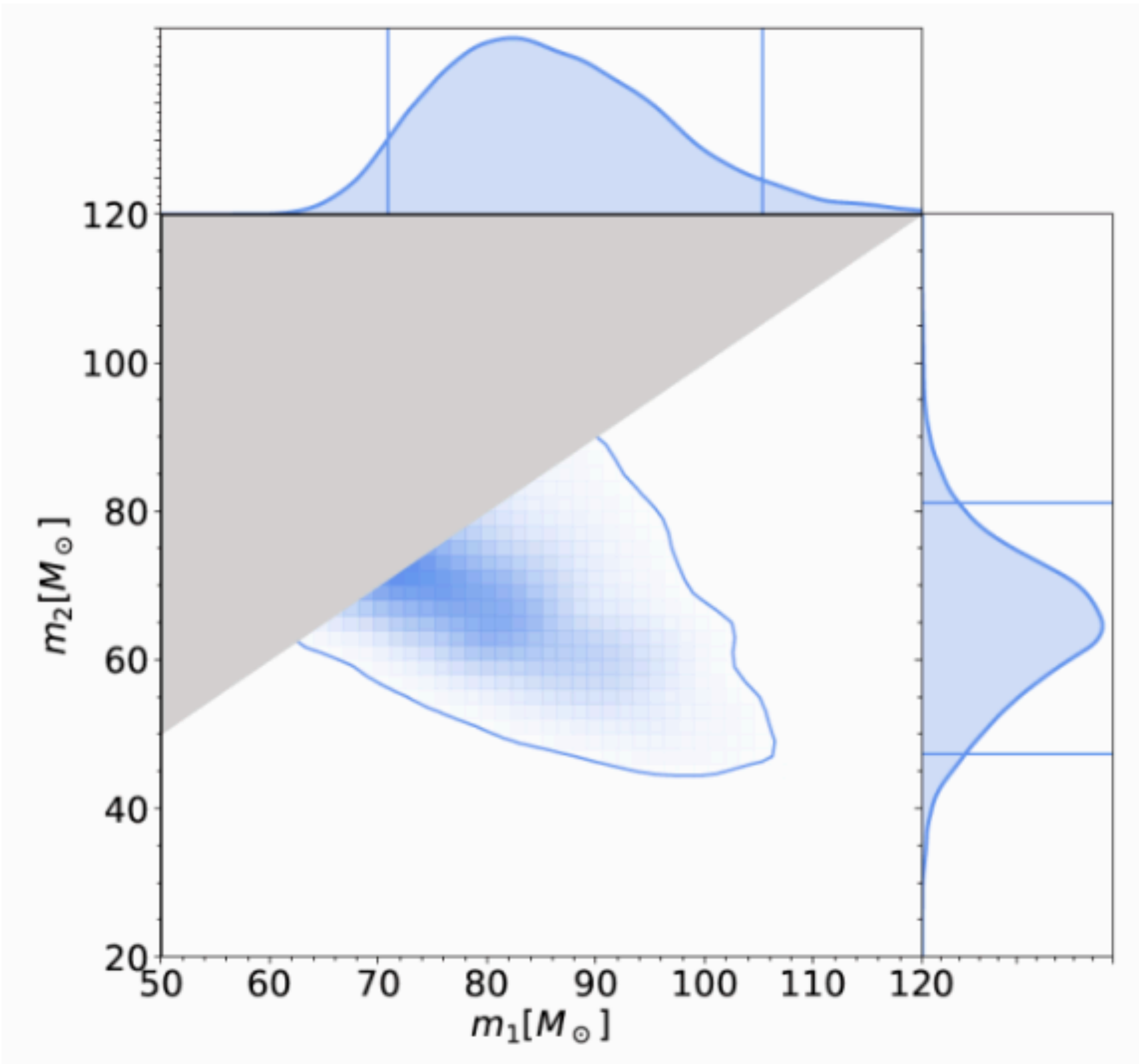

Mass 85^{+21}_{-14} M_{sun} + 66^{+17}_{-18} M_{sun} -> 142^{+28}_{-16} M_{sun}

Distance $5.3^{+2.4}_{-2.6}$ Gpc, z= $0.82^{+0.28}_{-0.34}$

100 10^5 M_{sun}

Stellar-mass BH **Intermediate-massBH** **Super-massive BH**

Existence of BH over 100 M_{sun} !

No formation scenario for BH over 65 M_{sun} in the standard model.

Second generation of mergers

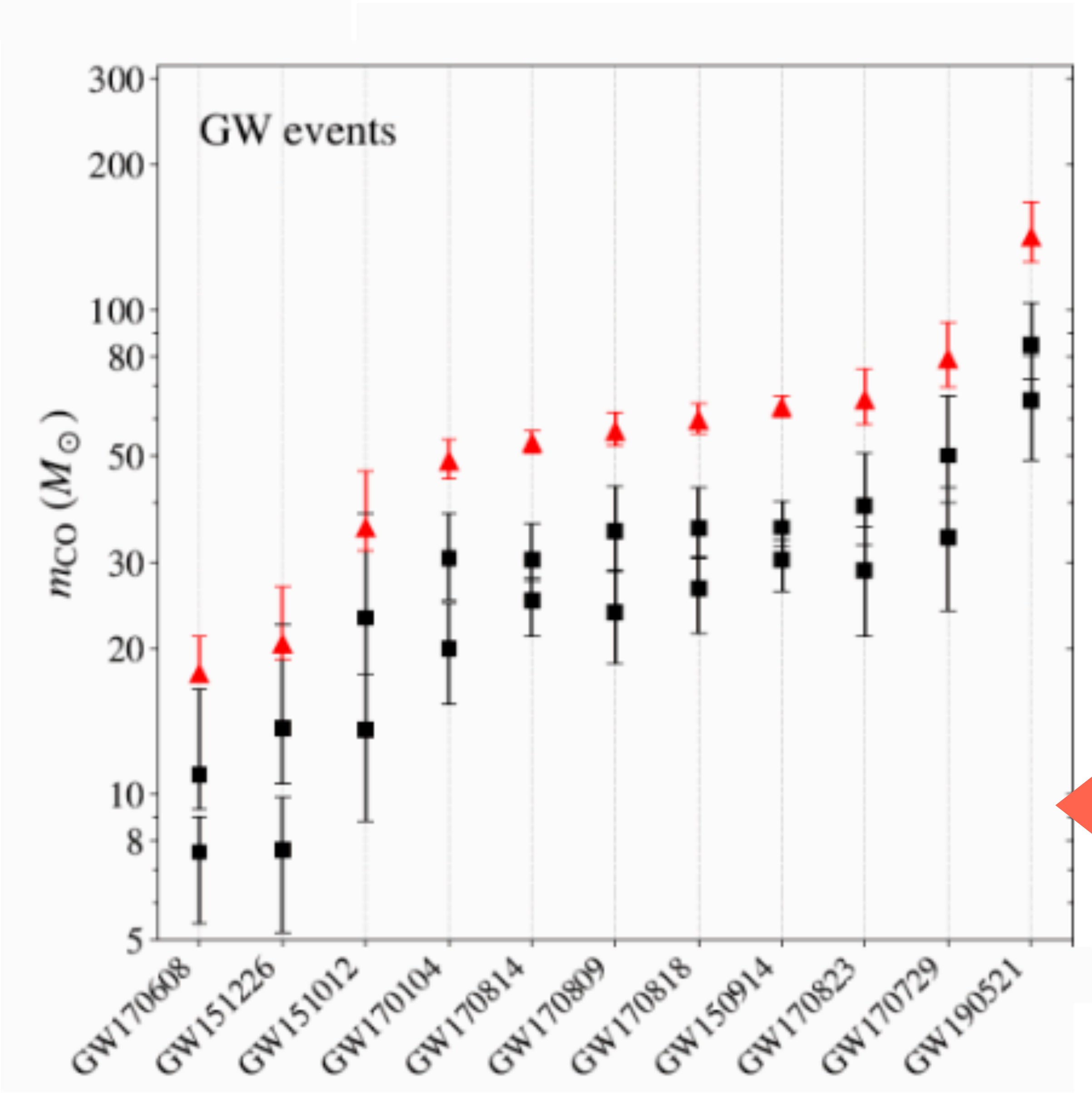

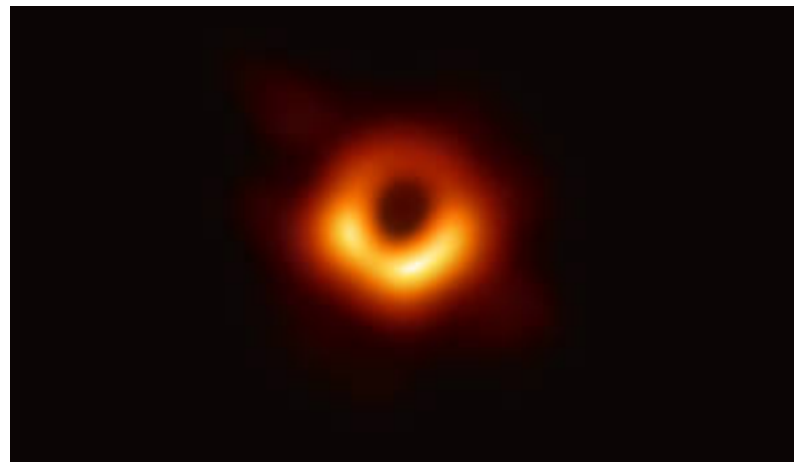

M87 by EHT

mass 6.5 $10^9 M_{sun}$

distance

55 Mly

16.9 Mpc

GWTC-3 (Gravitational Wave Transient Catalog 3) Nov 5, 2021 arXiv:2111.03606

arXiv:2111.03634 Population properties

arXiv:2112.xxxxx Test of GR

* added 35 events in O3b 90 events in total
  32 BHBH, 0 NSNS, 3 NSBH
* 1048 events of FAR < 2 / day
* FAR < 2/ day & P_{astro} > 0.5
* O3b made 39 public alerts
  —> 18 were real
  —> 17 newly added as events

	GWTC-3
BHBH	add 32 (total 83)
NSNS	+0 (2)
NSBH	+3 (3)
BH+unknown	+0 (2)
Total	+ 35 (90)

BHBH

GW200220_061928	87M + 61M -> 148M	Largest in O3b
GW191204_171526	12M + 8 M -> 19 M	Effective inspiral spin > 0
GW191129_134029	10.7 M + 6.7 M -> 16.8 M	Smallest in O3b
GW191109_010717	65 M+ 47 M - > 107 M	Effective inspiral spin < 0

**Discovery of NSBH ApJL 915; L5 (2021)

GW191219_163120	31M + 1.2 M
~~GW200105_162426**~~	~~9M+1.9M~~
GW200115_042309**	6M + 1.4 M
GW200210_092254	24M+2.8M

retracted since P_{astro} = 0.36

GWTC-3（Gravitational Wave Transient Catalog 3） Nov 5, 2021 arXiv:2111.03606

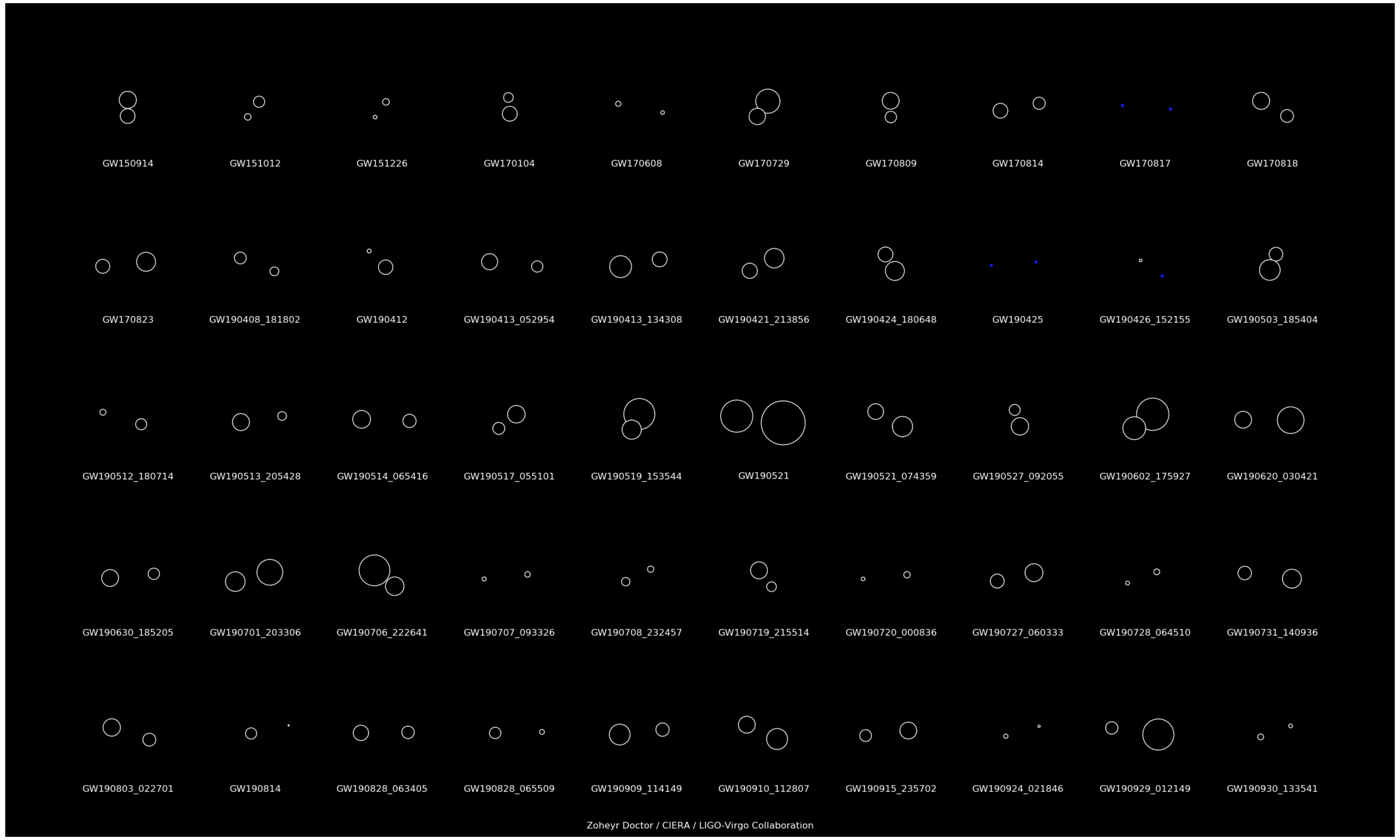

Gravitational-Wave Transient Catalog 3

compact binary coalescences from
the second part of the third observing run (O3b)

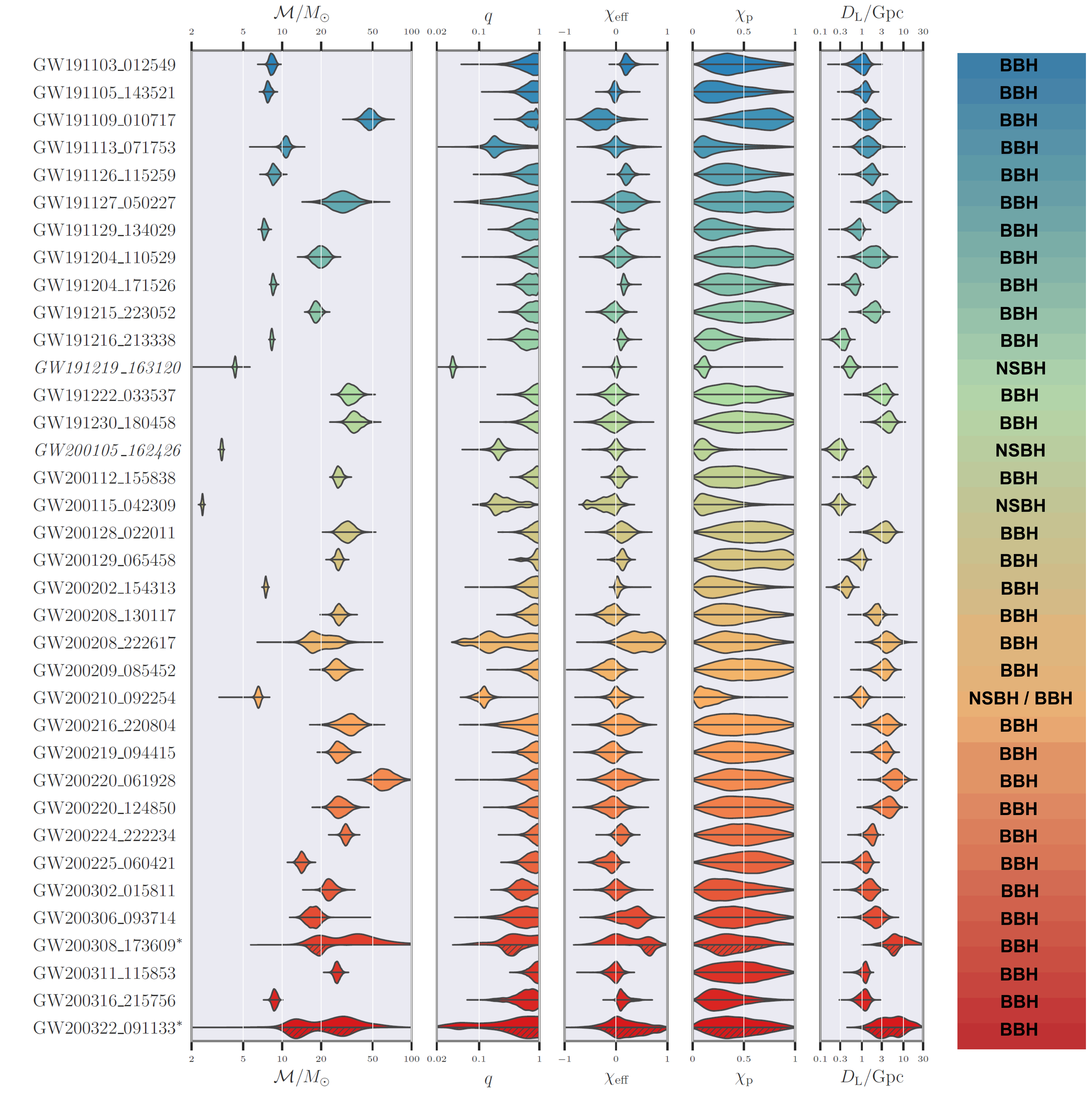

Properties of the events reported in the O3b catalog are listed above: chirp mass $\mathcal{M}$, in solar masses, mass ratio q, effective inspiral spin $\chi_{\rm eff}$, effective precession spin $\chi_{\rm p}$, and distance $D_{\rm L}$, in Gigaparsecs.

Also listed for each event is the most likely source classification. Events labelled BBH are those that we are confident are binary black hole coalescences. Events labelled NSBH are those that are possible neutron star and black hole coalescences. (We consider compact objects that are likely to have masses less than 3 times the mass of our sun to be possible neutron star candidates).

Credits: Martin Hendry, Hannah Middleton

LIGO/Virgo/KAGRA

GWTC-3（Gravitational Wave Transient Catalog 3）

Nov 5, 2021 arXiv:2111.03606

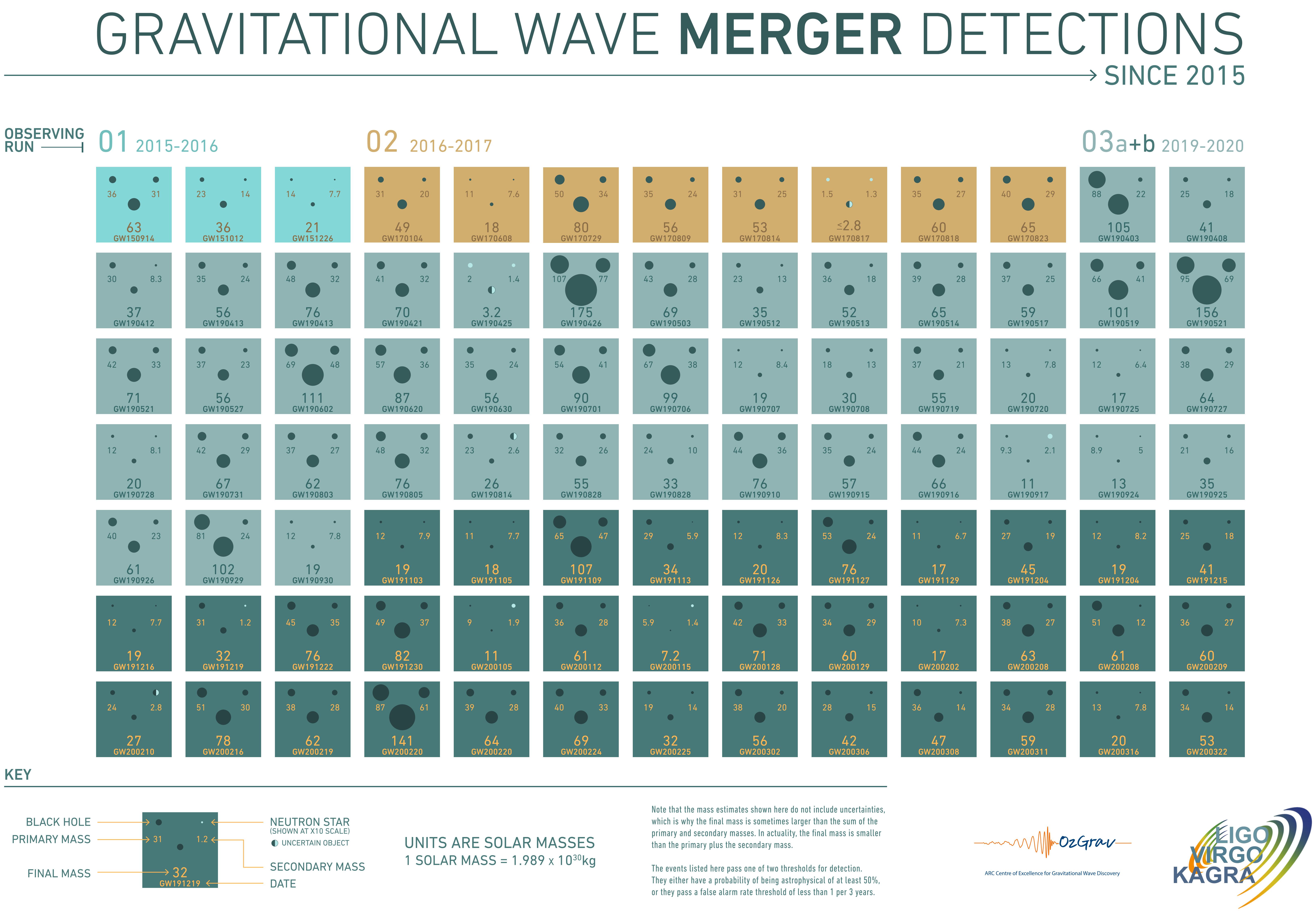

Consistency of GWTC-2 & 3

arXiv:2111.03634

＊ Populations of 77 events of FAR < 1 / year

The observations in GWTC-3 are consistent with the predictions from GWTC-2

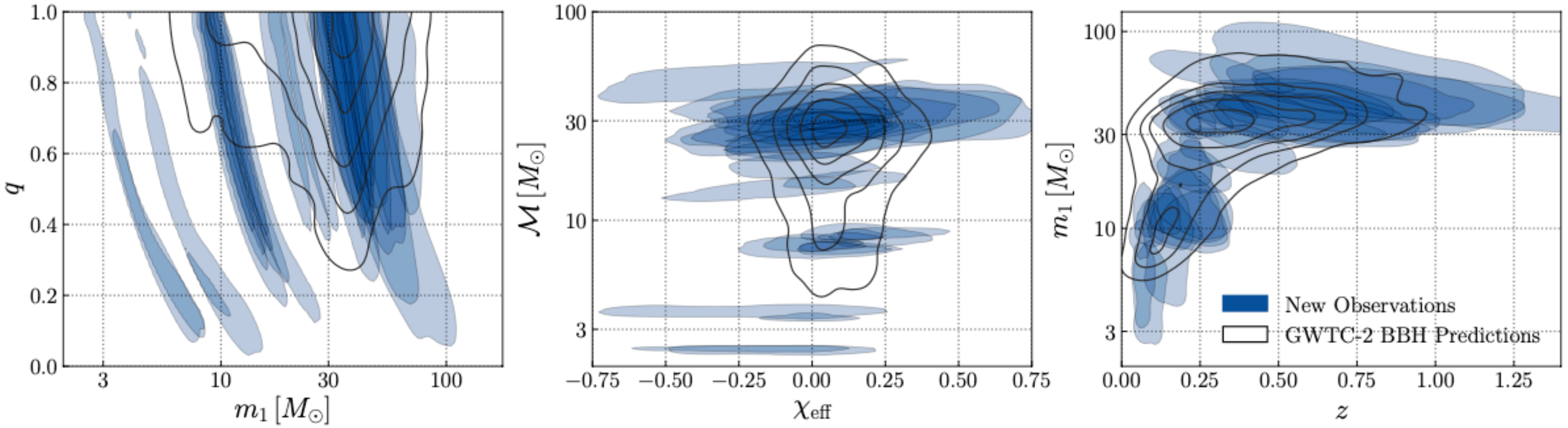

FIG. 1. New observations since GWTC-2. The measured properties of new CBC candidates announced since GWTC-2 with FAR< 1/yr and reported parameters (blue shaded regions), compared to the expected population of detected BBHs (black contours) as inferred from past analysis of GWTC-2 with the same FAR threshold [25]. The left hand plot shows the inferred primary mass m_1 and mass ratio q; the center plot shows the effective spin $\chi_{\rm eff}$ and chirp mass $\mathcal{M}$ and the right plot shows redshift z and primary mass. The least-massive sources in this sample include NSBH events GW200105 and GW200115.

$$q = m_2/m_1 \qquad \mathcal{M} = \frac{(m_1 m_2)^{3/5}}{(m_1+m_2)^{1/5}} \qquad \chi_{\rm eff} = \frac{(m_1\boldsymbol{\chi}_1 + m_2\boldsymbol{\chi}_2)\cdot\hat{\boldsymbol{L}}}{m_1+m_2}$$

- dimensionless spin of BH $\boldsymbol{\chi}_i = \boldsymbol{S}_i/m_i^2$
- orbital angular momentum $\hat{\boldsymbol{L}}$

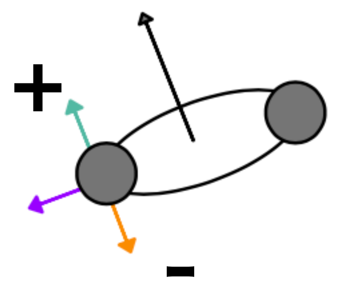

Neutron Stars

arXiv:2111.03634

＊ 7 events with NS

Name	$\mathrm{FAR_{min}}$ (yr^{-1})	$P(m < M_{\mathrm{max,TOV}})$	$P(m < M_{\mathrm{low}}^{\mathrm{gap}})$	Classification
GW170817	$< 1 \times 10^{-5}$	0.99	0.98	BNS
GW190425	3.38×10^{-02}	0.68	0.73	BNS
GW190814	$< 1 \times 10^{-5}$	0.06	0.19	BBH
GW200105	2.04×10^{-01}	0.94	0.74	NSBH
GW200115	$< 1 \times 10^{-5}$	0.95	0.97	NSBH
GW190426	9.12×10^{-01}	0.82	–	NSBH
GW190917	6.56×10^{-01}	0.56	–	NSBH

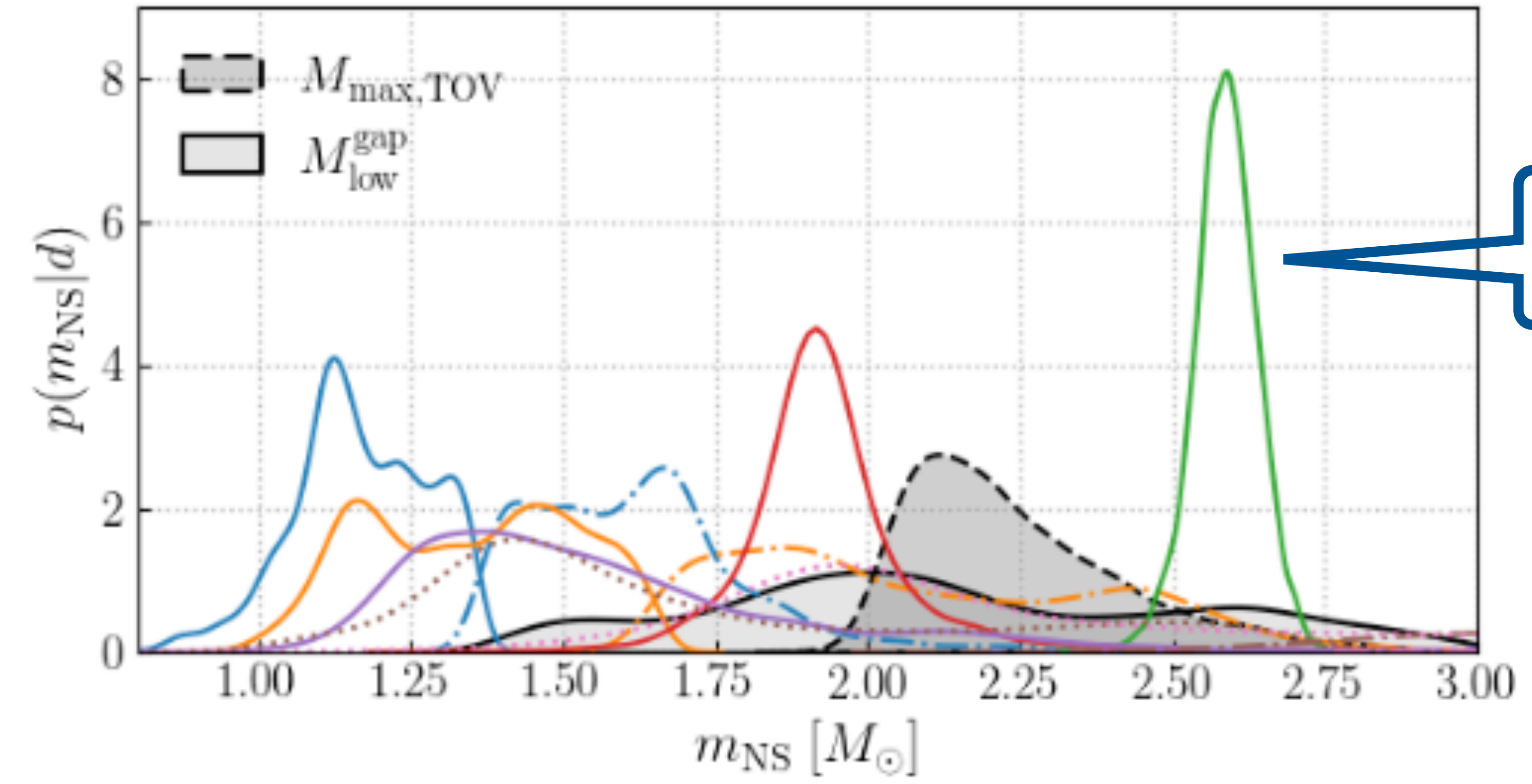

GW190814 is outlier

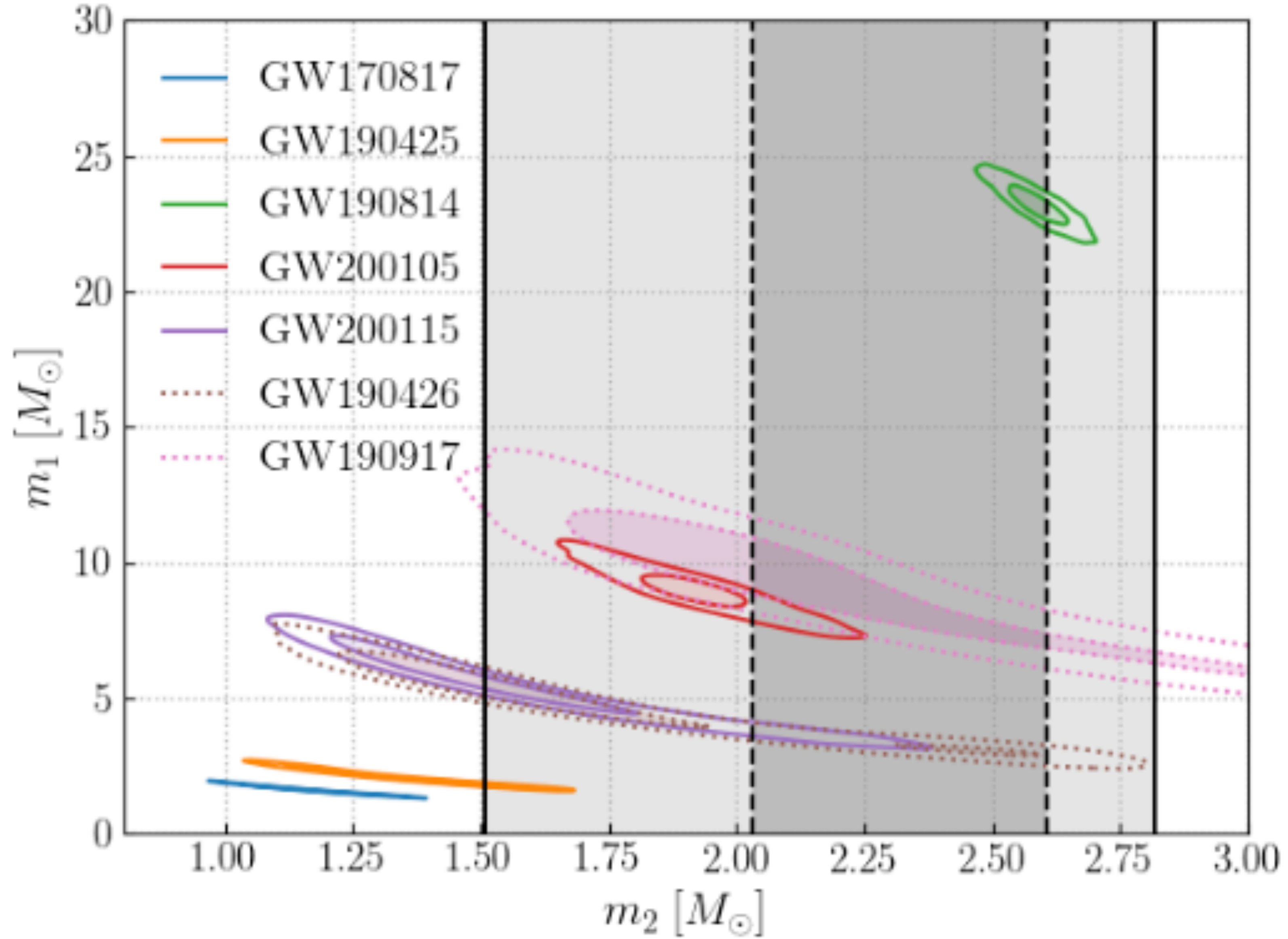

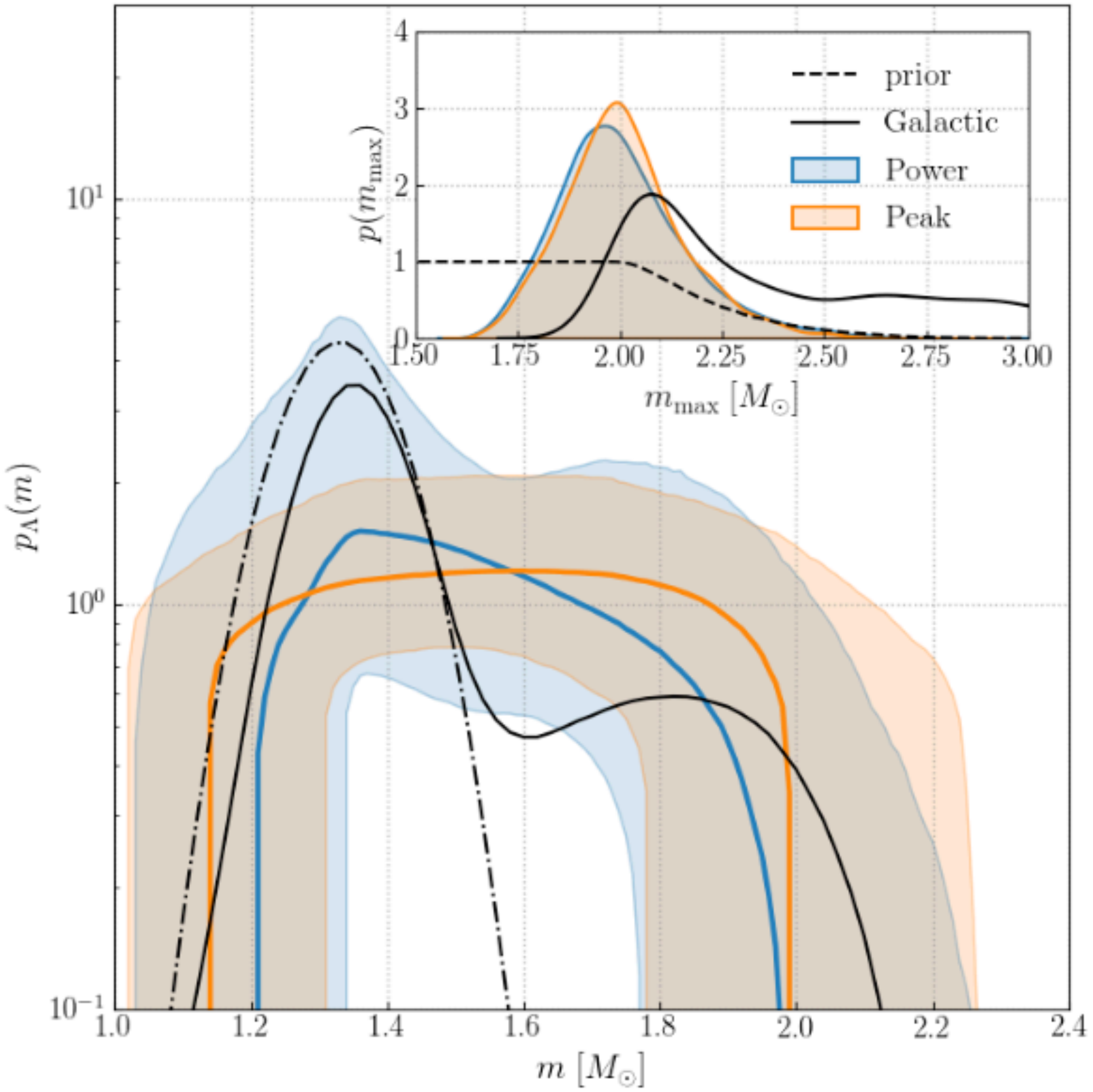

Mmax is consistent with galactic pulsars.

consistent with uniform distribution.

Population Properties in GWTC-3（3）

LIGO/Virgo/KAGRA

Black Holes

arXiv:2111.03634

binary parameters

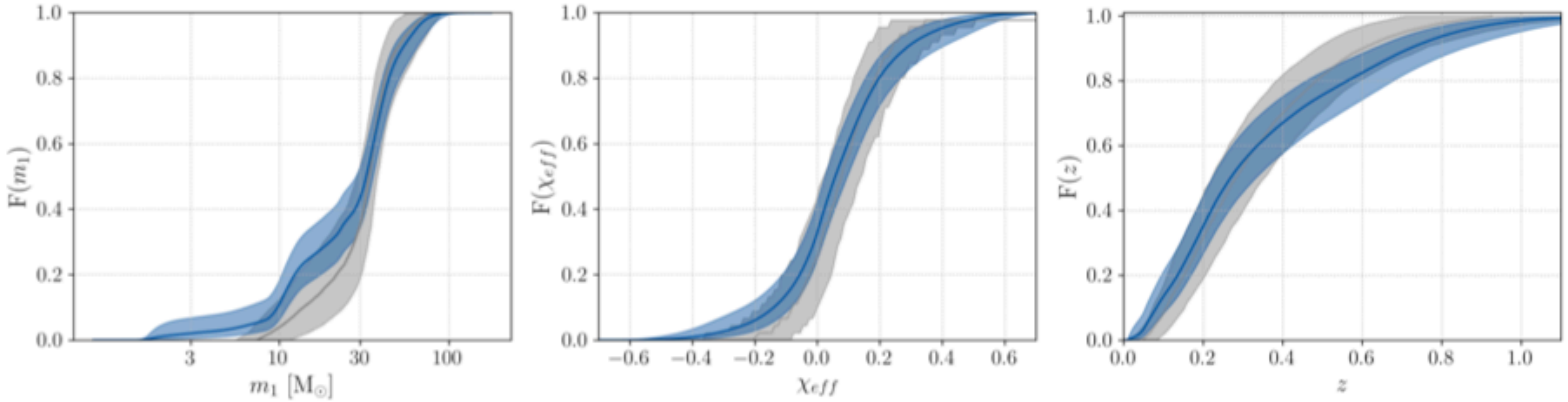

FIG. 9. The empirical cumulative density function $\hat{F} = \sum_k P_k(x)/N$ of observed binary parameter distributions (derived from the single-event cumulative distributions $P_k(x)$ for each parameter x) are shown in black for primary mass (left), effective inspiral spin (center), and redshift (right). All binaries used in this study with FAR< 1/4yr are included, and each is analyzed using our fiducial noninformative prior. For comparison, the gray bands show the expected observed distributions, based on our previous analysis of GWTC-2 BBH. Solid lines show the medians, while the shading indicates a 90% credible interval on the empirical cumulative estimate and selection-weighted reconstructed population, respectively. GW190814 is excluded from this analysis.

primary mass m_1 mass ratio q

power-low with single peak at 35M fits well the distribution

few events over 45M comparing with GWTC-2

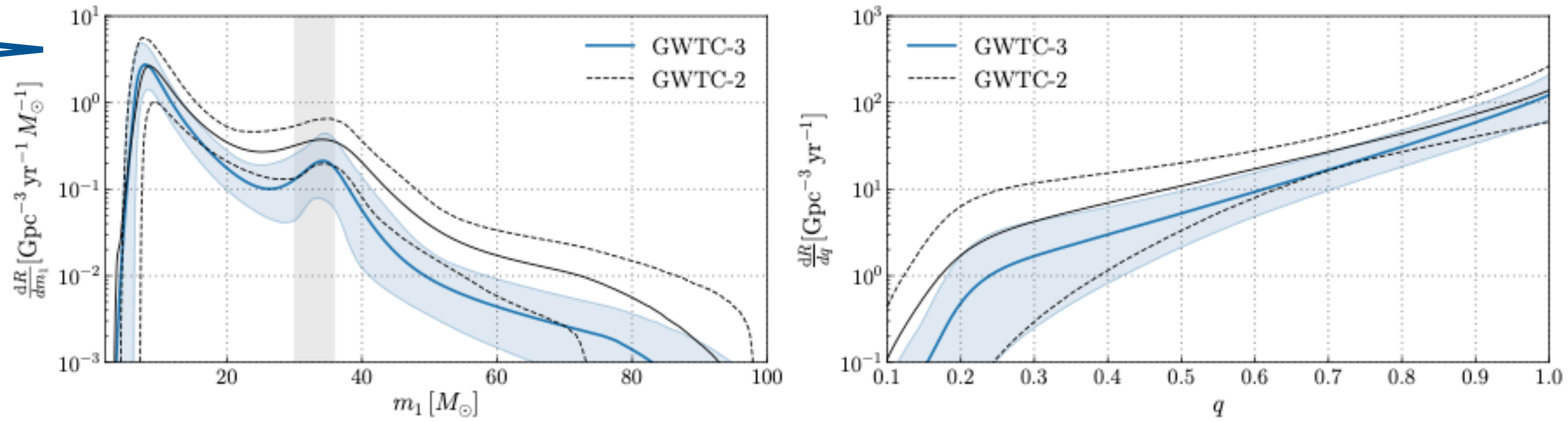

FIG. 10. The astrophysical BBH primary mass (left) and mass ratio (right) distributions for the fiducial PP model, showing the differential merger rate as a function of primary mass or mass ratio. The solid blue curve shows the posterior population distribution (PPD) with the shaded region showing the 90% credible interval. The black solid and dashed lines show the PPD and 90% credible interval from analyzing GWTC-2 as reported in [11]. The vertical gray band in the primary mass plot shows 90% credible intervals on the location of the mean of the Gaussian peak for the fiducial model.

Black Hole Spins

arXiv:2111.03634

$$\chi_{\rm eff} = \frac{(m_1\boldsymbol{\chi}_1 + m_2\boldsymbol{\chi}_2)\cdot\hat{\boldsymbol{L}}}{m_1+m_2}$$

- dimensionless spin of BH $\boldsymbol{\chi}_i = \boldsymbol{S}_i/m_i^2$
- orbital angular momentum $\hat{\boldsymbol{L}}$

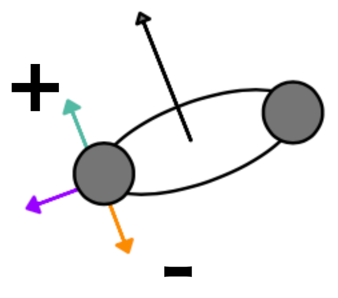

binary formation was
+ co-evolution
- dynamical

power-low with single peak
at 35M fits well the distribution

$\chi_{\rm eff}$ centered at 0.05

GW191204_171526	12M + 8 M -> 19 M	Effective inspiral spin > 0 0.16-0.05+0.08
GW191109_010717	65 M+ 47 M - > 107 M	Effective inspiral spin < 0 -0.29-0.31+0.42

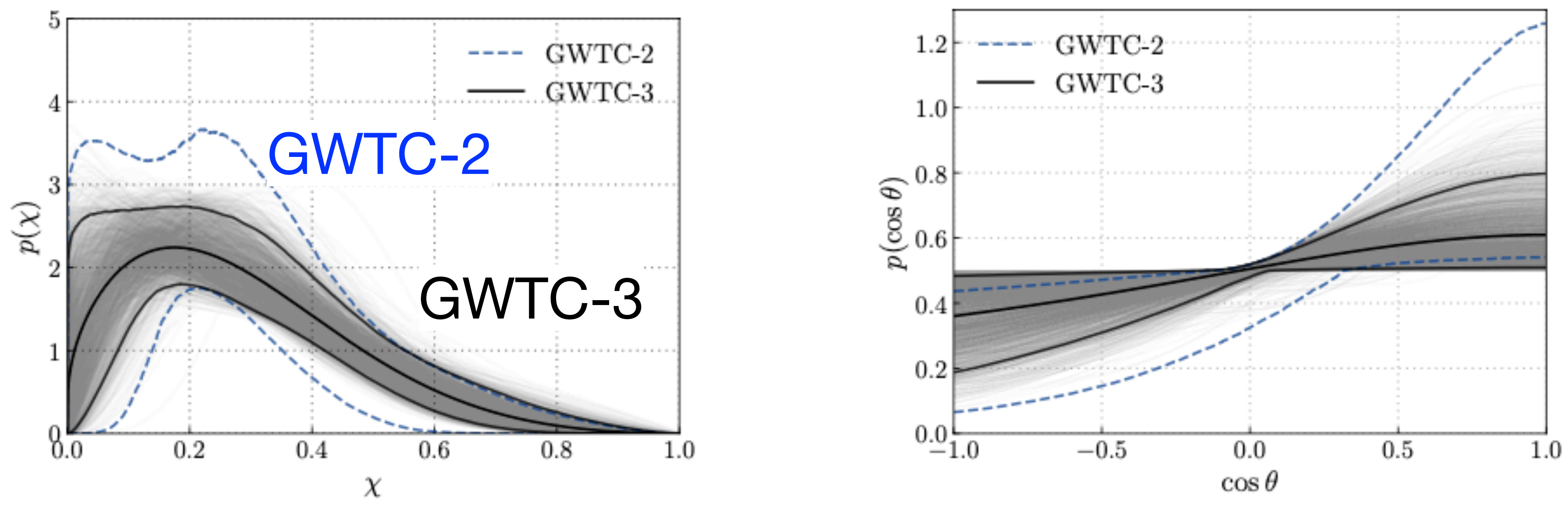

FIG. 15. The distributions of component spin magnitudes χ (*left*) and spin-orbit misalignment angles θ (*right*) among binary black hole mergers, inferred using the DEFAULT component spin model described further in Sect. B 2 a; e.g., both spin magnitudes are drawn from the same distribution. In each figure, solid black lines denote the median and central 90% credible bounds inferred on $p(\chi)$ and $p(\cos\theta)$ using GWTC-3. The light grey traces show individual draws from our posterior distribution on the DEFAULT model parameters, while the blue traces show our previously published results obtained using GWTC-2. As with GWTC-2, in GWTC-3 we conclude that the spin magnitude distribution peaks near $\chi_i \approx 0.2$, with a tail extending towards larger values. Meanwhile, we now more strongly favor isotropy, obtaining a broad $\cos\theta_i$ distribution that may peak at alignment ($\cos\theta_i = 1$) but that is otherwise largely uniform across all $\cos\theta$.

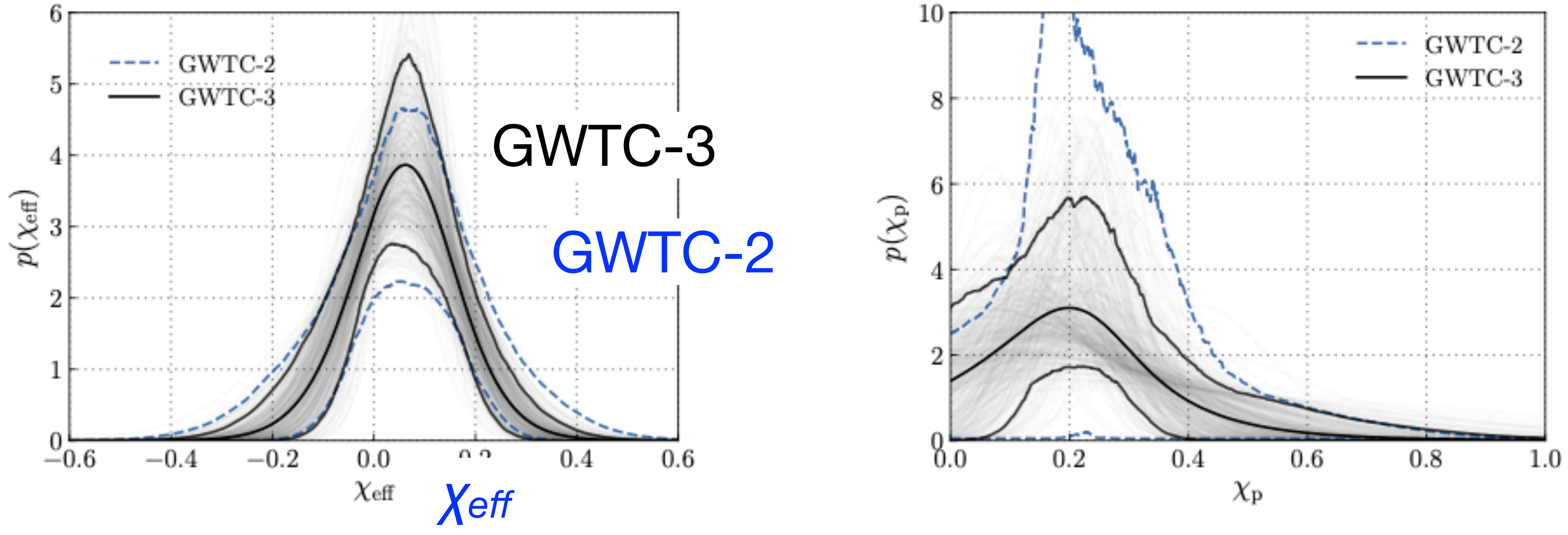

FIG. 16. *Left panel*: Inferred distribution of $\chi_{\rm eff}$ for our latest full analysis in black. For comparison, the blue distribution and interval shows our inferences derived from GWTC2. *Right panel*: Corresponding result for $\chi_{\rm p}$. While both panels in this figure are derived using the Gaussian spin model, we find similar conclusions with the other spin models used to analyze GWTC-2.

Population Properties in GWTC-3 (4)

LIGO/Virgo/KAGRA

Merger Rates

arXiv:2111.03634

	BNS	NSBH	BBH	NS-Gap	BBH-gap	Full
	$m_1 \in [1, 2.5] M_\odot$	$m_1 \in [2.5, 50] M_\odot$	$m_1 \in [2.5, 100] M_\odot$	$m_1 \in [2.5, 5] M_\odot$	$m_1 \in [2.5, 100] M_\odot$	$m_1 \in [1, 100] M_\odot$
	$m_2 \in [1, 2.5] M_\odot$	$m_2 \in [1, 2.5] M_\odot$	$m_2 \in [2.5, 100] M_\odot$	$m_2 \in [1, 2.5] M_\odot$	$m_2 \in [2.5, 5] M_\odot$	$m_2 \in [1, 100] M_\odot$
PDB (pair)	960^{+1700}_{-700}	59^{+81}_{-38}	25^{+10}_{-7}	41^{+69}_{-30}	$9.3^{+19.0}_{-7.6}$	1100^{+1700}_{-750}
PDB (ind)	250^{+640}_{-200}	170^{+150}_{-89}	22^{+9}_{-6}	29^{+55}_{-23}	10^{+15}_{-8}	470^{+830}_{-300}
MS	470^{+1400}_{-410}	57^{+120}_{-42}	42^{+88}_{-20}	$3.7^{+20}_{-3.4}$	$0.17^{+56}_{-0.16}$	650^{+1600}_{-460}
BGP	99^{+260}_{-86}	32^{+62}_{-25}	33^{+16}_{-10}	$2.1^{+33}_{-2.1}$	$5.1^{+12}_{-4.0}$	180^{+260}_{-110}
MERGED	13 – 1900	7.4 – 320	16 – 130	0.029 – 84	0.01 – 56	71 – 2200

TABLE II. Merger rates in $\mathrm{Gpc}^{-3}\,\mathrm{yr}^{-1}$ for the various mass bins, assuming merger rates per unit comoving volume are redshift-independent. BNS, NSBH and BBH regions are based solely upon component masses, with the split between NS and BH taken to be $2.5 M_\odot$. We also provide rates for binaries with one component in the purported mass gap between $2.5 M_\odot$ and $5 M_\odot$. For all but the last row, merger rates are quoted at the 90% credible interval. For the last row, we provide the union of 90% credible intervals for the preceding three rows, as our most conservative realistic estimate of the merger rate for each class accounting for model systematics. The PDB (pair) model is distinct from the other three models due to its use of a pairing function [107] and is therefore excluded from the union of credible intervals in the final row. In Sec. VI we estimate the merger rate for BBH alone, accounting for variation in merger rate versus redshift.

GWTC-2

$$\mathcal{R}_{\rm BBH} = 23.9^{+14.9}_{-8.6}\,\mathrm{Gpc}^{-3}\,\mathrm{yr}^{-1}$$

$$\mathcal{R}_{\rm BNS} = 320^{+490}_{-240}\,\mathrm{Gpc}^{-3}\,\mathrm{yr}^{-1}$$

GWTC-3

$$\mathcal{R}_{\rm BBH} = 17.3\text{–}45\ \mathrm{Gpc}^{-3}\,\mathrm{yr}^{-1}\ \text{at}\ z = 0.2$$

$$\mathcal{R}_{\rm BNS} = 13\text{–}1900\ \mathrm{Gpc}^{-3}\,\mathrm{yr}^{-1}$$

$$\mathcal{R}_{\rm NSBH} = 7.4\text{–}320\ \mathrm{Gpc}^{-3}\,\mathrm{yr}^{-1}$$

GW transient catalog

O3b (2020/11/1 - 2021/3/27) **After O3b : GWTC-3 (2021/11/7 released)**

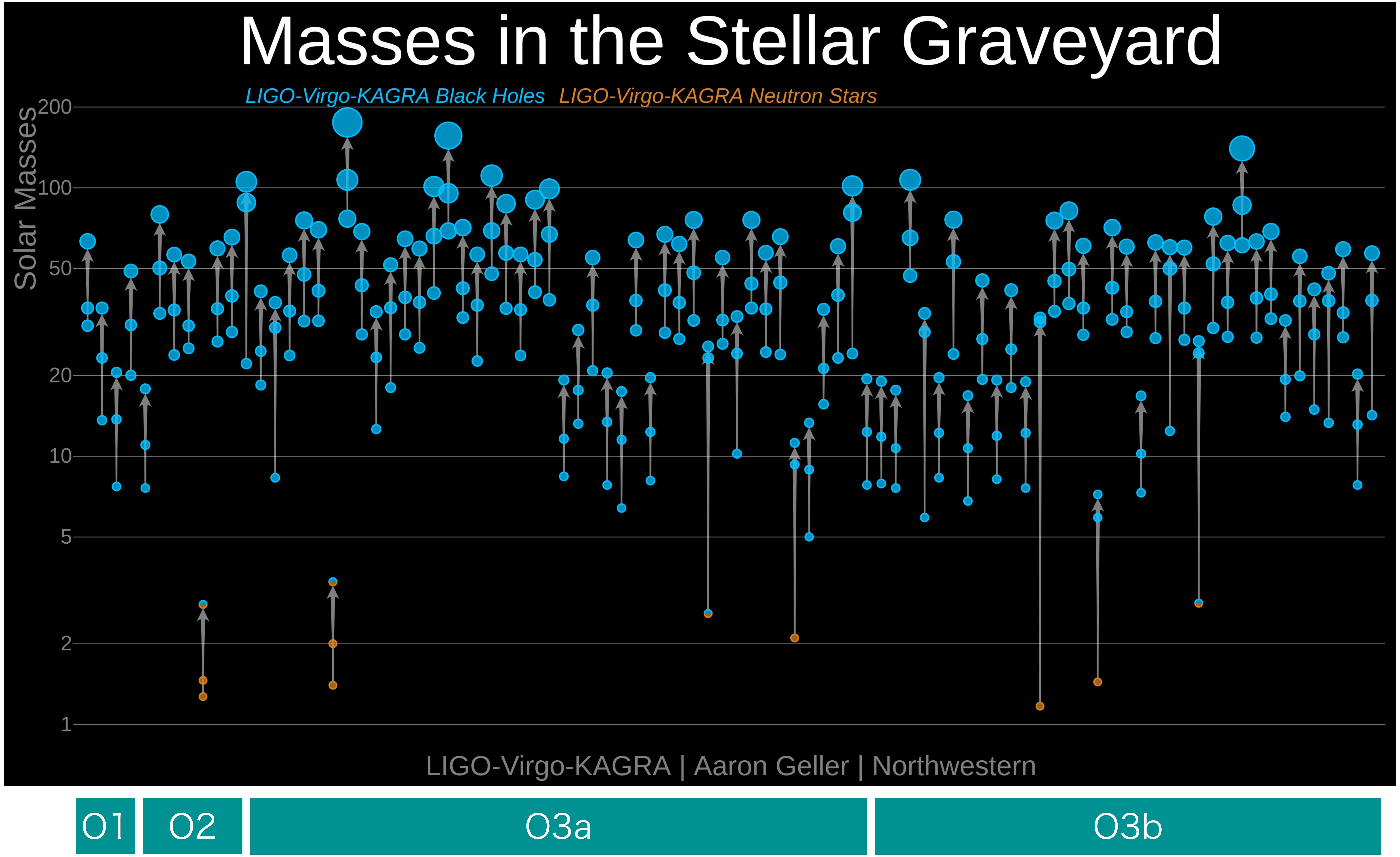

https://media.ligo.northwestern.edu/gallery/mass-plot

GWTC-3

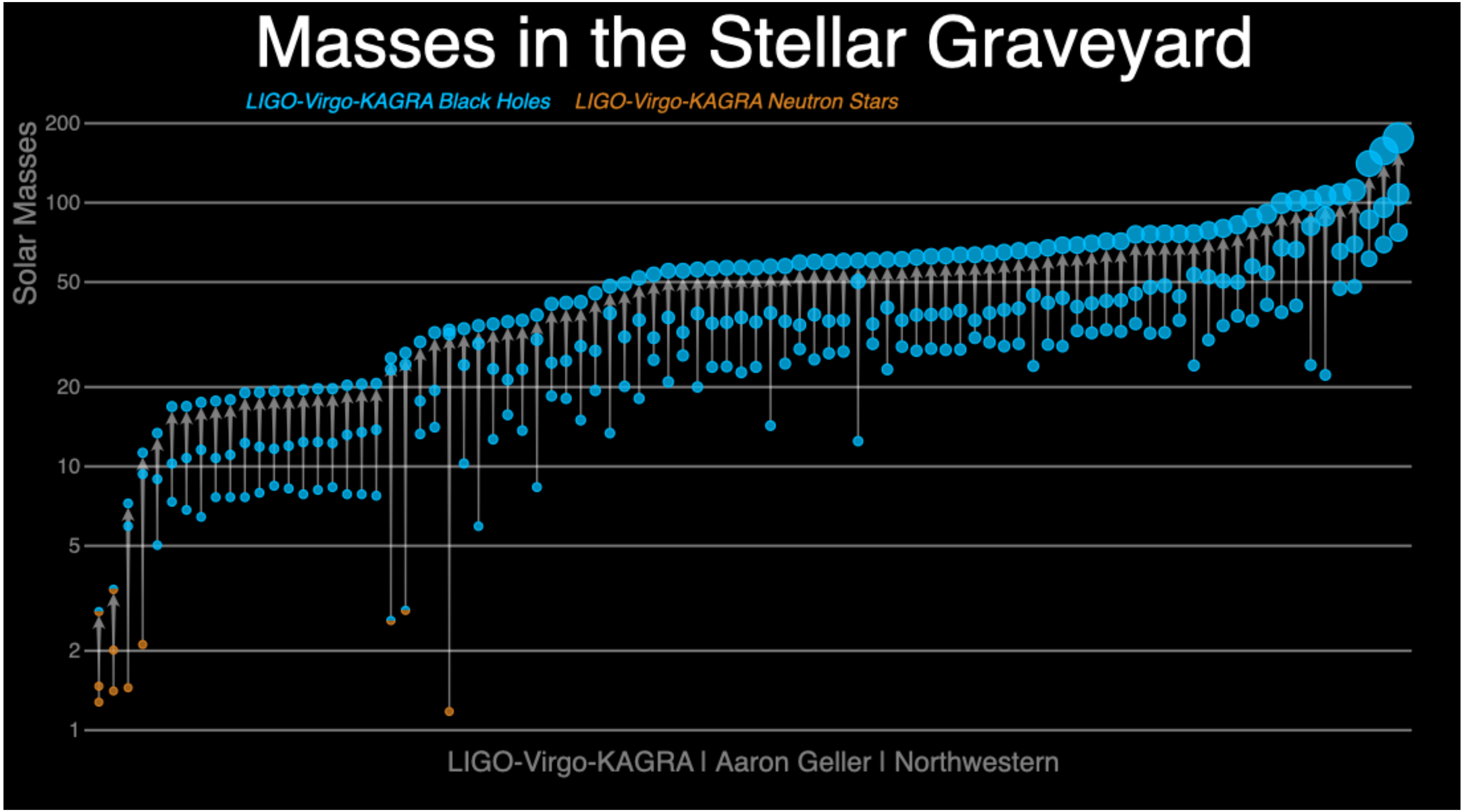
Masses in the Stellar Graveyard
LIGO-Virgo-KAGRA Black Holes
LIGO-Virgo-KAGRA Neutron Stars
Solar Masses
200
100
50
20
10
5
2
1
LIGO-Virgo-KAGRA | Aaron Geller | Northwestern

GWTC-3

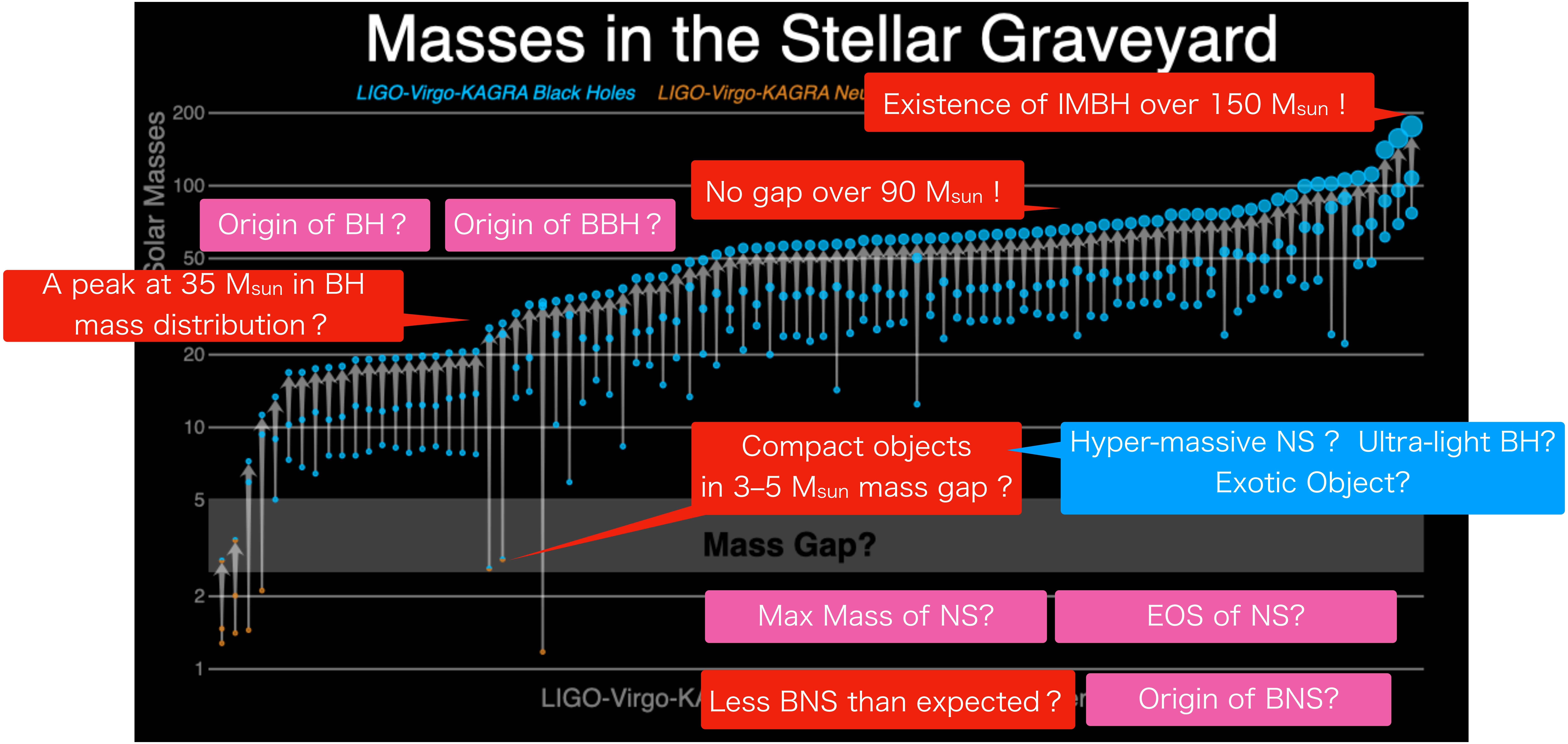
Masses in the Stellar Graveyard
LIGO-Virgo-KAGRA Black Holes
LIGO-Virgo-KAGRA Neu
Solar Masses
200
100
50
20
10
5
2
1
Mass Gap?
LIGO-Virgo-K
Existence of IMBH over 150 Msun !
No gap over 90 Msun !
Origin of BH？
Origin of BBH？
A peak at 35 Msun in BH mass distribution？
Compact objects in 3–5 Msun mass gap？
Hyper-massive NS？ Ultra-light BH? Exotic Object?
Max Mass of NS?
EOS of NS?
Less BNS than expected？
Origin of BNS?

LVK papers http://www.oit.ac.jp/is/shinkai/linkGW.html

Only for selected ones before O3a, and all for after O3b.

	abbrev	title	arXiv, publ	Science Summary
LVK	O3bAstroDist	The population of merging compact binaries inferred using gravitational waves through GWTC-3	arXiv:2111.03634	Eng , Jap Nov 5, 2021
LVK	O3bGRB	Search for Gravitational Waves Associated with Gamma-Ray Bursts Detected by Fermi and Swift During the LIGO-Virgo Run O3b	arXiv:2111.03608	Eng , Jap Nov 5, 2021
LVK	O3bCatalog	GWTC-3: Compact Binary Coalescences Observed by LIGO and Virgo During the Second Part of the Third Observing Run	arXiv:2111.03606	Eng , Jap Nov 5, 2021
LVK	O3Cosmology	Constraints on the cosmic expansion history from GWTC-3	arXiv:2111.03604	Eng , Jap Nov 5, 2021
LVK	O3Radiometer	All-sky, all-frequency directional search for persistent gravitational-waves from Advanced LIGO's and Advanced Virgo's first three observing runs	arXiv:2110.09834	Eng , Jap Oct 27, 2021
LV	O3aSSM	Search for subsolar-mass binaries in the first half of Advanced LIGO and Virgo's third observing run	arXiv:2109.12197	Eng , Jap Sep 28, 2021
LVK	O3LMXBsAMXPs	Search for continuous gravitational waves from 20 accreting millisecond X-ray pulsars in O3 LIGO data	arXiv:2109.09255	Eng , Jap Sep 20, 2021
LV	GWTC2.1	GWTC-2.1: Deep Extended Catalog of Compact Binary Coalescences Observed by LIGO and Virgo During the First Half of the Third Observing Run	arXiv:2108.01045	Eng , Jap Aug 2, 2021
LVK	O3LongBurst	All-sky search for long-duration gravitational-wave bursts in the third Advanced LIGO and Advanced Virgo run	arXiv: 2107.13796	Eng , Jap July 30, 2021
LVK	O3ShortBurst	All-sky search for short gravitational-wave bursts in the third Advanced LIGO and Advanced Virgo run	arXiv: 2107.03701	Eng , Jap July 9, 2021
LVK	O3ShortBurst	All-sky Search for Continuous Gravitational Waves from Isolated Neutron Stars in the Early O3 LIGO Data	arXiv: 2107.00600	Eng , Jap July 1, 2021
LVK	NSBH	Observation of Gravitational Waves from Two Neutron Star–Black Hole Coalescences	ApJL 915; L5 (2021)	Eng , Jap June 30, 2021
LVK	O3IMBH	Search for intermediate mass black hole binaries in the third observing run of Advanced LIGO and Advanced Virgo	arXiv:2105.15120 submitted to	Eng , Jap May 31, 2021
LVK	O3DarkPhoton	Constraints on dark photon dark matter using data from LIGO's and Virgo's third observing run	arXiv:2105.13085 submitted to	Eng , Jap May 27, 2021
LVK	O3DirectedSNR	Searches for continuous gravitational waves from young supernova remnants in the early third observing run of Advanced LIGO and Virgo	arXiv:2105.11641 submitted to	Eng , Jap May 26, 2021
LV	O3aLensing	Search for lensing signatures in the gravitational-wave observations from the first half of LIGO-Virgo's third observing run	arXiv:2105.06384 submitted to	Eng , Jap May 13, 2021
LVK	O3aRmode	Constraints from LIGO O3 data on gravitational-wave emission due to r-modes in the glitching pulsar PSR J0537-6910	arXiv:2104.14417 submitted to	Eng , Jap Apr 30, 2021
LV	O2H0	A Gravitational-wave Measurement of the Hubble Constant Following the Second Observing Run of Advanced LIGO and Virgo	arXiv: ApJ 909:218 (2021)	Eng , Jap Mar 19, 2021
LVK	O3StochDirectional	Search for anisotropic gravitational-wave backgrounds using data from Advanced LIGO's and Advanced Virgo's first three observing runs	arXiv:2103.08520 submitted to	Eng , Jap Mar 16, 2021
LVK	O3StochIso	Upper Limits on the Isotropic Gravitational-Wave Background from Advanced LIGO's and Advanced Virgo's Third Observing Run	arXiv:2101.12130 submitted to PRD	Eng, Jap Feb 01, 2021
LVK	O3CosmicString	Constraints on cosmic strings using data from the third Advanced LIGO-Virgo observing run	arXiv:2101.12248 PRL126, 241102 (2021)	Eng, Jap Feb 01, 2021
LVK	PSR J0537-6910	Diving below the spin-down limit: Constraints on gravitational waves from the energetic young pulsar PSR J0537-6910	arXiv:2012.12926 ApJL 913 L27 (2021)	Eng, Jap Dec 25, 2020

LVK-EPO (Education & Public Outreach) provides Science Summaries

LIGO Scientific Collaboration

News | Detections | Our science explained | Multimedia | Educational resources | For researcher

Intro to LIGO & Gravitational Waves | Science Summaries | Popular Articles | Frequently Asked

SUMMARIES OF LSC/LVK SCIENTIFIC PUBLICATIONS

For each of our new research articles, we feature a summary of the paper's key points written for the general public. Simply click on any of the titles for an online version, or on the '[flyer]' links for a downloadable file in PDF format. Translations into several languages are also available for some of these summaries. Where not noted separately, translations can be accessed through their language acronyms (e.g. 'es' for Spanish, also see details in the sidebar) or from the top of the English online versions. Most recent papers, and their summaries, are written together by the LIGO Scientific Collaboration (LSC), the Virgo Collaboration and the KAGRA Collaboration, forming the LVK collaboration.

LATEST DETECTIONS

GWTC-3 (Nov 07, 2021) GWTC-3, a third catalog of gravitational-wave detections [flyer]

Also in: Chinese (simplified) [zh-Hans] | Chinese (traditional) [zh-Hant] | French [fr] | German [de] | Japanese [ja] | Polish [pl] | Spanish [es]

Companion papers: (also available in some other languages):

- Uncovering the population properties of black holes and neutron stars following LIGO and Virgo's third observing run [flyer] | [fr] | [ja] | [pl] | [zh-Hant]
- Improving measurements of the cosmic expansion with gravitational waves [flyer] | [fr] | [el] | [ja] | [zh-Hant]
- Searching for quiet gravitational waves produced by gamma-ray bursts in O3b [flyer] | [fr] | [zh-Hant]

https://www.ligo.org/science/outreach.php

LIGO-Virgo-KAGRA network for hunting gravitational waves

Contents

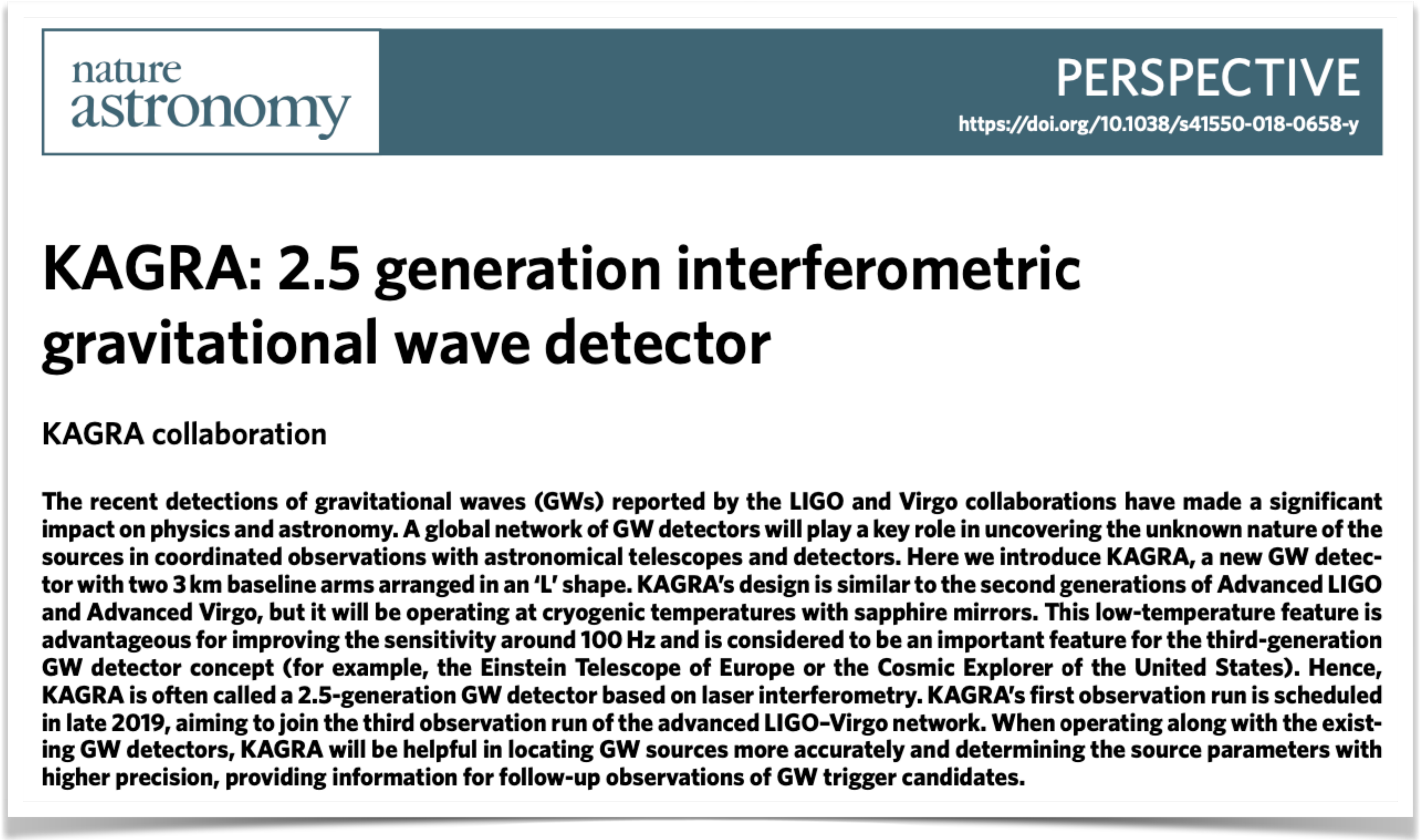

nature astronomy

PERSPECTIVE

https://doi.org/10.1038/s41550-018-0658-y

KAGRA: 2.5 generation interferometric gravitational wave detector

KAGRA collaboration

The recent detections of gravitational waves (GWs) reported by the LIGO and Virgo collaborations have made a significant impact on physics and astronomy. A global network of GW detectors will play a key role in uncovering the unknown nature of the sources in coordinated observations with astronomical telescopes and detectors. Here we introduce KAGRA, a new GW detector with two 3 km baseline arms arranged in an 'L' shape. KAGRA's design is similar to the second generations of Advanced LIGO and Advanced Virgo, but it will be operating at cryogenic temperatures with sapphire mirrors. This low-temperature feature is advantageous for improving the sensitivity around 100 Hz and is considered to be an important feature for the third-generation GW detector concept (for example, the Einstein Telescope of Europe or the Cosmic Explorer of the United States). Hence, KAGRA is often called a 2.5-generation GW detector based on laser interferometry. KAGRA's first observation run is scheduled in late 2019, aiming to join the third observation run of the advanced LIGO–Virgo network. When operating along with the existing GW detectors, KAGRA will be helpful in locating GW sources more accurately and determining the source parameters with higher precision, providing information for follow-up observations of GW trigger candidates.

Nature Astronomy 3, 35 (2019)
https://www.nature.com/articles/s41550-018-0658-y

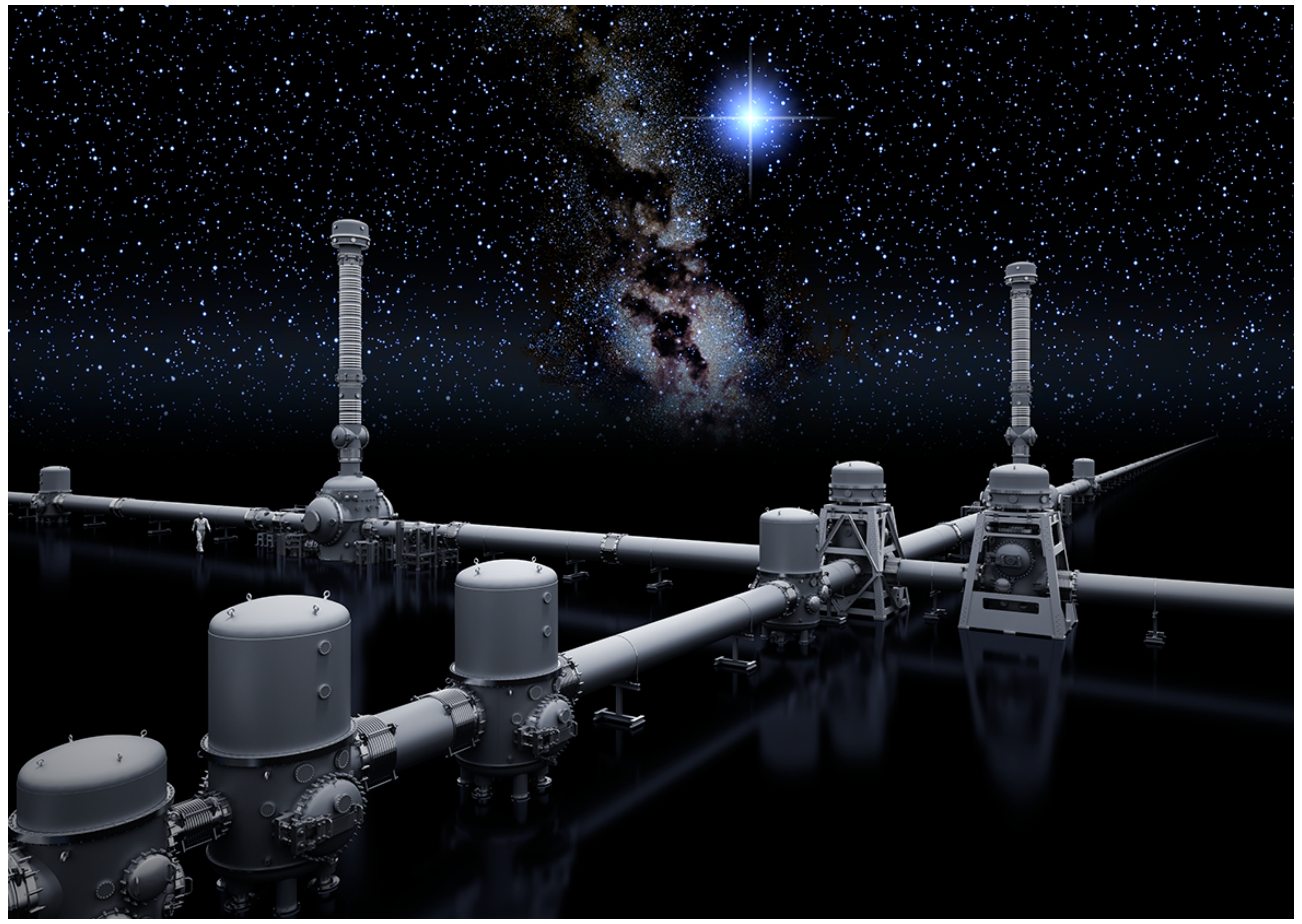

(c) KAGRA Collaboration / Rey.Hori

Hisaaki Shinkai (Osaka Inst. Tech.)
真貝寿明（大阪工業大学）

KAGRA Scientific Congress, board chair
on behalf of KAGRA collaboration

KAGRA (Kamioka Gravitational-Wave Observatory)

Mozumi
control office.
(15 min)

Toyama City
(60 min)

1000m under the summit of the Mt.

358m above the sea level.

http://gwcenter.icrr.u-tokyo.ac.jp/en/

（大型低温重力波望遠鏡）

former name LCGT = large cryogenic gravitational telescope

named by public naming contest, 神楽（かぐら）dance music in front of Gods

KAGRA (Kamioka Gravitational-Wave Observatory)

TAMA 300 m (NAOJ, Tokyo area, 2008)

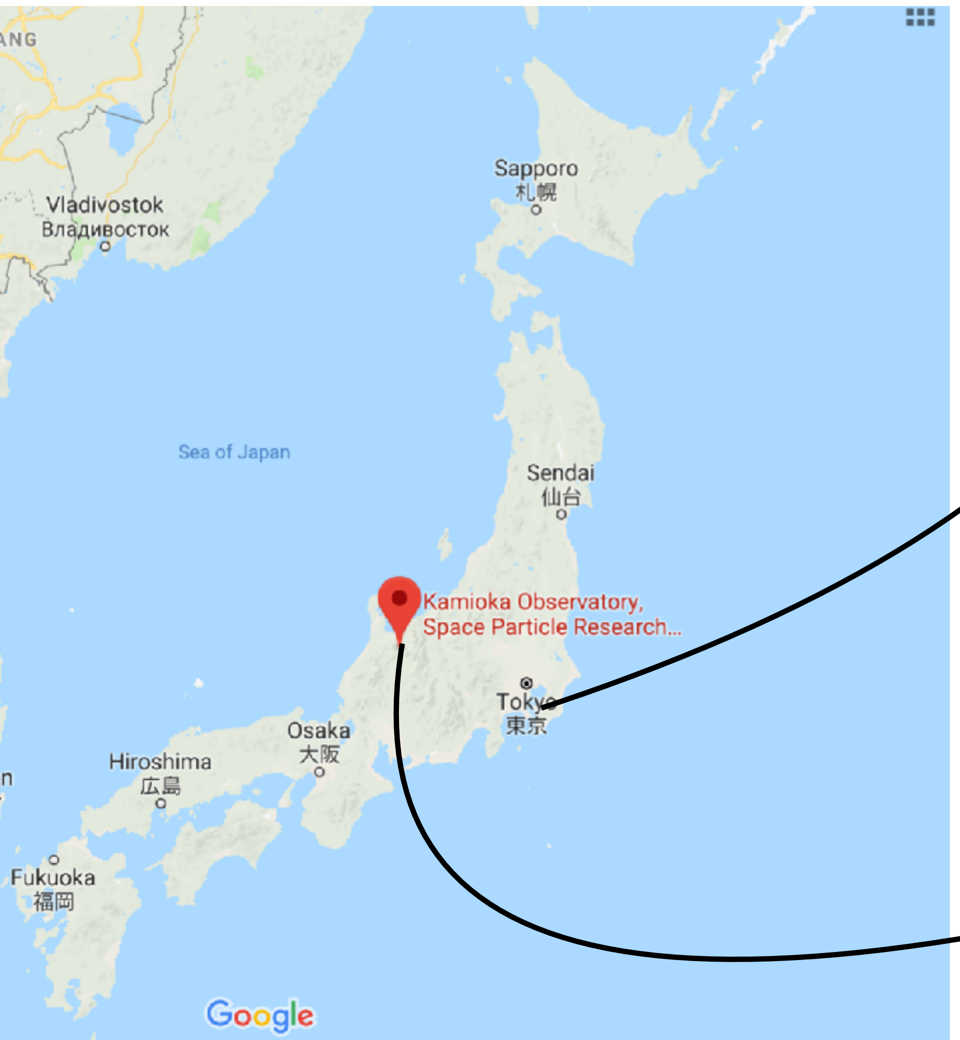

CLIO 20 m (Kamioka, 2010)

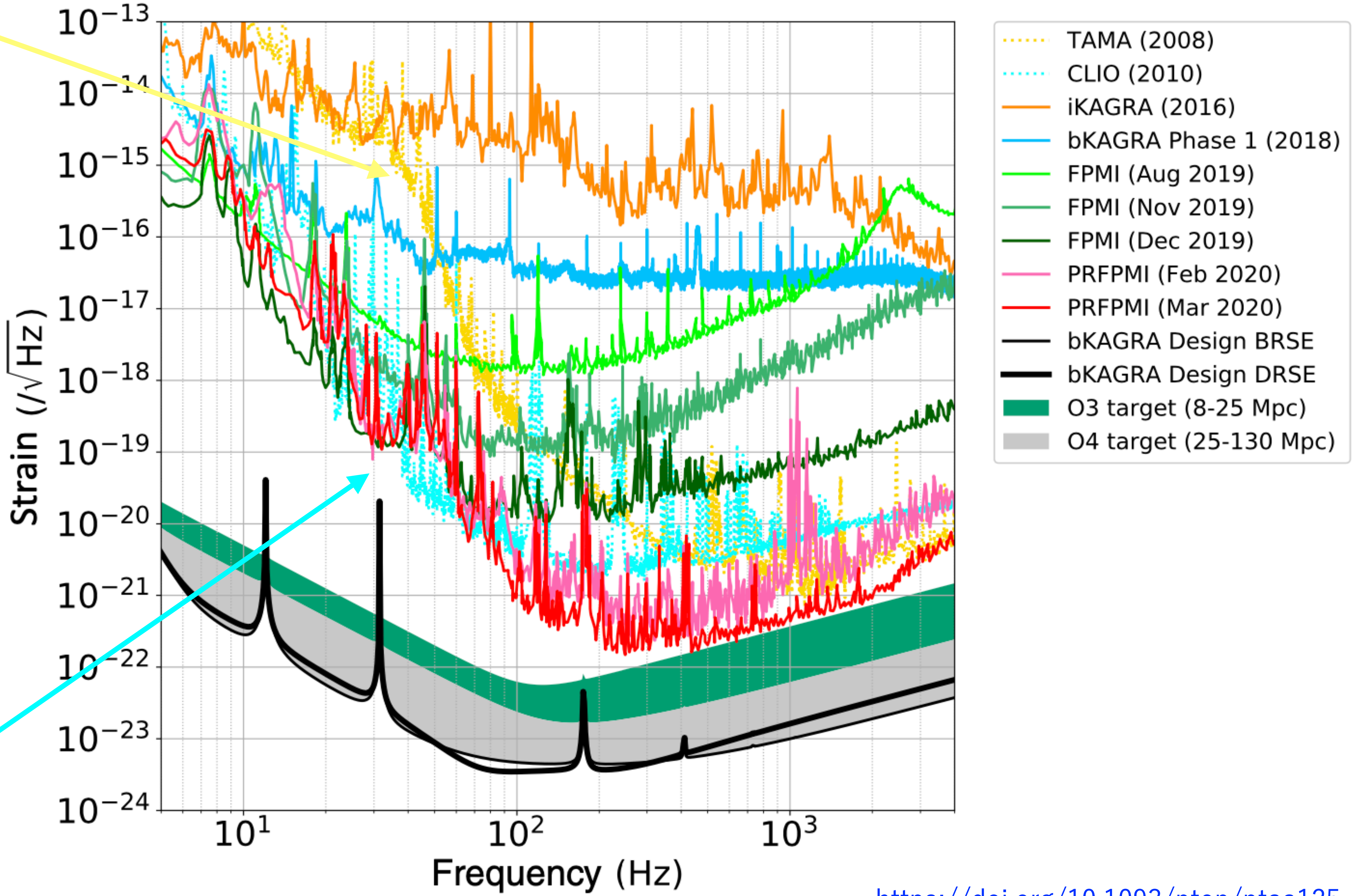

https://doi.org/10.1093/ptep/ptaa125

arXiv: 2005.05574

Brief History of KAGRA

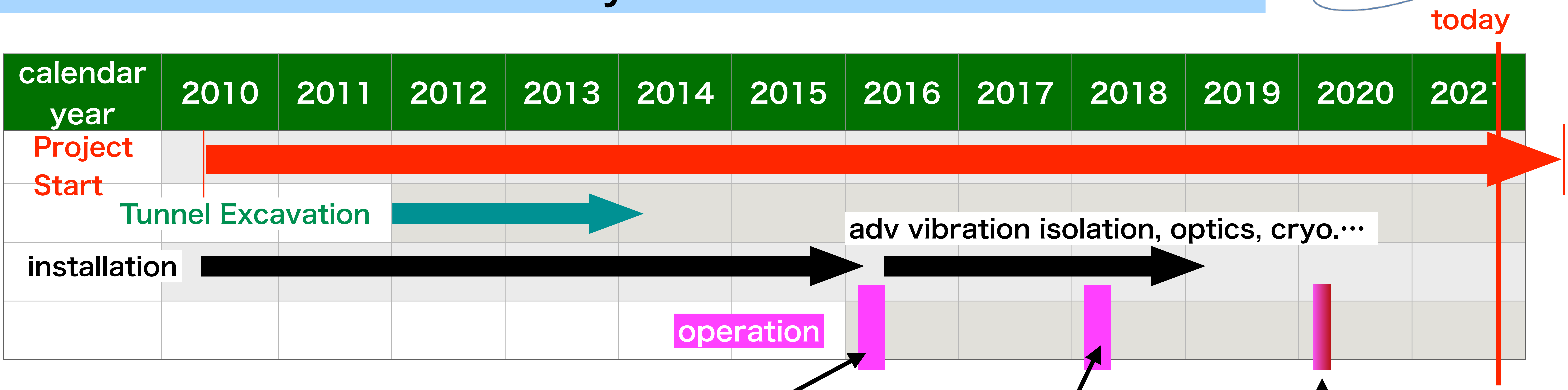

iKAGRA = initial KAGRA
bKAGRA = baseline KAGRA

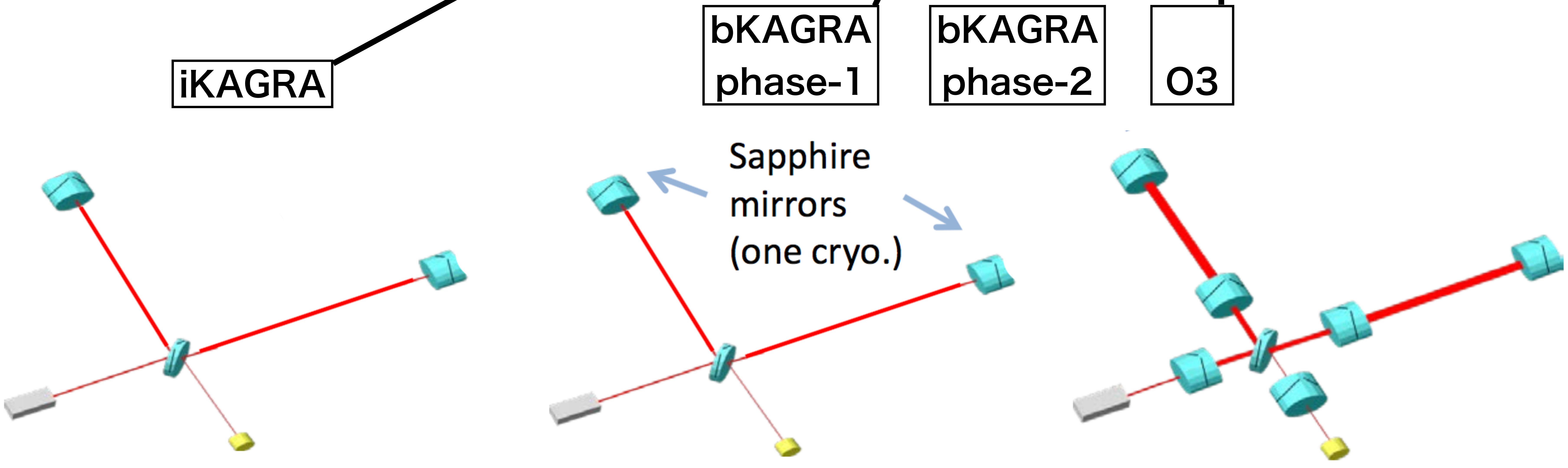

[arXiv:1712.00148]

[arXiv:1901.03569]

Basic Idea of the Interferometer

"Michelson" interferometer

Longer arm-length makes better sensitivity

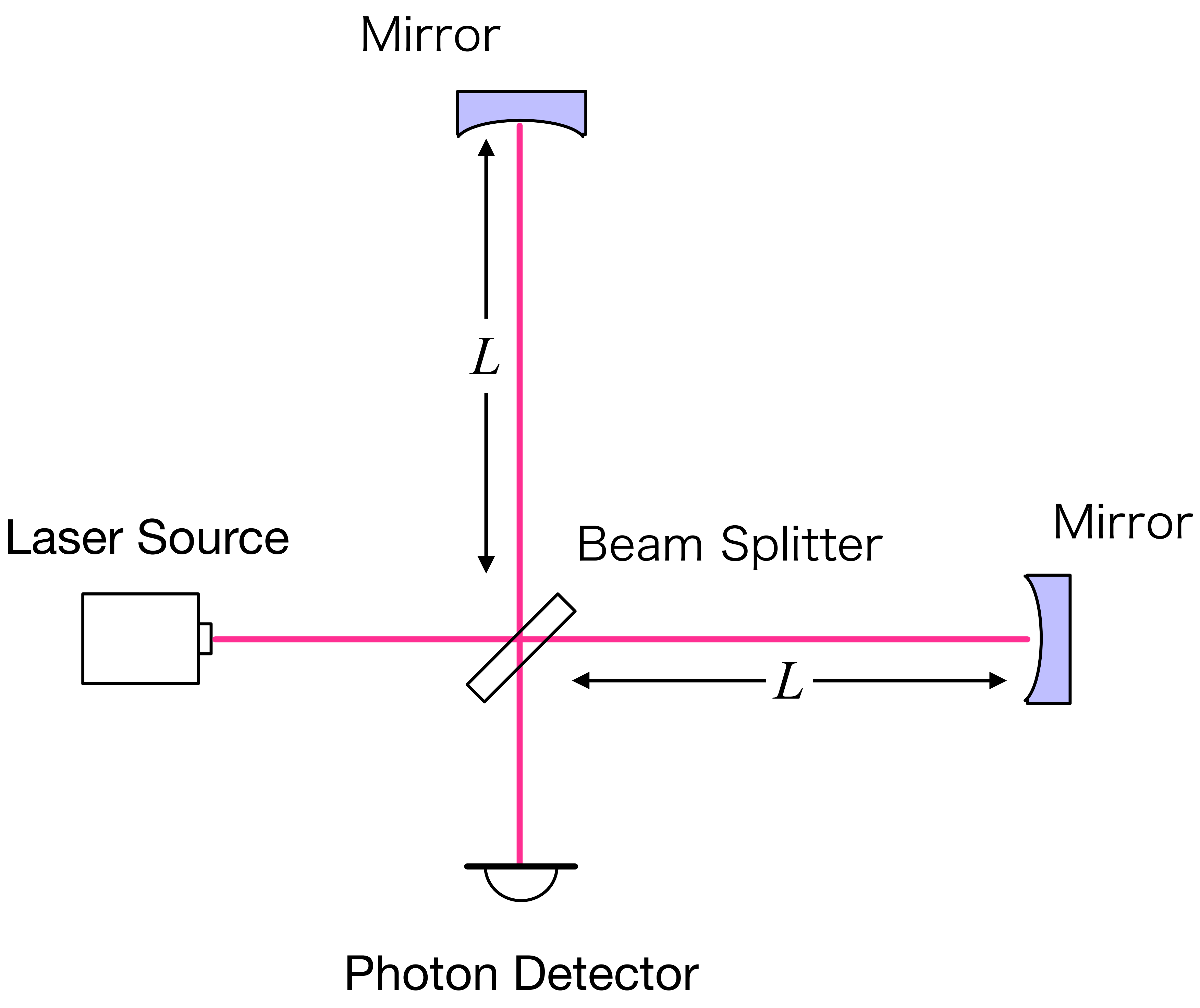

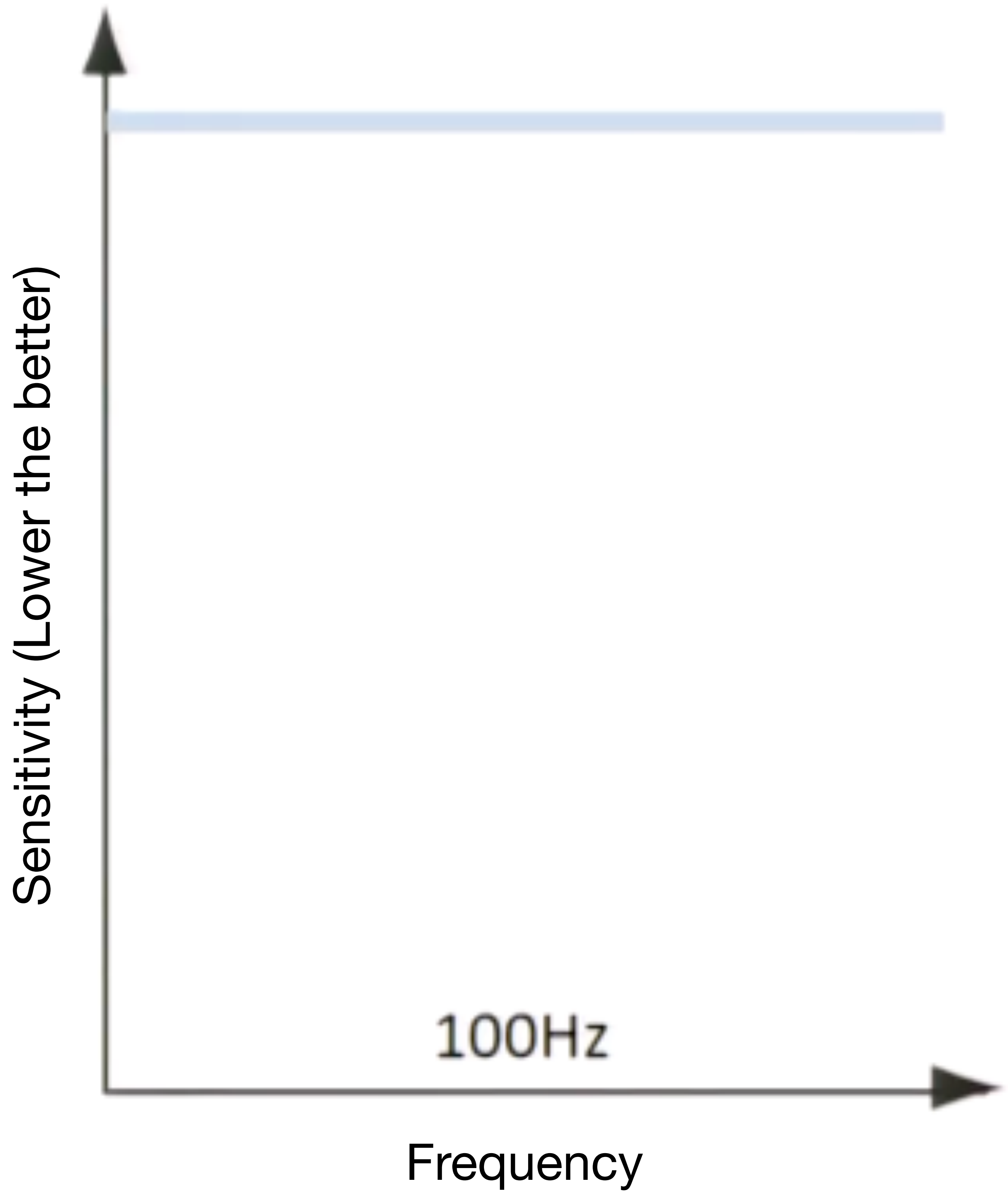

Basic Idea of the Interferometer

"Michelson" interferometer

Longer arm-length makes better sensitivity

Best sensitivity for 100 Hz is $L = 750$ km

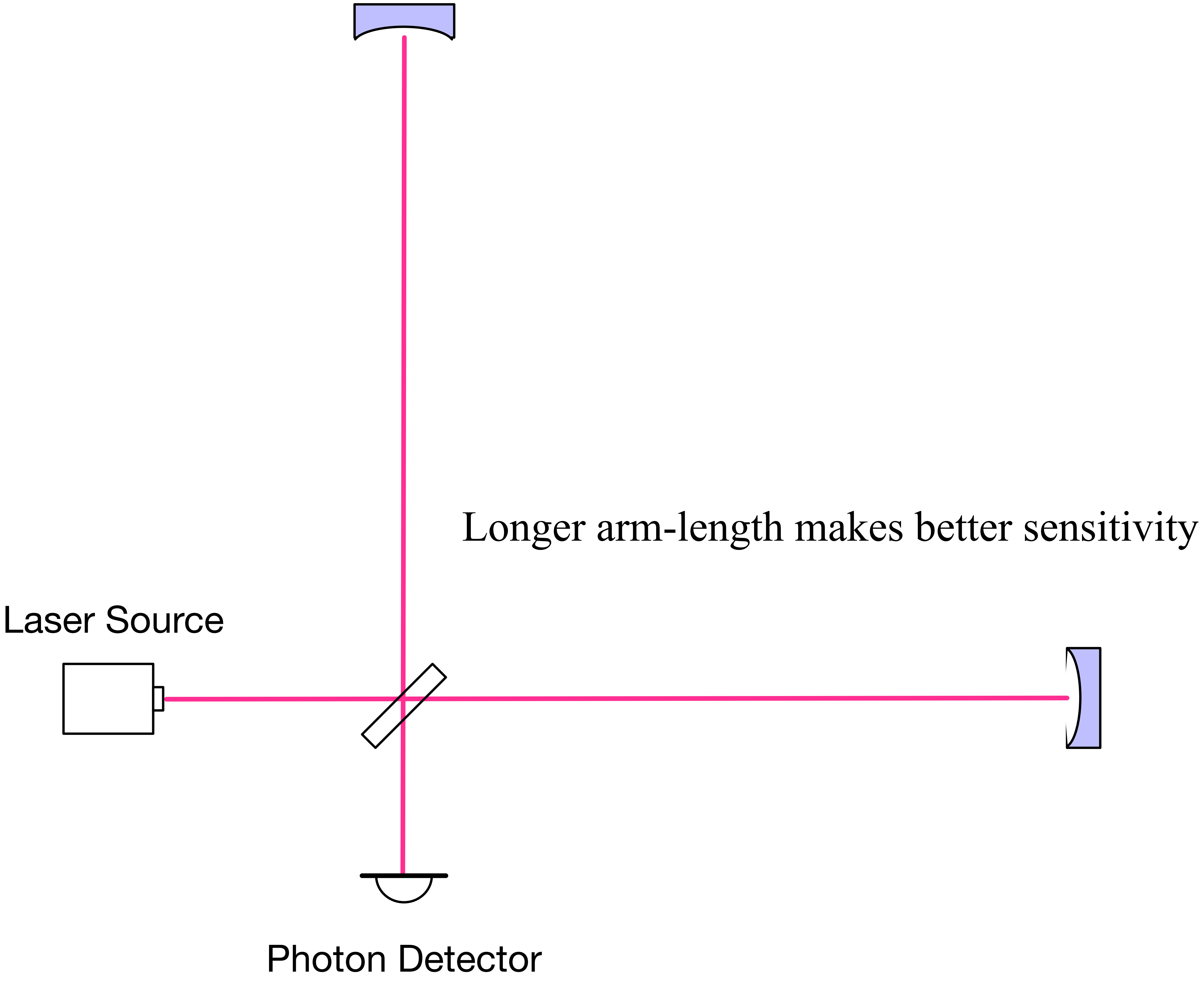

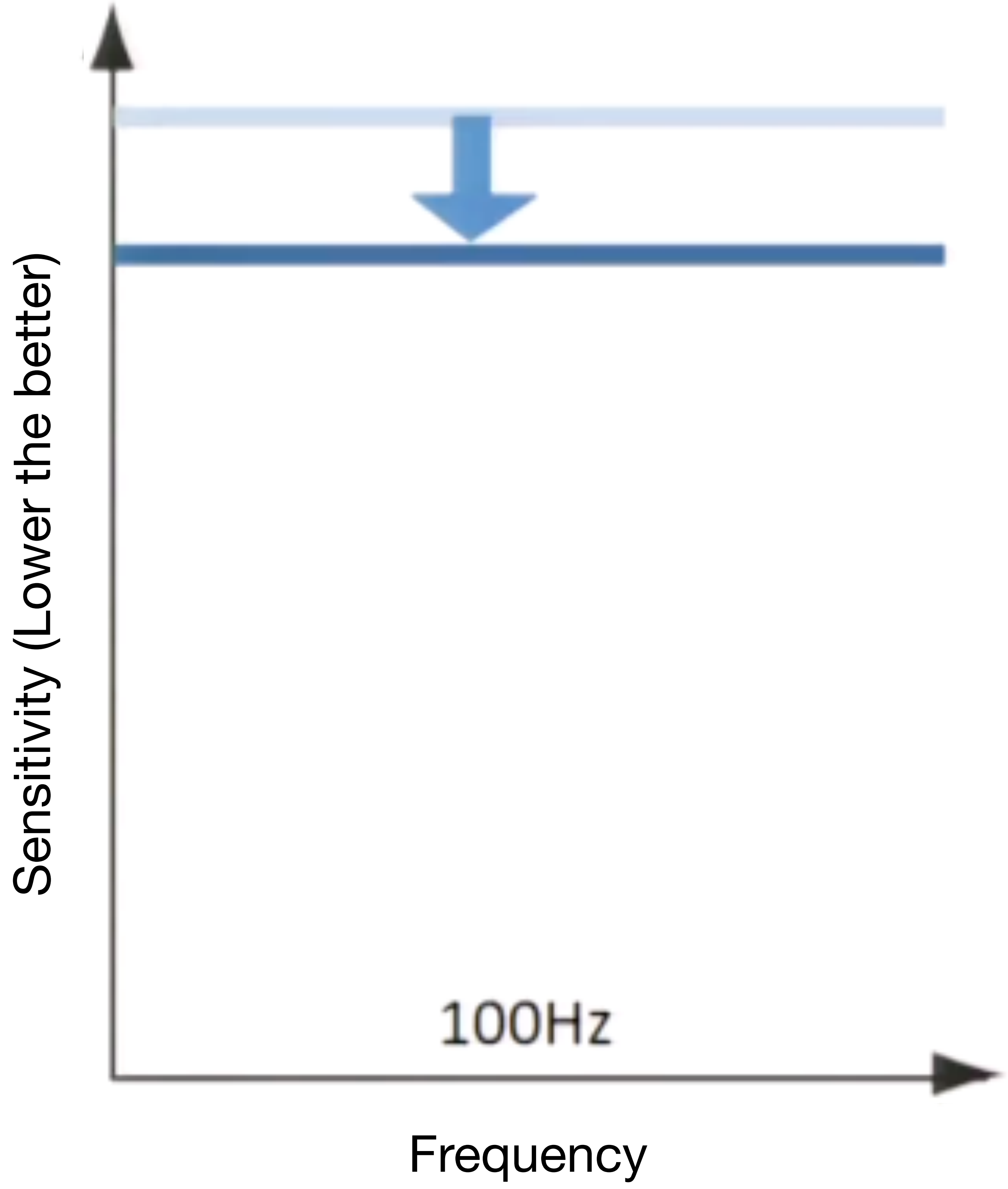

Basic Idea of the Interferometer

"Fabry-Pérot Michelson" interferometer

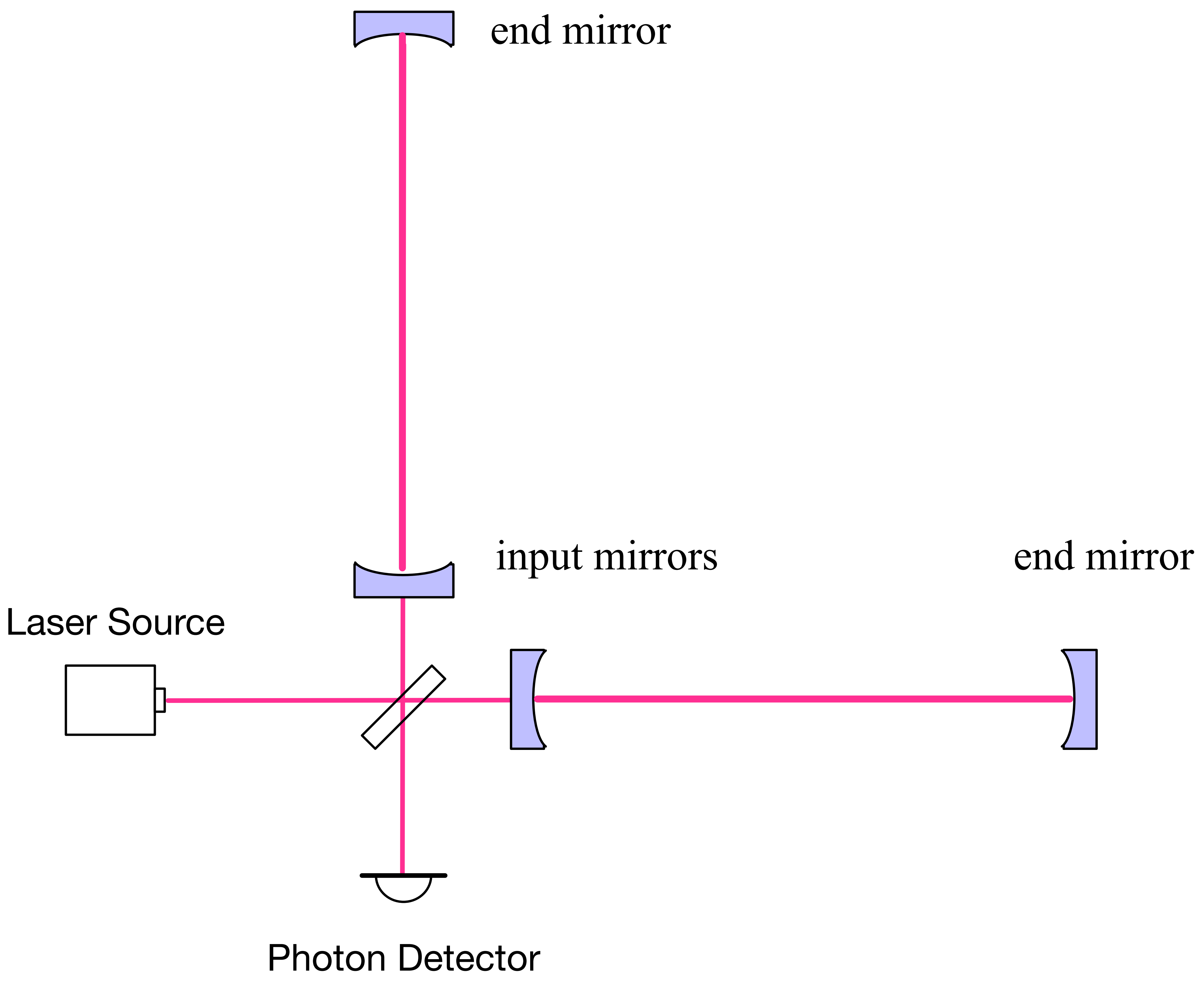

Longer arm-length makes better sensitivity

Best sensitivity for 100 Hz is L= 750 km

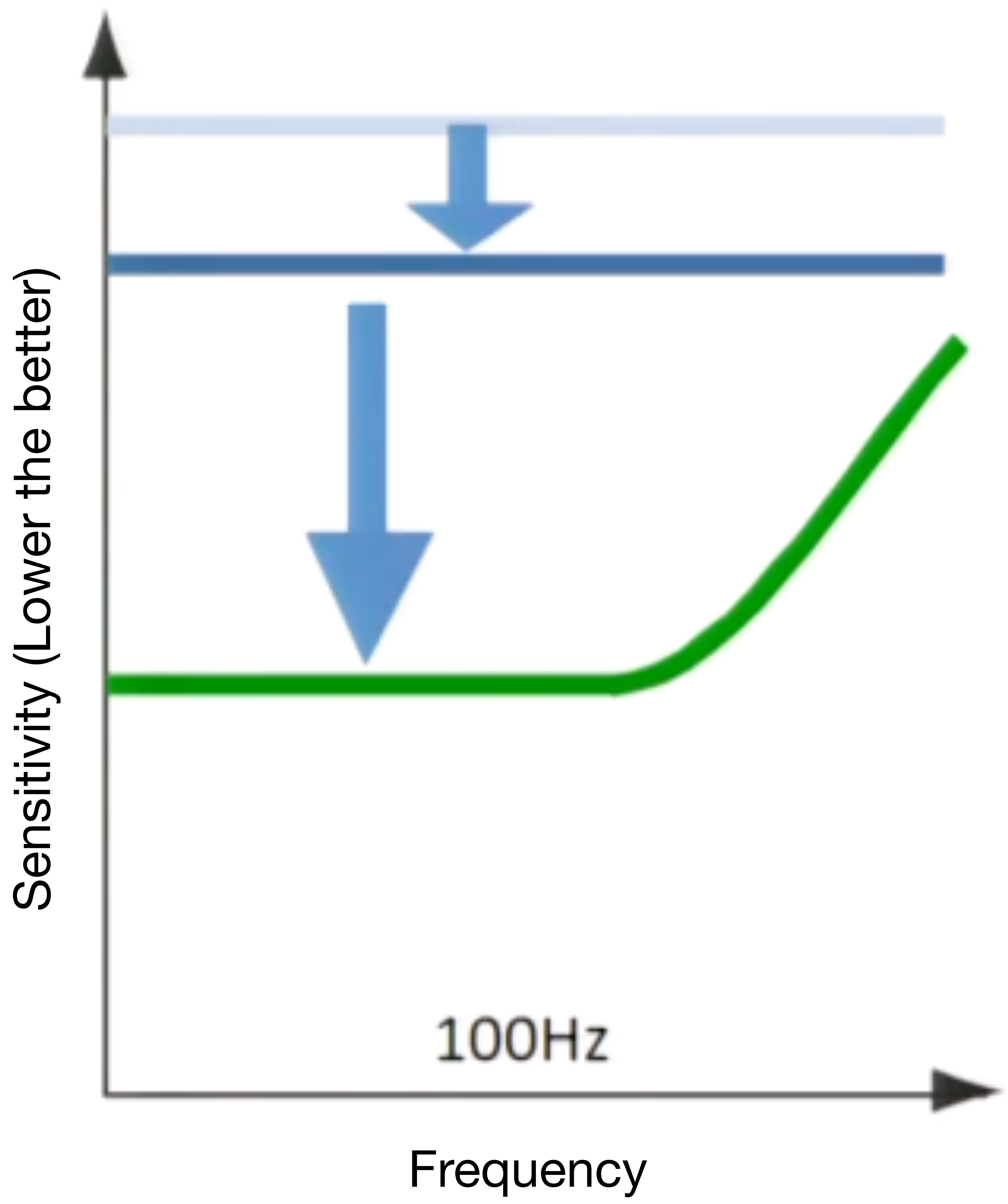

Not so good for high freq. due to GW cancellation.

Basic Idea of the Interferometer

"Fabry-Pérot Michelson" interferometer

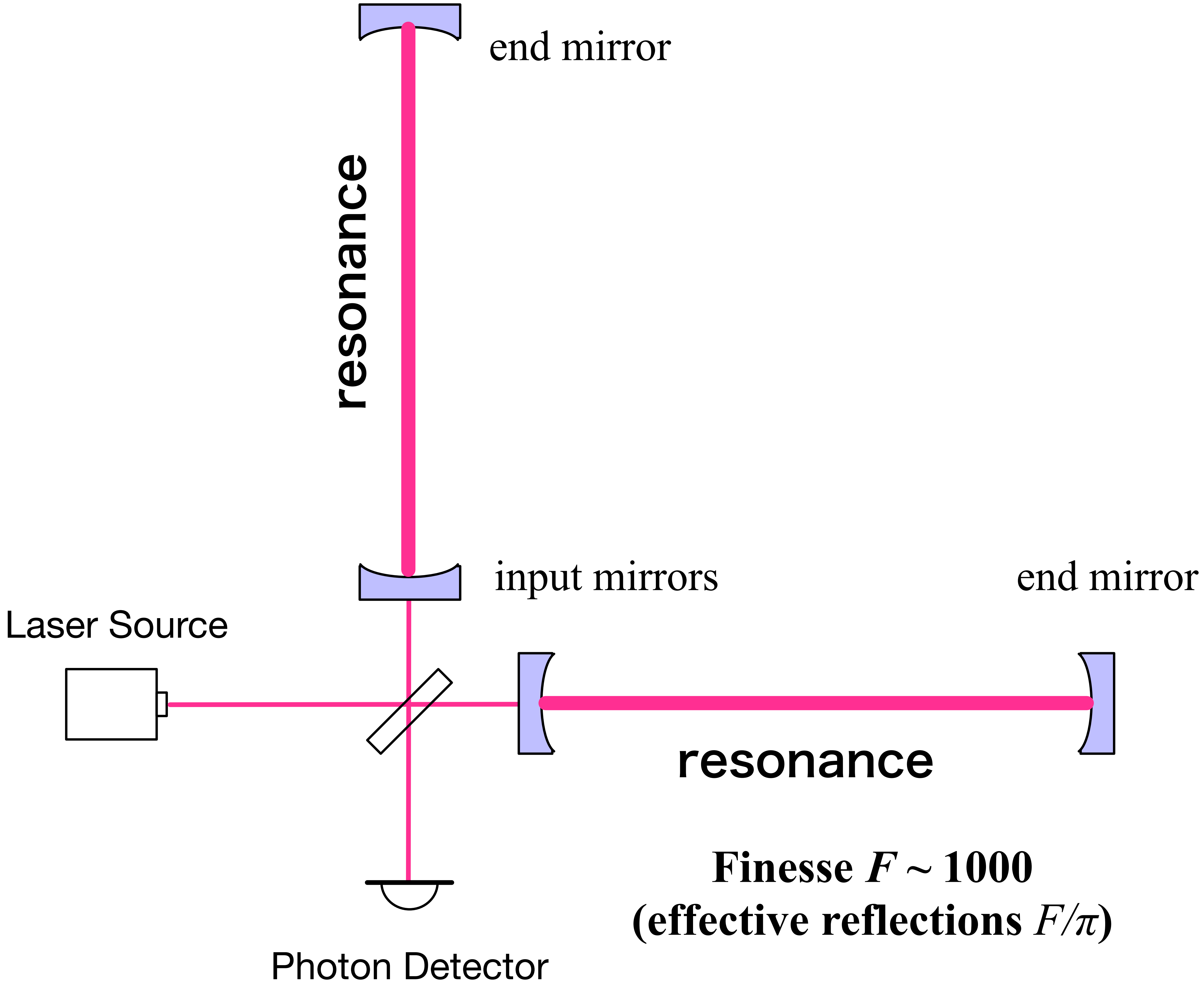

Finesse $F \sim 1000$
(effective reflections F/π)

Longer arm-length makes better sensitivity

Best sensitivity for 100 Hz is $L = 750$ km

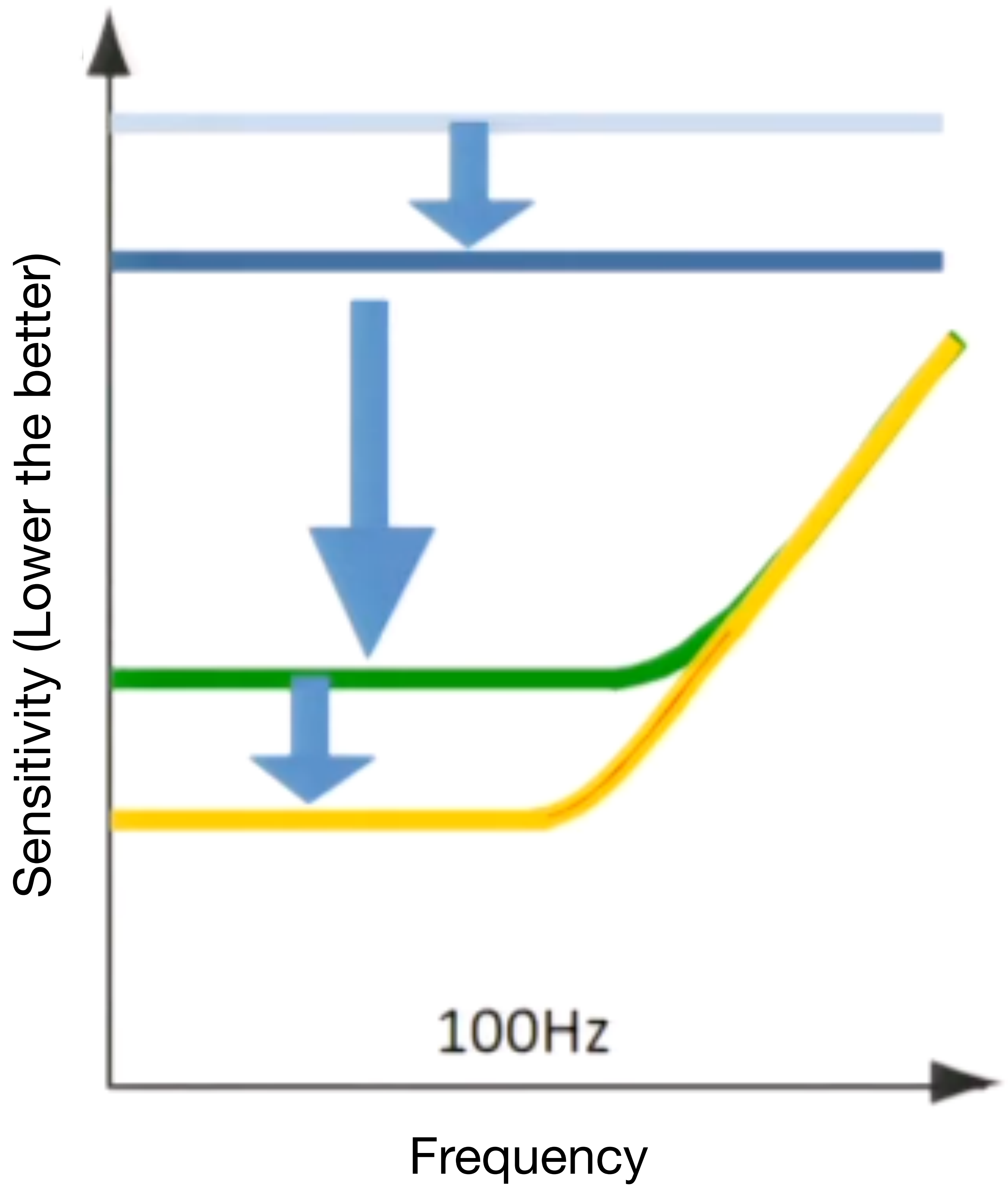

Not so good for high freq. due to GW cancellation.

High finesse introduces optical losses at mirrors

Basic Idea of the Interferometer

“Power-Recycled” Fabry-Pérot Michelson interferometer (TAMA300, initial LIGO, Virgo)

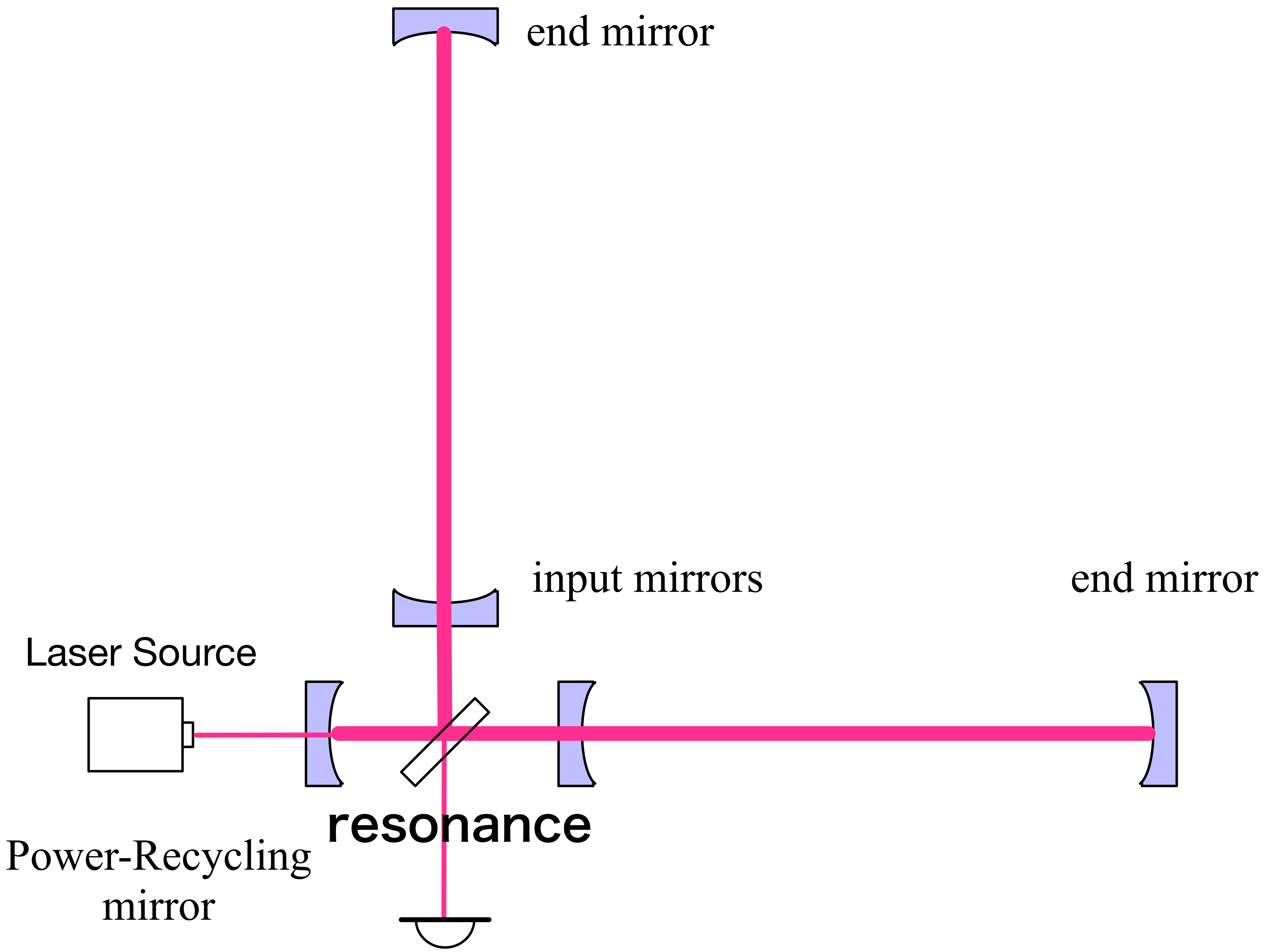

get more effective laser power

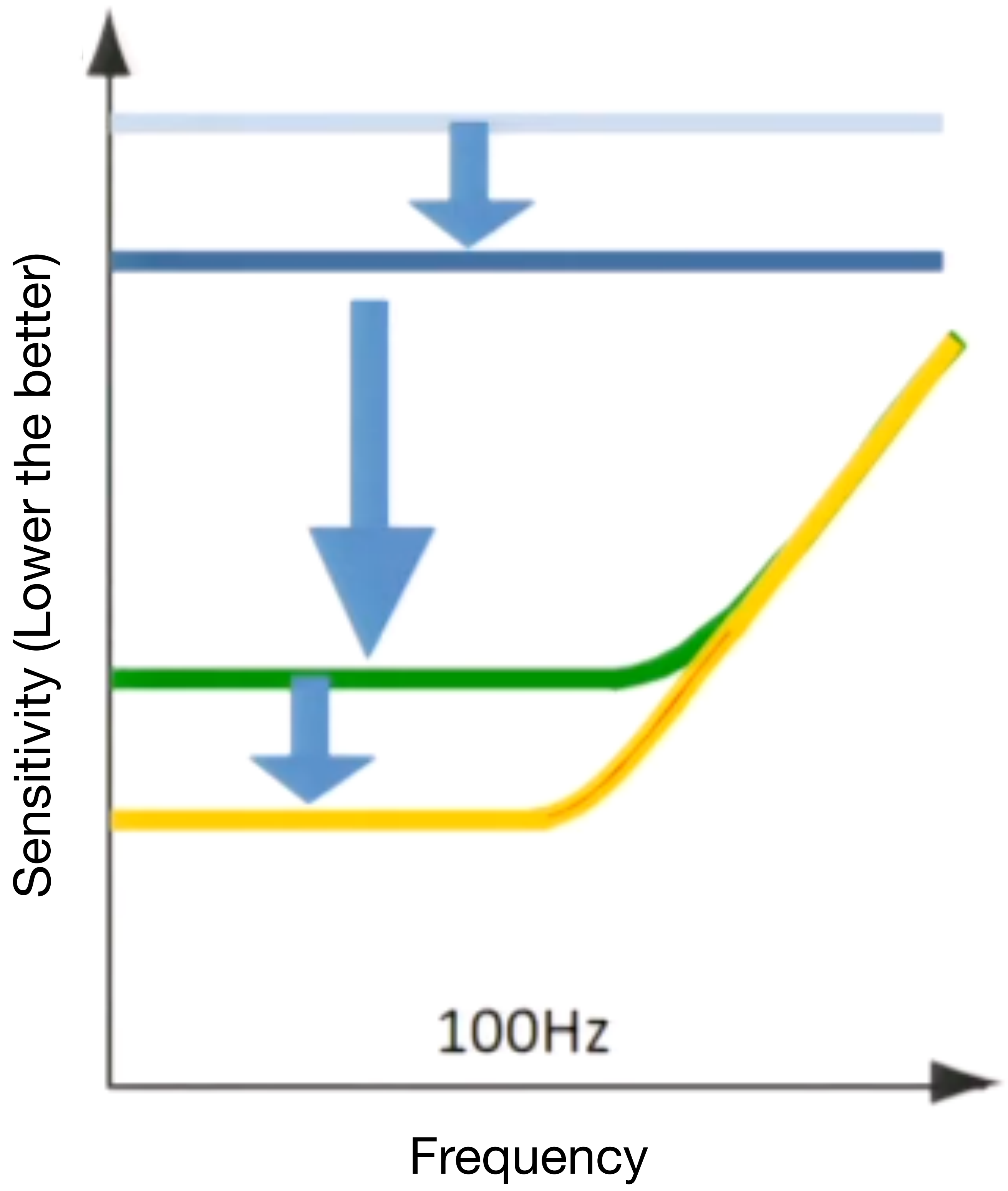

Reduce shot-noise of laser

Basic Idea of the Interferometer

“Signal-Recycled” Fabry-Pérot Michelson interferometer (GEO600)

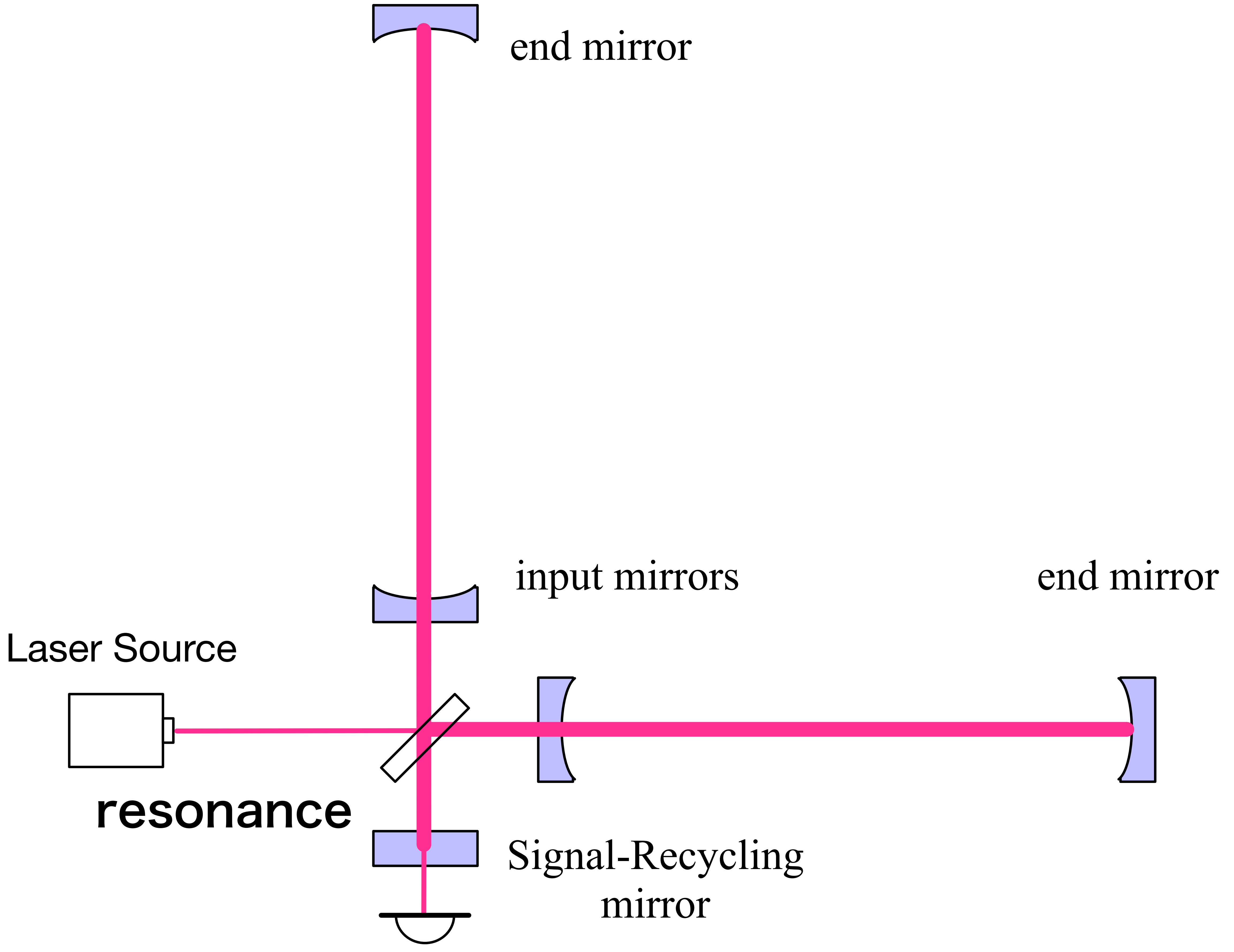

get more effective GW signals
resonance (N+1/2) wavelength between SR & IM

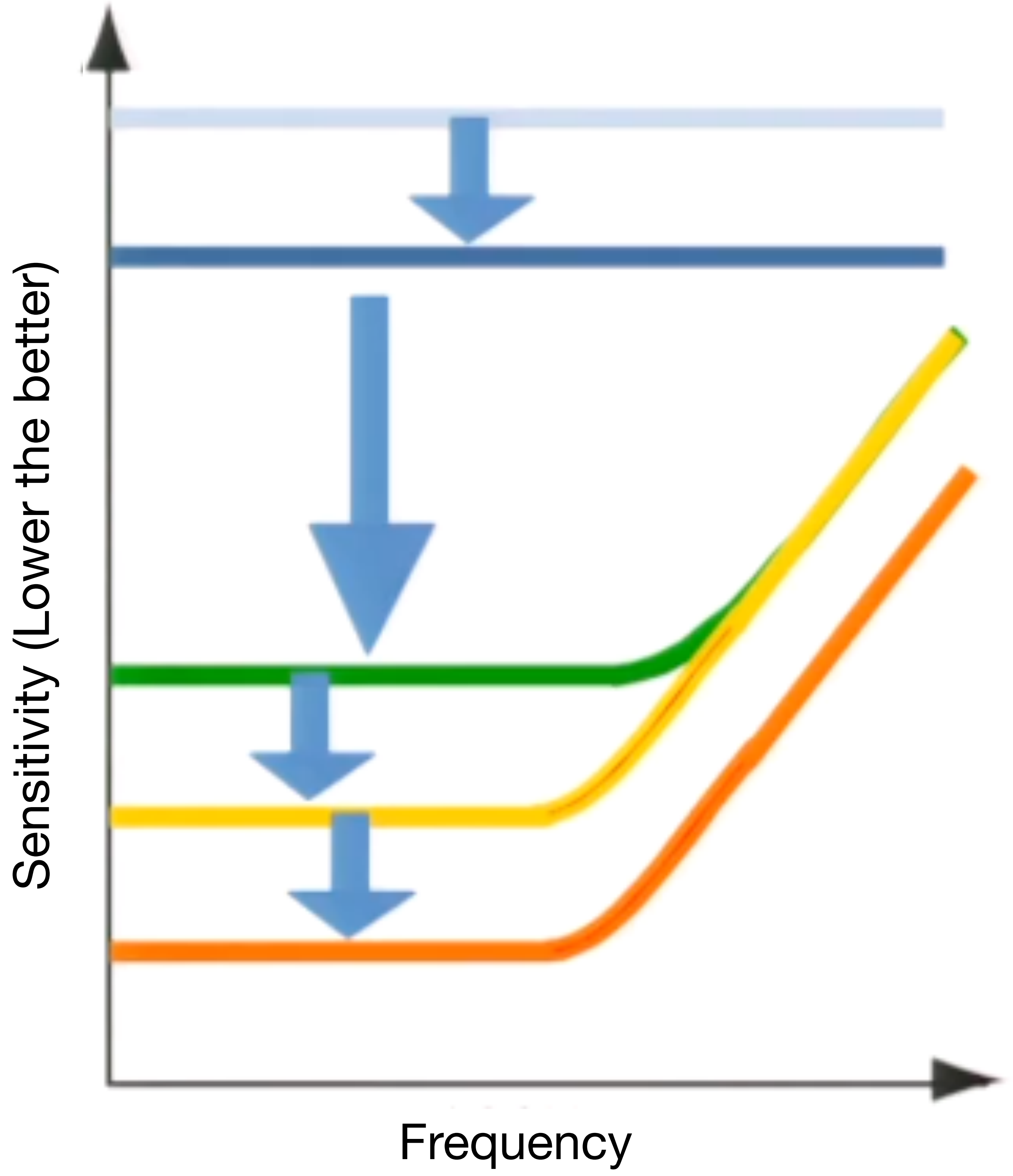

get more finesse
with SR mirror

Basic Idea of the Interferometer

“Resonant Side-band Extraction” interferometer (KAGRA, Advanced LIGO, Advanced Virgo)

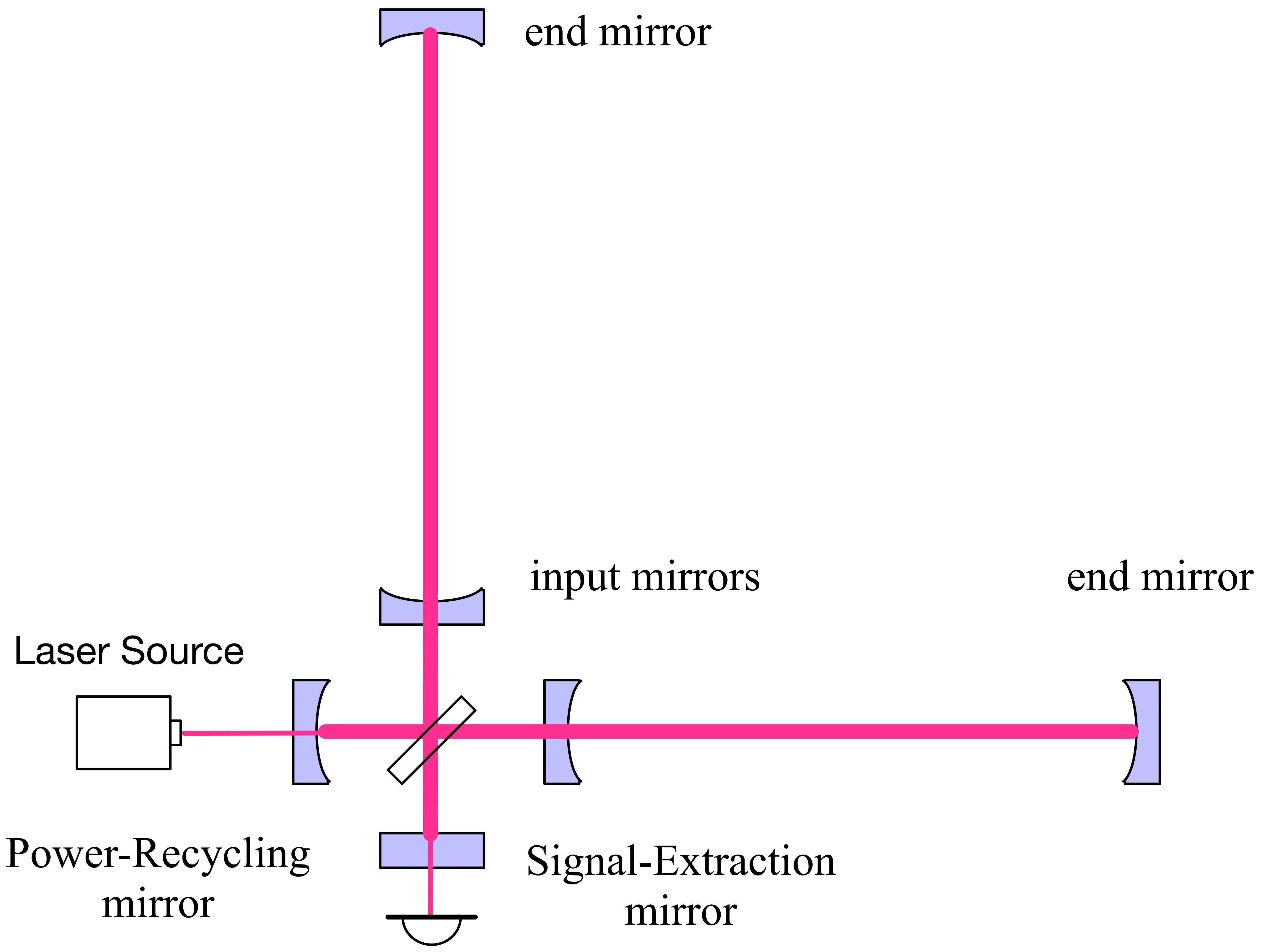

get more effective GW signals
resonance N wavelength

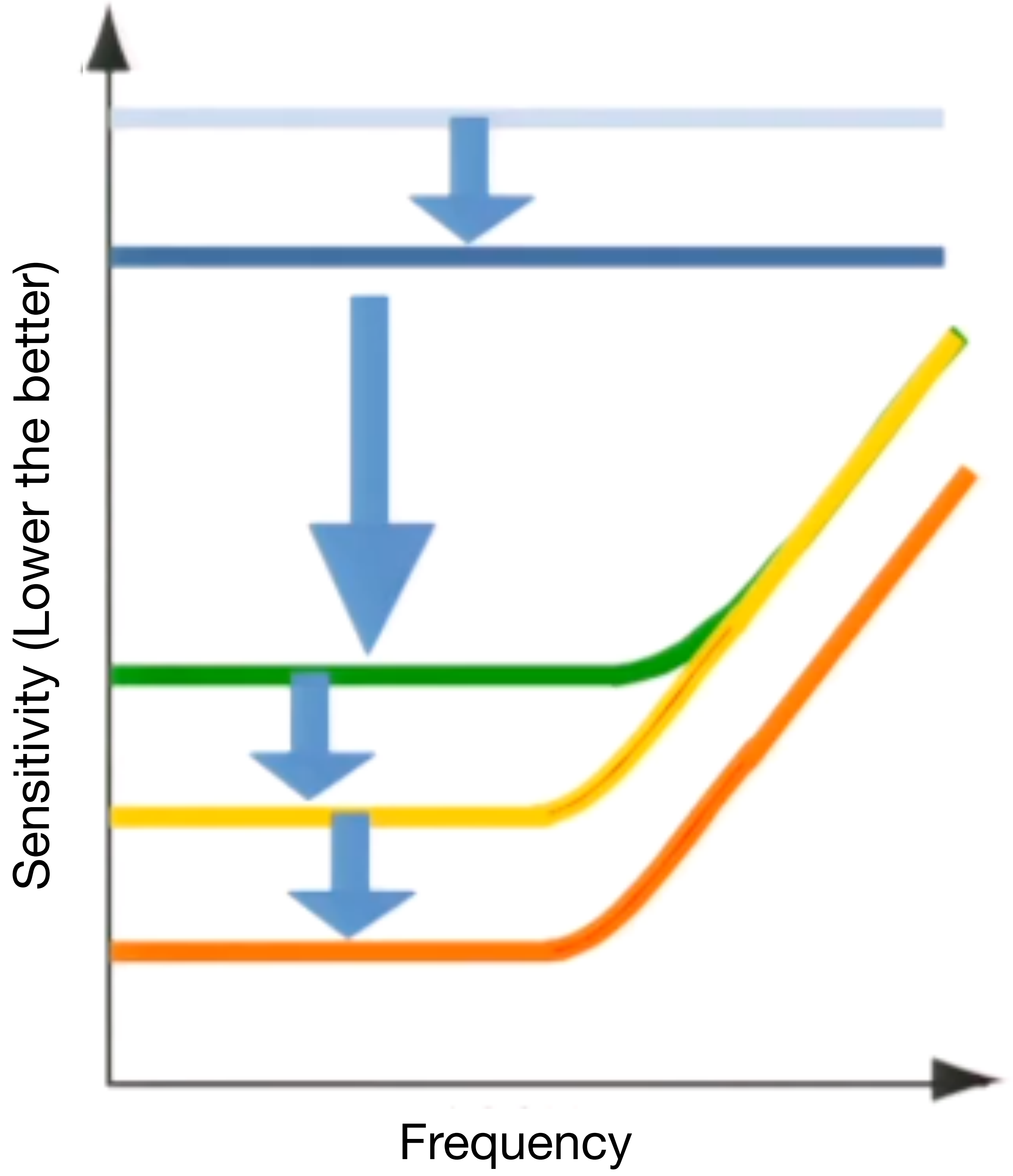

keep at relative low finesse
with SE mirror

for optical losses
for GW cancellation

Basic Idea of the Interferometer

"**Resonant Side-band Extraction**" **interferometer** (KAGRA, Advanced LIGO, Advanced Virgo)

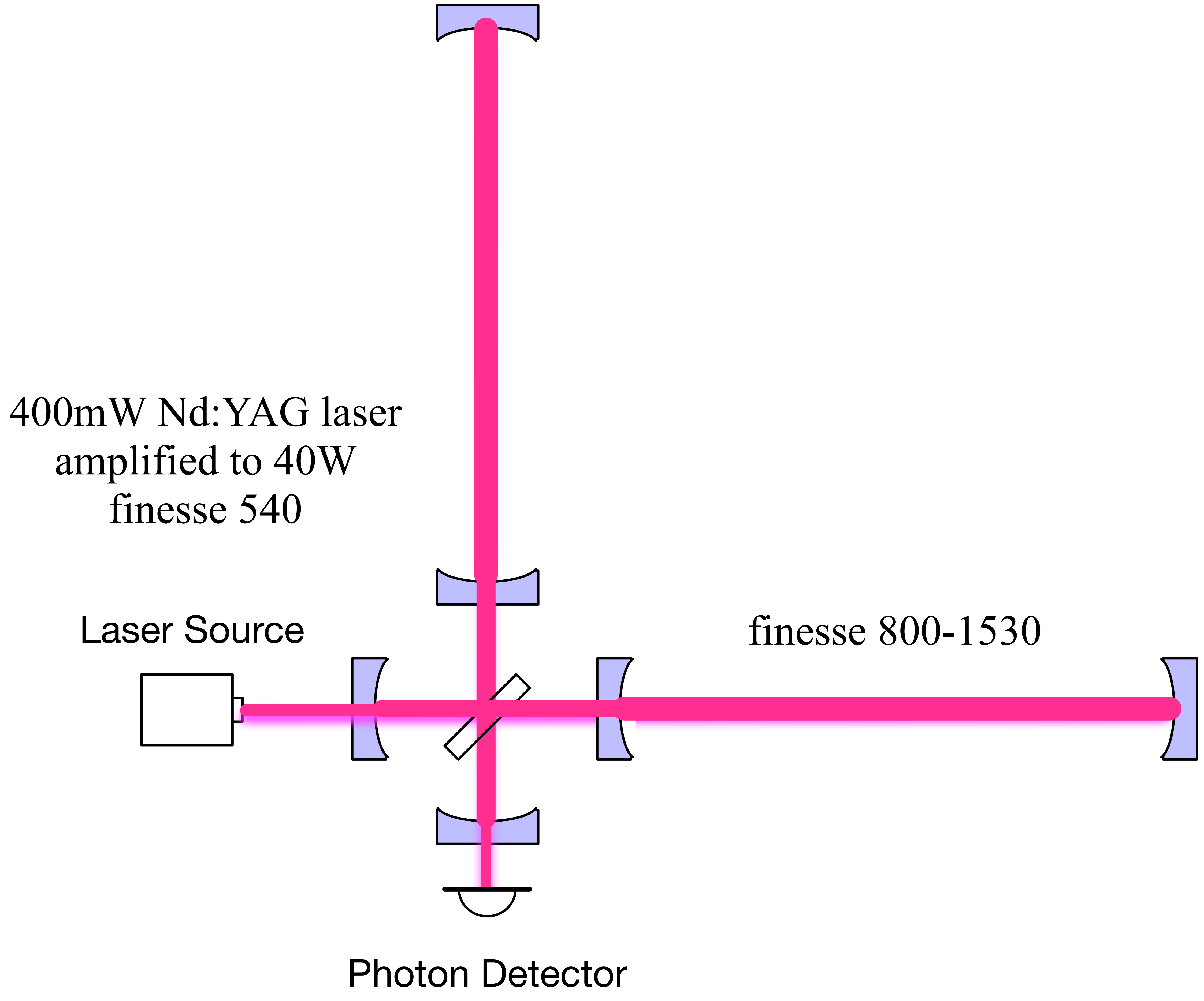

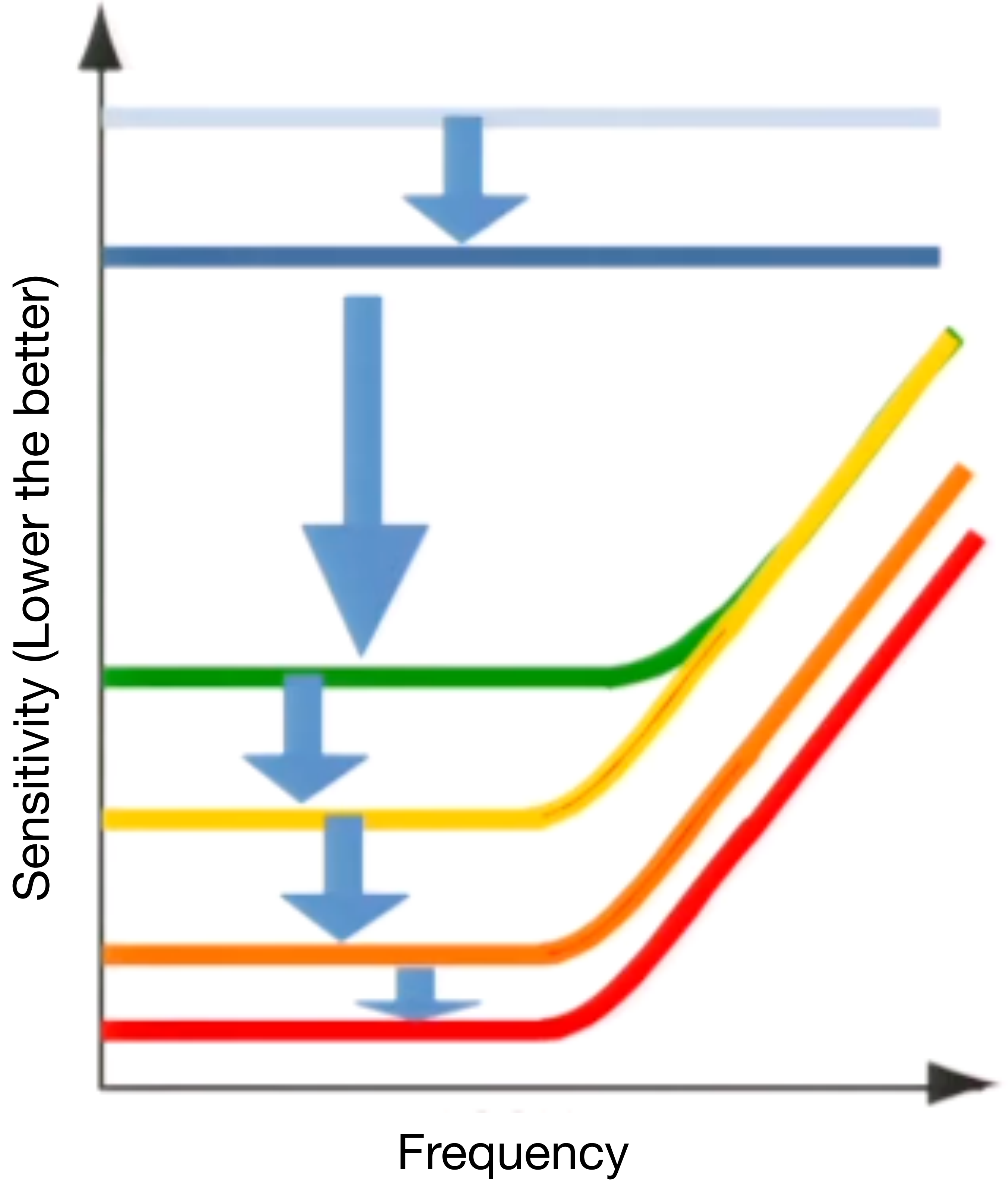

more laser power

Basic Idea of the Interferometer

“Resonant Side-band Extraction” interferometer

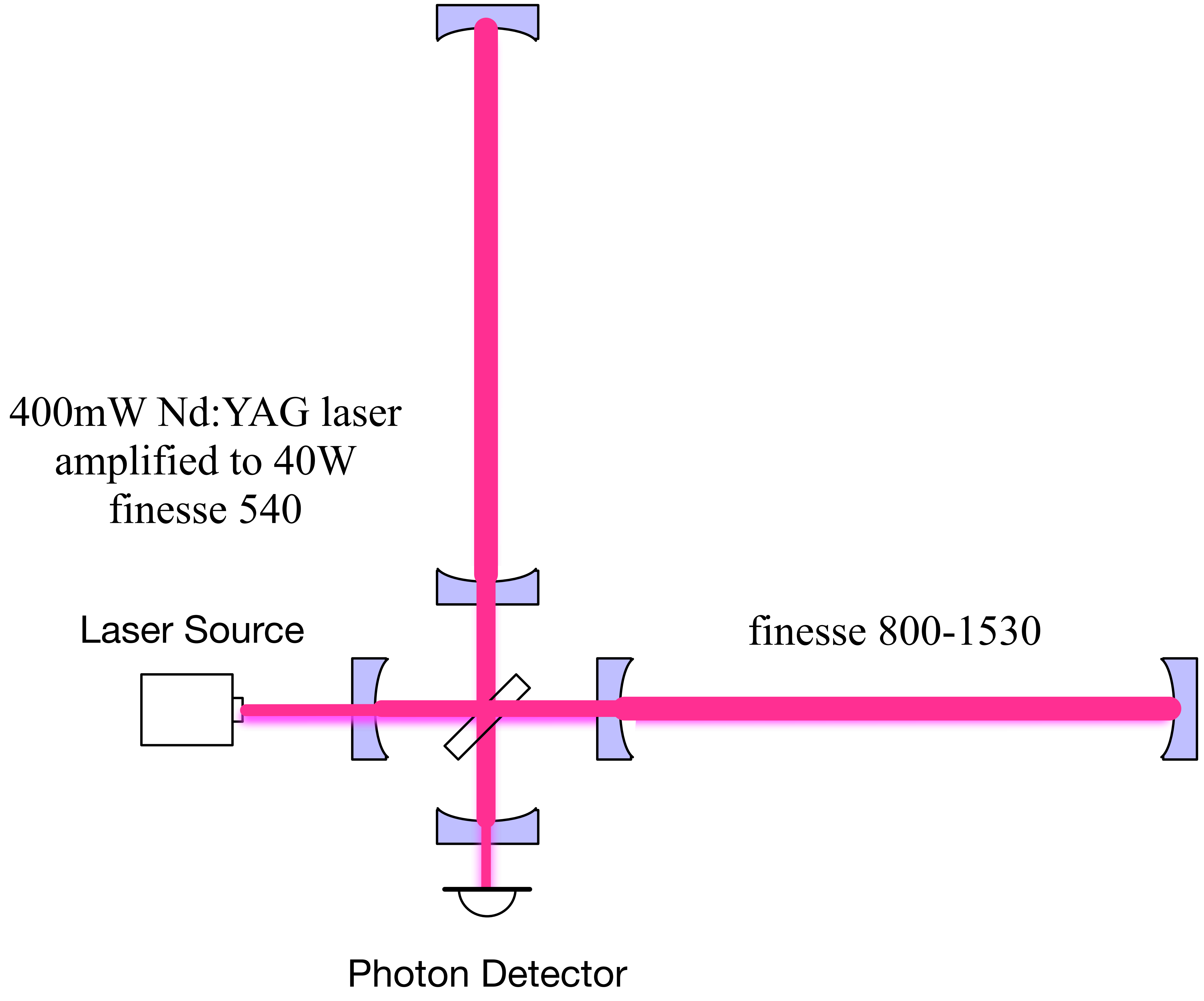

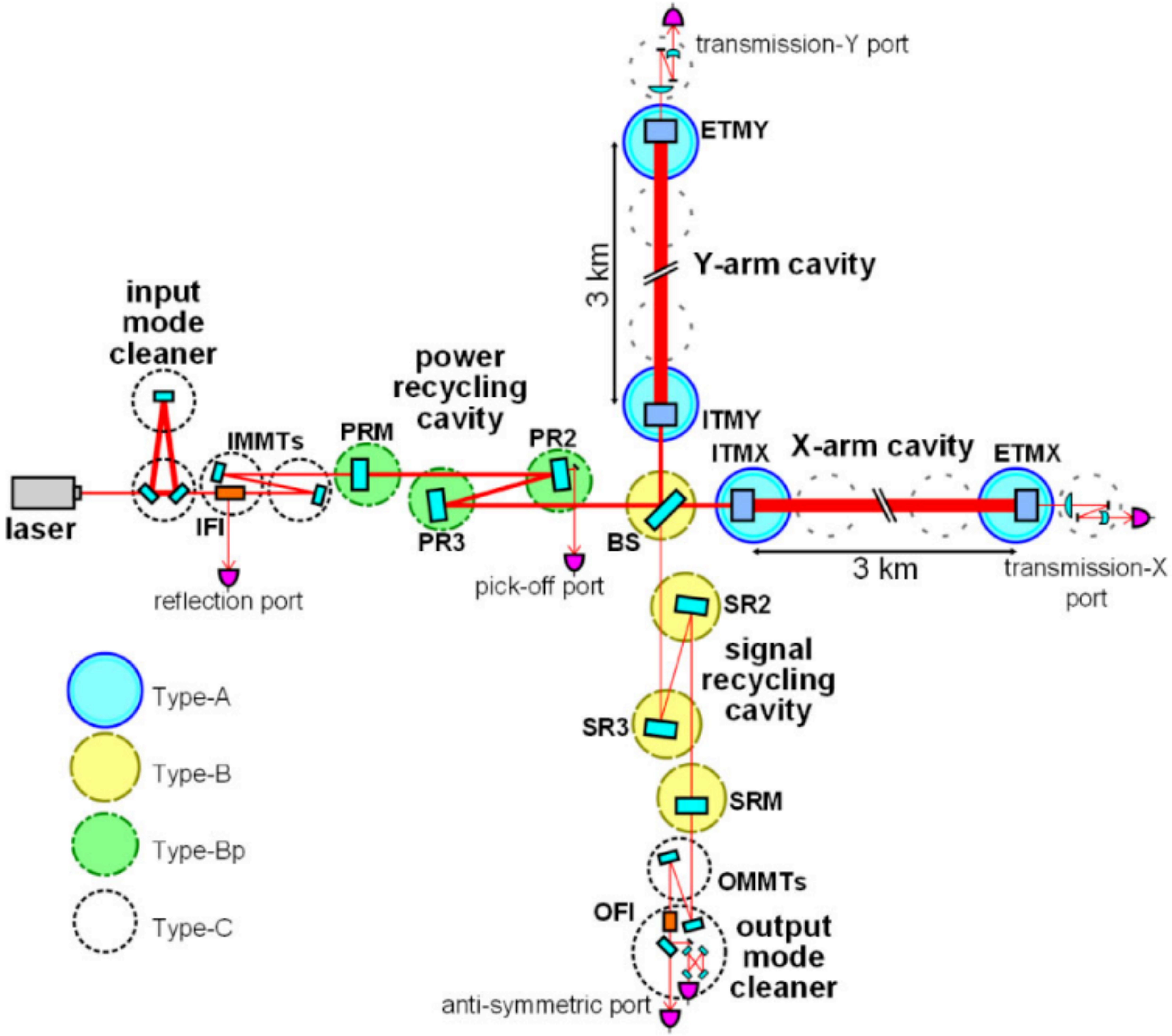

Basic Idea of Suspension System

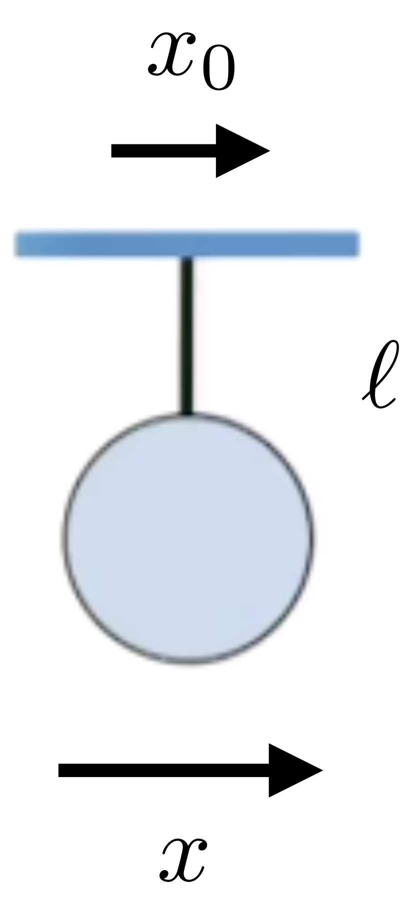

$$M\ddot{x} = -\frac{Mg}{\ell}(x - x_0)$$

$$x/x_0 = \frac{f_0^2}{f_0^2 - f^2}, \text{ where } f_0 = \frac{1}{2\pi}\sqrt{\frac{g}{\ell}}$$

$$\delta x_{\rm seis} \sim \left(\frac{1\rm Hz}{f}\right)^2 \times 10^{-7}\ {\rm m}/\sqrt{\rm Hz}$$

For 100 Hz, $\delta x_{\rm seis} \sim 10^{-11} {\rm m}/\sqrt{\rm Hz}$.

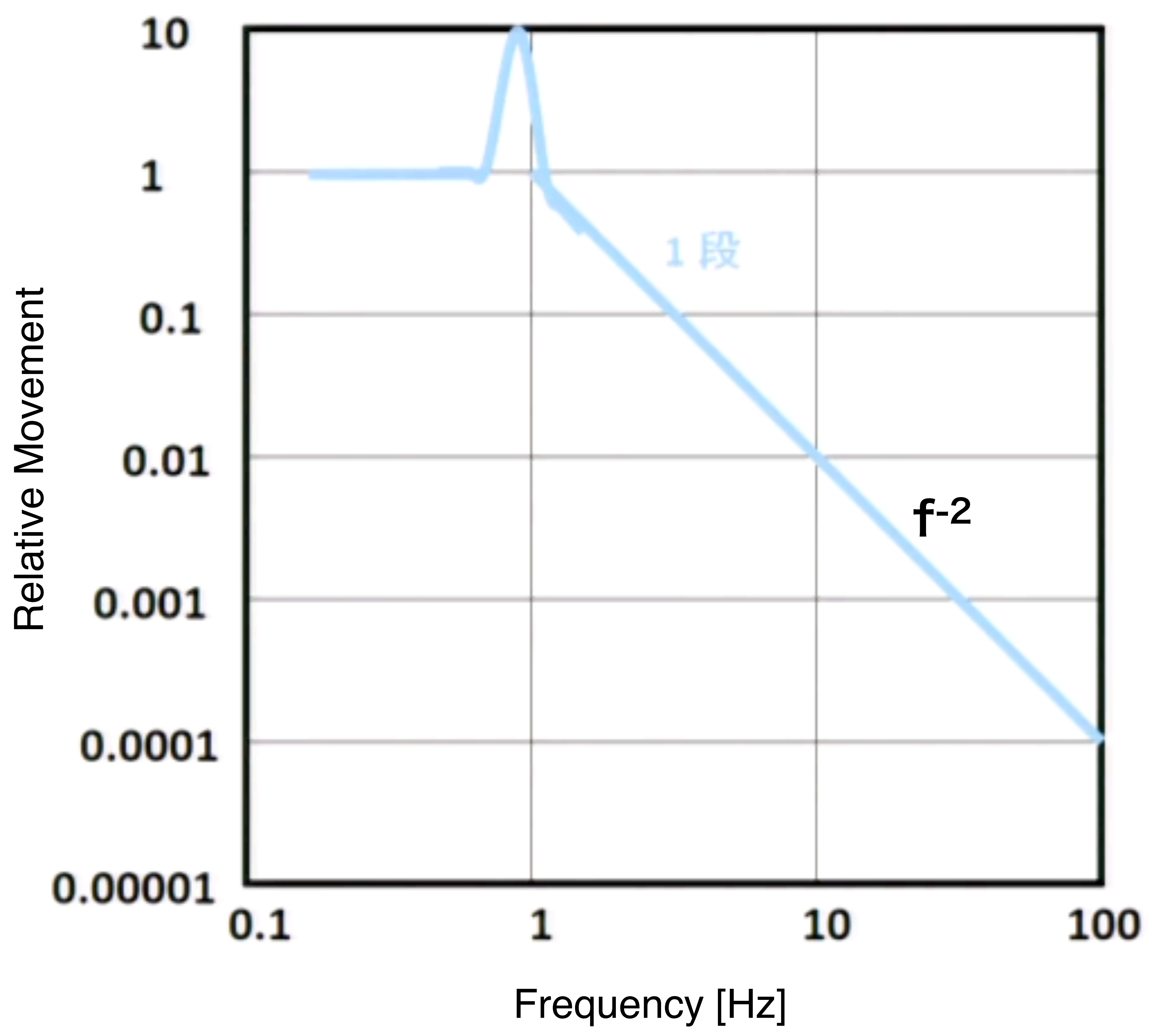

Basic Idea of Suspension System

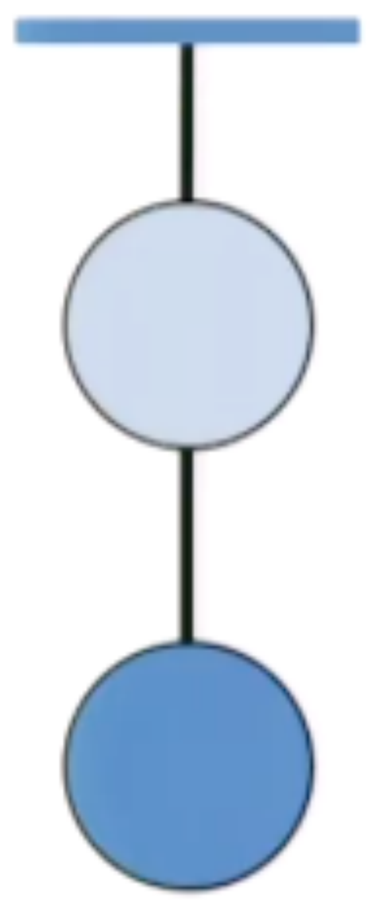

$$M\ddot{x} = -\frac{Mg}{\ell}(x - x_0)$$

$$x/x_0 = \frac{f_0^2}{f_0^2 - f^2}, \text{ where } f_0 = \frac{1}{2\pi}\sqrt{\frac{g}{\ell}}$$

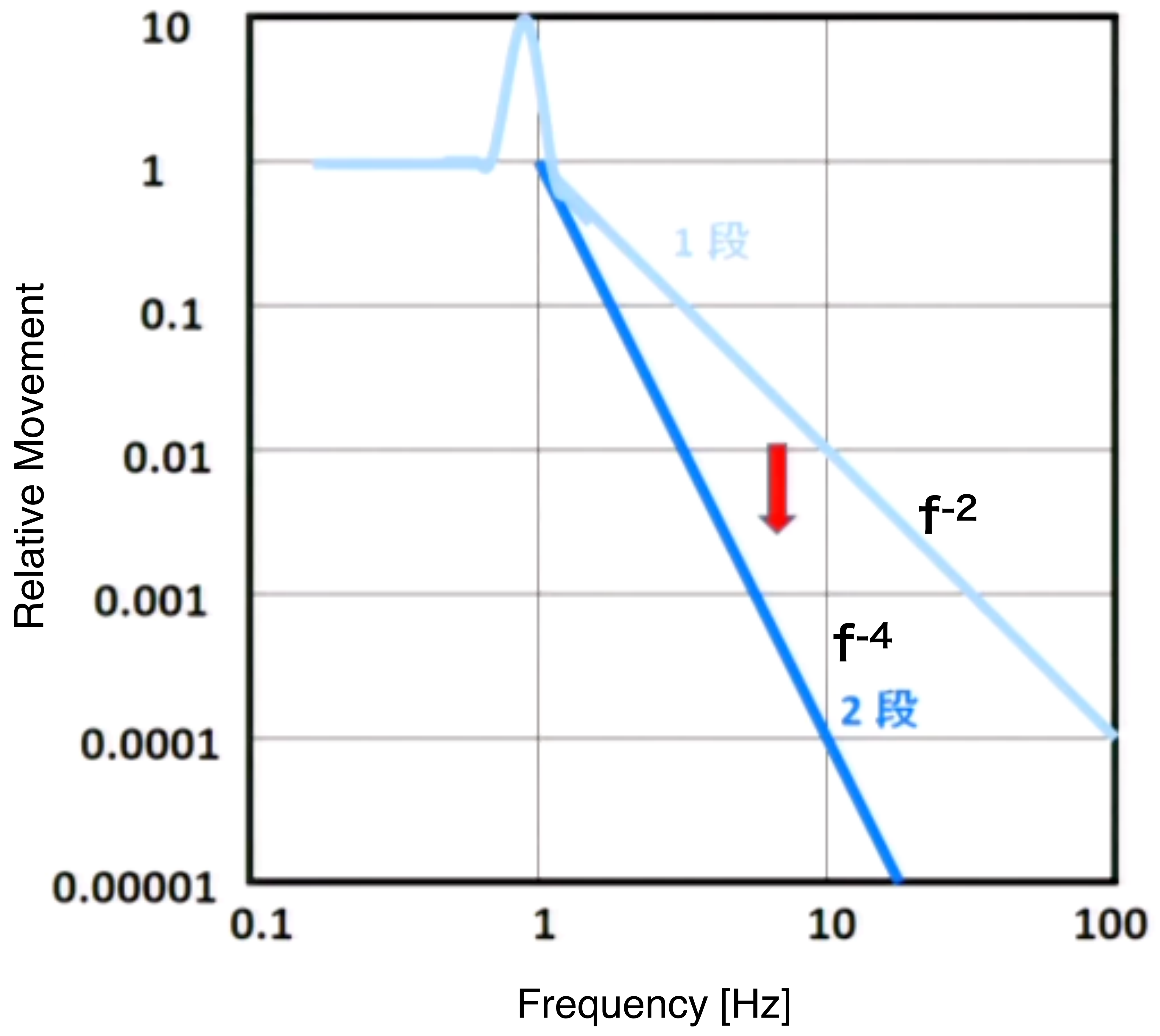

Basic Idea of Suspension System

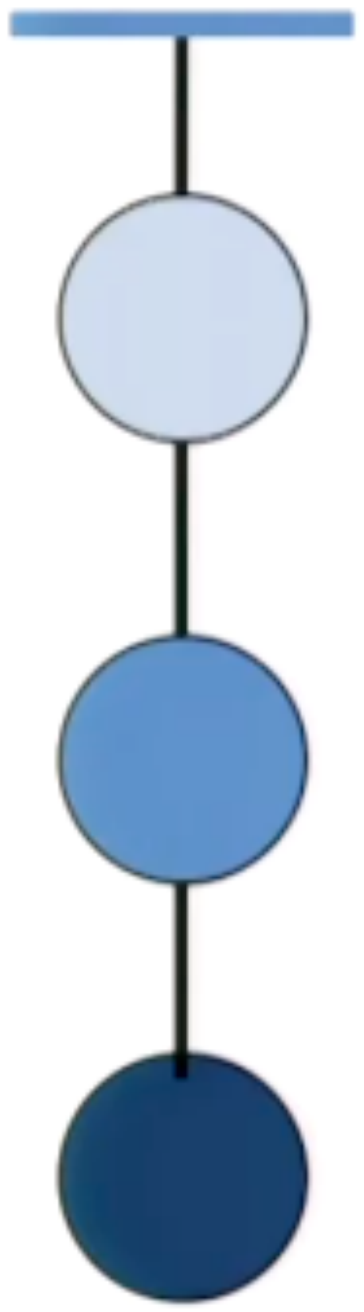

$$M\ddot{x} = -\frac{Mg}{\ell}(x - x_0)$$

$$x/x_0 = \frac{f_0^2}{f_0^2 - f^2}, \text{ where } f_0 = \frac{1}{2\pi}\sqrt{\frac{g}{\ell}}$$

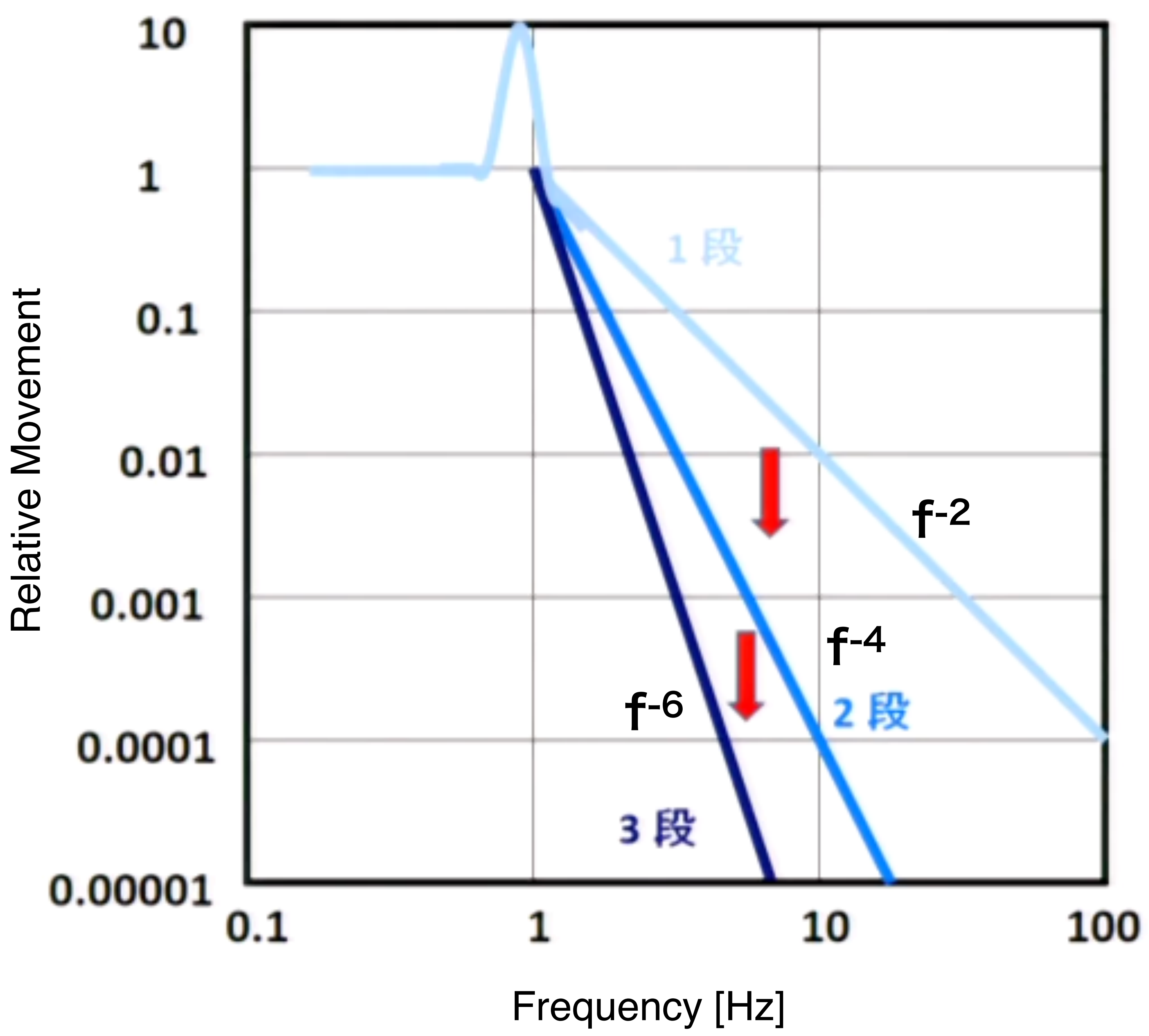

Basic Idea of Suspension System

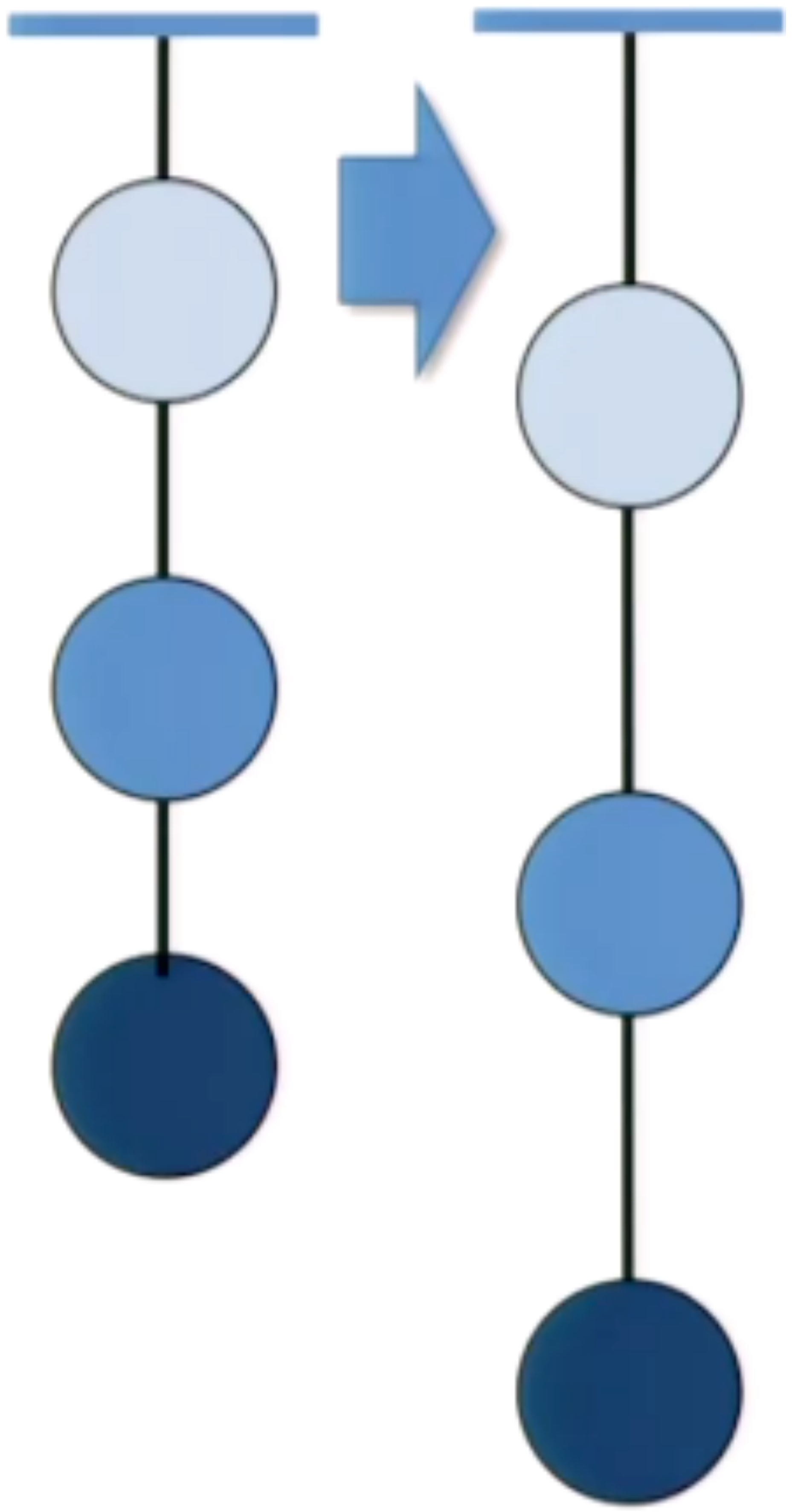

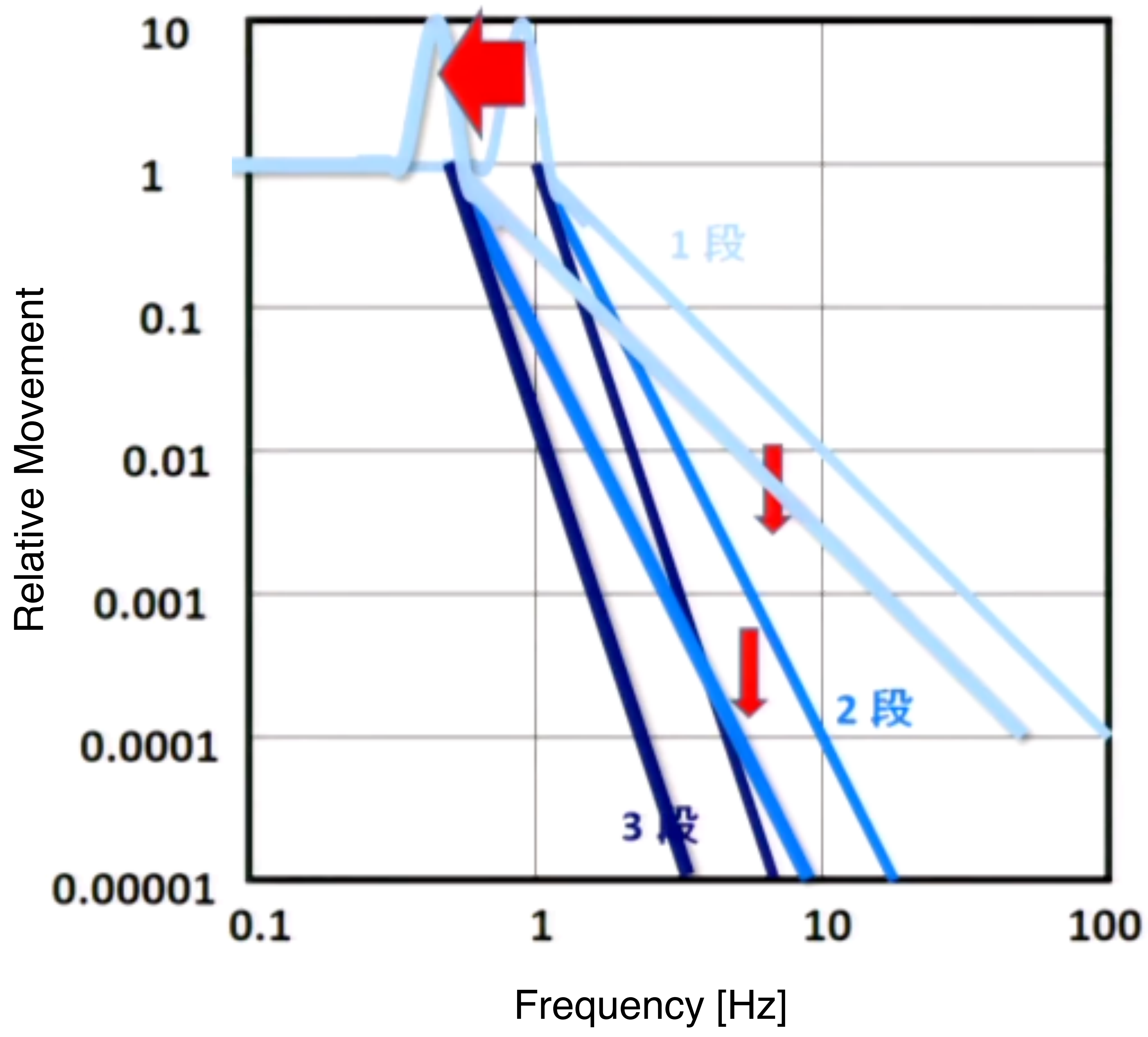

Basic Idea of Suspension System

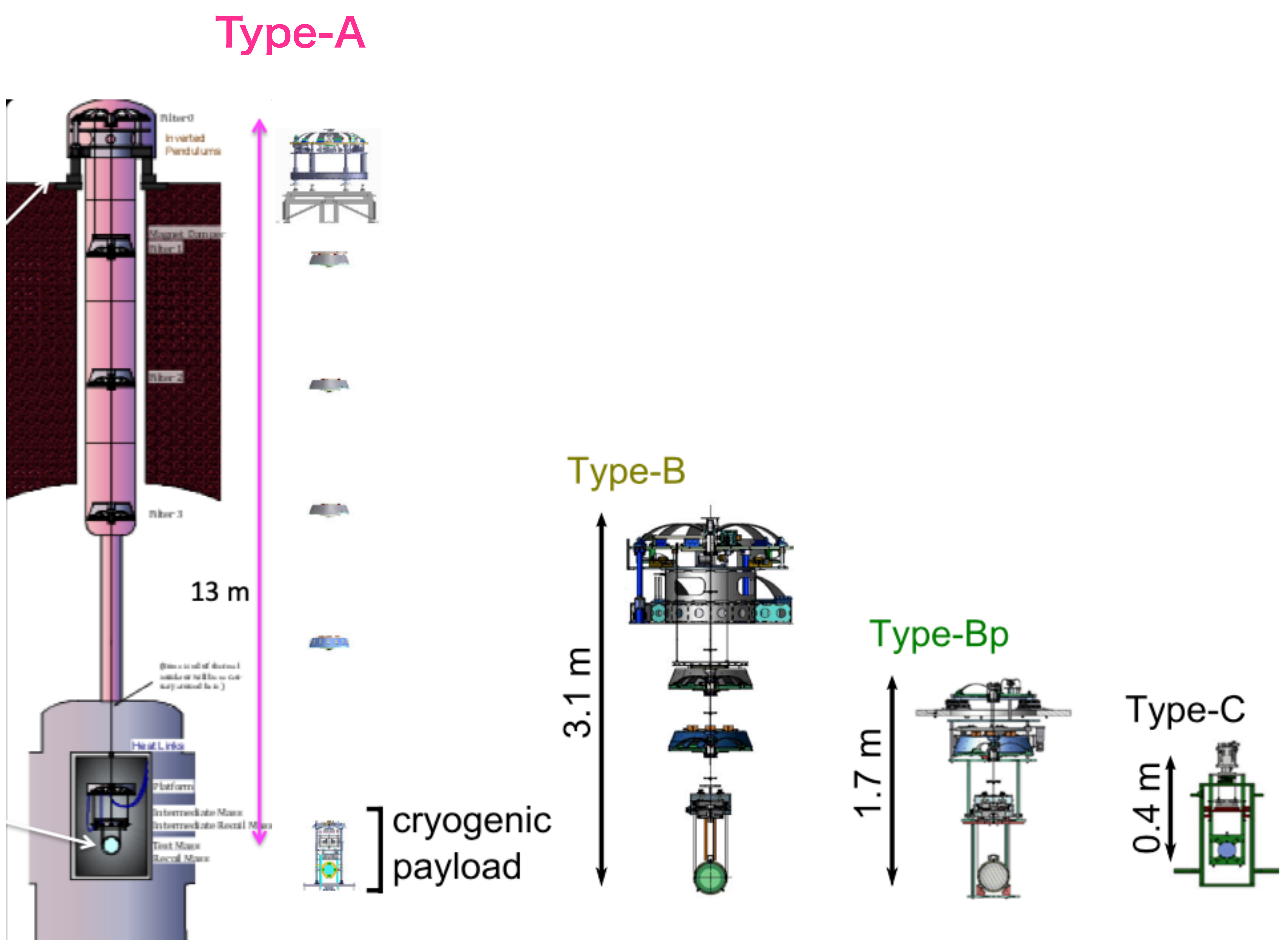

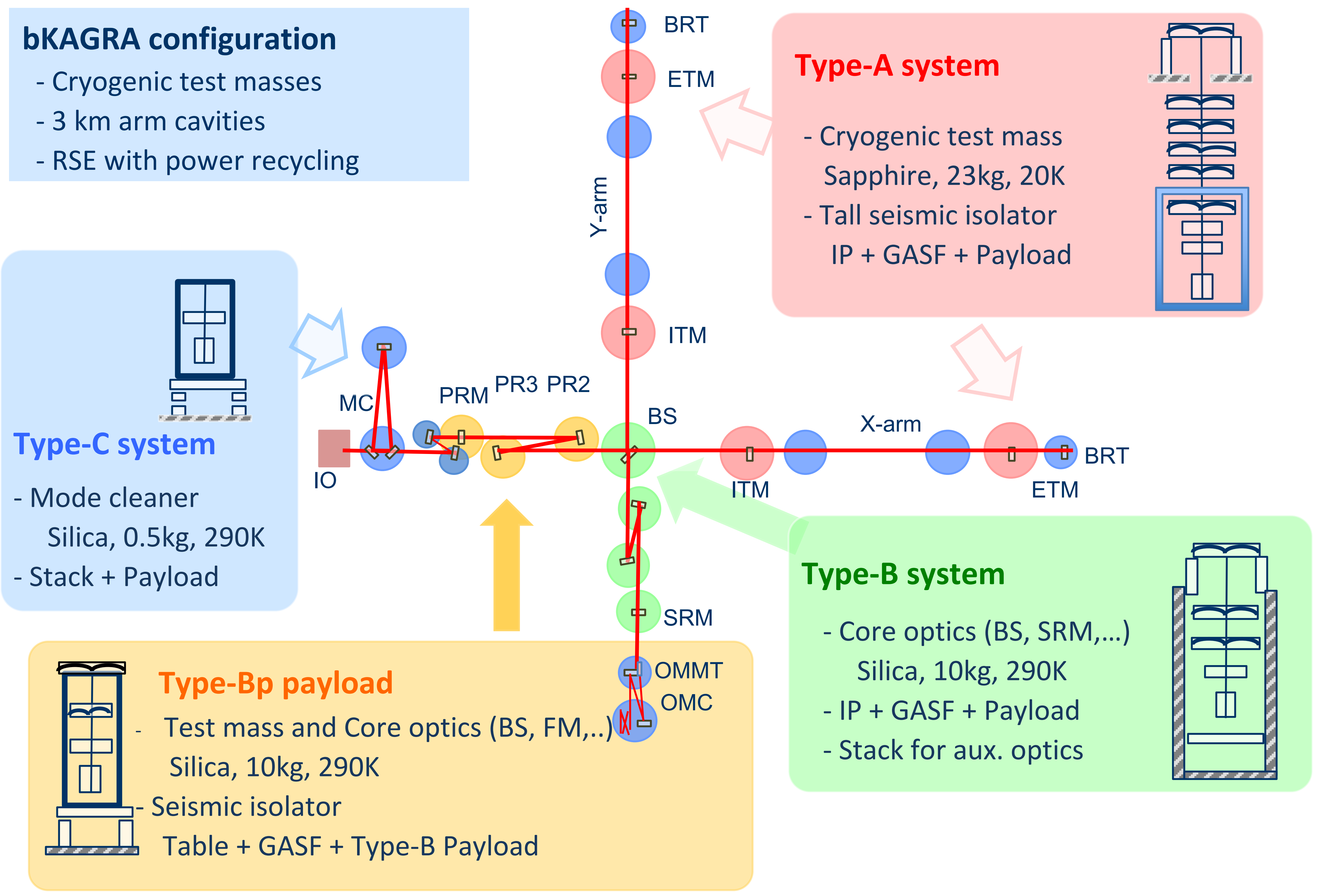

as the configuration of April 2020 (O3GK)

Class. Quantum Grav. **36** (2019) 165008

Cryogenic System

$$\text{Thermal Noise} \propto \sqrt{\frac{4k_B T}{m\omega_0^2 \omega Q}}$$

low temperature
large mass

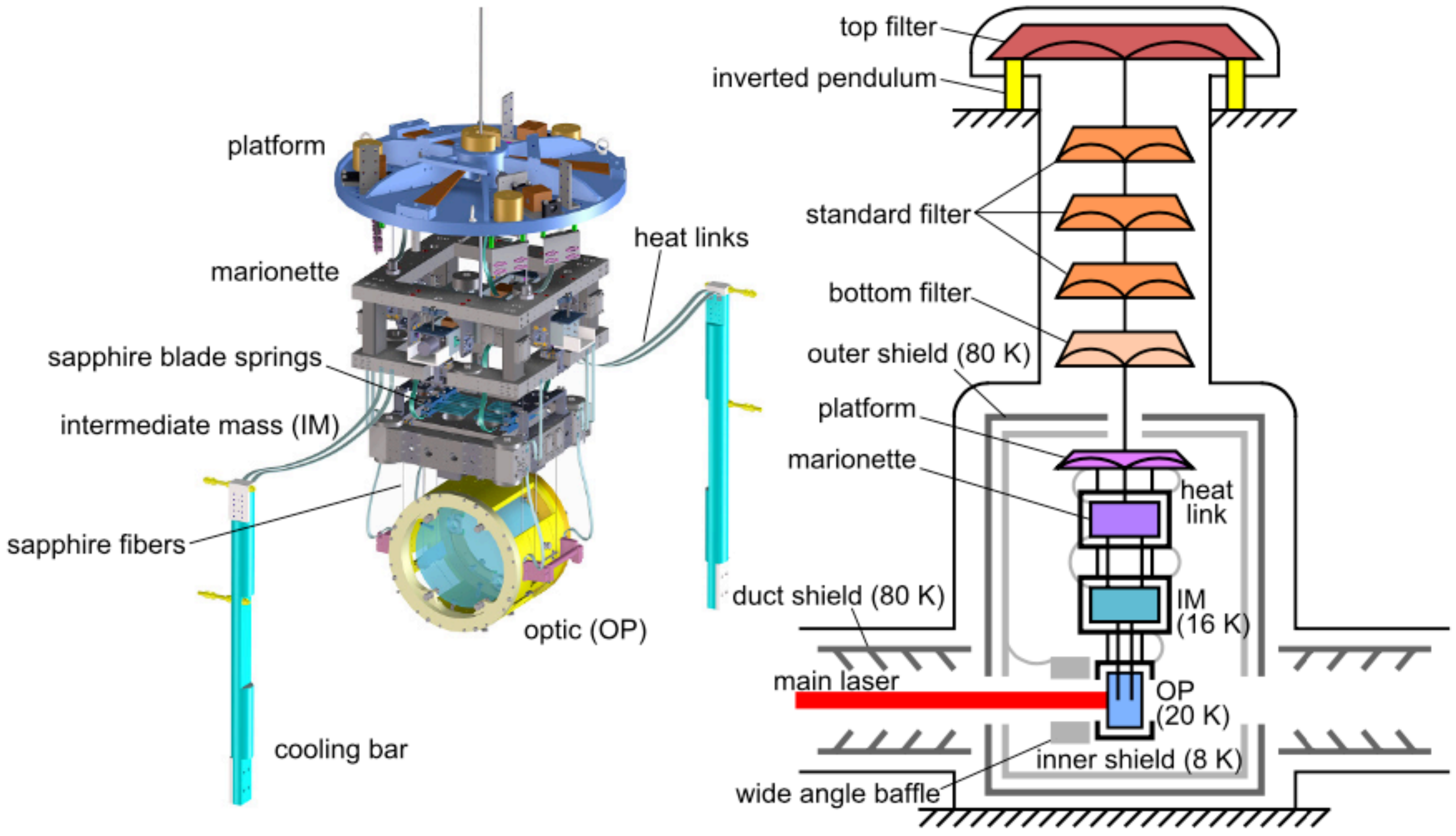

Figure 3. The CAD drawing of the cryogenic payload under Type-A (left) and the schematic of the cryogenic suspension system of sapphire test masses (right). Suspension stages outside of the outer shield are at room temperature.

Class. Quantum Grav. **36** (2019) 165008

sapphire mirror

22.8 kg
diameter 22cm
thickness 15cm

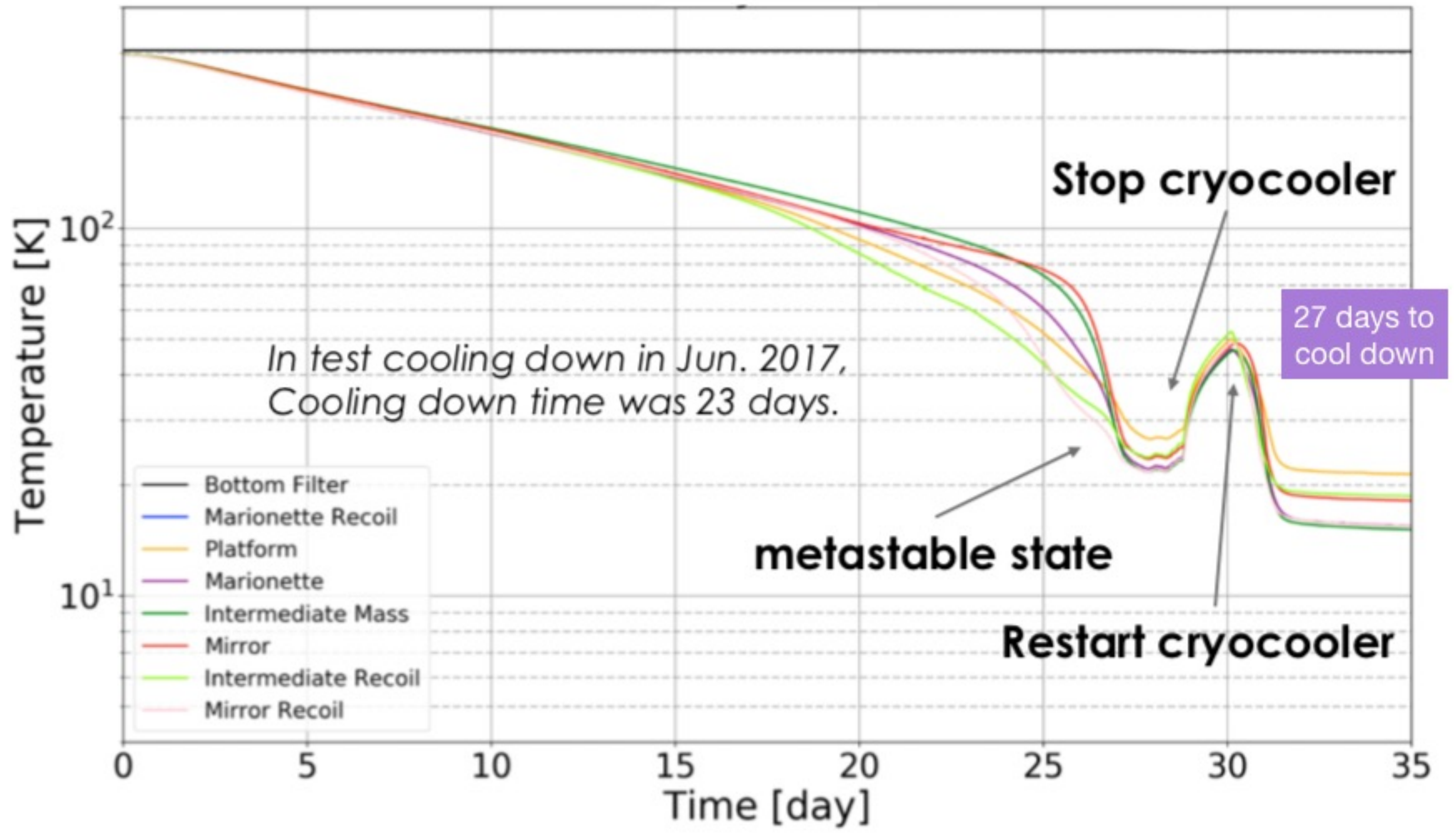

20 K
in 4 weeks

KAGRA (Kamioka Gravitational-Wave Observatory)

KAGRA (Kamioka Gravitational-Wave Observatory)

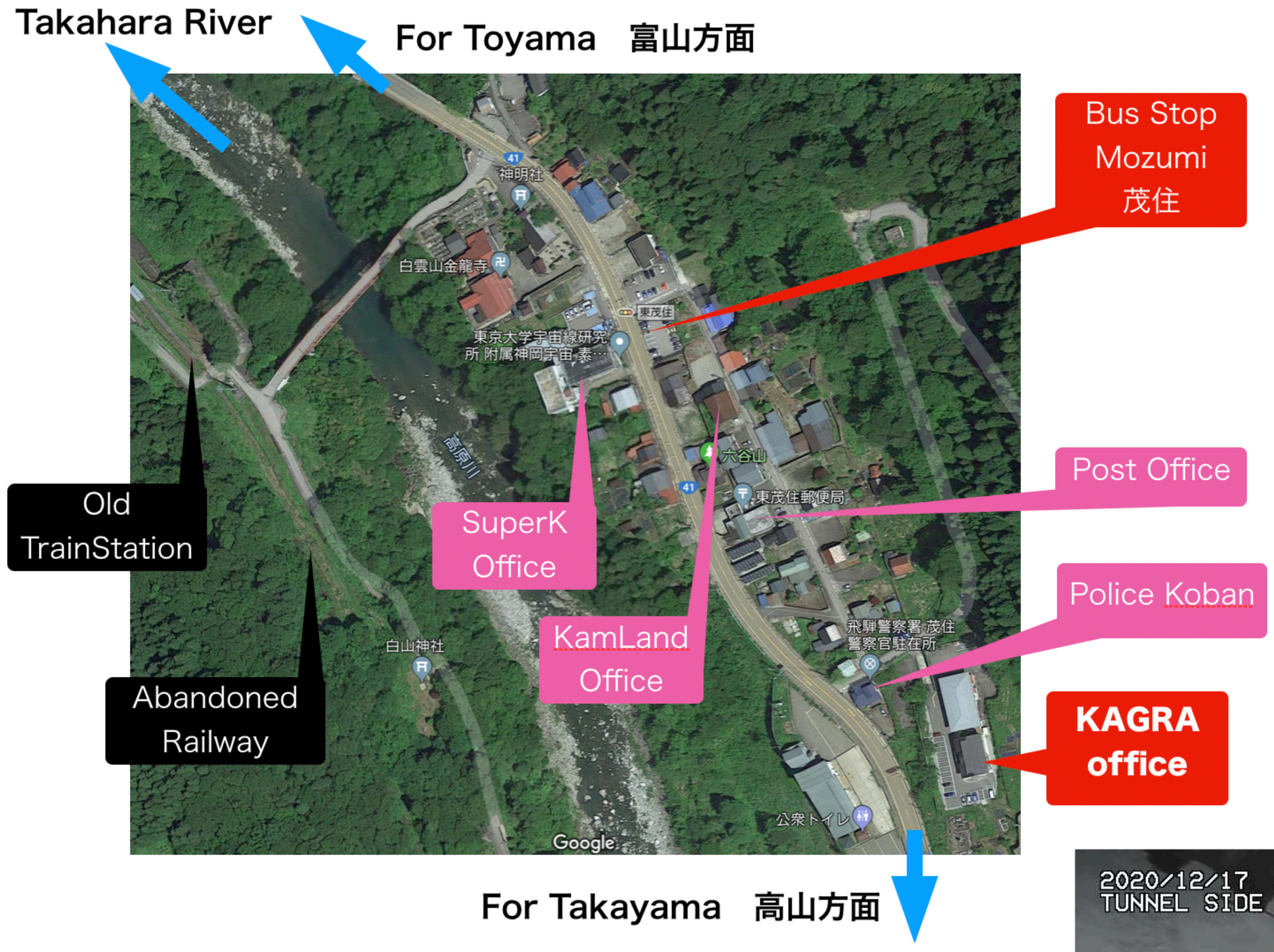

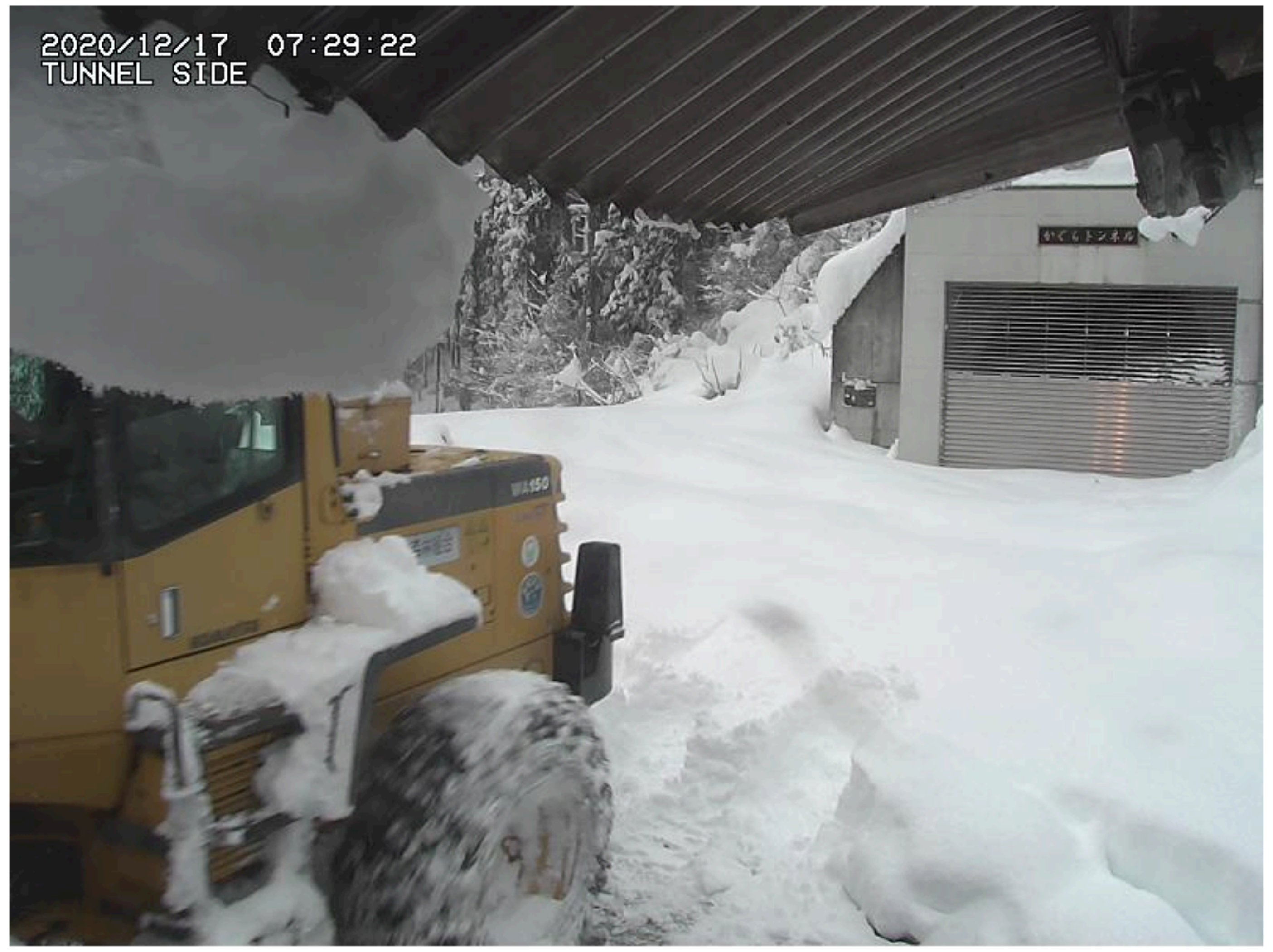

90cm snow in one night, Dec 17 2020

Joint Research MoA signed LIGO-Virgo-KAGRA

October 4, 2019 @ Ceremony of MoA signing

main part (10 pages)
Concept, Definitions, Purposes

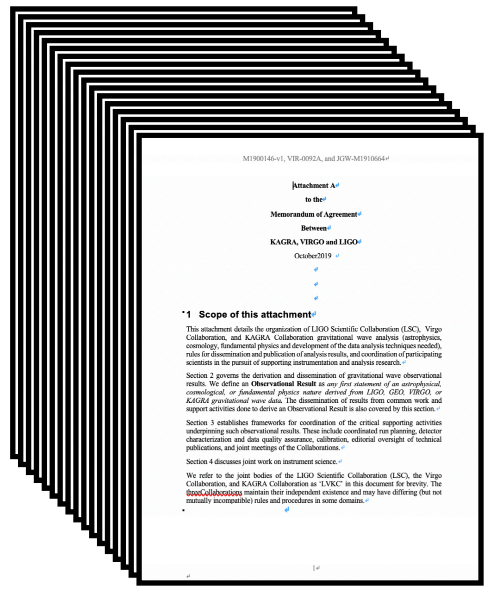

Appendix A (17 pages)
Organizations, Procedures

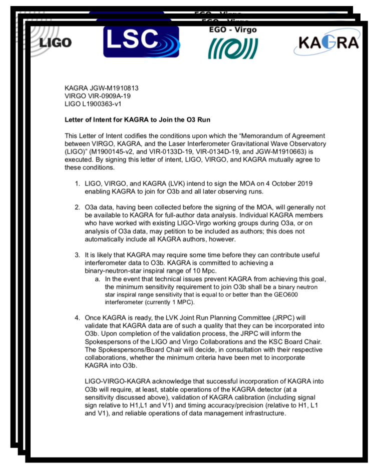

Letter of Intent (3 pages)
KAGRA's Join to O3

＊ 1 Mpc (BNS) is required to join the observation.

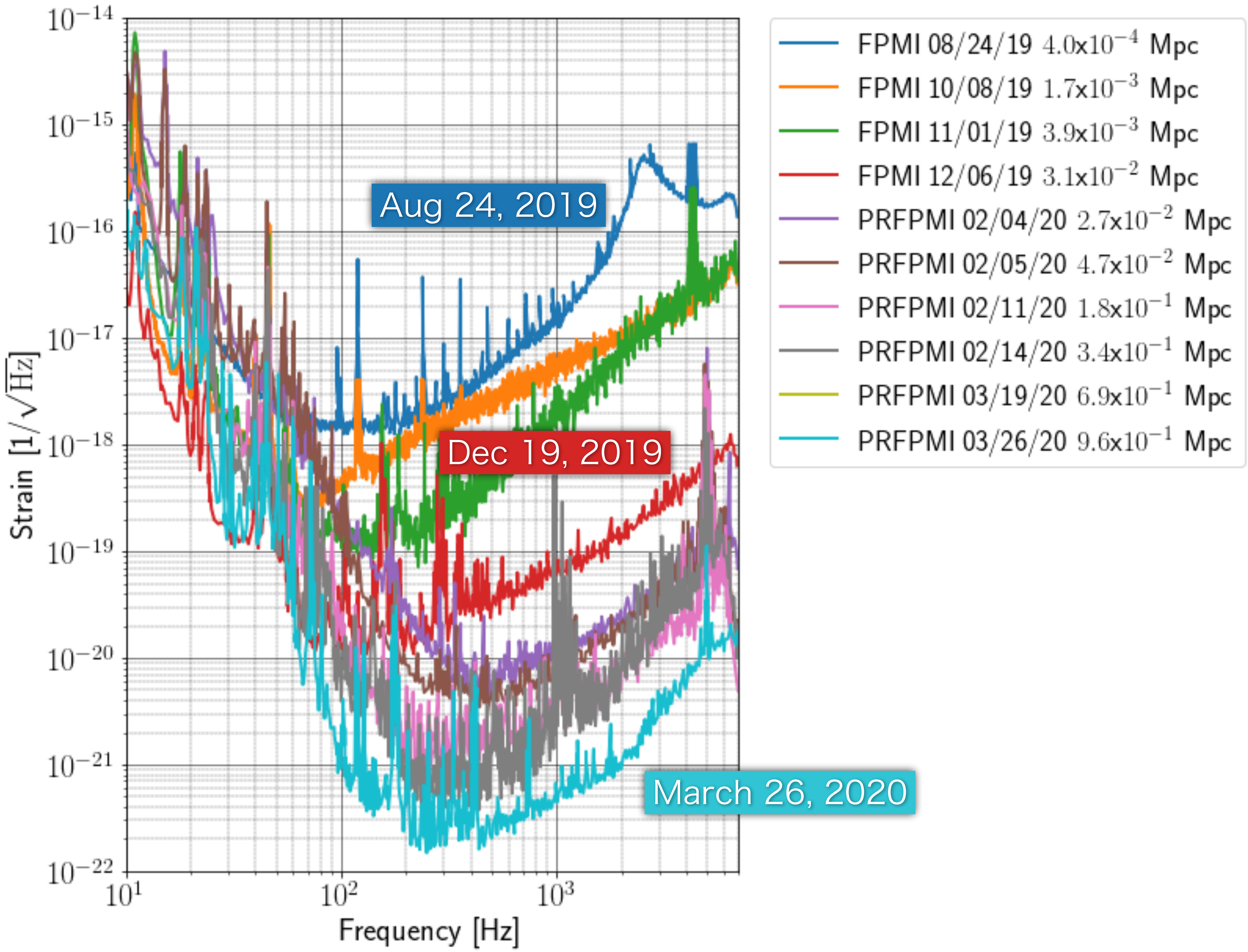

＊ Finally, over 1 Mpc in the end of March 26, 2020.

O3b, O3GK, and after that

KAGRA

2019 | 2020

12	1	2	3	4	5	6	7	8	9

O3b (planned)

O3b (LV)

GEO600 Astrowatch ~ 1.2 Mpc

KAGRA

Dec 17-25 ER

Feb25-Mar10 Obs.

Apr 7-21 Obs.

O3GK

* O3GK observation (LVK paper)

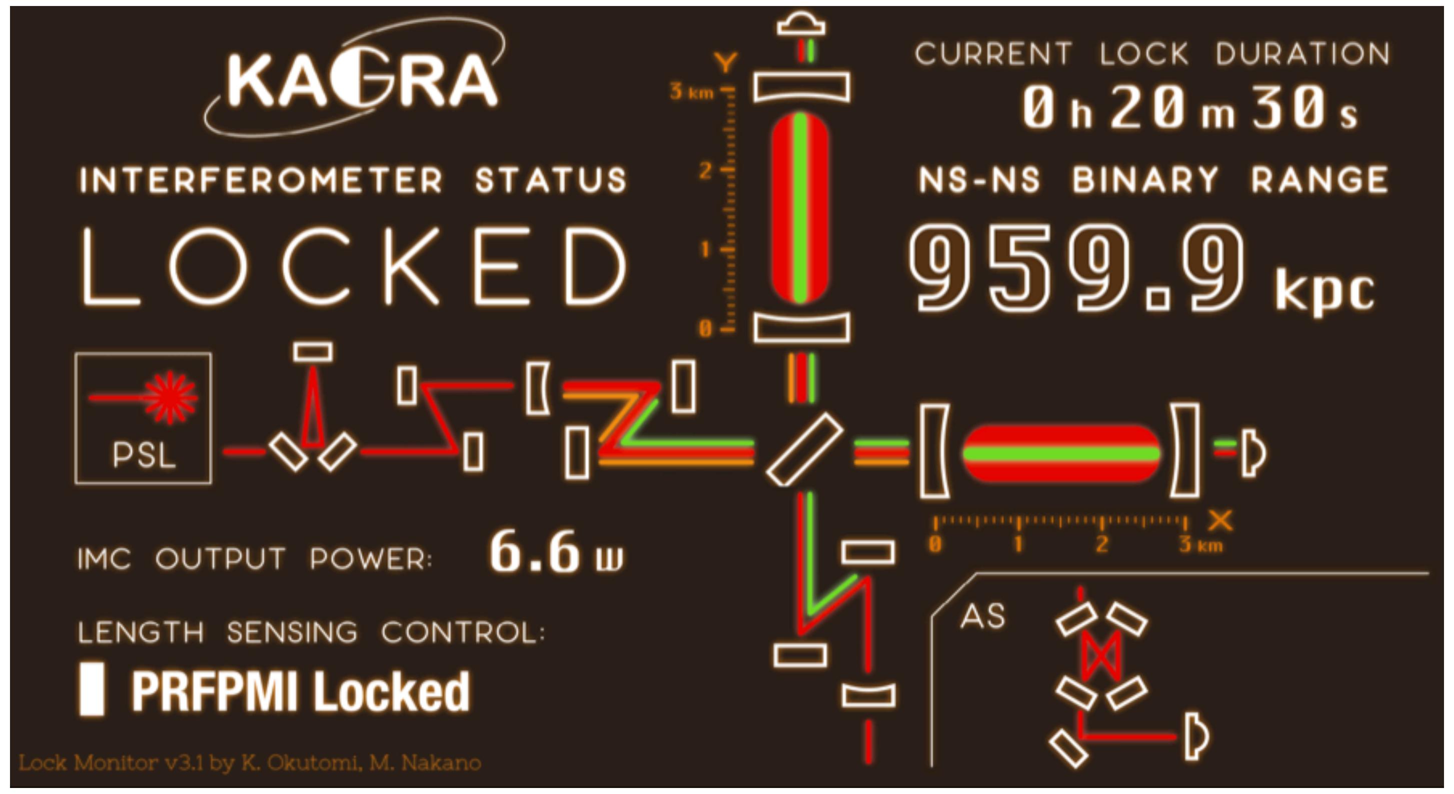

March 29, 2020

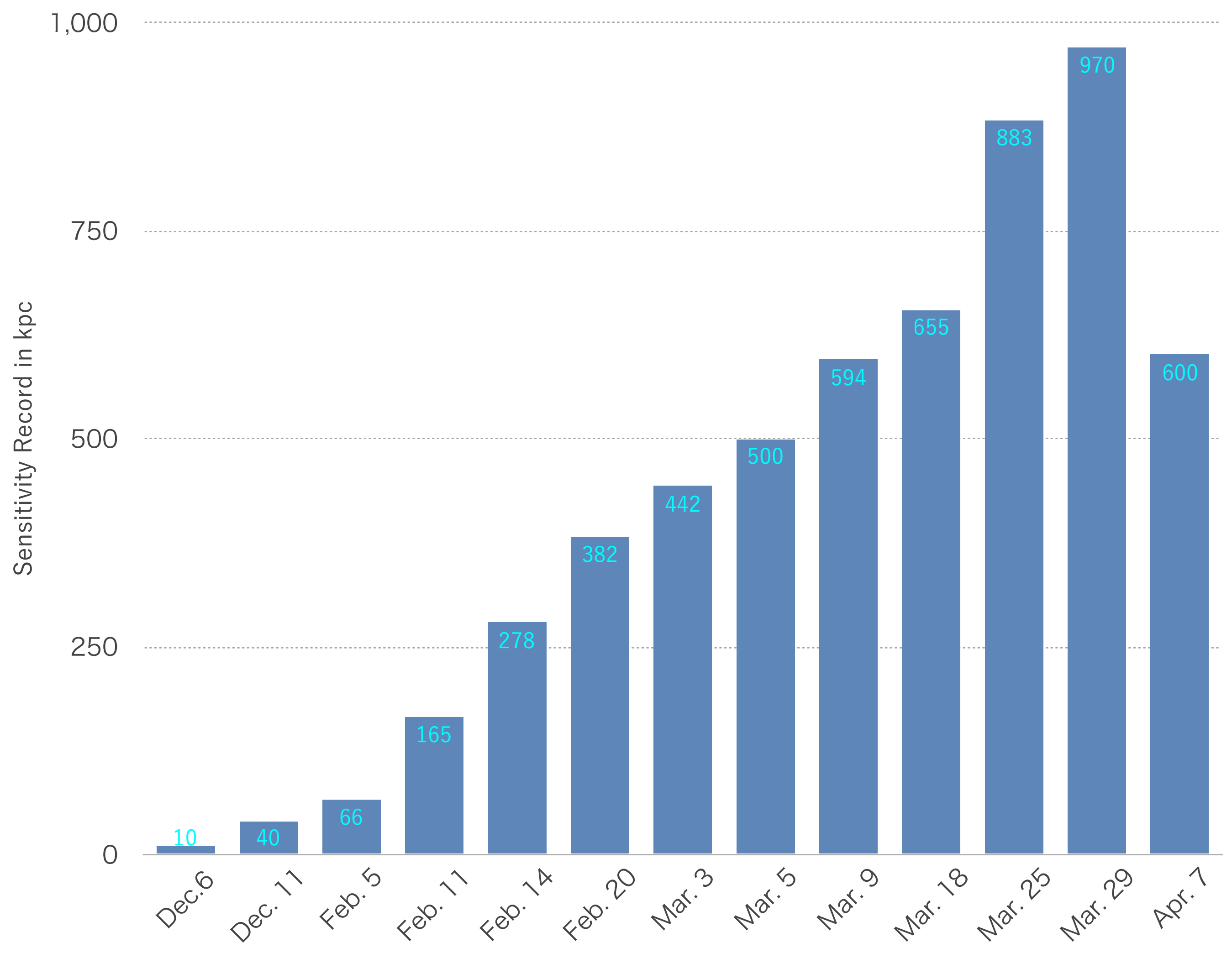

O3GK（April 7-21, 2020）

Official start and end time

Start : April 7 8:00 2020 UTC, GPS Time : 1270281618

End : April 21 0:00 2020 UTC, GPS Time 1271462418

KAGRA Duty Cycle : Locked 69%, Observing 58%

Longest lock 8h05m

Sensitivity : 500-700 kpc

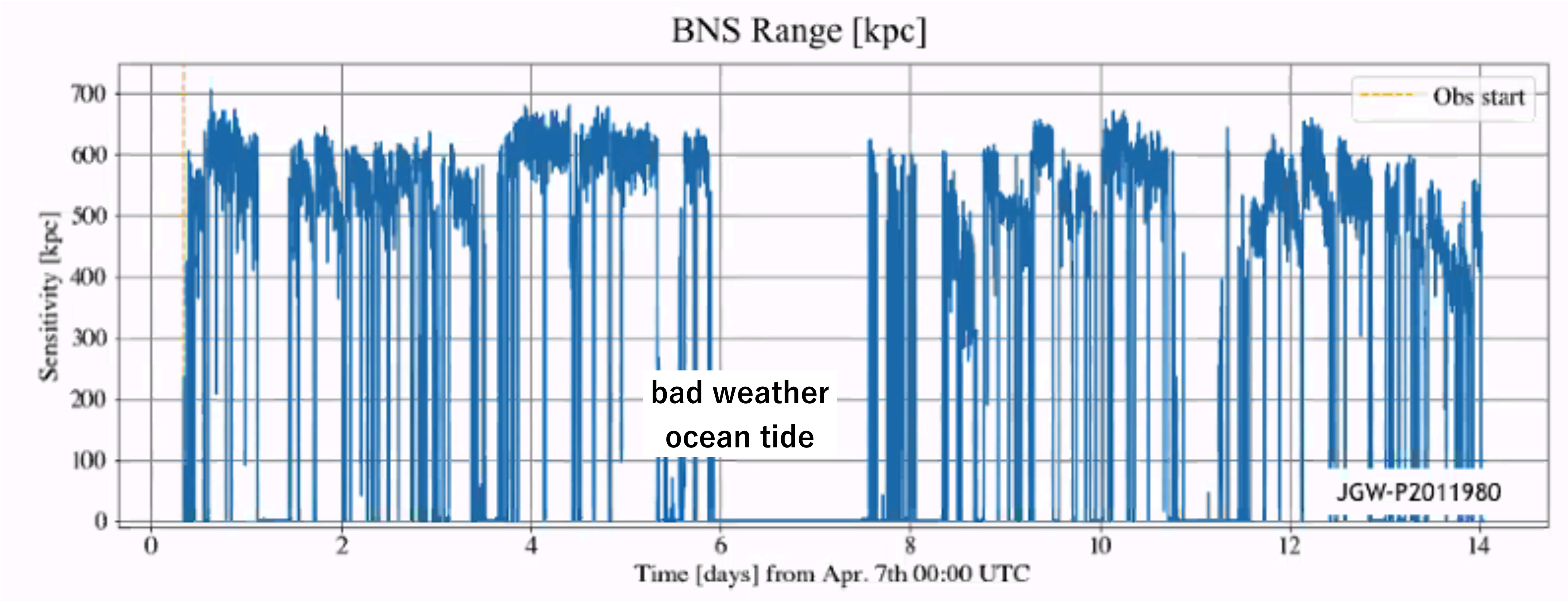

Takahiro Yamamoto, JGW-P2011980

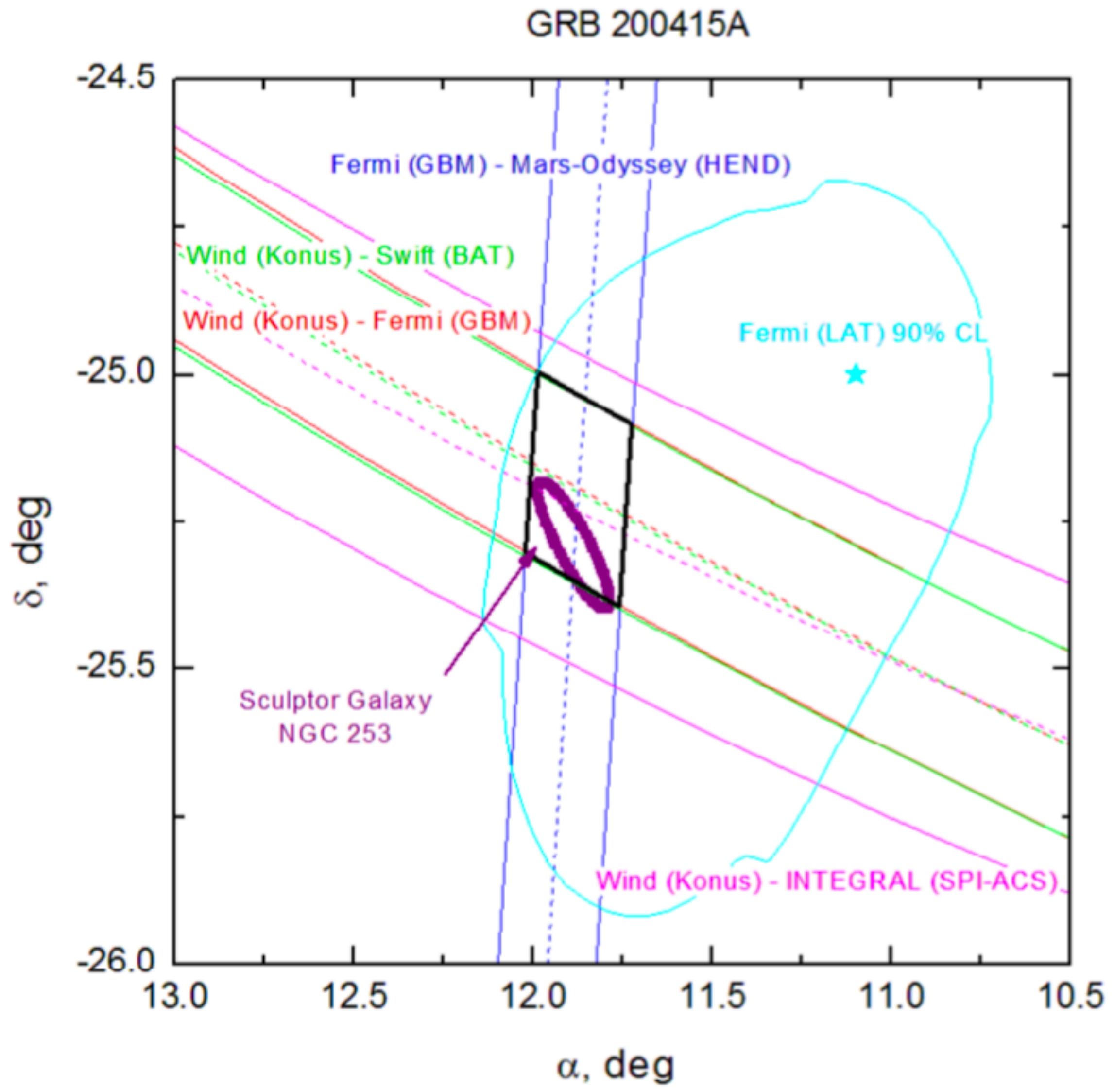

GRB200415A

NGC 235 (Sculptor galaxy)

3.5 Mpc, one of the brightest galaxies

https://gcn.gsfc.nasa.gov/fermi_grbs.html

GRB200415A

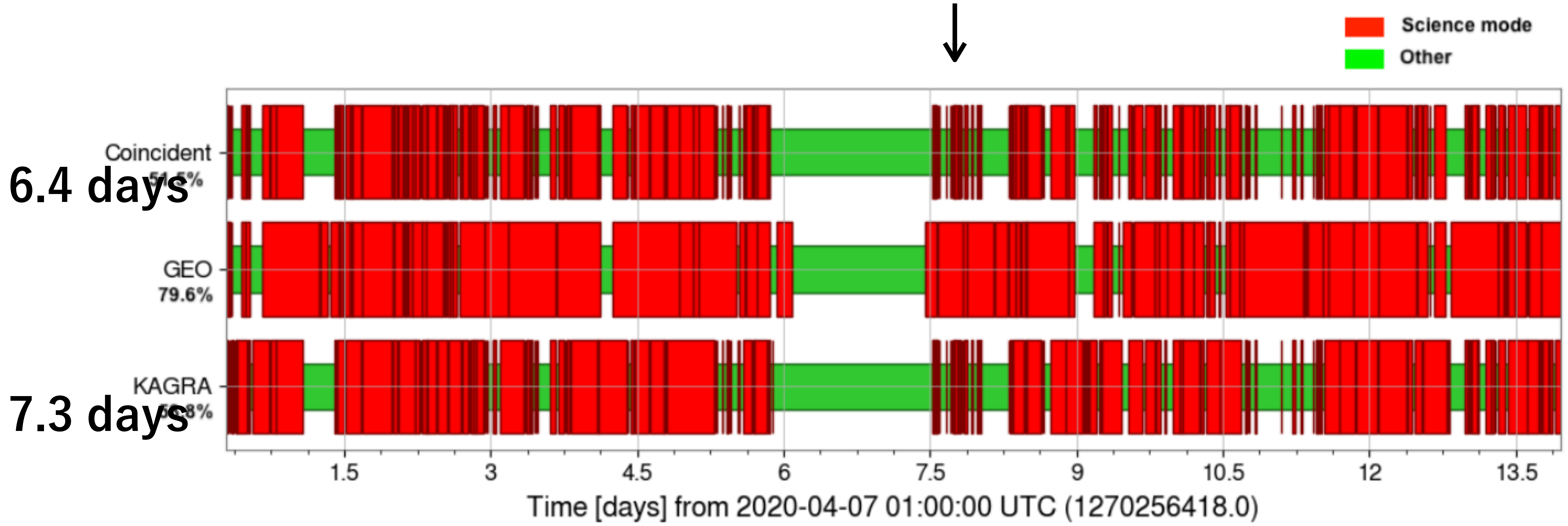

Jim Lough, LIGO-G2001554

Overview of KAGRA: reviews in PTEP 2020-2021

ACCEPTED MANUSCRIPT

Overview of KAGRA : Detector design and construction history

T Akutsu, M Ando, K Arai, Y Arai, S Araki, A Araya, N Aritomi, Y Aso, S Bae, Y Bae ... Show more

Progress of Theoretical and Experimental Physics, ptaa125, https://doi.org/10.1093/ptep/ptaa125

Published: 17 August 2020 **Article history** ▾

published PTEP 2020
KAGRA history

https://doi.org/10.1093/ptep/ptaa125

arXiv: 2005.05574

ACCEPTED MANUSCRIPT

Overview of KAGRA: KAGRA science

T Akutsu, M Ando, K Arai, Y Arai, S Araki, A Araya, N Aritomi, H Asada, Y Aso, S Bae ... Show more

Progress of Theoretical and Experimental Physics, ptaa120, https://doi.org/10.1093/ptep/ptaa120

Published: 12 August 2020 **Article history** ▾

PDF | Split View | Cite | Permissions | Share ▾

published PTEP 2020
KAGRA Science

https://doi.org/10.1093/ptep/ptaa120

arXiv: 2008.02921

Overview of KAGRA: Calibration, detector characterization, physical environmental monitors, and the geophysics interferometer

T Akutsu, M Ando, K Arai, Y Arai, S Araki, A Araya, N Aritomi, H Asada, Y Aso, S Bae ... Show more

Progress of Theoretical and Experimental Physics, Volume 2021, Issue 5, May 2021, 05A102, https://doi.org/10.1093/ptep/ptab018

Published: 22 February 2021 **Article history** ▾

published PTEP 2021
KAGRA Calibration, Detector characerization, physical environment monitors

https://doi.org/10.1093/ptep/ptab018

arXiv: 2009.09305

in preparation

* Overview of KAGRA : Noise Budget
* Overview of KAGRA : Data transfer and management
* Overview of KAGRA : Data analysis methods

PAPER

Vibration isolation systems for the beam splitter and signal recycling mirrors of the KAGRA gravitational wave detector

T Akutsu[1,2], M Ando[1,3,4], K Arai[5], Y Arai[5], S Araki[6], A Araya[7], N Aritomi[3], H Asada[8], Y Aso[9,10], S Bae[11] + Show full author list

Published 5 March 2021 • © 2021 IOP Publishing Ltd

Classical and Quantum Gravity, Volume 38, Number 6

Citation T Akutsu *et al* 2021 *Class. Quantum Grav.* **38** 065011

https://iopscience.iop.org/article/10.1088/1361-6382/abd922

Class. Quant. Grav. 38 (2020) 065011

Toward O4

* **Target Sensitivity 25 - 130 Mpc**
* Recent estimate: **less than 25 Mpc**
  due to heat absorption of sapphire mirrors

by reducing laser noise, low-f noise,

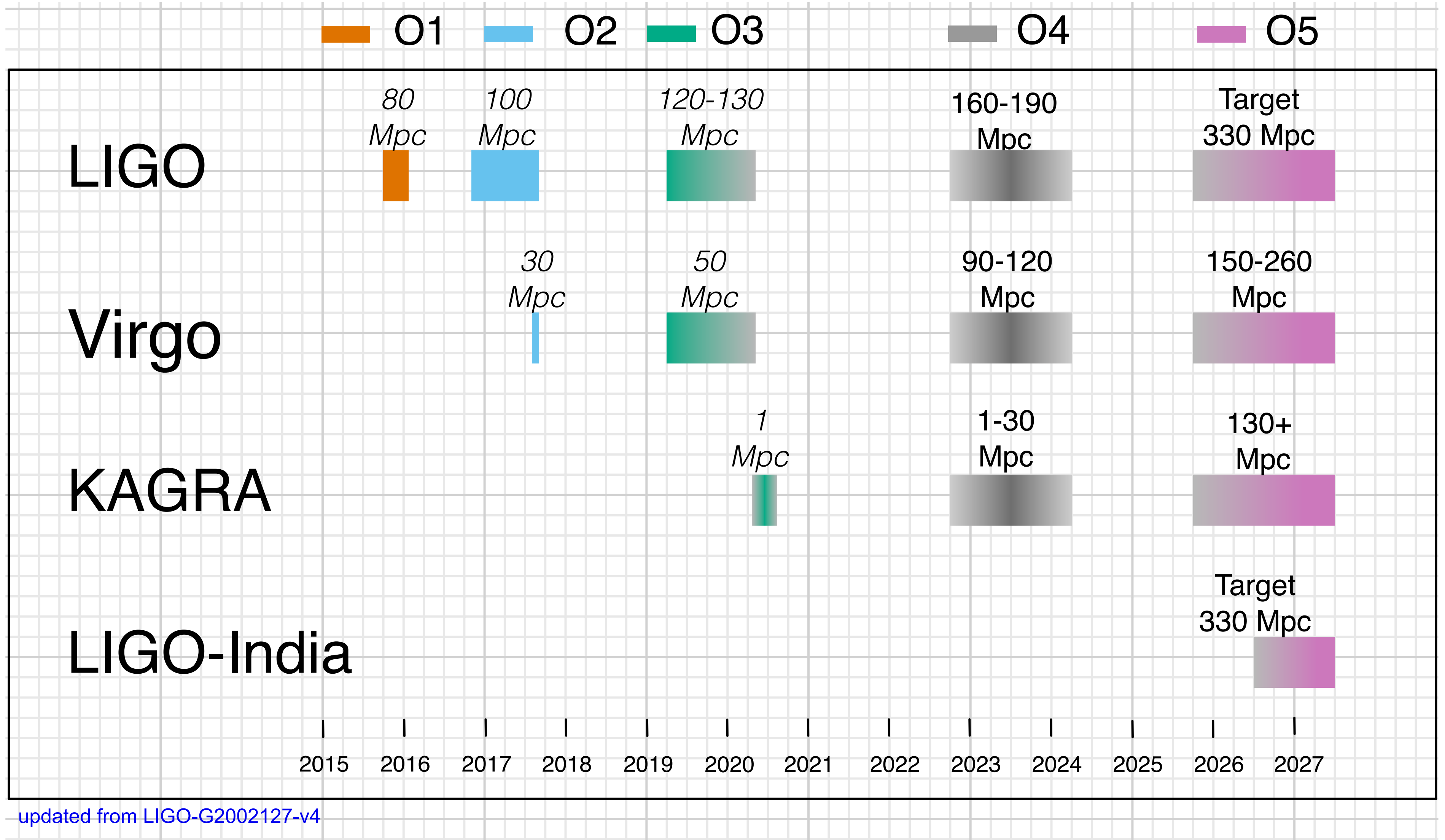

- [x] less than 100K
- [ ] dual recycling
  - [x] lock trials by the end of September 2020
- [ ] suspension noise control for low freq.
  - [x] one-order reduced in July
- [ ] de-frosting mirrors
- [ ] de-frosting windows for oplev light

x20 sensitivity at mid-freq.

commissioning

December 2022
O4 starts

repair & installation

- Cryo-Payload repairing
- ETMY tower repairing
- install laser beam baffles
- Cryocoolers replacement (CRY)
- Intensity noise reduction system (IOO)
- DGS/AEL upgrade (DGS/AEL)
- Stray light around IOO (AOS)
- Suspension frame modification (AOS, VIS)
- Temperature monitors (VIS)
- and more

Last 5 years

★ The first detection of GW was 6 years ago. Since then we detected 90 events.
Most of them are BBH, and 2 BNS, 2 BHNS and 2 BH+unknown.
Recent GW studies cover the constraints to the lensed events, stochastic backgrounds, spinning NSs, and also to cosmic string's model, dark matter candidates.

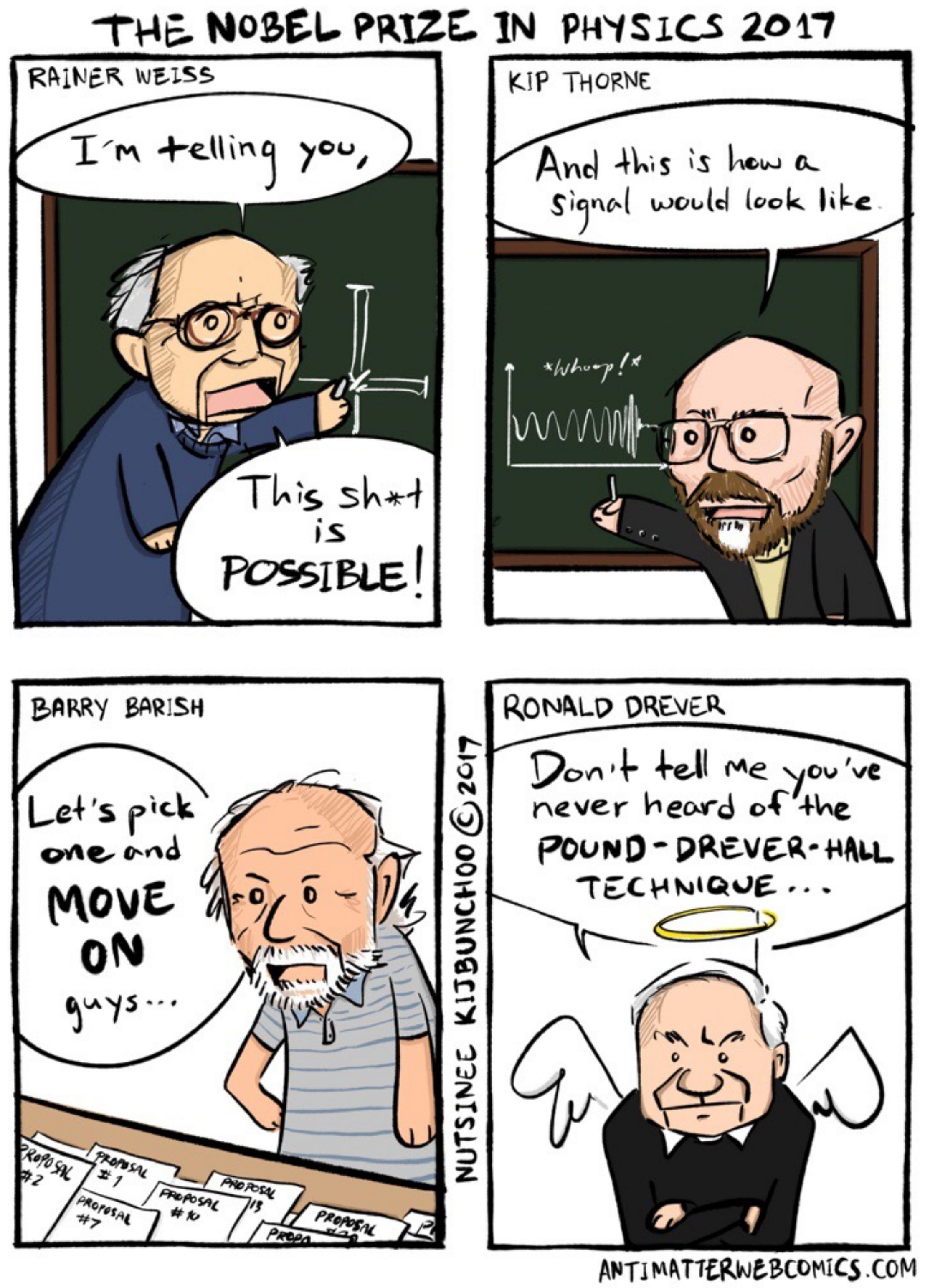

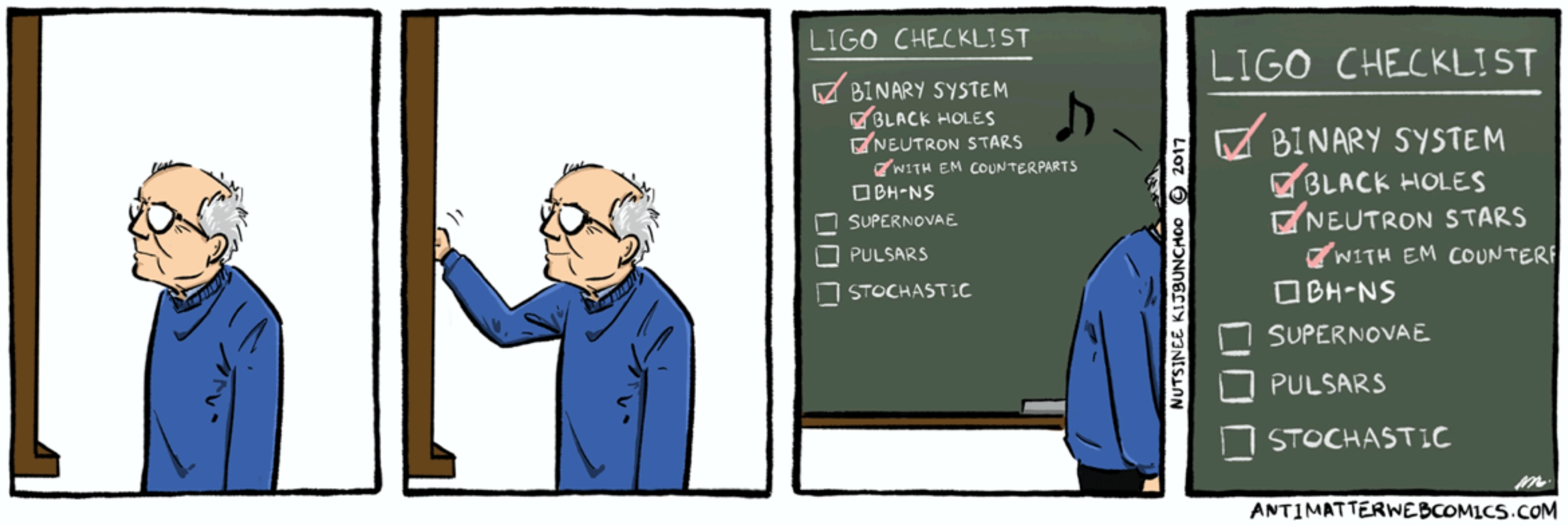

https://antimatterwebcomics.com/comic/physics-nobel-prize-2017/
https://antimatterwebcomics.com/comic/gw170817/

Next 5 years

★ A+, AdV+, and KAGRA projects involve significant upgrades in O5. The sensitivity of LIGO-Virgo-KAGRA network should improve 2-3 times over O3; one binary merger per day.

★ Alert system will also be improved.
In O3, the alerts were made within minutes of data acquisition for compact binary mergers.
Improved alerts for BNS in O5 will be seconds to minutes before its merger.

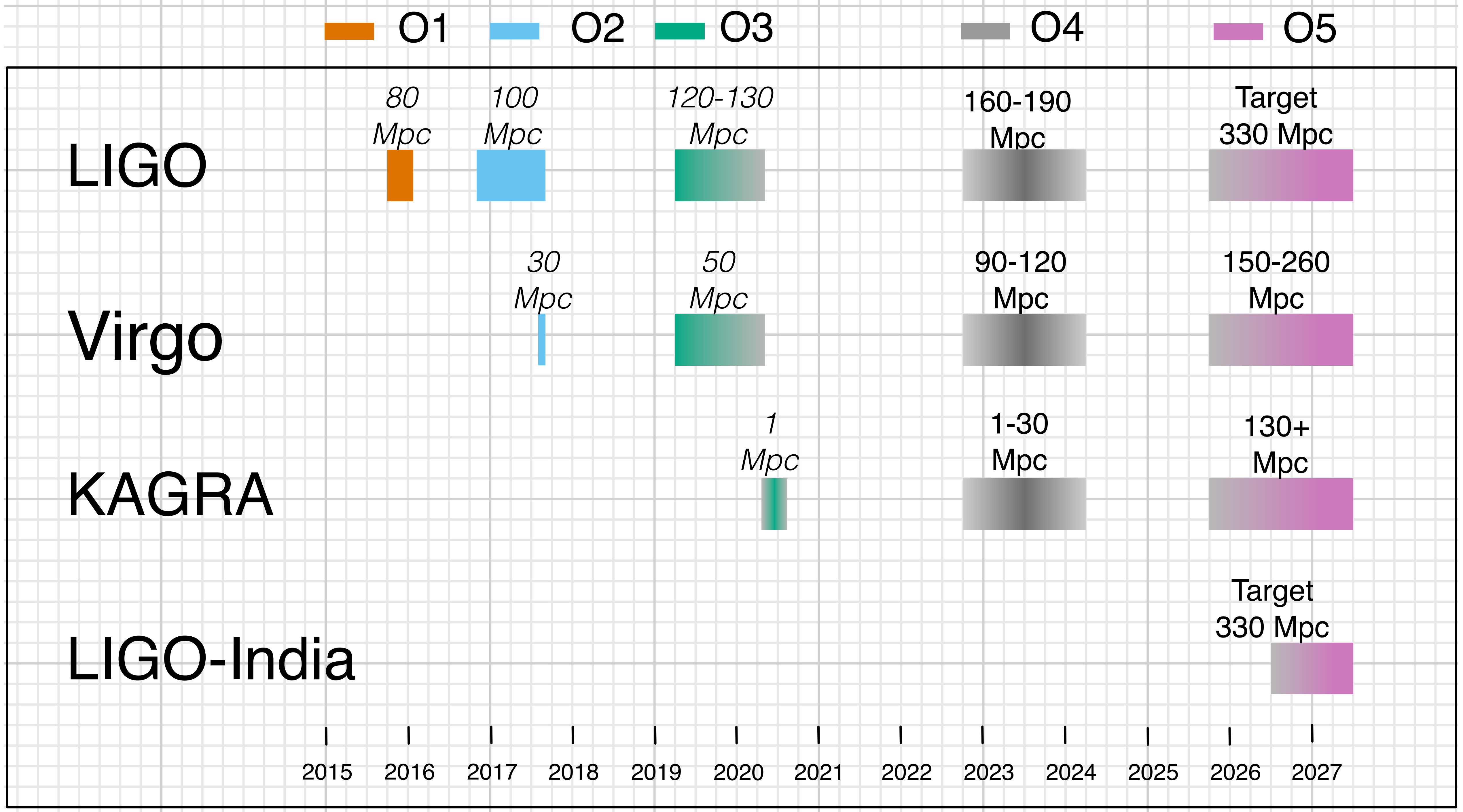

updated from LIGO-G2002127-v4

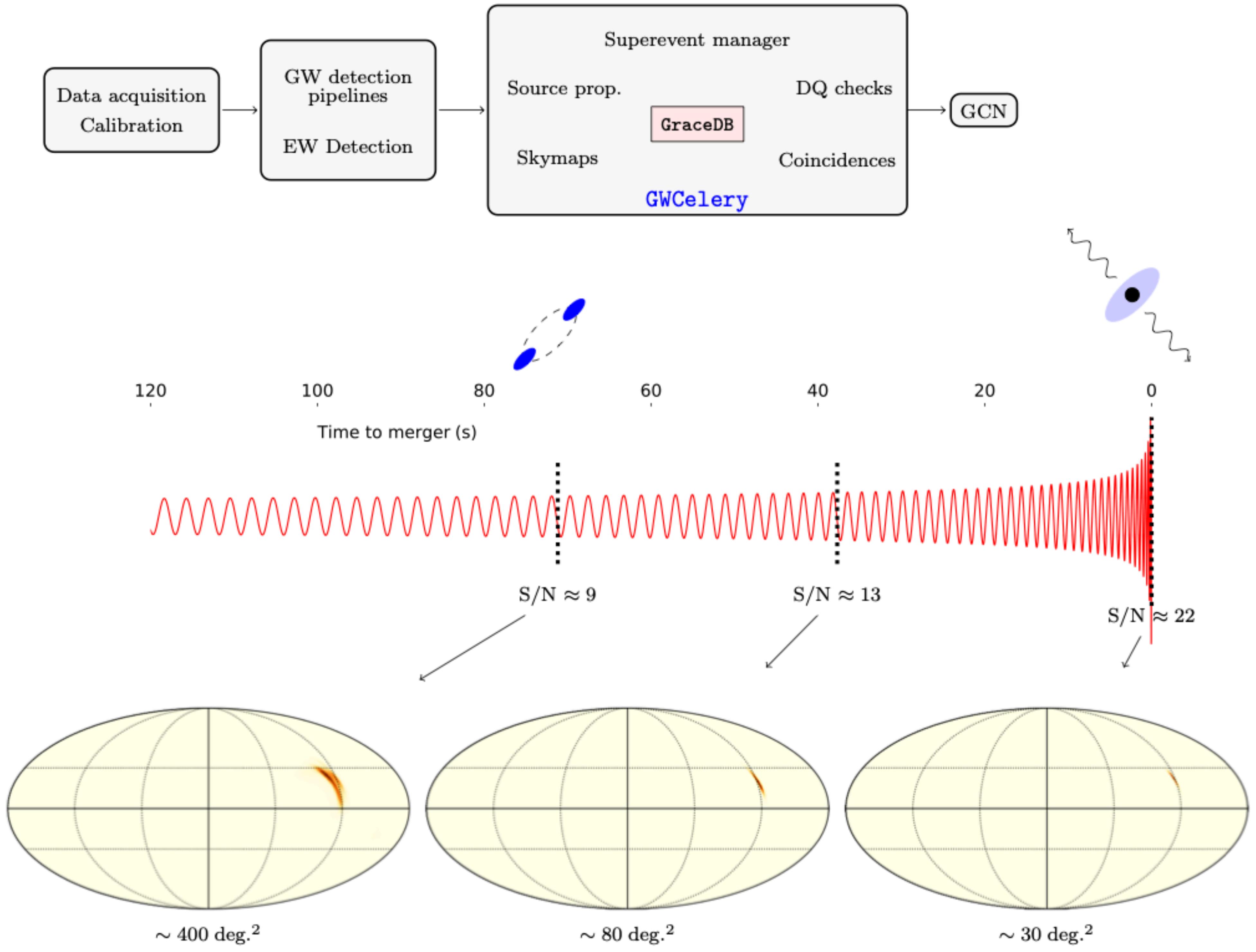

R Magee et al 2021 ApJL 910 L21 [arXiv:2102.04555]

Gravitational Wave Physics & Astronomy : Outlook (3)

Next 10 years

★ The 3rd generation GW detectors, Cosmic Explorer (US) and Einstein Telescope (Europe), will observe the entire Universe.

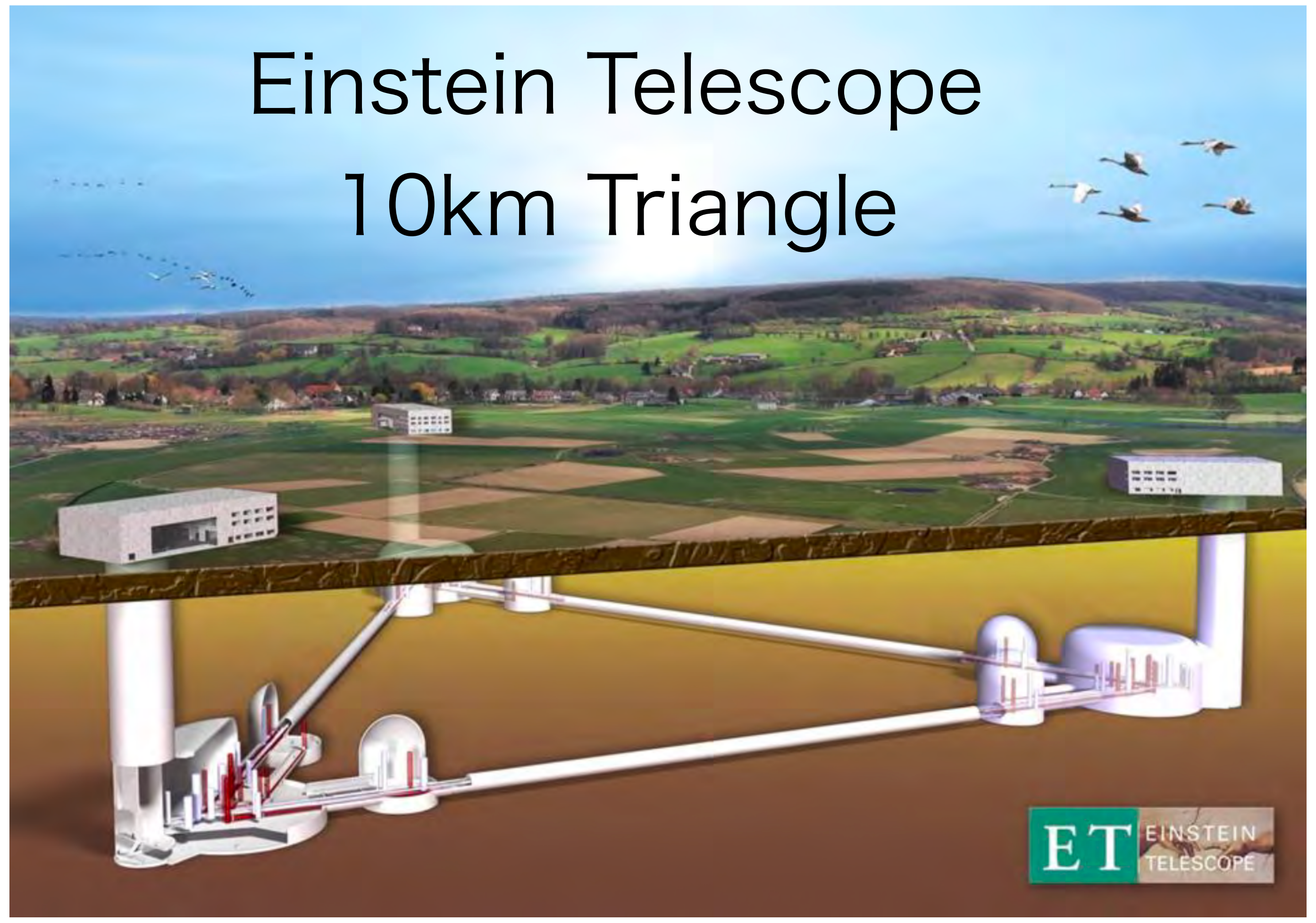

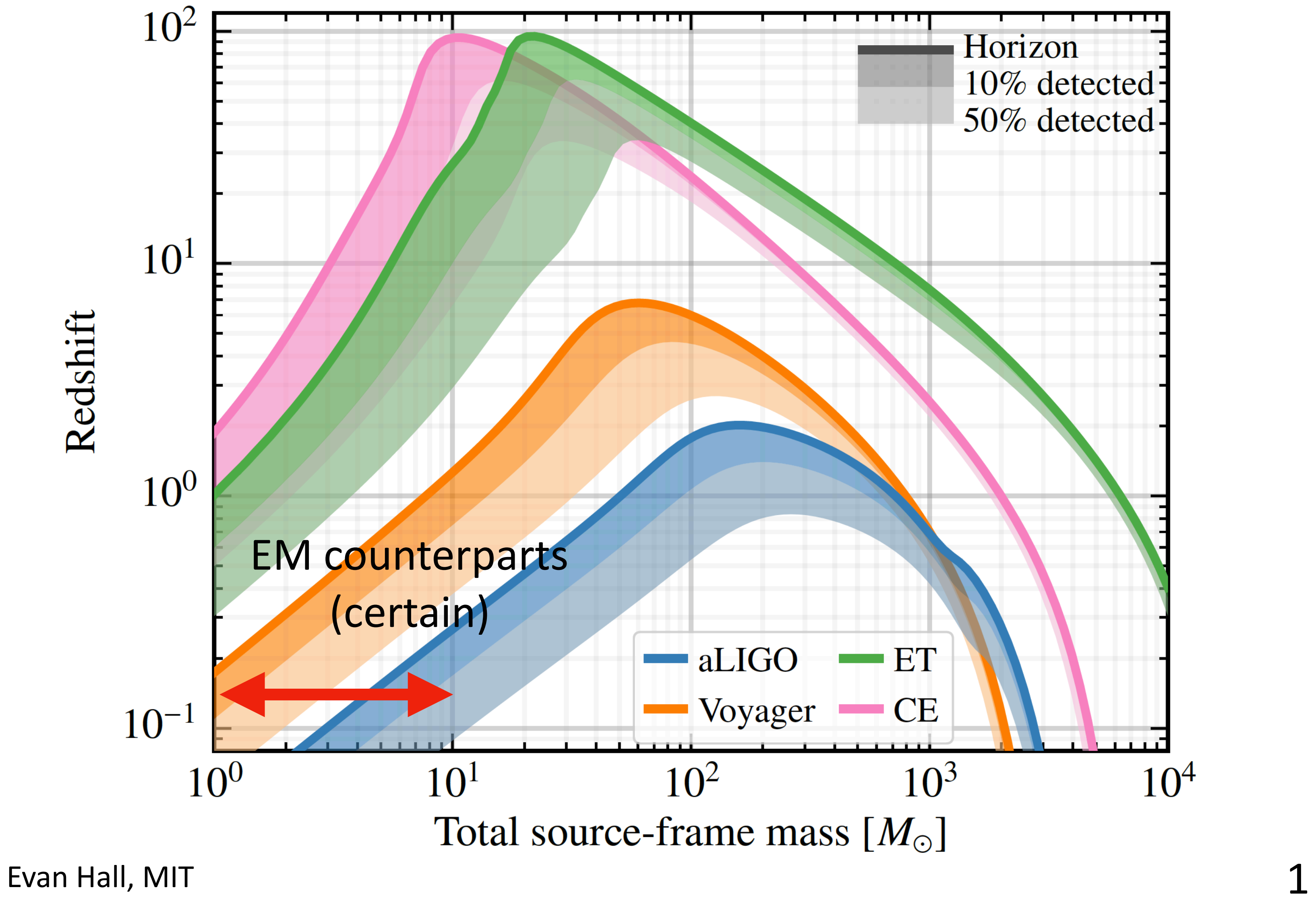

★ Space mission, LISA and with other proposed missions projects (DECIGO, BBO, ALIA, TianQin, …) will explore new GW phenomena in low frequency.